Fluid Dynamics

Flow Decomposition and Vortex Dynamics

(Draft)

I-Liang Chern

Department of Mathematics
National Taiwan University

Contents

1 Thermodynamics of Fluids **1**

1.1 The Thermodynamics of Gases . . . 1

1.1.1 Basic concepts . . . 1

1.1.2 Work and the First Law . . . 2

1.1.3 Characterizing Adiabatic Processes . . . 4

1.1.4 Heat, Entropy and Temperature . . . 6

1.1.5 Ideal Gases and Polytropic Gases . . . 10

1.2 Thermodynamic Potentials and Legendre Transform . . . 14

1.2.1 Enthalpy, Helmholtz, Gibbs Free Energies . . . 14

1.2.2 Maxwell Relations . . . 16

1.2.3 Legendre Transformation . . . 17

1.3 Thermodynamic Stability . . . 19

1.3.1 Stability Characterized by the Potentials . . . 19

1.3.2 Stability Characterized by the Thermodynamic Response Functions . . . 19

1.4 Construction of the Constitutive Law from Measurements . . . 24

1.5 Historial Note . . . 25

2 Dynamics of Fluid Flows **27**

2.1 Fluid Dynamics in the Eulerian Frame . . . 27

2.1.1 Conservation of mass, momentum and energy . . . 27

2.1.2 Initial conditions and boundary conditions . . . 30

2.1.3 Systems of Balance Laws in the Eulerian Frame . . . 31

2.2 Fluid Dynamics in the Lagrangian Frame . . . 32

2.2.1 Flow Maps and Velocity Fields . . . 32

2.2.2 Deformation Gradients . . . 32

2.2.3 Systems of Balance Laws in the Lagrangian Frame . . . 33

2.3 Material Derivatives . . . 36

2.3.1 Rate-of-changes of Geometric Variables . . . 37

2.3.2 Rate-of-change of Kinematic Variables . . . 38

2.3.3 Rate-of-change of Thermodynamic Variables . . . 39

3 Viscous Fluids **41**

3.1 Viscosity . . . 41

3.1.1 Stress . . . 41

3.1.2 Strain Rate . . . 42

3.1.3 The Stress–Strain Rate Relation for Newtonian Fluids . . . 44
3.2 The Navier–Stokes Equation for Viscous Flows . . . 45
3.2.1 The Momentum Equation for Viscous Flows . . . 45
3.2.2 Energy Equation and Heat Conduction . . . 46
3.3 Second Law of Thermodynamics for Viscous Flows . . . 46
3.3.1 Dissipation of Kinetic Energy . . . 46
3.3.2 Entropy Production and the Clausius–Duhem Inequality . . . 48
3.4 Dimensional Analysis . . . 50
3.4.1 Nondimensional Compressible Navier-Stokes Equations . . . 50
3.4.2 Physical Interpretation of Dimensionless Parameters . . . 53

4 Flow Invariants for Inviscid Fluid Flows 57
4.1 Introduction . . . 57
4.1.1 The Euler Equation in Lamb Form . . . 57
4.2 Bernoulli Principle . . . 58
4.2.1 Introduction . . . 58
4.2.2 Bernoulli Principle for Steady Isentropic Flows . . . 59
4.2.3 Special Cases of the Bernoulli Principle . . . 60
4.2.4 Bernoulli Principle for Unsteady Irrotational Flow . . . 62
4.2.5 Applications of Bernoulli Principle . . . 63
4.3 Vorticity and Circulation Theorem . . . 64
4.3.1 Motivation and Definition of Circulation . . . 64
4.3.2 Circulation Theorems . . . 65
4.3.3 Vorticity Transport Equation . . . 69
4.3.4 Helmholtz's Vorticity Equation . . . 74
4.3.5 Potential Vorticity . . . 76
4.3.6 Summary . . . 78
4.4 Vorticity Equation for Viscous Fluid Flows . . . 79

5 Variational and Hamiltonian Fluid Mechanics 81
5.1 Introduction and Main Ideas . . . 81
5.2 Hamilton's Principle in Material Coordinates . . . 82
5.2.1 The Motion Map and Material Variables . . . 82
5.2.2 The Material Action . . . 83
5.2.3 First Variation of the Action . . . 83
5.2.4 Euler–Lagrange Equations in Material Coordinates . . . 84
5.2.5 Recovery of the Compressible Euler Equations . . . 84
5.3 Canonical Form and Lagrangian Poisson Structure . . . 85
5.3.1 Material Momentum and Legendre Transform . . . 85
5.3.2 Canonical Hamiltonian Equations . . . 85
5.3.3 Canonical Symplectic Form . . . 86
5.3.4 Hamiltonian Vector Fields and the Poisson Bracket . . . 86
5.3.5 The Lagrangian Poisson Bracket . . . 87
5.3.6 Advantages of the Hamiltonian Viewpoint . . . 88
5.4 Eulerian Reduction and Dynamically Accessible Variations . . . 89
5.4.1 The Reduced Lagrangian . . . 89

5.4.2 Eulerian Variation Field . . . 89
5.4.3 Variations of Density and Entropy . . . 90
5.4.4 Eulerian Form of Hamilton's Principle . . . 91
5.5 The Euler–Poincare Equations . . . 91
5.5.1 Application to Compressible Ideal Fluids . . . 93
5.5.2 Meaning of the Euler–Poincare Form . . . 94
5.6 Noether's Theorem: Symmetry and Invariants . . . 94
5.6.1 Spatial Symmetries and Classical Conservation Laws . . . 95
5.6.2 Particle Relabelling Symmetry and Fluid Invariants . . . 96
5.7 Clebsch Representation . . . 99
5.7.1 Clebsch Ansatz and Variational Meaning . . . 99
5.7.2 Herivel–Lin Constrained Variations . . . 100
5.7.3 Why Lin Labels Are Needed . . . 100
5.7.4 Evolution Equations for the Clebsch Variables . . . 101
5.7.5 Geometric Interpretation and Local Validity . . . 102
5.8 Eulerian Poisson Structure . . . 103
5.8.1 Variational Derivatives of the Hamiltonian . . . 104
5.8.2 From the Lagrangian Bracket to the Eulerian Bracket . . . 104
5.8.3 The Noncanonical Poisson Bracket . . . 105
5.8.4 Hamiltonian Form of the Compressible Euler Equations . . . 105
5.9 Casimirs and Advected Invariants . . . 107
5.9.1 Entropy Casimirs . . . 107
5.9.2 Potential-Vorticity Casimirs . . . 108
5.9.3 Relation to Relabelling Symmetry . . . 109
5.10 Summary and Further Reading . . . 109

6 Flow Decomposition, Topology, and Applications 111
6.1 Introduction . . . 111
6.2 Helmholtz Decomposition in Euclidean Space . . . 111
6.3 The Hodge–Morrey–Friedrichs Decomposition and Reconstruction . . . 113
6.3.1 The Hodge–Morrey–Friedrichs Theorem . . . 113
6.3.2 The Scalar potential φ . . . 115
6.3.3 Vector Potential and Gauge . . . 115
6.3.4 Boundary Conditions and Orthogonality . . . 116
6.3.5 Relation to the Four-Component Theorem . . . 117
6.4 Harmonic Fields, Topology, and Examples . . . 117
6.4.1 Circulation, Cohomology, and Harmonic Coefficients . . . 117
6.4.2 Handles, Cavities, and Flux . . . 118
6.4.3 Pure Harmonic Circulation: Annulus and Multiple Obstacles . . . 119
6.4.4 A Solid Torus and Exterior Domains . . . 119
6.4.5 Constant Harmonic Flows on a Periodic Domain . . . 119
6.5 Applications to Incompressible and Compressible Flow . . . 120
6.5.1 Fixed Impermeable Boundaries . . . 120
6.5.2 Nonzero Normal Velocity and Viscous Walls . . . 120
6.5.3 The Pressure Projection . . . 121
6.6 Evolution of the Decomposed Components . . . 121

6.6.1 Vorticity and the Potential Component . . . 121
6.6.2 Harmonic Evolution by Projection . . . 122
6.6.3 Kelvin Circulation and the Distinction Between Coefficients . . . 122
6.6.4 Reconstruction at Each Time . . . 123
6.7 Clebsch Representation and Hodge Decomposition . . . 123
6.8 Summary, Further Reading, and the Next Chapters . . . 123

7 Irrotational Flows **125**
7.1 Introduction . . . 125
7.1.1 Why Irrotational Flows Form a Natural Class . . . 126
7.1.2 Incompressible Irrotational Flow . . . 126
7.1.3 Steady and Unsteady Potential Flows . . . 127
7.2 Steady Incompressible Potential Flows . . . 127
7.2.1 Uniform Flow . . . 128
7.2.2 Source and Sink . . . 129
7.2.3 Doublet Flow . . . 129
7.2.4 Flow Around a Circular Cylinder . . . 129
7.2.5 Flow Around a Cylinder with Circulation . . . 131
7.2.6 Flow Around a Sphere . . . 132
7.2.7 Flow Outside a Solid Torus . . . 134
7.2.8 Harmonic Flow on a Three-Dimensional Periodic Box . . . 135
7.2.9 Summary: Topology and Harmonic Circulation . . . 137
7.2.10 Time Dependence of Harmonic Circulation . . . 138
7.3 Unsteady Incompressible Potential Flows . . . 139
7.3.1 Unsteady Bernoulli Equation . . . 140
7.3.2 Accelerating Uniform Flow . . . 140
7.3.3 Accelerating Flow Around a Cylinder . . . 141
7.3.4 Accelerating Flow Around a Sphere . . . 141
7.3.5 Time-Dependent Circulation . . . 142
7.4 Forces and Momentum in Potential Flow . . . 142
7.4.1 Pressure from Bernoulli's Law . . . 143
7.4.2 Force on a Solid Body . . . 143
7.4.3 D'Alembert's Paradox . . . 143
7.4.4 Kutta–Joukowski Lift and Circulation . . . 144
7.4.5 Added Mass . . . 146
7.4.6 Impulse and Unsteady Motion . . . 147
7.5 Compressible Potential Flows . . . 147
7.5.1 Isentropic Compressible Potential Flow Equation . . . 148
7.5.2 Polytropic Gas . . . 149
7.5.3 Steady Isentropic Compressible Potential Flow . . . 149
7.5.4 Subsonic Potential Flow . . . 150
7.5.5 Small Perturbations and Acoustic Limit . . . 150
7.5.6 Nozzle and Jet Examples . . . 151
7.5.7 Remarks on Transonic and Supersonic Flows . . . 152
7.6 Transition to Vortex Dynamics . . . 152
7.7 Summary and Further Reading . . . 152

8 Vortex Dynamics and Applications **155**
8.1 Introduction: From Irrotational Flow to Vortex Dynamics . . . 155
8.2 What Is a Vortex? . . . 156
8.2.1 Vortex Lines and Vortex Tubes . . . 156
8.2.2 Vortex Filaments . . . 157
8.2.3 Vortex Patches . . . 158
8.2.4 Vortex Sheets . . . 158
8.3 Vorticity Dynamics Laws . . . 159
8.3.1 Recall of the Vorticity Laws . . . 159
8.3.2 Consequences for Vortex Structures . . . 160
8.4 Velocity Reconstruction from Vorticity . . . 162
8.4.1 Biot–Savart Law in Free Space . . . 162
8.4.2 Boundary-Compatible Reconstruction . . . 163
8.5 Vortex Formation and Growth . . . 166
8.5.1 Generation and Concentration of Vorticity . . . 166
8.5.2 Vortex Stretching and Intensification . . . 168
8.5.3 Merging, Concentration, and Coherent Structures . . . 170
8.5.4 Summary . . . 171
8.6 Two-Dimensional Vortex Dynamics . . . 171
8.6.1 Point Vortices . . . 171
8.6.2 Hamiltonian Structure of Point Vortices . . . 172
8.6.3 Rotating and Translating Vortex Pairs . . . 173
8.6.4 Von Karman Vortex Street . . . 175
8.6.5 Viscous Vortex: Lamb–Oseen Vortex . . . 177
8.6.6 Vortex Patches and Contour Dynamics . . . 177
8.6.7 Interaction and Merging of Vortex Patches . . . 184
8.6.8 Vortex Sheets and Kelvin–Helmholtz Instability . . . 185
8.7 Three-Dimensional Vortex Dynamics . . . 188
8.7.1 Vortex Filaments . . . 188
8.7.2 Vortex Rings . . . 192
8.7.3 A 3D Viscous Vortex: Burgers Vortex . . . 193
8.7.4 Swirling Vortices and Tornado-Type Flows . . . 194
8.7.5 Aircraft Wake Dipoles . . . 196
8.8 Helicity, Linking, and Knotting . . . 197
8.8.1 Linking Number . . . 197
8.8.2 Twist, Writhe, and Self-Linking . . . 198
8.8.3 Knots . . . 199
8.8.4 Helicity of Thin Vortex Tubes . . . 199
8.8.5 Conservation of Helicity . . . 201
8.9 Impulse, Momentum, and Forces . . . 203
8.9.1 Classical Impulse and Hydrodynamic Impulse . . . 203
8.9.2 Impulse of pair of point vortices in 2D . . . 206
8.9.3 Impulse of a Vortex Ring . . . 209
8.9.4 Lift, Bound Circulation, and Starting Vortices . . . 215
8.9.5 Wake Momentum and Drag . . . 215

8.10 Summary and Further Reading 215

Chapter 1

Thermodynamics of Fluids

Thermodynamics is a branch of physics which studies the energy exchange of homogeneous materials at equilibrium. These materials can be gases, liquids, solids, plasma, metals, concrete, soil, and more. The properties of these materials are described by state variables. Homogeneity in materials refers to the absence of spatial variations at a macroscopic scale. Examples of homogeneous materials are gases confined in a cylinder, or parcels of fluids. Properties such as density, temperature, and pressure are spatially uniform. The relevant forms of energy include the internal energy, mechanical work, and heat.

The formulation of thermodynamics in this Chapter follows the axiomatic foundations laid by Carathéodory (1909) and the modern development by Lieb and Yngvason (1999).

1.1 The Thermodynamics of Gases

Goal: We will study the thermodynamics of *single-component* gases confined in a cylinder. The cylinder is equipped with a movable piston on one end, allowing for the exchange of mechanical work with the external world (see Figure 1.1). Additionally, we can introduce or extract heat from the system. The theory of thermodynamics for gases aims to describe the exchange of energy between *heat*, *work*, and the *internal energy* of the system.

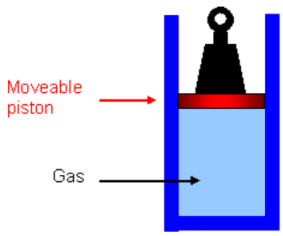


Figure 1.1: Gas in a cylinder with piston. Copied from `http://galileo.phys.virginia.edu/classes/152.mf1i.spring02/Boyle.htm`

1.1.1 Basic concepts

- **Closed system**: A closed system does not exchange matter, but can exchange energy (heat/-work).

- **Macroscopic scales**: The macroscopic scale refers to conditions where:

  (i) The time scale dt is much larger than the time scale of particle motion τ, which is typically defined as the "mean time of free particle motion."

  (ii) The spatial scales dx^1, dx^2, and dx^3 are much larger than the "mean distance of free particle motion."

  For example, on the Earth's surface, the actual dx is approximately 68 nm for a container with 2.7×10^{25} molecules per square meter and experiencing a pressure of 759.8 Torr. Further information can be found in the Mean Free Path article on Wikipedia. For the mean time of free motion, which is the inverse of collision frequency, you can consult the Collision Frequency article on Wikipedia.

- **Equilibrium**: A thermodynamic system is considered to be in equilibrium if it remains unchanged at the macroscopic scale.

- **Thermodynamic parameters** A simple thermodynamic system consists of gases confined in a cylinder. Several measurable quantities characterize this system at equilibrium, including:

  (i) V (specific volume), representing the volume of gas per unit mass,

  (ii) p (pressure),

  (iii) T (temperature),

  (iv) n (mole numbers).

  The volume is a geometric quantity, while pressure is a response of the system to changes in volume. The term "thermodynamic parameters" refers to these quantities. More parameters such as entropy S, internal energy U, etc., will be introduced later.

- **Equation of state** Let us fix the mole number of the system, say $n = 1$ mole. The rest of thermodynamic parameters T, p, and V associated with equilibrium are not independent. Experimental observations lead to an equation $f(T, p, V) = 0$, known as the equation of state. This relation is substance-dependent. For one mole ideal gases, $f(T, p, V) = pV - RT = 0$. Here, R is the gas constant. Another common and important example is the Van der Waals equation: $f(T, p, V) = \left(p + \frac{a}{V^2}\right)(V - b) - RT = 0$, where the constant a corrects for attractive forces between gas molecules and the constant b corrects for the volume occupied by the gas molecules themselves.

  Generally, *we postulate that such a thermodynamic system has only* 2 *degrees of freedom.* It forms a surface in the p-V-T space, and its projection on the p-V plane is termed a p-V diagram. A point (p, V) on the p-V plane is an independent *thermodynamic state.* Isotherms, representing curves with constant temperatures, can be observed on the p-V plane, see subfigure (a) in Figure 1.2.

1.1.2 Work and the First Law

1. Doing work to/by the system We can alter the state of the system through various physical processes. Let us introduce the following terminologies.

- **Quasi-Static Process**: A quasi-static process is characterized by its slow occurrence, ensuring the system remains in equilibrium at every instant during the process. In a continuous quasi-static process, the system is represented by a curve on the p-V plane.

- **Adiabatic Process**: An adiabatic process is a type of quasi-static process where there is no heat exchange; energy is transferred only via work.

- **Adiabatically reachable**: Two states (p_1, V_1) and (p_2, V_2) are considered adiabatically reachable if there exists an adiabatic process connecting them. We denote the work for such an adiabatic process moving from (p_1, V_1) to (p_2, V_2) as $W(p_1, V_1; p_2, V_2)$. Please refer to Figure 1.2.

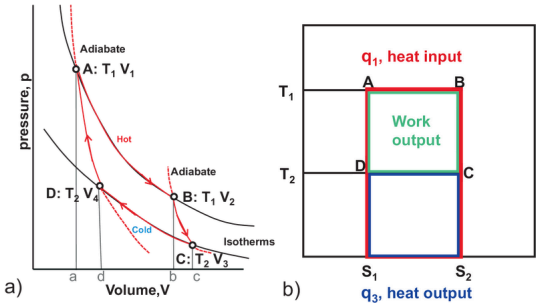


Figure 1.2: Carnot cycle on the thermodynamic plane. The left figure represents the p-V plane, while the right figure represents the T-S plane. Image source: `https://www.tf.uni-kiel.de/matwis/amat/td_kin_i/kap_1/backbone/r_se31.html`

2. First Law of Thermodynamics for adiabatic processes We now introduce an axiomatic formulation of the First Law of Thermodynamics based on the concept of *adiabatic accessibility*. This approach allows the definition of internal energy without reference to microscopic models.

- **Adiabatic Accessibility**: Given two equilibrium states (p_1, V_1) and (p_2, V_2), we say that (p_2, V_2) is *adiabatically accessible* from (p_1, V_1) if there exists a process involving only mechanical work (i.e., no heat transfer) that transforms the system from state 1 to state 2. Although work is generally path-dependent, in the case of quasi-static adiabatic processes, we postulate that the work between any two adiabatically connected states depends only on the endpoints

- **First Law of Thermodynamics for Adiabatic Processes**: *For any sequence of adiabatic processes connecting a chain of states*

$$(p_1, V_1) \to (p', V') \to (p_2, V_2),$$

the total work is additive:

$$W(p_1, V_1; p_2, V_2) = W(p_1, V_1; p', V') + W(p', V'; p_2, V_2).$$

- **Internal Energy Function**: Under this assumption, we infer the existence of a scalar state function $U(p, V)$ satisfying:

$$U(p_2, V_2) - U(p_1, V_1) = W(p_1, V_1; p_2, V_2) \tag{1.1}$$

for all adiabatically reachable states. It is natural to choose $U(p, V)$ to represent the system's internal energy at the state (p, V). The system's internal energy is the sum of all energies of the particles (translational rotational, etc.) it contains. The function $U(p, V)$ is uniquely determined up to a constant.

- **Mechanical Equation of State**: The relation

$$U = U(p, V)$$

between the internal energy U and the state (p, V) is known as the *mechanical equation of state*. This relation encodes the material properties of the system. For example, in the case of an ideal gas, the relation becomes:

$$U = U(p, V) = \frac{c_V}{R} pV.$$

This mechanical equation of state plays a central role in connecting internal energy to measurable quantities like pressure and volume, even before introducing the concept of temperature, which will emerge from entropy in the next section.

- **Remark** This formulation does not rely on the concept of heat initially. The internal energy U is defined through adiabatic processes and the associated work. In the next subsection, we will state the full first law of thermodynamics beyond the adiabatic processes, the Carathéodory's Principle Carathéodory (1909), leading to the existence of the entropy S and the absolute temperature T. This framework sets the foundation for introducing entropy as a monotonic function under adiabatic accessibility.

3. Monotonicity assumption of the mechanical equation of state We postulate the following monotonicity condition on the internal energy $U(p, V)$:

$$\boxed{\left(\frac{\partial U}{\partial p}\right)_V > 0, \quad \left(\frac{\partial U}{\partial V}\right)_p > 0, \quad \text{for all } p > 0 \ \& \ V > 0.} \tag{1.2}$$

This assumption reflects physically reasonable behavior: increasing pressure or volume typically leads to an increase in internal energy. It ensures that $U(p, V)$ is well-behaved and invertible ($p = p(U, V)$). In other words, it allows us to use U to parameterize adiabatic state curves in the p-V plane.

1.1.3 Characterizing Adiabatic Processes

In this subsection, we aim to characterize adiabatic processes by the level sets of the *entropy function* on the P-V plane.

Infinitesimal Work along an adiabatic process Let us consider a gas cylinder containing a unit mass of gases. The cylinder has a piston on one end, allowing its volume to change by pushing or pulling the piston. The cylinder's wall is assumed to be thermally isolated, enabling the piston to move through an adiabatic process with no energy exchange between the gases inside the cylinder and its environment except for the work done by the piston.

For an infinitesimal pushing of the piston, the work done by the piston to the system is $dW = -p\,dV$. Here, the volume change is $-dV = -dx \cdot A$, where A is the area of the cross-section of the cylinder. The term pA represents the force F exerted on the piston per unit area A by the gas particles, and $-Fdx$ is the work done by the piston on the gas particles in the cylinder. The first law of thermodynamics gives

$$dU = -p\,dV \tag{1.3}$$

along an adiabatic process.

Existence of the entropy function We will now demonstrate that the relationship $U = U(p, V)$ and equation (1.3) lead to the existence of a function called *entropy*, denoted by σ. This entropy is another thermodynamic parameter that characterizes various adiabatic processes. In other words, the level sets of σ represent adiabatic processes. This derivation, attributed to Carathéodory, establishes the mathematical foundation of thermodynamics. * Here are the steps for the existence of an entropy function σ:

1. Let us plug $U = U(p, V)$ into (1.3) to get

   $$U_p dp + (U_V + p)dV = 0.$$

   This is called a *Pfaffian equation*. It is equivalent to the ODE:

   $$\frac{dp}{dV} = -\frac{U_V(p, V) + p}{U_p(p, V)}. \tag{1.4}$$

   Note that from (1.2), the right-hand side of (1.4) is always less than 0 in the region $(p > 0, V > 0)$. Thus, (1.4) is always solvable in this region.

2. A curve in the p-V plane is called an integral curve of (1.3) (or (1.4)) if it satisfies (1.3). A function $\sigma(p, V)$ is called an integral of (1.3) if its level set (i.e. $\sigma(p, V) =$ constant) is an integral curve of (1.4), that is:

   $$d\sigma = 0 \quad \Leftrightarrow \quad dU + pdV = 0. \tag{1.5}$$

   The solutions of (1.4) form a one-parameter family of curves: $\sigma(p, V) = C$, where C is the parameter. Each curve $\sigma(p, V) = C$ represents a specific adiabatic process. An integral of (1.3) is termed an *entropy function* of the system.

3. From (1.5), there exists a function $\mu(p, V) \neq 0$ (referred to as the integration factor) such that

   $$d\sigma = \sigma_p dp + \sigma_V dV = \mu \cdot (dU + pdV). \tag{1.6}$$

   We shall choose $\mu > 0$ so that entropy increases with energy. This gives $\sigma_p > 0$ and $\sigma_V > 0$ in the region $(p > 0, V > 0)$.

*See Pogliani and Berberan-Santos (2000).

4. The solutions of μ and σ are not unique. In fact, suppose σ is a solution, we can easily construct a new integration factor $\bar{\mu} := \nu(\sigma)\mu$, where $\nu(\sigma)$ is an arbitrary chosen function. In fact, by multiplying (1.6) by $\nu(\sigma)$:

$$\nu(\sigma)d\sigma = \nu(\sigma)\mu \cdot (dU + pdV),$$

we see that $\bar{\sigma}$ with $d\bar{\sigma} = \nu(\sigma)d\sigma$ is a new entropy function.

Characterizing heat

1. **Entropy Function Discovery:** From the preceding paragraph, we have

$$dU = \frac{1}{\mu}d\sigma - pdV.$$

This suggests that (σ, V) is a natural independent variable for the internal energy. For this purpose, we make a change of variable:

$$(p, V) \mapsto (\sigma, V)$$

using the formula

$$\sigma = \sigma(p, V).$$

This inversion $p = p(\sigma, V)$ is always possible in the region $(p > 0, V > 0)$ because $\sigma_p > 0$ there. Using (σ, V) as the new state variables, we express equation (1.6) as:

$$dU = \tau d\sigma - pdV, \tag{1.7}$$

where $\tau = 1/\mu = U_\sigma$.

2. **Interpretation of Formula (1.7):** This formula has a meaningful interpretation: When $d\sigma = 0$ (i.e., adiabatic process), the change in internal energy is attributed to the work exerted from outside, represented by $-pdV$. When $dV = 0$ (i.e., no exerted work), the change in U is due to $\tau d\sigma$, denoting the heat added from outside to the system.

3. **Uniqueness of Integration Factor and Entropy Function:** As previously mentioned, the integration factor $1/\tau$ and the integral (entropy function) σ lack uniqueness. Later on, we will introduce the concepts of intensive variables and extensive variables. By selecting τ as an intensive variable (termed the absolute temperature), the corresponding σ becomes the physical entropy S.

1.1.4 Heat, Entropy and Temperature

Intensive and extensive variables There are two kinds of thermodynamic state variables, the intensive and extensive variables. A variable is considered intensive if it is independent of the system's size. In other words, for the combined system of two subsystems I and II, an intensive variable x remains unchanged ($x_{I+II} = x_I = x_{II}$), while an extensive variable x adds up ($x_{I+II} = x_I + x_{II}$). Examples of extensive variables include volume (V) and internal energy (U), while temperature (T) and pressure (p) are intensive. Notably, if x and y are extensive variables, then $\partial y/\partial x$ is intensive.

In the first law of thermodynamics

$$dU = \tau d\sigma - pdV$$

U, V are extensive, while p is intensive. Choosing τ to be intensive makes σ extensive. A natural choice of τ is the temperature, the corresponding σ becomes the entropy. The temperature is further characterized below.

Equilibrium and empirical temperature

- **Thermo equilibrium** When two systems $\mathcal{S}_1$ and $\mathcal{S}_2$ are in contact, allowing energy transfer but not with the outside, they reach a steady state on the macroscopic scale, signifying thermo equilibrium ($\mathcal{S}_1 \sim \mathcal{S}_2$).

- **The zeroth law of thermodynamics:**

  $$\text{If } \mathcal{S}_1 \sim \mathcal{S}_2 \text{ and } \mathcal{S}_2 \sim \mathcal{S}_3, \text{ then } \mathcal{S}_1 \sim \mathcal{S}_3.$$

  This law establishes an equivalence relation among all states, represented by the temperature.

- **Ideal gas thermometer** The ideal gas is postulated to satisfy $pV = constant$ in an equilibrium equivalent class. The temperature label for this class is

  $$\theta = pV/R,$$

  where R is the gas constant.

- **Heat bed and empirical temperature** By merging a small system $\mathcal{S}$ into a heat bed filled with ideal gases, we measure its temperature. The empirical temperature of the heat bed represents the temperature of $\mathcal{S}$. Thus, each state of $\mathcal{S}(p, V)$ is associated with an empirical temperature $\theta(p, V)$.

Caloric equation of state

- **Existence Postulate** The zeroth law of thermodynamics can be postulated by the *existence of a state function $\theta(p, V)$, characterizing thermo equilibrium states.* characterizing thermo equilibrium states. Two states (p_1, V_1) and (p_2, V_2) are in thermo equilibrium if $\theta(p_1, V_1) = \theta(p_2, V_2)$.

- **Monotonicity assumption:** The state function $\theta(p, V)$ is postulated to be strictly increasing in both arguments:

  $$\frac{\partial \theta}{\partial p} > 0, \quad \frac{\partial \theta}{\partial V} > 0, \quad \text{for all } p > 0 \ \& \ V > 0. \tag{1.8}$$

  The monotonicity condition on $\theta(p, V)$ ensures that empirical temperature increases with pressure and volume across the physically relevant state space. This reflects the fact that, in a simple compressible system, increasing pressure at fixed volume or expanding volume at fixed pressure typically requires adding energy to the system, thus raising its temperature. Monotonicity guarantees that θ behaves like a well-posed thermometer: it assigns increasing values to physically "hotter" states and supports a consistent foliation of state space by isotherms.

Absolute temperature T and the entropy S Let us revisit the solution of the Pfaffin equation (1.3). Let σ be one of its solution and $1/\tau$ be the corresponding integration factor. We relate τ and the empirical temperature θ by the following steps.

1. We divide the system $\mathcal{S}$ into two subsystems $\mathcal{S}_1$ and $\mathcal{S}_2$, which are in thermodynamic equilibrium with a common empirical temperature θ.

2. We shall use (σ, θ) as our new state variables instead of (σ, V). It can be verified that $\theta = \theta(\sigma, V)$ satisfies $\left(\frac{\partial\theta}{\partial V}\right)_\sigma \neq 0$, allowing us to invert θ and V in the formula $\theta = \theta(\sigma, V)$.

3. At thermodynamic equilibrium, $\mathcal{S} = (\sigma, \theta)$, $\mathcal{S}_1 = (\sigma_1, \theta)$, $\mathcal{S}_2 = (\sigma_2, \theta)$, and by adding heat to $\mathcal{S}$ without doing work, equation (1.7) gives:

$$\tau(\theta, \sigma)d\sigma = \tau_1(\theta, \sigma_1)d\sigma_1 + \tau_2(\theta, \sigma_2)d\sigma_2. \tag{1.9}$$

   This implies that the entropy function σ of the combined system $\mathcal{S}$, originally a function of $(\theta, \sigma_1, \sigma_2)$, is independent of θ.

4. Therefore, $\sigma = \sigma(\sigma_1, \sigma_2)$ and

$$\begin{aligned}\frac{\tau_1(\theta, \sigma_1)}{\tau(\theta, \sigma)} &= \left(\frac{\partial\sigma}{\partial\sigma_1}\right)_{\sigma_2} = \phi(\sigma_1, \sigma_2),\\ \frac{\tau_2(\theta, \sigma_2)}{\tau(\theta, \sigma)} &= \left(\frac{\partial\sigma}{\partial\sigma_2}\right)_{\sigma_1} = \psi(\sigma_1, \sigma_2),\end{aligned}$$

   are independent of θ.

5. This implies the existence of functions $T(\theta)$, $\nu_1(\sigma_1)$, $\nu_2(\sigma_2)$, $\nu(\sigma)$ such that

$$\begin{aligned}\tau_1(\theta, \sigma_1) &= T(\theta)\nu_1(\sigma_1),\\ \tau_2(\theta, \sigma_2) &= T(\theta)\nu_2(\sigma_2),\\ \tau(\theta, \sigma) &= T(\theta)\nu(\sigma).\end{aligned}$$

   Equation (1.9) becomes

$$T\nu(\sigma)d\sigma = T\nu_1(\sigma_1)d\sigma_1 + T\nu_2(\sigma_2)d\sigma_2. \tag{1.10}$$

6. If we define

$$S_i(\sigma_i) := \int^{\sigma_i} \nu_i(\sigma_i)\, d\sigma_i, \quad , i = 1, 2,$$

   then (1.10) implies

$$dS = dS_1 + dS_2. \tag{1.11}$$

7. The function $T(\theta)$ defined above is called the *absolute temperature* of the system. Note that $T \neq 0$. So, we choose

$$T > 0.$$

Choosing the integration factor $\mu := 1/T$ implies that the corresponding entropy function has the property (1.11). If $\mathcal{S}$ is divided into m subsystems, then

$$dS = \sum_{i=1}^{m} dS_i.$$

Since S can be determined uniquely up to an integration constant, we can choose S so that

$$S = \sum_{i=1}^{m} S_i. \tag{1.12}$$

Measuring system's entropy On the thermodynamic p–V plane, one can draw isothermal curves (Figure 1.2). Along an isothermal curve, the line integral

$$S_2 - S_1 = \int_{S_1}^{S_2} \frac{dQ}{T}$$

gives the entropy difference between two states. This provides a practical method to assign or measure the entropy of a thermodynamic state (p, V), once a reference entropy is chosen.

Gibbs relation: The first law of thermodynamics now reads

$$\boxed{dU = TdS - pdV.} \tag{1.13}$$

The term dU represents the change in the internal energy of the system, the first term on the right TdS is the heat added to the system, and the second term $-pdV$ is the mechanical work done on the system by the surroundings. Formula (1.13) is called the *Gibbs relation*.

Constitutive Law Using (S, V) as the independent variable, the internal energy can be expressed as

$$\boxed{U = U(S, V).} \tag{1.14}$$

This is called the constitutive law of the gas system. The temperature T and the pressure p are derived parameters:

$$T = \left(\frac{\partial U}{\partial S}\right)_V, \quad p = -\left(\frac{\partial U}{\partial V}\right)_S.$$

Summary: Complete characterization of the gas thermodynamic system The thermodynamics of a gas system is completely characterized by the constitutive relation

$$U = U(S, V).$$

The first law of thermodynamics

$$dU = TdS - pdV,$$

leads to

$$T = \left(\frac{\partial U}{\partial S}\right)_V, \quad p = -\left(\frac{\partial U}{\partial V}\right)_S.$$

Conversely, one can use the first law of thermodynamics together with two equations of states:

- mechanical equation of state: $U = U(p, V)$,
- caloric equation of state: $T = \theta(p, V)$,

to obtain the constitutive law $U = U(S, V)$.

1.1.5 Ideal Gases and Polytropic Gases

In a gas thermodynamic system, we deal with five thermodynamic variables (V, p, S, T, U), with only two of them being independent. The first law of thermodynamics (**??**), and two equations of states: kinetic and caloric, govern these variables, deriving from either measurements or statistical mechanics. Here, we illustrate a specific examples of a gas thermodynamic system, known as the ideal gases and the polytropic gases Courant and Friedrichs (1948).

Ideal gas law

- **Mechanical equation of state - Ideal gas law:** The ideal gas law, representing Boyle's and Gay-Lussac's laws, is given by:
$$pV = RT, \tag{1.15}$$
where R is the universal gas constant (approximately $8.314462618\ \mathrm{J} \cdot \mathrm{K}^{-1} \cdot \mathrm{mol}^{-1}$), see Gas Constant, Wiki. Under a mild assumption (stated below), the ideal gas law and the Gibbs relation imply that U is solely a function of T.
- **Theorem:** *Under a mild assumption (1.17) below, the ideal gas law and the Gibbs relation imply that U is only a function of T.* [†]
Derivation:

  1. From the first law of thermodynamics (1.13), treating (S, V) as the independent variables, we obtain:
$$p = -\left(\frac{\partial U}{\partial V}\right)_S \quad \text{and} \quad T = \left(\frac{\partial U}{\partial S}\right)_V.$$
Plugging these into the ideal gas law (1.15), we get a partial differential equation (PDE) for U in (S, V):
$$R\frac{\partial U}{\partial S} + V\frac{\partial U}{\partial V} = 0.$$
This linear first-order equation can be solved by the method of characteristics as shown below.
  2. Let us rewrite this equation as a directional differentiation:
$$\left(R\frac{\partial}{\partial S} + V\frac{\partial}{\partial V}\right) U = 0. \tag{1.16}$$
It means that U is unchanged along the direction: $(dS, dV) \parallel (R, V)$. The integral curves of these directions are the solutions of the differential equation
$$\frac{dV}{dS} = \frac{V}{R}.$$

[†]This derivation is referred to in Courant-Friedrichs' Courant and Friedrichs (1948) and Callen's Callen (1985) books.

They are called the characteristic curves. This equation can be integrated as

$$\frac{dV}{V} - \frac{dS}{R} = 0 \quad \Rightarrow \quad \ln V - \frac{S}{R} = C \quad \Rightarrow \quad V\exp(-S/R) = e^C.$$

Here, C is an integration constant. Thus, (1.16) implies that $U(V,S)$ is constant whenever $\phi := V\exp(-S/R)$ is a constant. This means that U and ϕ are functionally dependent, which implies that there exists a function $h : \mathbb{R}^+ \to \mathbb{R}$ such that

$$U = h(\phi).$$

3. We claim that U is a function of T only. This can be derived by the following arguments. First, we note that $h' < 0$ because

$$p = -(\frac{\partial U}{\partial V})_S = -\exp(-S/R)h'(V\exp(-S/R)) > 0.$$

Next, from

$$T = (\frac{\partial U}{\partial S})_V = h'(\phi)\left(\frac{\partial \phi}{\partial S}\right)_V = h'(\phi)\left(-\frac{V}{R}e^{-S/R}\right) = -\frac{1}{R}h'(\phi)\cdot\phi,$$

we see that T is a function of ϕ.

4. We shall make an assumption that this function is invertible. That is, the derivative

$$\big(h'(\phi)\phi\big)' > 0 \text{ for } \phi > 0. \tag{1.17}$$

We get that T is a decreasing function of ϕ. With this, we can invert the relation between T and ϕ and treat ϕ as a decreasing function of T. By inverting U and ϕ, and T and ϕ, we get that U is an increasing function of T:

$$\boxed{U = U(T).}$$

We shall make this our second constitutive relation.

The heat capacities

- **Specific heat capacities** Let us denote by $dQ = TdS$ the heat added to the system. From Gibbs' relation, $dQ = dU + pdV$. Using $RT = pV$, we have

$$\begin{aligned} dQ &= dU + pdV \\ &= U'(T)dT + pdV \\ &= U'(T)dT + RdT - Vdp. \end{aligned}$$

The first and the third equalities lead to the following derived quantities:

$$\begin{aligned} c_v &:= \left(\frac{\partial Q}{\partial T}\right)_V = U'(T), \\ c_p &:= \left(\frac{\partial Q}{\partial T}\right)_p = U'(T) + R, \end{aligned}$$

called the *specific heat capacities at constant volume and constant pressure*, respectively. The expressions for c_v and c_p follow classical thermodynamic derivations (see Callen Callen (1985), FermiFermi (1956)). Since $R > 0$, we have $c_p > c_v$. Recall that c_p is the amount of heat added to a system per unit mass at constant pressure. When we heat the system at constant pressure, the volume has to expand to maintain constant pressure, the extra amount of work for expansion is supplied by the extra amount of heat, which is R per unit mass.

- **Heat capacity ratio** $\gamma := c_p/c_v$

  1. Let γ be the ratio between c_p and c_v:

  $$\gamma = \frac{c_p}{c_v} = \frac{c_v + R}{c_v}.$$

  This heat capacity ratio is also called the adiabatic index. It plays a central role in adiabatic processes Kittel and Kroemer (1980).

  2. For a monatomic gas molecule (like helium or argon), there are three translational degrees of freedom. Every atom has an average kinetic energy of $\frac{3}{2}k_BT$ in thermal equilibrium, where k_B is the Boltzmann constant. For 1 mole of gas, this becomes $U = \frac{3}{2}RT$. Thus, $c_v = U'(T) = \frac{3}{2}R$. Note that the number 3 comes from the three translational degrees of freedom. Each degree of freedom contribute $RT/2$ amount of energy.

  3. For ideal gas with f degrees of freedom, $U = \frac{f}{2}RT$, and the corresponding

  $$c_v = \frac{f}{2}R.$$

  This is a consequence of the equipartition theorem [wiki] in statistical mechanics. For a diatomic molecule (like oxygen or nitrogen), in addition to translational motion (in $\mathbb{R}^3$), there are two rotational degrees of freedom (in S^2). This totals to $f = 5$ degrees of freedom.

  4. Thus, we have

  $$\gamma = \frac{c_v + R}{c_v} = \frac{f+2}{f}, \quad 1 < \gamma \leq \frac{5}{3} \tag{1.18}$$

  for ideal gases. When γ is closer to $5/3$, the gas is harder to compress because all work input is reacted by the translation of the mono-atoms. On the other hand, when γ is closer to 1, the gas is easily compressed as the input energy is transferred to other modes of molecular energies. For further discussion about γ, we refer to [wiki: Heat Capacity Ratio].

Polytropic gases

- **Caloric equation of state:** If $U(T) = c_vT$, the energy we add to the system is proportional to the temperature, we call such gases the *polytropic gases.* The ratio c_v is called the specific heat capacity at constant volume.

- **Algebraic relations of the polytropic gases**

1. We have five thermodynamic variables p, V, U, S, T, and three relations:

$$\begin{cases} pV &= RT \\ U &= c_v T \\ dU &= TdS - pdV \end{cases}.$$

2. Plugging the two constitutive relations

$$pV = RT \text{ and } U = c_v T \tag{1.19}$$

into the first law of thermodynamics (1.13), we obtain

$$\begin{aligned} dU &= TdS - pdV \\ \frac{c_v}{R} d(pV) &= \frac{pV}{R} dS - pdV \\ c_v \frac{d(pV)}{pV} &= dS - R\frac{dV}{V} \\ dS &= d\ln\left((pV)^{c_v}\right) + d\ln\left(V^R\right) \\ &= d\ln\left(p^{c_v} \cdot V^{c_v+R}\right) \\ S - S_0 &= \ln\left(p^{c_v} \cdot V^{c_v+R}\right) \\ e^{S-S_0} &= \left(pV^{(c_v+R)/c_v}\right)^{c_v} \\ e^{(S-S_0)/c_v} &= p\, V^{(c_v+R)/c_v}. \end{aligned}$$

3. Define

$$\gamma := 1 + R/c_v, \quad A(S) := \exp((S - S_0)/c_v),$$

then, the algebraic relations of the thermodynamic variables in terms of (S, V) are

$$\begin{cases} p = A(S)V^{-\gamma} \\ T = \frac{A(S)}{R} V^{-\gamma+1} \\ U = \frac{c_v A(S)}{R} V^{-\gamma+1}. \end{cases} \tag{1.20}$$

Summary of algebraic relations of state variables for polytropic gases For ideal gases, these two equations of states are the ideal gas law: $pV = RT$ and $U = c_v T$. The algebraic relations of the state variables are listed below.

- In terms of (ρ, U):

$$p = (\gamma - 1)\rho U, \quad T = \frac{\gamma - 1}{R} U,$$

$$S - S_0 = \frac{R}{\gamma - 1} \ln\left(U\rho^{-\gamma+1}\right).$$

- In terms of (V, S):

$$U = (\gamma - 1)^{-1} A(S) V^{-\gamma+1}, \quad A(S) = \exp\left(\frac{\gamma - 1}{R}(S - S_0)\right),$$

$$p = A(S)V^{-\gamma}, \quad T = \frac{1}{R} A(S) V^{-\gamma+1}.$$

- In terms of (ρ, p):

$$U = \frac{1}{\gamma - 1} p\rho^{-1}, \quad T = \frac{1}{R} p\rho^{-1},$$
$$S - S_0 = \frac{R}{\gamma - 1} \ln\left(\frac{1}{\gamma - 1} p\rho^{-\gamma}\right).$$

See also the summary expressions of polytropic gases in [Fermi, Wikipedia].

Homeworks

1. Prove that adiabats (lines of constant entropy) have a steeper slope than isotherms (lines of constant temperature) for an ideal gas on a p-V diagram, where the pressure p is the ordinate and the volume per unit mass V the abscissa. Again, carefully draw a diagram of a Carnot cycle, and compute the slopes of the isotherms and adiabats in terms of p and V.
2. Write a short report on Carnot cycle for an ideal gas.

1.2 Thermodynamic Potentials and Legendre Transform

1.2.1 Enthalpy, Helmholtz, Gibbs Free Energies

In the Gibbs relation

$$dU = TdS - p\,dV,$$

the system's energy U can be varied by changing the volume at constant entropy, or by adding heat at constant volume. The relative changes give

$$-p = \left(\frac{\partial U}{\partial V}\right)_S \quad \text{and} \quad T = \left(\frac{\partial U}{\partial S}\right)_V,$$

respectively. We say that (S, V) are the natural independent variables for U.

While the internal energy $U(S, V)$ provides a complete thermodynamic description of the system, in practice, we often control or observe different variables than (S, V). For example, in many experimental or engineering setups, pressure p is easier to control or measure than volume V, while entropy S remains an inaccessible variable. Therefore, it is convenient to reformulate the energy description using new independent variables better aligned with the physical constraints of the system.

Enthalpy We choose (S, p) as the independent variables. This suggests the following change of variable:

$$(S, V) \mapsto (S, p) \text{ through } p = -\left(\frac{\partial U(S, V)}{\partial V}\right)_S.$$

By adding $d(PV)$ in the Gibbs relation:

$$dU + d(pV) = TdS - pdV + d(pV) = TdS + V\,dp,$$

the natural independent variables become (S, p). The corresponding potential energy, $h(S, p) := U + pV$, is termed the *enthalpy*. Enthalpy comprises a system's internal energy and the work required to create the system by displacing its environment, establishing its volume and pressure. It is especially useful in processes that occur at constant pressure, such as chemical reactions and atmospheric thermodynamics.

Helmholtz Free Energy Using the change-of-variable formula:

$$(S, V) \mapsto (T, V) \text{ through } T = \left(\frac{\partial U}{\partial S}\right)_T,$$

and noting

$$dU - d(TS) = TdS - pdV - TdS - SdT = -SdT - pdV,$$

we define the Helmholtz free energy $\Psi(T, V) := U - TS$, and get

$$d\Psi = -SdT - pdV.$$

The term TS represents the portion of the internal energy U that is unavailable for doing mechanical work at temperature T. It accounts for the energy associated with the system's entropy S, which reflects the level of thermal disorder or microscopic irreversibility. Thus, the Helmholtz free energy $\Psi = U - TS$ quantifies the maximum useful work that can be extracted from a system at constant temperature and volume. It is particularly useful for systems in contact with a thermal reservoir where temperature is controlled, such as in physical, chemical, or statistical mechanical models.

Gibbs Free Energy: We consider the change-of-variable:

$$(S, V) \mapsto (T, p)$$

through both

$$-p = \left(\frac{\partial U}{\partial V}\right)_S \text{ and } T = \left(\frac{\partial U}{\partial S}\right)_T$$

Define the Gibbs free energy

$$G(T, p) := U + pV - TS.$$

We have

$$dG = TdS - pdV + d(pV) - d(TS) = -SdT + Vdp.$$

In the Gibbs free energy $G(T, p) = U + pV - TS$, the term TS represents the thermal energy associated with the system's entropy S at temperature T. This energy is not available to do useful work because it reflects the microscopic disorder inherent in the system. Subtracting TS from the total enthalpy $U + pV$ yields the Gibbs free energy G, which measures the maximum amount of non-expansion work a system can perform at constant temperature and pressure. This makes G the most important thermodynamic potential in chemical thermodynamics, where reactions typically occur at constant pressure and temperature. A decrease in G indicates a spontaneous process.

The Gibbs free energy $G(T, p) := U + pV - TS$, as we have mentioned, represents the maximum amount of non-expansion work a system can perform at constant temperature and pressure. It subtracts the energy unavailable due to entropy (TS) and includes the work needed to maintain pressure (pV).

In isothermal and isobaric processes, G is minimized at equilibrium. This makes it the most important thermodynamic potential in chemical thermodynamics, where reactions typically occur at constant pressure and temperature. A decrease in G indicates a spontaneous process.

Potential	Definition	Natural Variables	Physical Meaning
U	$U(S,V)$	S,V	Internal energy of the system
h	$U+pV$	S,p	Total energy for isobaric processes
Ψ	$U-TS$	T,V	Maximum useful work at constant T, V
G	$U+pV-TS$	T,p	Maximum non-expansion work at const T, p

Table 1.1: Comparison of Thermodynamic Potentials

Summary of thermodynamic potentials

- **Comparison**
- **First Law of Thermodynamics:**

$$\begin{aligned} dU &= TdS - pdV \\ dh &= TdS + Vdp \\ d\Psi &= -SdT - pdV \\ dG &= -SdT + Vdp \end{aligned}$$

- **Process's names with Fixed Thermo Variables:**

Adiabatic: $dS=0$, Isochoric: $dV=0$,
Isothermal: $dT=0$, Isobaric: $dp=0$.

1.2.2 Maxwell Relations

Thermo relations The thermo relations are expressed in terms of two independent thermo variables.

- Using (S,V) as independent variables:

$$T=\left(\frac{\partial U}{\partial S}\right)_V, \quad -p=\left(\frac{\partial U}{\partial V}\right)_S,$$

- Using (S,p) as independent variables:

$$T=\left(\frac{\partial h}{\partial S}\right)_p, \quad V=\left(\frac{\partial h}{\partial p}\right)_S,$$

- Using (T,V) as independent variables:

$$-S=\left(\frac{\partial \Psi}{\partial T}\right)_V, \quad -p=\left(\frac{\partial \Psi}{\partial V}\right)_T$$

- Using (T,p) as independent variables:

$$-S=\left(\frac{\partial G}{\partial T}\right)_p, \quad V=\left(\frac{\partial G}{\partial p}\right)_T$$

Maxwell relations From

$$\frac{\partial^2 U}{\partial V \partial S} = \frac{\partial^2 U}{\partial S \partial V}, \quad T = \left(\frac{\partial U}{\partial S}\right)_V, \quad -p = \left(\frac{\partial U}{\partial V}\right)_S,$$

we get

$$\left(\frac{\partial T}{\partial V}\right)_S = -\left(\frac{\partial p}{\partial S}\right)_V.$$

In general, we have the following Maxwell relations:

$$\left(\frac{\partial T}{\partial V}\right)_S = -\left(\frac{\partial p}{\partial S}\right)_V = \frac{\partial^2 U}{\partial S \partial V} \tag{1.21}$$

$$\left(\frac{\partial T}{\partial p}\right)_S = \left(\frac{\partial V}{\partial S}\right)_p = \frac{\partial^2 h}{\partial S \partial p} \tag{1.22}$$

$$\left(\frac{\partial S}{\partial V}\right)_T = \left(\frac{\partial p}{\partial T}\right)_V = -\frac{\partial^2 \Psi}{\partial T \partial V} \tag{1.23}$$

$$-\left(\frac{\partial S}{\partial p}\right)_T = \left(\frac{\partial V}{\partial T}\right)_p = \frac{\partial^2 G}{\partial T \partial p}. \tag{1.24}$$

1.2.3 Legendre Transformation

The transformations from U to h, Ψ, and G are called Legendre transformations. Let us introduce this mathematical concept.

Legendre transform for convex functions

- Let $f : \mathbb{R}^n \to \mathbb{R}$ be a convex function. If $f \in C^2$, then the (strong) convexity of f is equivalent to the Hessian of f being positive semi-definite (i.e. $H_f(x) \succeq 0$ for all x). [Convex function (Wiki)].

- We are interested in the differential $df(x) = \nabla_x f(x) \cdot dx$. Let us introduce a new variable $y = \nabla_x f(x)(x)$ and express

  $$df = y \cdot dx.$$

  We consider the change-of-variable:

  $$x \mapsto y = \nabla_x f(x) \tag{1.25}$$

  This mapping is invertible because the convexity of f leading to $\nabla_x f(x)$ being a monotonic function. Now we define

  $$f^*(y) := x \cdot y - f(x).$$

  Here, x is treated as a function of y through (1.25). Then we have

  $$df^*(y) = d(x \cdot y) - \nabla_x f(x) \cdot dx = d(x \cdot y) - y \cdot dx = x \cdot dy.$$

  From this formula, we get

  $$x = \nabla_y f^*(y). \tag{1.26}$$

- When f is a convex function, there is another equivalent expression for $f^*(y)$:

$$f^*(y) := \sup_x [x \cdot y - f(x)].$$

  The maximum occurs at $y = \nabla_x f(x)$. This formula also shows that f^* is a convex function.

- The transform: $f \to f^*$ is called the Legendre transform. The function f^* is called the conjugate function of f, or the Legendre transform of f, while the variable $y := \nabla_x f(x)$ the conjugate variable of x.

- **Lemma.** f^* is convex.

- **Lemma.** If f is convex, then $f^{**}(x) = f(x)$ [Convex function (Wiki)].

- **Lemma.** If f is convex, then the inverse of $y = \nabla_x f(x)$ is given by $x = \nabla_y f^*(y)$. Let us denote it by $x(y)$. Then $f^*(y) = x(y) \cdot y - f(x(y))$. Its gradient $\nabla_y f^*(y)$ is $x(y)$. Its Hessian of f is the inversion of the Hessian of f^*:

$$H_{f^*}(y) = [H_f(x)]^{-1} \quad \text{with } y = \nabla_x f(x).$$

- The functions $-h$, $-\Psi$ and $-G$ are the Legendre transformations of the internal energy $U(S, V)$:

$$\begin{aligned} -h(S,p) &= \sup_V [(-p)V - U(S,V)] \\ -\Psi(T,V) &= \sup_S [ST - U(S,V)] \\ -G(T,p) &= \sup_V \sup_S [(-p)V + ST - U(S,V)], \end{aligned}$$

  with respective to V, S, and (S, V), respectively. Equivalently, we can express them as

$$\begin{aligned} h(S,p) &= \inf_V [U(S,V) + pV] \\ \Psi(T,V) &= \inf_S [U(S,V) - TS] \\ G(T,p) &= \inf_{V,S} [U(S,V) + pV - TS] \end{aligned}$$

- Both (p, V) and (T, S) are conjugate pairs.

- To have a legitimate Legendre transformations, we require U to be convex in (S, V). This is the thermodynamic stability condition, which will be discussed in the next section.

Homeworks.

1. Let $f(x, y)$ be a convex function in $\mathbb{R}^2$. Let $g(z, w) := \sup_{x,y}[xz + yw - f(x, y)]$. Show that

$$\begin{bmatrix} g_{zz} & g_{zw} \\ g_{wz} & g_{ww} \end{bmatrix} = \begin{bmatrix} f_{xx} & f_{xy} \\ f_{yx} & f_{yy} \end{bmatrix}^{-1}, \quad \begin{bmatrix} z \\ w \end{bmatrix} = \begin{bmatrix} f_x(x,y) \\ f_y(x,y) \end{bmatrix}.$$

2. Let $f(x, y)$ be a convex function in $\mathbb{R}^2$. Let $h(z, y) := \sup_x [xz - f(x, y)]$. Show that

$$\begin{bmatrix} h_{zz} & h_{zy} \\ h_{zy} & h_{yy} \end{bmatrix} = \frac{1}{f_{xx}} \begin{bmatrix} 1 & -f_{xy} \\ -f_{xy} & f_{xy}^2 - f_{xx} f_{yy} \end{bmatrix}.$$

1.3 Thermodynamic Stability

1.3.1 Stability Characterized by the Potentials

Thermodynamic Stability. In physical terms, a thermodynamic system is said to be *stable* if, when subject to small perturbations, it returns to equilibrium without undergoing spontaneous changes in its macroscopic state. This means that the system resists arbitrary fluctuations in entropy, volume, or other extensive variables.

Mathematically, the condition for stability is that *the internal energy $U(S, V)$ is a convex function of its extensive variables (S, V)* (see Callen Callen (1985), Landau & Lifshitz Landau and Lifshitz (1980)). This is equivalent to requiring that the second variation of U is non-negative for all non-zero perturbations:

$$\delta^2 U = \frac{\partial^2 U}{\partial S^2}(\delta S)^2 + 2\frac{\partial^2 U}{\partial S \partial V}\delta S \delta V + \frac{\partial^2 U}{\partial V^2}(\delta V)^2 \geq 0.$$

Or, the Hessian matrix of $U(S, V)$ must be *positive semi-definite*:

$$H_U = \begin{bmatrix} \frac{\partial^2 U}{\partial S^2} & \frac{\partial^2 U}{\partial S \partial V} \\ \frac{\partial^2 U}{\partial V \partial S} & \frac{\partial^2 U}{\partial V^2} \end{bmatrix} \succeq 0.$$

In terms of the Gibbs free energy G, the stability condition states that *G is concave in the intensive variables (T, p)* (see Callen Callen (1985), Reichl Reichl (2016)). Equivalently, the Hessian matrix of G is negative semi-definite:

$$H_G \preceq 0.$$

Strong Thermodynamical Stability If U is *strictly convex*, we call the system is *strongly thermodynamically stable*. This is equivalent to $H_U \succ 0$.

Sylvester's criterion Let $\mathbf{A} = \begin{bmatrix} A & B \\ B & C \end{bmatrix}$ be a symmetric matrix, $\Delta = \det \mathbf{A}$. We have

- $\mathbf{A} \succ 0 \quad \Leftrightarrow \quad (A > 0 \text{ and } \Delta > 0)$.
- $\mathbf{A} \succeq 0 \quad \Leftrightarrow \quad (A \geq 0 \ \& \ C \geq 0 \ \& \ \Delta \geq 0)$.

Homeworks.

1. For the above matrix $\mathbf{A}$, show that it is negative semi-definite if and only if $(A \leq 0 \ \& \ C \leq 0 \ \& \ \Delta \leq 0)$.

1.3.2 Stability Characterized by the Thermodynamic Response Functions

Material properties can be characterized by their response to external probes, such as heat input, pressure variation, or thermal expansion. For instance, we can measure how much heat to add to the system in order to increase its temperature by one degree. This is the heat capacity (dQ/dT). We can measure the volume change under increase of pressure. This is the (negative) compressibility $(-\frac{1}{V}\frac{dV}{dp})$. We can measure volume change under increase of temperature (dV/dT). This is the expansion rate.

Heat capacity Let us define $dQ = TdS$, the heat added to the system. Define heat capacity to be the heat added to the system per unit temperature, with either V or p fixed. That is,

$$c_v := \left(\frac{dQ}{dT}\right)_V = T\left(\frac{\partial S}{\partial T}\right)_V = -T\left(\frac{\partial^2 \Psi}{\partial T^2}\right)_V, \tag{1.27}$$

$$c_p := \left(\frac{dQ}{dT}\right)_p = T\left(\frac{\partial S}{\partial T}\right)_p = -T\left(\frac{\partial^2 G}{\partial T^2}\right)_p. \tag{1.28}$$

Compression rate The isentropic/isothermal compressibility rate are defined as

$$\kappa_S := -\frac{1}{V}\left(\frac{\partial V}{\partial p}\right)_S = -\frac{1}{V}\left(\frac{\partial^2 H}{\partial p^2}\right)_S, \tag{1.29}$$

$$\kappa_T := -\frac{1}{V}\left(\frac{\partial V}{\partial p}\right)_T = -\frac{1}{V}\left(\frac{\partial^2 G}{\partial p^2}\right)_T. \tag{1.30}$$

Expansion rate: The expansion rate is defined as

$$\alpha := \frac{1}{V}\left(\frac{\partial V}{\partial T}\right)_p = \frac{1}{V}\left(\frac{\partial}{\partial T}\right)_p \left(\frac{\partial G}{\partial p}\right)_T.$$

Remark. These quantities are commonly referred to as thermodynamic response functions Callen (1985); Greiner et al. (1995). They are functions of (S, V).

Proposition 1.1. *Assuming the Hessian of U is nonzero at (S_0, V_0). Then in a small neighborhood of (S_0, V_0), we have*

$$\kappa_T(c_p - c_v) = TV\alpha^2 \tag{1.31}$$

$$c_p(\kappa_T - \kappa_S) = TV\alpha^2, \tag{1.32}$$

and

$$\frac{c_p}{c_v} = \frac{\kappa_T}{\kappa_S}.$$

Thus, there are five parameters with two independent relations. Further,

$$c_p \geq c_V, \quad \kappa_T \geq \kappa_S.$$

Remarks.

- The inequality $c_p > c_V$ reflects the fact that, under constant pressure, a system does additional expansion work as it absorbs heat, requiring more energy than at constant volume. Similarly, $\kappa_T > \kappa_S$ expresses that a system is more compressible when heat exchange is allowed (isothermal) than when entropy is held fixed (adiabatic), since thermal fluctuations assist compression under constant temperature.
- For gases, the ratio $\gamma = \frac{c_p}{c_V} = \frac{\kappa_T}{\kappa_S}$ is known as the adiabatic index or heat capacity ratio. It quantifies how easily a gas responds to adiabatic compression compared to isothermal compression, and determines the relation between pressure and volume in adiabatic processes: $pV^\gamma = \text{const}$. The value of γ influences wave speeds and shock behavior in compressible flows and appears in the formula for the speed of sound: $c = \sqrt{\gamma p/\rho}$.

Proof. 1. Let us consider the Legendre transform of $U(S,V)$ to $-G(T,p)$ through

$$\begin{pmatrix} S \\ V \end{pmatrix} \mapsto \begin{pmatrix} T \\ p \end{pmatrix} = \begin{pmatrix} U_S(S,V) \\ -U_V(S,V) \end{pmatrix}.$$

When the Hessian of U is nonzero, by the inverse function theorem, the above mapping has an inverse locally. Let us denote the inverse of this mapping by $(S(T,p), V(T,p))$.

2. Differentiate $S(T, V(T,p))$ in T with fixed p:

$$\left(\frac{\partial S}{\partial T}\right)_p = \left(\frac{\partial S}{\partial T}\right)_V + \left(\frac{\partial S}{\partial V}\right)_T \left(\frac{\partial V}{\partial T}\right)_p,$$

then multiply it by T, we get

$$c_p = c_v + T\left(\frac{\partial S}{\partial V}\right)_T \left(\frac{\partial V}{\partial T}\right)_p.$$

Multiply this by $\kappa_T = -\frac{1}{V}\left(\frac{\partial V}{\partial p}\right)_T$, we get

$$\begin{aligned}
\kappa_T(c_p - c_v) &= -\frac{T}{V}\left(\frac{\partial V}{\partial p}\right)_T \left(\frac{\partial S}{\partial V}\right)_T \left(\frac{\partial V}{\partial T}\right)_p \\
&= -\frac{T}{V}\left(\frac{\partial S}{\partial p}\right)_T \left(\frac{\partial V}{\partial T}\right)_p && \because \text{chain rule} \\
&= +\frac{T}{V}\left(\frac{\partial V}{\partial T}\right)_p \left(\frac{\partial V}{\partial T}\right)_p && \because (1.24) \\
&= TV\left(\frac{1}{V}\left(\frac{\partial V}{\partial T}\right)_p\right)^2 \\
&= TV\alpha^2
\end{aligned}$$

3. Differentiate $V(S(T,p),p)$ in p with fixed T:

$$\left(\frac{\partial V}{\partial p}\right)_T = \left(\frac{\partial V}{\partial p}\right)_S + \left(\frac{\partial V}{\partial S}\right)_p \left(\frac{\partial S}{\partial p}\right)_T.$$

Multiply it by $-1/V$, we get

$$\kappa_T = \kappa_S - \frac{1}{V}\left(\frac{\partial V}{\partial S}\right)_p \left(\frac{\partial S}{\partial p}\right)_T.$$

Then multiply it by $c_p = T\left(\frac{\partial S}{\partial T}\right)_p$, we get

$$\begin{aligned}
c_p\left(\kappa_T - \kappa_S\right) &= -\frac{T}{V}\left(\frac{\partial S}{\partial T}\right)_p \left(\frac{\partial V}{\partial S}\right)_p \left(\frac{\partial S}{\partial p}\right)_T \\
&= -\frac{T}{V}\left(\frac{\partial V}{\partial T}\right)_p \left(\frac{\partial S}{\partial p}\right)_T && \because \text{chain rule}
\end{aligned}$$

$$
\begin{aligned}
&= \frac{T}{V}\left(\frac{\partial S}{\partial p}\right)_T\left(\frac{\partial S}{\partial p}\right)_T \qquad \because (1.24)\\
&= \frac{T}{V}\left(\frac{\partial V}{\partial T}\right)_p^2\\
&= TV\left(\frac{1}{V}\left(\frac{\partial V}{\partial T}\right)_p\right)^2\\
&= TV\alpha^2.
\end{aligned}
$$

□

Hessian of the potentials in terms of the response functions

- The response functions, such as $\kappa_S = \frac{1}{V}\left(\frac{\partial V}{\partial p}\right)_S$ or $c_v = T\left(\frac{\partial S}{\partial T}\right)_V$, are differentiations of V or S with respect to p or T. In order to express the Hessian of the potentials in terms of these response functions, it is easier to find H_G, because G is a function of (T, p). Its Hessian involves the derivatives of (S, V) with respect to (T, p). The Hessian H_U can be obtained from $H_U = -H_G^{-1}$.
- The Hessian of G is

$$
\begin{bmatrix} G_{TT} & G_{Tp} \\ G_{Tp} & G_{pp} \end{bmatrix} = \begin{bmatrix} -\left(\frac{\partial S}{\partial T}\right)_p & -\left(\frac{\partial S}{\partial p}\right)_T \\ \left(\frac{\partial V}{\partial T}\right)_p & \left(\frac{\partial V}{\partial p}\right)_T \end{bmatrix} = \begin{bmatrix} -\frac{c_p}{T} & \alpha V \\ \alpha V & -V\kappa_T \end{bmatrix}
$$

  Its determinant

$$
\Delta_G = \frac{V}{T}\kappa_T c_p - \alpha^2 V^2 = \frac{V}{T}c_v\kappa_T = \frac{V}{T}c_p\kappa_S.
$$

  Here, we have used (1.31).

- Hessian H_U:

$$
H_U = -H_G^{-1} = -\frac{1}{\Delta_G}\begin{bmatrix} -V\kappa_T & -\alpha V \\ -\alpha V & -\frac{c_p}{T} \end{bmatrix} = \begin{bmatrix} \frac{T}{c_V} & \frac{T\alpha}{c_V\kappa_T} \\ \frac{T\alpha}{c_V\kappa_T} & \frac{1}{V\kappa_S} \end{bmatrix}
$$

  Or we can can compute the Hessian H_U directly:

  * $\left(\frac{\partial^2 U}{\partial S^2}\right)_V = \left(\frac{\partial T}{\partial S}\right)_V = \frac{T}{T\left(\frac{\partial S}{\partial T}\right)_V} = \frac{T}{c_V}$.
  * $\left(\frac{\partial^2 U}{\partial V^2}\right)_S = -\left(\frac{\partial p}{\partial V}\right)_S = \frac{1}{V\kappa_S}$.
  * $\frac{\partial^2 U}{\partial S \partial V} = -\left(\frac{\partial p}{\partial S}\right)_V = -\left(\frac{\partial p}{\partial V}\right)_T\left(\frac{\partial V}{\partial T}\right)_p\left(\frac{\partial T}{\partial S}\right)_V = \frac{T\alpha}{c_V\kappa_T}$.

Homework Show the following expression of the Hessians of h and Ψ in terms of the response functions:

- Hessian of h:
  * $\left(\frac{\partial^2 h}{\partial S^2}\right)_p = \left(\frac{\partial T}{\partial S}\right)_p = \frac{T}{T\left(\frac{\partial S}{\partial T}\right)_p} = \frac{T}{c_p}$.

* $\left(\frac{\partial^2 h}{\partial p^2}\right)_S = \left(\frac{\partial V}{\partial p}\right)_S = -V\kappa_S.$
* $\frac{\partial^2 h}{\partial S \partial p} = \left(\frac{\partial V}{\partial S}\right)_p = \frac{\left(\frac{\partial V}{\partial T}\right)_p}{\left(\frac{\partial S}{\partial T}\right)_p} = \frac{\alpha V T}{c_p}$

- Hessian of Ψ:
  * $\left(\frac{\partial^2 \Psi}{\partial T^2}\right)_V = -\left(\frac{\partial S}{\partial T}\right)_V = -\frac{c_V}{T}$
  * $\left(\frac{\partial^2 \Psi}{\partial V^2}\right)_T = -\left(\frac{\partial p}{\partial V}\right)_T = -\frac{V}{V\left(\frac{\partial V}{\partial p}\right)_T} = \frac{1}{V\kappa_T}$
  * $\frac{\partial^2 \Psi}{\partial V \partial T} = -\left(\frac{\partial p}{\partial T}\right)_V = -\frac{\left(\frac{\partial V}{\partial T}\right)_p}{\left(\frac{\partial V}{\partial p}\right)_T} = \frac{\alpha}{\kappa_T}$

Theorem 1.2. *In the region $S > 0$, $V > 0$, $T > 0$,*

(i) the thermodynamical strong stability (i.e. U is strictly convex) $\Leftrightarrow$ $0 < c_V, \kappa_T < \infty$ or $0 < c_p, \kappa_S < \infty$;

(ii) the thermodynamical stability (i.e. U is convex) $\Leftrightarrow$ $0 \le c_V, c_p, \kappa_S, \kappa_T \le \infty$.

Proof. 1. Note that

$$\Delta_U = \frac{T}{V}\frac{1}{c_p \kappa_S} = \frac{T}{V}\frac{1}{c_v \kappa_T} \neq 0$$

provided $0 < c_V, \kappa_T < \infty$ or $0 < c_p, \kappa_S < \infty$. The positive definiteness of H_U is equivalent to

$$\left(U_{SS} = \frac{T}{c_V} > 0 \text{ or } U_{VV} = \frac{1}{V\kappa_S} > 0\right) \text{ and } (\Delta_U > 0)\,.$$

These are equivalent to $(c_V > 0, \kappa_T > 0)$ or $(c_p > 0, \kappa_S > 0)$.

2. The positive semi-definiteness of H_U is equivalent to

$$U_{SS} = \frac{T}{c_V} \ge 0, \quad U_{VV} = \frac{1}{V\kappa_S} \ge 0, \quad \Delta_U = \frac{T}{V}\frac{1}{c_p \kappa_S} = \frac{T}{V}\frac{1}{c_V \kappa_T} \ge 0.$$

These are equivalent to

$$0 \le c_V, c_p, \kappa_S, \kappa_T \le \infty.$$

□

Remarks

- The stability is characterized by the following statement:
  A potential is convex in its extensive variable and concave in its intensive variable Callen Callen (1985).
- This stability condition $U_{VV} > 0$ is equivalent to the condition of finite sound speed. The sound speed is defined by

$$c^2 := \left(\frac{\partial p(\rho, S)}{\partial \rho}\right)_S,$$

which is also

$$c^2 = \left(\frac{\partial V}{\partial \rho}\right)_S \left(\frac{\partial}{\partial V}\right)_S \left(-\frac{\partial U}{\partial V}\right)_S = V^2 \left(\frac{\partial^2 U}{\partial V^2}\right)_S .$$

The positivity on the right-hand side of the above equation gives real value of sound speed. This property leads to finite speed propagation of signal in rest gases. Namely, the governing equation for the perturbed gas is

$$u_{tt} = c^2 u_{xx},$$

where $u = \delta\rho$ is the perturbed density. If initial data is e^{ikx}, then the solution has the form $e^{i(kx \pm \omega(k)t)}$, where $\omega(k)$ satisfies the dispersion relation: $\omega^2 = c^2 k^2$. If c is not real, then u will grow exponentially in time. This is unstable.

- For γ-law gases, the stability $\left(\frac{\partial p}{\partial \rho}\right)_S > 0$ is equivalent to $\gamma > 1$.

For most simple equilibrium systems, the weak stability conditions $c_v > 0$ and $\kappa_S > 0$ imply the strong stability conditions involving the full Hessian of the thermodynamic potential. However, near critical points or in systems with long-range correlations, quantities such as c_p or κ_T can diverge, and the Hessian may become degenerate. In such cases, weak stability may hold while strong stability fails. Additionally, artificially engineered metamaterials can be designed to violate strong stability conditions while maintaining positive diagonal response coefficients.

1.4 Construction of the Constitutive Law from Measurements

The mechanical relation $f(p, V, T)$ and the caloric relation: $(\partial U/\partial T)_V$ are measurable

- We recall that any of the relations:

$$U = U(S, V), \quad h = h(S, p), \quad \Psi = \Psi(T, V), \quad G = G(T, p)$$

constitutes a constitutive law of the thermodynamic system. These relations are interconnected through Legendre transforms. To determine all of them, we need only to construct any one of these expressions.

- In practice, p, V, and T are measurable quantities. We can obtain a mechanical equation of state of the form:

$$p = p(T, V) \tag{1.33}$$

through measurements of p, V, and T. For instance, ideal gases satisfy $pV = RT$, which serves as one form of a mechanical equation of state.

- The caloric equation of state can be obtained by measuring the heat capacity c_V:

$$c_V = \left(\frac{\partial U}{\partial T}\right)_V .$$

Using the Gibbs relation with (T, V) being the independent variables, we have

$$dU(T, V) = T dS(T, V) - p dV$$

$$= T\left[\left(\frac{\partial S}{\partial T}\right)_V dT + \left(\frac{\partial S}{\partial V}\right)_T dV\right] - p dV$$
$$= T\left(\frac{\partial S}{\partial T}\right)_V dT + \left[T\left(\frac{\partial p}{\partial T}\right)_V - p\right] dV$$

From this, we obtain

$$\left(\frac{\partial U}{\partial V}\right)_T = T\left(\frac{\partial p}{\partial T}\right)_V - p.$$

$$\left(\frac{\partial U}{\partial T}\right)_V = c_V(T,V), \quad \left(\frac{\partial U}{\partial V}\right)_T = T\left(\frac{\partial p}{\partial T}\right)_V - p \quad \Rightarrow \quad U = U(T,V)$$

- Once we have $p = p(T,V)$ and $U = U(T,V)$, we can find $S(T,V)$ using the Gibbs relation:

$$dS = \frac{1}{T}(dU + p\,dV) \quad \Rightarrow \quad S = S(T,V).$$

This method of constructing the constitutive law from measured quantities such as $p(T,V)$ and $c_V(T,V)$ is widely used in experimental thermodynamics, engineering applications, and computational modeling. It provides a practical path from observable data to a complete thermodynamic state description, enabling the reconstruction of energy and entropy functions needed to model real materials. (see, e.g., Callen Callen (1985), Reif Reif (1965), or Greiner Greiner et al. (1995))

1.5 Historial Note

The axiomatic formulation of thermodynamics has evolved over more than a century. The earliest mathematically systematic approach was developed by J. Willard Gibbs Gibbs (1928) in the late 19th century, who introduced the idea of thermodynamic potentials and equilibrium principles using variational and geometric methods.

A rigorous mathematical foundation for the second law was provided by Constantin Carathéodory in 1909 Carathéodory (1909), who reformulated thermodynamics in terms of differential geometry and integrability. His key insight was that entropy arises as an integrating factor from the inaccessibility of certain adiabatic paths.

In recent decades, Elliott Lieb and Jakob Yngvason Lieb and Yngvason (1999) introduced a modern axiomatic system based on the concept of adiabatic accessibility and the ordering of thermodynamic states. In their framework, entropy is constructed as a monotonic, extensive, and concave function over a state space, satisfying a set of natural axioms.

These contributions underpin much of the modern understanding of thermodynamic stability, entropy, and the structure of equilibrium state spaces.

Chapter 2

Dynamics of Fluid Flows

There are two formulations of fluid dynamics: Eulerian and Lagrangian. The former is described from the observer's frame of reference, while the latter is described from the material frame (or reference frame), meaning that the fluid particles are initially labeled, and the description is from each labeled particle's point of view.

Suppose the fluid (the continuum object) occupies a region $\hat{M}$ initially and evolves to a domain M_t at time t. We will refer to M_t as the observer's domain, while $\hat{M}$ is the material (reference) domain.

- In the Lagrangian formulation, we assume $\hat{M} \subset \mathbb{R}^3$, and the coordinate of the reference domain $\hat{M}$ is called the Lagrangian coordinate, material coordinate, reference coordinate, or label coordinate. It will be denoted by X. Its components are denoted by X^α, $\alpha = 1, 2, 3$. The embedding $\hat{M} \subset \mathbb{R}^3$ induces a natural volume element $\hat{\mu} = dX = dX^1 \wedge dX^2 \wedge dX^3$ in $\hat{M}$.

- The coordinate of the observer's domain M_t is called the Eulerian coordinate or the observer's coordinate. It is denoted by $\mathbf{x}$. Its components are denoted by x^i, $i = 1, 2, 3$. The domain $M_t \subset \mathbb{R}^3$ has a natural volume form $\mu_t = d\mathbf{x} = dx^1 \wedge dx^2 \wedge dx^3$.

2.1 Fluid Dynamics in the Eulerian Frame

The governing equations of fluid flow are derived from three fundamental physical laws: conservation of mass, momentum, and energy. Leonhard Euler derived the equations in 1755 under the assumptions of adiabatic flow and negligible viscous effects, without an explicit energy equation (Euler, 1755). The entropy equation was later introduced by Pierre-Simon Laplace (Laplace, 1816). Subsequently, the effects of viscosity and thermal conductivity were incorporated, leading to the developments of Claude-Louis Navier and George Gabriel Stokes (Navier, 1822; Stokes, 1850).

2.1.1 Conservation of mass, momentum and energy

Conservation of mass Consider an arbitrary domain $\Omega \subset M_t$. The change of mass per unit time in Ω is given by

$$\frac{d}{dt} \int_\Omega \rho \, d\mathbf{x}.$$

This quantity is equal to the mass flowing into Ω through its boundary $\partial\Omega$ per unit time. To measure the mass flows through $\partial\Omega$, the concept of *mass flux* is introduced. For a small area dA on the surface $\partial\Omega$ with an outer normal $\mathbf{n}$, and flow velocity $\mathbf{v}$ in its vicinity, the mass flux is defined as $\rho\mathbf{v}\cdot(-\mathbf{n})$. * Here, $-\mathbf{n}$ represents the inner normal, indicating the flow into Ω from outside. The mass flux is integrated over $\partial\Omega$ to obtain the total mass flow into Ω per unit time:

$$\int_{\partial\Omega} \rho\mathbf{v}\cdot(-\mathbf{n})\, dA.$$

The conservation of mass is expressed as

$$\frac{d}{dt}\int_\Omega \rho\, d\mathbf{x} = \int_{\partial\Omega} [-\rho\mathbf{v}\cdot\mathbf{n}] dA = -\int_\Omega \nabla\cdot(\rho\,\mathbf{v})\, d\mathbf{x},$$

or

$$\int_\Omega \left(\frac{\partial\rho}{\partial t} + \nabla\cdot(\rho\mathbf{v})\right) d\mathbf{x} = 0.$$

This holds for arbitrary domain Ω. This leads to the *continuity equation:*

$$\boxed{\frac{\partial\rho}{\partial t} + \nabla\cdot(\rho\,\mathbf{v}) = 0.} \tag{2.1}$$

Conservation of Momentum The momentum change in Ω per unit time is given by

$$\frac{d}{dt}\int_\Omega \rho\mathbf{v}\, d\mathbf{x}.$$

This change results from:

(a) the momentum carried into Ω through the boundary $\partial\Omega$, given by $(\rho\mathbf{v})[\mathbf{v}\cdot(-\mathbf{n})]$,

(b) a surface force (per unit area) $\mathbf{t}$ on the boundary $\partial\Omega$,

(c) a body force (per unit volume) $\mathbf{f}$ in Ω.

Here, the surface force $\mathbf{t}$ comes from the impacts of particles on the surface. It is assumed that

$$\mathbf{t} = \boldsymbol{\sigma}\cdot\mathbf{n},$$

where $\boldsymbol{\sigma}$ is a rank-2 tensor: $\boldsymbol{\sigma} = (\sigma_{ij})$, termed the Cauchy stress tensor. † This leads to the momentum conservation equation:

$$\begin{aligned}\frac{d}{dt}\int_\Omega \rho\mathbf{v}\, d\mathbf{x} &= \int_{\partial\Omega} \rho\mathbf{v}[\mathbf{v}\cdot(-\mathbf{n})]\, dA + \int_{\partial\Omega} \boldsymbol{\sigma}\cdot\mathbf{n}\, dA + \int_\Omega \mathbf{f}\, d\mathbf{x} \\ &= \int_\Omega [\nabla\cdot(-\rho\mathbf{v}\mathbf{v} + \boldsymbol{\sigma}) + \mathbf{f}\,]\, d\mathbf{x}.\end{aligned}$$

*The mass in the parallelogram spanned by dA and the vector $\mathbf{v}\Delta t$ will flow into Ω through dA in the period Δt. The volume of this parallelogram is $(\mathbf{v}\Delta t\cdot\mathbf{n})dA$. The mass in this parallelogram is $\rho(\mathbf{v}\Delta t\cdot\mathbf{n})dA$. Thus the mass flows into Ω through dA per unit time, per unit area is $\rho\mathbf{v}\cdot(-\mathbf{n})$.

†This will be proven that $\mathbf{t}$ is a linear function of the outer normal $\mathbf{n}$. For a full derivation of the surface force law $\mathbf{t} = \boldsymbol{\sigma}\cdot\mathbf{n}$ from continuum mechanics principles, see Aris Aris (1989), or Cauchy's Stress in the later chapter.

This holds for arbitrary domain Ω. Thus, we obtain [‡]

$$\boxed{\frac{\partial(\rho \mathbf{v})}{\partial t} + \nabla \cdot (\rho\, \mathbf{v}\mathbf{v}) = \nabla \cdot \boldsymbol{\sigma} + \mathbf{f}.} \tag{2.2}$$

This is the conservation of momentum equation in Eulerian form (see Batchelor Batchelor (1967), Chorin & Marsden Chorin and Marsden (2000), Landau & Lifshitz Landau and Lifshitz (1987)).

For each velocity component v^i, the momentum conservation equation is:

$$\begin{aligned} \frac{d}{dt}\int_\Omega \rho v^i \, d\mathbf{x} &= \int_{\partial\Omega} [-\rho v^i v^j + \sigma^{ij}]\nu^j \, dA + \int_\Omega f^i \, d\mathbf{x} \\ &= \int_\Omega \partial_j [-\rho v^i v^j + \sigma^{ij}] + f^i \, d\mathbf{x}. \end{aligned}$$

Inviscid assumption for gas flows In gas flows, the stress mainly comes from the impact of gas particles on the surface, which gives a stress of the form

$$\boldsymbol{\sigma} = -pI,$$

where p is the pressure and I is the 3×3 identity matrix. The minus sign means that the surface force $\boldsymbol{\sigma} \cdot \mathbf{n} = -p\mathbf{n}$ is inward to Ω. The stress has the form pI, meaning that the gas is *isotropic*, i.e., the particle impacts at a point have no preferred direction.

Note that gas particles can also *interact* with one another through collisions or intermolecular forces such as Van der Waals interactions. These effects contribute to the *viscous stress*, introducing internal friction and anisotropic behavior in the stress tensor. However, they are typically secondary in dilute gases or high-speed flows. We will neglect them in our present treatment and adopt the *inviscid assumption*, modeling the gas as an ideal fluid with isotropic pressure and no shear stress.

With $\boldsymbol{\sigma} = -pI$, the momentum equation now reads

$$\boxed{\frac{\partial(\rho \mathbf{v})}{\partial t} + \nabla \cdot (\rho\, \mathbf{v}\mathbf{v}) = -\nabla p + \mathbf{f}.} \tag{2.3}$$

Conservation of energy The total energy per unit volume is

$$\rho E := \frac{1}{2}\rho\, |\mathbf{v}|^2 + \rho U,$$

the sum of kinetic energy and internal energy. The energy change in a region Ω per unit time is due to

(a) the energy carried in through the boundary $\partial\Omega$, which is $\rho E \mathbf{v} \cdot (-\mathbf{n})$ $\left(= -\rho E v^i \nu^i\right)$,

(b) the work done by the stress from the boundary, which is $\mathbf{v} \cdot \boldsymbol{\sigma} \cdot \mathbf{n}$ $\left(= v^i \sigma_{ij} \nu^j\right)$,

(c) the work done by the body force in Ω, which is $\mathbf{v} \cdot \mathbf{f}$ $\left(= v^i f^i\right)$,

(d) the heat transfer into Ω through boundary, which is $\mathbf{q} \cdot (-\mathbf{n})$. Here, $\mathbf{q}$, is the *heat flux*.

[‡]The notation $\mathbf{vv}$ stands for a tensor: $\mathbf{vv} = (v^i v^j)$, and $\nabla \cdot (\rho \mathbf{vv})$ stands for a vector whose ith component is $\partial_j(\rho v^i v^j)$.

The conservation of energy reads

$$\frac{d}{dt}\int_\Omega \rho E\, d\mathbf{x} = \int_{\partial\Omega} [-\rho E \mathbf{v}\cdot\mathbf{n} + \boldsymbol{\sigma}\cdot\mathbf{v}\cdot\mathbf{n} - \mathbf{q}\cdot\mathbf{n}]\, dA + \int_\Omega \mathbf{f}\cdot\mathbf{v}\, d\mathbf{x}.$$

By applying the divergence theorem, we obtain the energy equation: [§]

$$\boxed{\frac{\partial(\rho E)}{\partial t} + \nabla\cdot[(\rho E\mathbf{I} - \boldsymbol{\sigma})\cdot\mathbf{v} + \mathbf{q}] = \mathbf{v}\cdot\mathbf{f}.} \tag{2.4}$$

This is the conservation of energy in differential form, accounting for mechanical work and heat transport (see Batchelor Batchelor (1967), Landau & Lifshitz Landau and Lifshitz (1987), Chorin & Marsden Chorin and Marsden (2000)).

Adiabatic assumption for gas flows We shall assume no heat conduction for inviscid gas flows. This means that $\mathbf{q} = 0$.

Compressible Euler equations System (2.1),(2.3),(2.4) is called the (compressible) Euler equations. There are 5 equations (momentum equation has 3 equations) for 5 unknowns (ρ, U, v^1, v^2, v^3). The pressure p is given as $p(\rho, U)$ from the equation-of-state. For ideal gases, this relation takes the form $p = (\gamma - 1)\rho U$, where γ is the adiabatic index.

2.1.2 Initial conditions and boundary conditions

We consider the fluid flows in a fixed domain $\hat{M} = M_t = M$.

Initial conditions The Euler equation is first-order in time and thus requires initial condition

$$\rho(0,\mathbf{x}) = \rho_0(\mathbf{x}), \quad U(0,\mathbf{x}) = U_0(\mathbf{x}), \quad \mathbf{v}(0,\mathbf{x}) = \mathbf{v}_0(\mathbf{x}), \quad \mathbf{x}\in M.$$

Boundary conditions Typically, we consider a *closed system*, implying that there are no transported fluxes from outside the domain. In other words:

$$\rho\mathbf{v}\cdot\mathbf{n} = 0, \quad \rho\mathbf{v}\mathbf{v}\cdot\mathbf{n} = 0, \quad \rho E\mathbf{v}\cdot\mathbf{n} = 0 \text{ on } \partial M.$$

This is equivalent to the following Neumann boundary condition (or no through boundary condition):

$$\boxed{\mathbf{v}\cdot\mathbf{n} = 0 \text{ on } \partial M.} \tag{2.5}$$

This boundary condition corresponds to an impermeable wall and is standard in the theory of compressible Euler flows (see Courant & Friedrichs Courant and Friedrichs (1948), Chorin & Marsden Chorin and Marsden (2000)).

[§]The notation $\nabla\cdot[\mathbf{v}\cdot\boldsymbol{\sigma}]$ is $\partial_j(v^i\sigma^{ij})$.

Remarks An important mathematical question is that *whether this boundary condition can determine the flow inside uniquely?* For classical solutions (i.e. the solution is continuously differentiable), this problem can be analyzed through the method of characteristics. *The answers to the uniqueness problem are:*

- *yes, for classical solutions;*
- *no, even in one dimension for weak solution;*
- *if we add so-called entropy condition, then the answer is yes in one dimension for weak solutions;*
- *no, in three dimensions for weak solutions.*

For classical solutions, we have $\mathbf{v} \cdot \mathbf{n} = 0$ on the boundary. The thermo variable S is known on the boundary because S stays constant along fluid parcels and the parcel stays on the boundary if it does initially. The other thermo variable, say V, is obtained from the interior through the characteristic curve. Details will be discussed in later Chapters.

2.1.3 Systems of Balance Laws in the Eulerian Frame

PDE formulation The fluid dynamics can be expressed in the following balance laws:

$$\boxed{\partial_t \mathscr{U} + \nabla_{\mathbf{x}} \cdot \mathscr{F} = \mathscr{R} \quad \mathbf{x} \in M, t > 0,} \tag{2.6}$$

where

$$\mathscr{U} = \begin{bmatrix} \rho \\ \rho \mathbf{v} \\ \rho E \end{bmatrix}, \quad \mathscr{F} = \begin{bmatrix} \rho \mathbf{v} \\ \rho \mathbf{v}\mathbf{v} - \boldsymbol{\sigma} \\ \mathbf{v} \cdot (\rho E \mathbf{I} - \boldsymbol{\sigma}) + \mathbf{q} \end{bmatrix}, \quad \mathscr{R} = \begin{bmatrix} 0 \\ \mathbf{f} \\ \mathbf{v} \cdot \mathbf{f} \end{bmatrix}.$$

Let us express these quantities in an abstract form: $\mathscr{U} = (u_1, ..., u_m)^T$, $\mathscr{R} = (r_1, ..., r_m)^T$, the flux $\mathscr{F}$ is an $m \times 3$ matrix, and expressed as $\mathscr{F} = (\mathscr{F}^1, \mathscr{F}^2, \mathscr{F}^3)$. The divergence of flux is $\nabla_{\mathbf{x}} \cdot \mathscr{F} := \partial_{x^i} \mathscr{F}^i$.

Integral form formulation By using the divergence theorem, the balance laws can be expressed in the following integral form:

$$\int_\Omega \partial_t \mathscr{U} \, d\mathbf{x} + \int_{\partial\Omega} \mathscr{F} \cdot \mathbf{n} \, dS_t = \int_\Omega \mathscr{R} \, d\mathbf{x}. \tag{2.7}$$

where $\Omega \subset M_t$ is an arbitrary subdomain and $\mathbf{n}$ is its outer normal.

Remark It was known by Rankine-Hugoit that the solutions of gas dynamics can exhibit shock waves, where the solution is discontinuous. A smooth solution where its derivatives can be understood in the ordinary sense is called a classical solution. Shock-wave solutions are called a weak solutions. The derivatives in the balance laws are interpreted as weak derivatives. On the other hand, in the integral forms of the balance laws, such formulation only require the solutions to be locally integrable. Thus, we can use this integral formulation as the definition of weak solutions. Rigorously, we have the following definition.

Weak solutions of balance laws A function $\mathscr{U}(\mathbf{x}, t)$ defined on $M \times (0, \infty)$ is called a weak solution of (2.6) if

$$\int \mathscr{U} \cdot \phi_t \, dx \, dt + \int \mathscr{F} \cdot \nabla \phi \, dx \, dt + \int \mathscr{R} \phi \, dx \, dt = 0. \tag{2.8}$$

for all text function $\phi = (\phi_1, ..., \phi_m)$ in $C_c^\infty(M \times (0, \infty))$.

2.2 Fluid Dynamics in the Lagrangian Frame

2.2.1 Flow Maps and Velocity Fields

Flow map and velocity field

- **Fluid parcel:** The fluid contained in a small reference volume dX centered at point X is referred to as a *fluid parcel at* X. Let $\mathbf{x}(\cdot, X)$ denote the trajectory of the parcel originating from X.
- **Velocity:** The time derivative $\dot{\mathbf{x}}(t, X)$ gives the velocity of the parcel, denoted by $\mathbf{V}$. In Lagrangian coordinates, this is defined as

  $$\mathbf{V}(t, X) := \dot{\mathbf{x}}(t, X).$$

  In Eulerian (spatial) coordinates, the velocity is expressed as $\mathbf{v}(t, \mathbf{x})$, satisfying

  $$\mathbf{v}(t, \mathbf{x}(t, X)) := \dot{\mathbf{x}}(t, X).$$

  In geometric language, we write $\mathbf{v}(t, \cdot)$ as $\mathbf{v}_t$ and treat it as a vector field in the tangent bundle TM_t. Given a velocity field $\mathbf{v}_t \in TM_t$, the trajectory $\mathbf{x}(t, X)$ satisfies the ordinary differential equation:

  $$\dot{\mathbf{x}}(t) = \mathbf{v}(t, \mathbf{x}), \quad \mathbf{x}(0, X) = X.$$

- **Flow map:** The mapping $\varphi_t : \hat{M} \to M_t$ defined by

  $$X \mapsto \mathbf{x}(t, X)$$

  is called the *flow map*. Specifying a flow map φ_t is equivalent to specifying the velocity field $\mathbf{v}_t$ on TM_t.
- Physical quantities may be expressed in Eulerian coordinates as $f(t, \mathbf{x})$ or in Lagrangian coordinates as $f(t, X) := f(t, \mathbf{x}(t, X))$. (By convention, we use the same symbol f in both cases.) The partial derivative $\partial/\partial t$ refers to variation at fixed spatial point $\mathbf{x}$, while the total derivative d/dt (or dot notation) refers to variation at fixed Lagrangian coordinate X.

2.2.2 Deformation Gradients

- The deformation gradient of the flow map $\varphi_t(X) = \mathbf{x}(t, X)$ is defined by

  $$F(t, X) := \frac{\partial \mathbf{x}}{\partial X}(t, X), \quad F_\alpha^i := \frac{\partial x^i}{\partial X^\alpha}. \tag{2.9}$$

  This tensor describes the local deformation of a fluid parcel. It is a fundamental object in continuum mechanics, encoding how material elements stretch and rotate over time (see Marsden & Hughes Marsden and Hughes (1994), Truesdell & Noll Truesdell and Noll (2004)).

- Because fluid flows may exhibit discontinuities (e.g., shocks or contact surfaces), the Eulerian velocity field $\mathbf{v}(t, \mathbf{x})$ is typically only piecewise smooth. As a result, the flow map φ_t is generally only Lipschitz continuous. Although the Lipschitz constant may depend on time, the deformation gradient $\partial \mathbf{x}/\partial X$ is well-defined and bounded for each fixed time t.

- We frequently use the following matrix expressions:

  - **Transpose:** $(F^T)_i^\alpha := F_\alpha^i = \frac{\partial x^i}{\partial X^\alpha}$.
  - **Inverse:** $(F^{-1})_i^\alpha := \frac{\partial X^\alpha}{\partial x^i}$, satisfying $(F \cdot F^{-1})_j^i = F_\alpha^i (F^{-1})_j^\alpha = \delta_j^i$.
  - **Inverse transpose:** $(F^{-T})_i^\alpha := (F^{-1})_i^\alpha = \frac{\partial X^\alpha}{\partial x^i}$.

- The Jacobian of the flow map is defined by

$$J(t, X) := \det\left(\frac{\partial \mathbf{x}}{\partial X}\right), \quad \text{so that} \quad d\mathbf{x}(t, X) = J(t, X)\, dX.$$

  We require that

$$J(t, X) > 0$$

  to ensure that the flow map φ_t is locally invertible.

2.2.3 Systems of Balance Laws in the Lagrangian Frame

To derive the fluid equations in the Lagrangian frame, we need to convert integrals over the current (spatial) domain to integrals over the reference domain, using the flow map. Two fundamental results are needed: the Reynolds transport theorem and the surface area transformation formula.

Reynolds Transport Theorem.

Theorem 2.1. *Let $\mathbf{v}(t, \mathbf{x})$ be a vector field, and φ_t be the flow map from $\hat{M}$ to M_t generated by $\mathbf{v}$. Suppose Ω_0 is a subdomain in $\hat{M}$ and $\Omega(t) := \varphi_t(\Omega_0)$. Then, for any function $f(t, \mathbf{x})$, we have*

$$\boxed{\frac{d}{dt}\int_{\Omega(t)} f(t, \mathbf{x})\, d\mathbf{x} = \int_{\Omega(t)} \frac{\partial}{\partial t} f(t, \mathbf{x})\, d\mathbf{x} + \int_{\partial\Omega(t)} f(t, \mathbf{x}) \mathbf{v} \cdot \mathbf{n}\, dS_t,} \tag{2.10}$$

where $\mathbf{n}$ is the outer normal on $\partial\Omega(t)$.

Proof. We have

$$\frac{d}{dt}\int_{\Omega(t)} f(t, \mathbf{x})\, d\mathbf{x} = \int_{\Omega(t)} \frac{\partial}{\partial t} f(t, \mathbf{x})\, d\mathbf{x} + \lim_{\Delta t \to 0} \frac{1}{\Delta t} \int_{\Omega(t+\Delta t) - \Omega(t)} f(t, \mathbf{x})\, d\mathbf{x}$$

and

$$\lim_{\Delta t \to 0} \frac{1}{\Delta t} \int_{\Omega(t+\Delta) - \Omega(t)} f(t, \mathbf{x})\, d\mathbf{x} = \lim_{\Delta t \to 0} \frac{1}{\Delta t} \int_{\partial\Omega(t)} f(t, \mathbf{x}) (\mathbf{v}\Delta t) \cdot \mathbf{n}\, dS_t.$$

□

Surface Area Transformation.

Proposition 2.2. *Let φ_t be the flow map from $\hat{M}$ to M_t. Then the normal surface area elements $\mathbf{n}dS_t$ on ∂M_t and $\mathbf{N}dS_0$ on $\partial\hat{M}$ satisfy the following transformation formula*

$$\boxed{\mathbf{n}dS_t = JF^{-T}\mathbf{N}\,dS_0,} \tag{2.11}$$

where $\mathbf{n}$ and $\mathbf{N}$ are respectively the outer normals of ∂M_t and $\partial\hat{M}$, $F = \partial\varphi_t/\partial X$, and $J = \det F$.

This geometric identity is central to the formulation of balance laws in Lagrangian coordinates (see Marsden & Hughes Marsden and Hughes (1994), Truesdell & Noll Truesdell and Noll (2004)).

Proof. Let dX_1 and dX_2 be a pair of two infinitesimal vectors on $\hat{M}$ forming an oriented surface patch. Their cross product defines the surface element: ¶

$$\mathbf{N}\,dS_0 = dX_1 \times dX_2.$$

Under the flow map φ_t, the corresponding vectors in M_t are:

$$d\mathbf{x}_1 = FdX_1, \quad d\mathbf{x}_2 = FdX_2.$$

Hence, the transformed surface element is:

$$\mathbf{n}\,dS_t = d\mathbf{x}_1 \times d\mathbf{x}_2 = (FdX_1) \times (FdX_2).$$

Using the identity for transforming a cross product under a linear map: ‖

$$FdX_1 \times FdX_2 = JF^{-T}(dX_1 \times dX_2),$$

we obtain:

$$\mathbf{n}\,dS_t = JF^{-T}\mathbf{N}\,dS_0.$$

□

Abstract Form of Balance Laws in the Lagrangian Frame We now express the system of balance laws in the Lagrangian frame using abstract notation. The starting point is the integral form in the Eulerian form (2.7):

$$\int_{\Omega(t)} \partial_t \mathscr{U}\,d\mathbf{x} + \int_{\partial\Omega(t)} \mathscr{F}\cdot\mathbf{n}\,dS_t = \int_{\Omega(t)} \mathscr{R}\,d\mathbf{x}.$$

¶We can parameterize $\hat{M}$ by (u_1, u_2) through a map $(u_1, u_2) \mapsto X(u_1, u_2)$. Then $dX_i = \frac{\partial X}{\partial u_i}du_i$, $i = 1, 2$.

$$dX_1 \times dX_2 = \left(\frac{\partial X}{\partial u_1} \times \frac{\partial X}{\partial u_2}\right) du_1 \wedge du_2 = \left(\frac{\frac{\partial X}{\partial u_1} \times \frac{\partial X}{\partial u_2}}{J}\right) J du_1 \wedge du_2 = \mathbf{N}dS_0, \quad \text{where } J := \left|\frac{\partial X}{\partial u_1} \times \frac{\partial X}{\partial u_2}\right|.$$

‖For a linear map $A : \mathbb{R}^3 \to \mathbb{R}^3$, for any two vectors $\mathbf{u}, \mathbf{v} \in \mathbb{R}^3$:

$$A\mathbf{u} \times A\mathbf{v} = (\det A)A^{-T}\mathbf{u} \times \mathbf{v}.$$

Here, we choose the arbitrary domain $\Omega = \Omega(t) := \varphi_t(\Omega_0)$ for some fixed domain $\Omega_0 \subset \hat{M}$. By the Renold transport Theorem (2.10), we have

$$\frac{d}{dt}\int_{\Omega(t)} \mathscr{U}\, d\mathbf{x} = \int_{\Omega(t)} \partial_t \mathscr{U}\, d\mathbf{x} + \int_{\partial\Omega_t} \mathscr{U}\,\mathbf{v}\cdot\mathbf{n}\, dS_t.$$

Thus the balance laws become

$$\frac{d}{dt}\int_{\Omega(t)} \mathscr{U}\, d\mathbf{x} + \int_{\partial\Omega(t)} (\mathscr{F} - \mathscr{U}\,\mathbf{v})\cdot\mathbf{n}\, dS_t = \int_{\Omega(t)} \mathscr{R}\, d\mathbf{x}.$$

Next, we pull back the integral from the Eulerian frame to the Lagrangian frame by φ_t^{-1}. We get

$$\frac{d}{dt}\int_{\Omega(0)} \mathscr{U} J\, dX + \int_{\partial\Omega(0)} (\mathscr{F} - \mathscr{U}\,\mathbf{v})\cdot JF^{-T}\cdot\mathbf{N}\, dS_0 = \int_{\Omega(0)} \mathscr{R} J\, dX.$$

Here, we have used

$$\mathbf{n} dS_t = JF^{-T}\cdot\mathbf{N}\, dS_0.$$

Using divergence theorem, the balance laws in the Lagrangian frame takes the form:

$$\boxed{\frac{d}{dt}\mathscr{W} + \nabla_X\cdot\mathscr{G} = \mathscr{R} J,} \tag{2.12}$$

where

$$\mathscr{W} = \mathscr{U} J, \quad \mathscr{G} := (\mathscr{F} - \mathscr{U}\,\mathbf{v})\cdot JF^{-T}. \tag{2.13}$$

Since $\rho J = \rho_0$ (see (2.22) in the next section), we get

$$\mathscr{U} J = \begin{bmatrix} \rho_0 \\ \rho_0\mathbf{V} \\ \rho_0 E \end{bmatrix}, \quad \mathscr{F} - \mathscr{U}\,\mathbf{v} = \begin{bmatrix} 0 \\ -\boldsymbol{\sigma} \\ -\mathbf{v}\cdot\boldsymbol{\sigma} + \mathbf{q} \end{bmatrix}, \quad \mathscr{G} = \begin{bmatrix} 0 \\ -P \\ -\mathbf{V}\cdot P + \mathbf{Q} \end{bmatrix}, \quad \mathscr{R} J = \begin{bmatrix} 0 \\ \mathbf{f} J \\ \mathbf{V}\cdot\mathbf{f} J \end{bmatrix}.$$

The stress term is transformed to

$$\boldsymbol{\sigma}\cdot\mathbf{n}\, dS_t = \boldsymbol{\sigma}\cdot JF^{-T}\cdot\mathbf{n}\, dS_0 := P\cdot\mathbf{N}\, dS_0,$$

with

$$P := J\boldsymbol{\sigma}F^{-T} \tag{2.14}$$

called the *first Piola stress*. In component form, it reads

$$P^i_\alpha = J\sigma^i_j (F^{-T})^j_\alpha = J\sigma^i_j (F^{-1})^\alpha_j = J\sigma^i_j \frac{\partial X^\alpha}{\partial x^j}.$$

The heat flux $\mathbf{Q}$ transformed to

$$\mathbf{q}\cdot\mathbf{n}\, dS_t = (J\mathbf{q}F^{-T})\cdot\mathbf{N}\, dS_0 := \mathbf{Q}\cdot\mathbf{n}\, dS_0,$$

with

$$\mathbf{Q} = J\mathbf{q}F^{-T}, \tag{2.15}$$

or

$$Q_\alpha = Jq_j (F^{-T})^j_\alpha = Jq_j \frac{\partial X^\alpha}{\partial x^j}.$$

The abstract balance laws formulations (2.12) is widely used in continuum mechanics and geometric models of fluid motion (see Marsden & Hughes Marsden and Hughes (1994), Truesdell & Noll Truesdell and Noll (2004)).

Evolution equation for the deformation gradient The above balance laws are not closed because the corresponding Piola stress P and the Lagrangian heat flux $\mathbf{Q}$ depend on the deformation gradient F, see (2.14),(2.15). We need an evolution equation for F. It can be derived from

$$\frac{d}{dt}F^i_\alpha(t,X) = \frac{\partial}{\partial t}\frac{\partial x^i}{\partial X^\alpha} = \frac{\partial}{\partial X^\alpha}\frac{\partial x^i}{\partial t} = \frac{\partial}{\partial X^\alpha}V^i(t,X).$$

In tensor form:

$$\boxed{\frac{dF(t,X)}{dt} = \frac{\partial \mathbf{V}(t,X)}{\partial X}.} \tag{2.16}$$

This PDE together with (2.12) closes the system with unknowns $(\mathbf{V}(t,X), E(t,X), F(t,X))$.

Remarks.

- The continuity equation becomes an algebraic equation for ρ:

  $$\rho(t,X)J(t,X) = \rho_0(X), \quad J = \det F.$$

  Thus, we can eliminate ρ from the list of unknowns.

- Instead of using the total energy E as the variable in the energy equation, we may choose the entropy S as the other thermodynamically independent variable. The pressure p then becomes a function of (ρ, S) via the equation of state.

- The Piola stress $\mathbf{P} = -pJF^{-T}$ is considerably more difficult to handle than the Cauchy stress $\boldsymbol{\sigma} = -pI$, both analytically and numerically. In numerical simulations, the stress is typically computed in Eulerian coordinates.

2.3 Material Derivatives

In continuum mechanics, it is essential to understand how physical quantities evolve as they are transported by the motion of a fluid. This leads naturally to the concept of the *material derivative*, which captures the rate-of-change experienced by a quantity following a fluid particle. Such derivatives form the backbone of the differential formulation of the balance laws.

This section provides a systematic treatment of material derivatives. We begin by analyzing the rate-of-change of scalar and tensor fields, focusing in particular on geometric quantities such as the deformation gradient and its determinant, the Jacobian. We then turn to thermodynamic variables—including density, velocity, energy, entropy, and temperature—whose evolution plays a central role in fluid dynamics.

Finally, we adopt the language of differential geometry to recast these notions in a coordinate-free framework. The use of differential forms not only provides elegant and compact formulations of classical laws but also offers a pathway toward modern geometric methods in continuum physics, which are especially relevant for numerical simulation and theoretical generalization.

2.3.1 Rate-of-changes of Geometric Variables

Rate-of-change of Scalar Fields For any scalar field $f(t, \mathbf{x})$, we can track its evolution along the flow by composing with the trajectory: $f(t, \mathbf{x}(t, X))$ where X is fixed. The derivative of this quantity is referred to **material derivative**

$$\left.\frac{d}{dt}\right|_X f(t, \mathbf{x}(t, X)) = \frac{\partial f}{\partial t} + \dot{\mathbf{x}}(t, X)\frac{\partial f}{\partial \mathbf{x}} = \left(\frac{\partial}{\partial t} + \mathbf{v} \cdot \nabla\right) f(t, \mathbf{x}(t, X)) \tag{2.17}$$

We sometimes abbreviate $\left.\frac{d}{dt}\right|_X$ as $\frac{d}{dt}$ or simply use the dot notation.

Rate-of-change of the Deformation Gradient The variation of the flow map $\mathbf{x}(t, X)$ with respect to X defines the *deformation gradient*

$$F(t, X) := \frac{\partial \mathbf{x}}{\partial X}(t, X), \quad \text{or component-wise} \quad F^i_\alpha := \frac{\partial x^i}{\partial X^\alpha}.$$

By differentiating

$$\dot{\mathbf{x}}(t, X) = \mathbf{v}(t, \mathbf{x}(t, X))$$

with respect to X, we obtain the evolution equation for F:

$$\frac{d}{dt}\frac{\partial x^i}{\partial X^\alpha} = \frac{\partial \dot{x}^i}{\partial X^\alpha} = \frac{\partial v^i}{\partial X^\alpha} = \frac{\partial v^i}{\partial x^k}\frac{\partial x^k}{\partial X^\alpha}$$

Writing this in tensor notation, we get:

$$\boxed{\dot{F} = (\nabla \mathbf{v})F}, \quad \text{or} \quad \dot{F}^i_\alpha = \frac{\partial v^i}{\partial x^k}F^k_\alpha. \tag{2.18}$$

where $\dot{F} := \frac{dF}{dt}$, and $\nabla \mathbf{v}$ is known as the *velocity gradient* or *deformation rate*.

Rate-of-change of the Jacobian Let $J = \det F$ be the Jacobian of the flow map, which measures the local volume change under deformation.

$$d\mathbf{x}(t, X) = J(t, X)dX.$$

Then the material derivative of J satisfies:

$$\boxed{\dot{J} = tr(\nabla \mathbf{v})J = (\nabla \cdot \mathbf{v})J.}$$

This follows from Jacobi's formula, recalled below:

Lemma 2.3 (Jacobi's formula)**.** *(i) Let A be an $n \times n$ matrix, and $J := detA$. It holds that*

$$\frac{\partial J}{\partial a_{ij}} = J(A^{-T})_{ij}. \tag{2.19}$$

(ii) Let $A(\varepsilon)$ be a smooth $n \times n$ matrix-valued function. Then

$$\frac{dJ}{d\varepsilon} = tr(\dot{A}A^{-1})J$$

Proof. 1. First, recall the Laplace expansion (cofactor formula) of $\det A$:

$$\sum_k a_{ik}A_{jk} = (\det A)\delta_{ij}, \quad \text{or} \quad A(\text{cof}A)^T = (\det A)I = J\,I,$$

where $\text{cof}\,A = (A_{ij})$ and A_{ij} is the signed cofactor of A at position (i, j). This gives:

$$A_{ij} = J(A^{-T})_{ij}.$$

2. To compute $\partial \det A/\partial a_{ij}$, write:

$$\det A = \sum_k a_{ik}A_{ik},$$

and observe that A_{ik} is independent of a_{ij} for $k \neq j$. Therefore,

$$\frac{\partial \det A}{\partial a_{ij}} = A_{ij}.$$

3. Differentiating J with respect to ε:

$$\begin{aligned}\dot{J} &= \frac{\partial J}{\partial a_{ij}}\frac{da_{ij}}{d\varepsilon} = \sum_{i,j}\dot{a}_{ij}A_{ij} \\ &= \sum_{i,j}\dot{a}_{ij}J(A^{-T})_{ij} = J\,tr(\dot{A}A^{-1}).\end{aligned}$$

In the last step, we use $\sum_{i,j} a_{ij}b_{ij} = tr(A^TB) = tr(AB^T)$.

□

2.3.2 Rate-of-change of Kinematic Variables

Rate-of-change of the velocity The momentum equation in Eulerian coordinate is

$$\partial_t(\rho\mathbf{v}) + \nabla\cdot(\rho\mathbf{v}\mathbf{v}) + \nabla p = 0.$$

Expanding the first two terms:

$$\rho\frac{\partial \mathbf{v}}{\partial t} + \frac{\partial \rho}{\partial t}\mathbf{v} + \nabla\cdot(\rho\mathbf{v})\mathbf{v} + \rho\mathbf{v}\cdot\nabla\mathbf{v} + \nabla p = 0.$$

Using the continuity equation, the second and third terms cancel, leading to:

$$\frac{\partial \mathbf{v}}{\partial t} + \mathbf{v}\cdot\nabla\mathbf{v} = -\frac{\nabla p}{\rho}. \tag{2.20}$$

Thus, the material derivative of velocity is:

$$\boxed{\frac{d\mathbf{v}}{dt} = -\frac{\nabla p}{\rho}.} \tag{2.21}$$

This equation expresses the acceleration of a fluid parcel due to pressure gradients. Note that this expression is a mix of Lagrangian representation ($d\mathbf{v}/dt$) and Eulerian representation ($\nabla_{\mathbf{x}}p$).

Rate-of-change of the kinetic energy We multiply (2.21) by $\rho\mathbf{v}$ to obtain:

$$\frac{d}{dt}\left(\frac{1}{2}\rho|\mathbf{v}|^2\right) = -\mathbf{v}\cdot\nabla p.$$

This shows that the rate-of-change of kinetic energy in a fluid parcel is due to the work done by the external pressure forces.

2.3.3 Rate-of-change of Thermodynamic Variables

Rate of change of the density A fluid parcel centered at X has initial mass $\rho_0(X)\,dX$. At time t, it occupies volume $d\mathbf{x}(t,X) = J(t,X)\,dX$, and its mass becomes

$$\rho(t,\mathbf{x}(t,X))\,d\mathbf{x} = \rho(t,\mathbf{x}(t,X))J(t,X)\,dX.$$

By conservation of mass, this must equal $\rho_0(X)\,dX$ at all times. Hence:

$$\boxed{\rho(t,\mathbf{x}(t,X))J(t,X) = \rho_0(X) \quad \text{or equivalently} \quad \frac{d}{dt}(\rho J) = 0.} \tag{2.22}$$

This is equivalent to:

$$\dot\rho J + \rho\dot J = \left(\frac{\partial\rho}{\partial t} + \nabla\rho\cdot\mathbf{v} + \rho\nabla\cdot\mathbf{v}\right)J = 0,$$

which recovers the Eulerian form of the continuity equation.

Thus, the conservation of mass in the Lagrangian frame is encoded by equation (2.22).

Dynamical form of density evolution The corresponding evolution equation for density is:

$$\frac{d\rho}{dt} + \rho\nabla\cdot\mathbf{v} = 0.$$

This yields the boxed relation:

$$\boxed{\nabla\cdot\mathbf{v} = -\frac{\dot\rho}{\rho} = \frac{\dot V}{V} = \frac{\dot J}{J},} \tag{2.23}$$

which expresses the relative rate of change of specific volume, or the *volumetric dilatation rate*.

A fluid flow is called *incompressible* if $\frac{d\rho}{dt} = 0$, or equivalently, $\nabla\cdot\mathbf{v} = 0$. Water is nearly incompressible under appropriate flow conditions.

Rate-of-change of the internal energy The energy equation is

$$\rho\left(\partial_t E + \mathbf{v}\cdot\nabla E\right) + \nabla\cdot(p\mathbf{v}) = 0,$$

or equivalently,

$$\rho\frac{d}{dt}\left(\frac{1}{2}|\mathbf{v}|^2 + U\right) + \nabla\cdot(p\mathbf{v}) = 0.$$

Subtracting the kinetic energy equation from the total energy equation yields the evolution equation for the internal energy:

$$\frac{dU}{dt} + \frac{p}{\rho}\nabla \cdot \mathbf{v} = 0. \tag{2.24}$$

From $\nabla \cdot \mathbf{v} = \frac{1}{V}\frac{dV}{dt}$, we get

$$\frac{dU}{dt} + p\frac{dV}{dt} = 0 \quad \because \rho V = 1.$$

This means that the change in internal energy is due to the work associated with the fluid's volume change.

Rate-of-change of the entropy The evolution equation for U, together with the Gibbs relation

$$dU = T\,dS - p\,dV,$$

leads to

$$\boxed{\frac{dS}{dt} = 0.} \tag{2.25}$$

This implies that S remains constant along the trajectory of each fluid particle. In other words, *the flow is adiabatic*—there is no heat transfer between different fluid parcels.

Rate-of-change of the temperature From the caloric equation of state $U(T)$ and the evolution equation for internal energy, we obtain

$$U'(T)\frac{dT}{dt} = -p\frac{dV}{dt}.$$

This yields

$$\frac{dT}{dt} = -\frac{p}{U'(T)}\frac{dV}{dt}. \tag{2.26}$$

Remark The material derivative represents differentiation along a fluid trajectory. However, as we shall see later, *inviscid fluid flows may exhibit discontinuities.* Across such discontinuities, the material derivative must be interpreted in a weak sense in the weak sense developed by Vol'pert and Hudjaev (1985), and *additional jump conditions must be satisfied.* Thus, *the constant entropy along parcel trajectories holds only in smooth region.* We will study these in a later chapter.

Chapter 3

Viscous Fluids

3.1 Viscosity

3.1.1 Stress

Cauchy's Principles for Stress In continuum mechanics, stress is a surface force arising from the collisions and interactions of nearby fluid particles. Cauchy postulated the following principles to characterize stress.

Consider a small surface element centered at $\mathbf{x}$ with area dA and outward normal $\boldsymbol{\nu}$. Suppose this surface is subjected to a force $\mathbf{t}\, dA$ exerted by neighboring particles. The following principles apply:

- **Cauchy's stress principle:** The surface force $\mathbf{t}$ depends only on the spatial point $\mathbf{x}$ and the normal vector $\boldsymbol{\nu}$.
- **Principle of linear momentum:** There exists a second-order tensor $\boldsymbol{\sigma}(\mathbf{x})$ such that

$$\mathbf{t} = \boldsymbol{\sigma}(\mathbf{x}) \cdot \boldsymbol{\nu}, \quad \text{or in components,} \quad t_i = \sigma_{ij}\nu^j. \tag{3.1}$$

- **Principle of angular momentum:** In the absence of internal torques, macroscopic angular momentum is conserved. This implies that

$$\boldsymbol{\sigma}(\mathbf{x}) \text{ is symmetric.}$$

We shall take these principles as given for now; their derivations will be provided in a later chapter.

Composition of the Stress Tensor The stress tensor $\boldsymbol{\sigma}$ consists of two parts: a hydrostatic (isotropic) part and a deviatoric part:

$$\boxed{\boldsymbol{\sigma} = -p\mathbf{I} + \boldsymbol{\tau}.} \tag{3.2}$$

The hydrostatic stress $-p\mathbf{I}$ arises from random microscopic collisions, and it exists even when the macroscopic velocity $\mathbf{v}$ is zero or spatially constant. Under the assumption of isotropy, this thermodynamic stress is modeled as $-p\mathbf{I}$.

The deviatoric stress $\boldsymbol{\tau}$ includes both restorative and resistive effects due to material motion. In solids, this includes elastic stress, but in fluids, the restorative (elastic) part is absent. Hence, in fluid mechanics, $\boldsymbol{\tau}$ is termed the *viscous stress tensor*.

This tensor reflects internal friction and arises when fluid parcels move with differing velocities. Therefore, $\boldsymbol{\tau}$ depends on $\nabla \mathbf{v}$ (and possibly higher derivatives), but vanishes when $\nabla \mathbf{v} = 0$.

For Newtonian fluids, we assume that:

- $\boldsymbol{\tau}$ is a linear function of $\nabla \mathbf{v}$.
- $\boldsymbol{\tau} = 0$ when $\mathbf{v}$ corresponds to a rigid-body motion, which implies that $\boldsymbol{\tau}$ depends only on the shear (deviatoric) part of $\nabla \mathbf{v}$.

We explore this structure next.

3.1.2 Strain Rate

Decomposition of the velocity gradient tensor Recall from (2.18) that the rate of change of the deformation gradient is

$$\dot{F} = (\nabla \mathbf{v})\, F.$$

Define the velocity gradient tensor by

$$L := \nabla \mathbf{v}.$$

This tensor characterizes the local rate of deformation and can be decomposed into symmetric and antisymmetric parts:

$$\nabla \mathbf{v} = \frac{1}{2}\left(\nabla \mathbf{v} + (\nabla \mathbf{v})^T\right) + \frac{1}{2}\left(\nabla \mathbf{v} - (\nabla \mathbf{v})^T\right) =: D + \boldsymbol{\omega}. \tag{3.3}$$

Here,

- D is the *strain-rate tensor* (also called the rate-of-strain tensor), which is symmetric,
- $\boldsymbol{\omega}$ is the *spin tensor*, which is antisymmetric and characterizes local rigid-body rotation.

The strain-rate tensor D can be further decomposed into a deviatoric part and an isotropic part:

$$D_s := D - \frac{1}{3}\operatorname{tr}(D)\,\mathbf{I}, \qquad D_b := \frac{1}{3}\operatorname{tr}(D)\,\mathbf{I}.$$

- D_s is called the *deviatoric strain-rate tensor* and describes shape-changing (shearing) motions,
- D_b is the *volumetric strain-rate tensor* and represents isotropic expansion or compression.

In summary, the velocity gradient tensor admits the decomposition

$$L = D_s + D_b + \boldsymbol{\omega}.$$

Examples We now consider two examples of velocity gradients $\nabla \mathbf{v}$ to understand how fluids respond to different types of deformation.

- **Rigid-body rotation:**

  For fluid undergoing a rigid-body rotation, experimental evidence shows that there is no viscous resistance force. Such a velocity field takes the form:

  $$\mathbf{v} = \boldsymbol{\alpha} \times \mathbf{x}, \qquad \boldsymbol{\alpha} = (\alpha_1, \alpha_2, \alpha_3)^T \text{ is the rotation vector.}$$

  Then, the velocity gradient is:

  $$\nabla \mathbf{v} = \begin{bmatrix} 0 & -\alpha_3 & \alpha_2 \\ \alpha_3 & 0 & -\alpha_1 \\ -\alpha_2 & \alpha_1 & 0 \end{bmatrix},$$

  which is an antisymmetric matrix. That is,

  $$\nabla \mathbf{v} + (\nabla \mathbf{v})^T = 0.$$

  For such flows, the strain-rate tensor $D = 0$ and the spin tensor $\boldsymbol{\omega} = \nabla \mathbf{v}$. Experimental observations show that $\boldsymbol{\tau} = 0$ in this case. Therefore, a physically reasonable constitutive law for Newtonian fluids should satisfy:

  $$\boxed{\boldsymbol{\tau} = 0 \quad \text{when} \quad \nabla \mathbf{v} + (\nabla \mathbf{v})^T = 0.}$$

- **Simple shear flow:**

  Consider the velocity field:

  $$v_1 = \dot{\gamma}_{21} x_2, \quad v_2 = 0, \quad v_3 = 0, \tag{3.4}$$

  where $\dot{\gamma}_{21}$ is a constant called the *shear rate*. The velocity gradient becomes:

  $$\nabla \mathbf{v} = \begin{bmatrix} 0 & \dot{\gamma}_{21} & 0 \\ 0 & 0 & 0 \\ 0 & 0 & 0 \end{bmatrix}.$$

  The symmetric part, i.e. the strain-rate tensor D, is:

  $$D = \frac{1}{2} \begin{bmatrix} 0 & \dot{\gamma}_{21} & 0 \\ \dot{\gamma}_{21} & 0 & 0 \\ 0 & 0 & 0 \end{bmatrix}.$$

  Experiments show that for many fluids (within a wide range of shear rates), the pressure p is independent of $\dot{\gamma}_{21}$, and

  $$\tau_{21} = \mu \dot{\gamma}_{21}$$

  for some constant μ. This constant μ is called the *shear viscosity*.

3.1.3 The Stress–Strain Rate Relation for Newtonian Fluids

Assumptions for Isotropic Newtonian Fluids We assume the following constitutive properties for the viscous stress tensor $\boldsymbol{\tau}$:

(1) $\boldsymbol{\tau}$ is a linear function of the strain-rate tensor $\nabla \mathbf{v}$;

(2) $\boldsymbol{\tau}$ is isotropic (invariant under coordinate rotations);

(3) $\boldsymbol{\tau}$ is symmetric.

From the linearity assumption, we may write:

$$\tau_{ij} = a_{ijkl} \frac{\partial v^k}{\partial x^l},$$

where a_{ijkl} is a fourth-order tensor of constants.

By isotropy, a_{ijkl} must take the general form of an isotropic fourth-order tensor:

$$a_{ijkl} = \alpha \delta_{ij}\delta_{kl} + \beta \delta_{ik}\delta_{jl} + \gamma \delta_{il}\delta_{jk}, \tag{3.5}$$

for some scalars α, β, γ. *

Imposing the symmetry condition $\tau_{ij} = \tau_{ji}$ requires that a_{ijkl} is symmetric in i and j, which implies $\beta = \gamma$. Hence, we have:

$$a_{ijkl} = \alpha \delta_{ij}\delta_{kl} + \beta \left(\delta_{ik}\delta_{jl} + \delta_{il}\delta_{jk}\right). \tag{3.6}$$

Substituting into the stress expression, we obtain:

$$\begin{aligned} \tau_{ij} &= a_{ijkl} \frac{\partial v^k}{\partial x^l} \\ &= \left[\alpha \delta_{ij}\delta_{kl} + \beta \left(\delta_{ik}\delta_{jl} + \delta_{il}\delta_{jk}\right)\right] \frac{\partial v^k}{\partial x^l} \\ &= \alpha \delta_{ij} \frac{\partial v^k}{\partial x^k} + \beta \left(\frac{\partial v^i}{\partial x^j} + \frac{\partial v^j}{\partial x^i} \right). \end{aligned}$$

Thus, the viscous stress tensor takes the form:

$$\boldsymbol{\tau} = 2\beta D + \alpha \ \mathrm{tr}(D)\mathbf{I},$$

where

$$D = \frac{1}{2}\left(\nabla \mathbf{v} + (\nabla \mathbf{v})^T\right) \tag{3.7}$$

is the strain-rate tensor, and $\mathrm{tr}(D) = \nabla \cdot \mathbf{v}$ is its trace.

We now decompose D into:

$$D_s := D - \frac{1}{3}\,\mathrm{tr}(D)\mathbf{I}, \qquad D_b := \frac{1}{3}\,\mathrm{tr}(D)\mathbf{I}.$$

*This follows from the representation theorem for isotropic tensors:

(a) Any isotropic rank-2 tensor must be of the form $Q_{ij} = \alpha \delta_{ij}$.

(b) Any isotropic rank-4 tensor must be a linear combination of $\delta_{ij}\delta_{kl}$, $\delta_{ik}\delta_{jl}$, and $\delta_{il}\delta_{jk}$, i.e., as in (3.5).

Here, - D_s is the *shear strain-rate tensor* (deviatoric part), and - D_b is the *bulk strain-rate tensor* (isotropic part).

Substituting into the expression for $\boldsymbol{\tau}$, we write:

$$\boxed{\boldsymbol{\tau} = 2\mu\, D_s(\mathbf{v}) + 2\zeta\, D_b(\mathbf{v}),}$$

where:

- $\mu := \beta$ is the *shear viscosity*, and
- $\zeta := \frac{1}{2}\alpha + \frac{1}{3}\beta$ is the *bulk viscosity*.

Physically, we require:

$$\boxed{\mu > 0, \qquad \zeta > 0.} \tag{3.8}$$

Remark Since the constitutive relation $\boldsymbol{\tau} = \mathcal{L}(\nabla\mathbf{v})$ is assumed to be linear, isotropic, and symmetric, it follows that the antisymmetric part of $\nabla\mathbf{v}$ cannot contribute to $\boldsymbol{\tau}$.

Indeed, any isotropic, linear tensor-valued function of a second-order tensor must depend only on the symmetric part of its argument. Therefore, the viscous stress $\boldsymbol{\tau}$ depends solely on the strain-rate tensor $D = \frac{1}{2}(\nabla\mathbf{v} + (\nabla\mathbf{v})^T)$, and is completely independent of the spin tensor $\boldsymbol{\omega} = \frac{1}{2}(\nabla\mathbf{v} - (\nabla\mathbf{v})^T)$.

This reflects an important physical principle: *rigid-body rotations do not generate viscous stresses* in a Newtonian fluid. They induce no deformation of fluid elements, only reorientation.

Homework Show that a rank-4 isotropic tensor must have the form

$$A_{ijkl} = \alpha\delta_{ij}\delta_{kl} + \beta\delta_{ik}\delta_{jl} + \gamma\delta_{il}\delta_{jk}$$

for some scalars α, β, γ.

3.2 The Navier–Stokes Equation for Viscous Flows

3.2.1 The Momentum Equation for Viscous Flows

Momentum Equation The viscous force is given by the divergence of the viscous stress tensor:

$$\begin{aligned}\nabla\cdot\boldsymbol{\tau} &= \nabla\cdot\left[\mu\left(\nabla\mathbf{v} + (\nabla\mathbf{v})^T - \frac{2}{3}(\nabla\cdot\mathbf{v})\,\mathbf{I}\right) + \zeta(\nabla\cdot\mathbf{v})\,\mathbf{I}\right]\\ &= \mu\nabla^2\mathbf{v} + \left(\zeta + \frac{\mu}{3}\right)\nabla(\nabla\cdot\mathbf{v}).\end{aligned}$$

In this derivation, we used the identity:

$$\begin{aligned}\partial_j\left(\partial_i v^j + \partial_j v^i - \frac{2}{3}\delta_i^j\partial_k v^k\right) &= \partial_j\partial_i v^j + \partial_j^2 v^i - \frac{2}{3}\partial_i(\partial_k v^k)\\ &= \nabla^2 v^i + \frac{1}{3}\partial_i(\nabla\cdot\mathbf{v}).\end{aligned}$$

Therefore, for compressible viscous flows, the momentum equation becomes:

$$\boxed{\rho\,(\partial_t\mathbf{v} + \mathbf{v}\cdot\nabla\mathbf{v}) + \nabla p = \mu\nabla^2\mathbf{v} + \left(\zeta + \frac{\mu}{3}\right)\nabla(\nabla\cdot\mathbf{v}).} \tag{3.9}$$

Boundary Condition For viscous flows near a fixed boundary, a natural boundary condition is the no-slip condition:

$$\mathbf{v} = \mathbf{0} \quad \text{on the boundary.}$$

3.2.2 Energy Equation and Heat Conduction

The energy equation accounts for the rate-of-work done by internal stress and external body forces, namely $\boldsymbol{\sigma} \cdot \mathbf{v}$ and $\mathbf{f} \cdot \mathbf{v}$.

When temperature gradients are present, microscopic particle motion induces a heat flux $\mathbf{q}$, which is modeled as a function of ∇T. In the linear approximation:

$$\boxed{\mathbf{q} = -\kappa \nabla T,} \tag{3.10}$$

where $\kappa > 0$ is the *thermal conductivity*. This is known as Fourier's law.

Incorporating mechanical work and heat conduction, the energy balance equation becomes:

$$\boxed{\frac{\partial(\rho E)}{\partial t} + \nabla \cdot (\rho E \mathbf{v} - \boldsymbol{\sigma}\mathbf{v} + \mathbf{q}) = \mathbf{f} \cdot \mathbf{v} + \rho r, \quad \text{with } \boldsymbol{\sigma} = -p\mathbf{I} + \boldsymbol{\tau},} \tag{3.11}$$

where $E = \frac{1}{2}|\mathbf{v}|^2 + U$ is the total energy per unit mass, U is the internal energy, and r is the external heat source per unit mass.

Thermal Boundary Conditions Since energy balance involves second derivatives of temperature, natural boundary conditions are of mixed type. Let the domain boundary Γ be decomposed into disjoint parts:

$$\Gamma = \Gamma_d \cup \Gamma_n \cup \Gamma_0, \quad \text{with } \operatorname{area}(\Gamma_0) = 0.$$

We prescribe:

$$\begin{cases} T(\mathbf{x}) = T_d(\mathbf{x}) & \text{on } \Gamma_d \quad \text{(Dirichlet)}, \\ \nabla T \cdot \boldsymbol{\nu}(\mathbf{x}) = g(\mathbf{x}) & \text{on } \Gamma_n \quad \text{(Neumann)}, \end{cases}$$

where $\boldsymbol{\nu}$ is the outward unit normal.

3.3 Second Law of Thermodynamics for Viscous Flows

3.3.1 Dissipation of Kinetic Energy

The kinetic energy density per unit mass is defined as $E_k := \dfrac{1}{2}|\mathbf{v}|^2$. We will show that the quantity ρE_k decays due to viscous friction. To analyze the evolution of kinetic energy, we follow the classical mechanics approach by taking the dot product of the momentum equation with the velocity field $\mathbf{v}$. On the left-hand side, this yields the time derivative of the kinetic energy density:

$$\begin{aligned} \mathbf{v} \cdot [\rho (\partial_t \mathbf{v} + \mathbf{v} \cdot \nabla \mathbf{v})] &= \partial_t \left(\frac{1}{2} \rho |\mathbf{v}|^2 \right) + \nabla \cdot (\rho \mathbf{v}) \cdot \frac{|\mathbf{v}|^2}{2} + \rho v^i v^j \partial_j v^i \\ &= \partial_t \left(\frac{1}{2} \rho |\mathbf{v}|^2 \right) + \nabla \cdot \left(\frac{1}{2} \rho |\mathbf{v}|^2 \mathbf{v} \right). \end{aligned}$$

The pressure gradient term in the momentum equation contributes:

$$\mathbf{v} \cdot \nabla p = \nabla \cdot (p\mathbf{v}) - p\nabla \cdot \mathbf{v}.$$

The viscous force contributes:

$$\begin{aligned}
\mathbf{v} \cdot (\nabla \cdot \boldsymbol{\tau}) &= \nabla \cdot (\boldsymbol{\tau} \cdot \mathbf{v}) - \nabla \mathbf{v} : \boldsymbol{\tau} \\
&= \nabla \cdot (\boldsymbol{\tau} \cdot \mathbf{v}) - \frac{1}{2} \left(\nabla \mathbf{v} + (\nabla \mathbf{v})^T \right) : \boldsymbol{\tau} \\
&= \nabla \cdot (\boldsymbol{\tau} \cdot \mathbf{v}) - \boldsymbol{\tau} : D,
\end{aligned}$$

where $A : B := \sum_{ij} a_{ij} b_{ij}$ denotes the Frobenius inner product of tensors. Note that in the second step above, we use the symmetry of $\boldsymbol{\tau}$ to write

$$\nabla \mathbf{v} : \boldsymbol{\tau} = \frac{1}{2} \left(\nabla \mathbf{v} + (\nabla \mathbf{v})^T \right) : \boldsymbol{\tau} = D : \boldsymbol{\tau}.$$

Recall the viscous stress expression:

$$\boldsymbol{\tau} = 2\mu D_s + 2\zeta D_b, \qquad D = D_s + D_b,$$

and note that $D_s : D_b = 0$ due to orthogonality. Therefore,

$$\boxed{\boldsymbol{\tau} : D = 2\mu |D_s|^2 + 2\zeta |D_b|^2 > 0,} \tag{3.12}$$

which represents the rate of viscous dissipation. Note that $|D_s|^2 = D_s : D_s$.

Putting all terms together, we obtain the kinetic energy balance:

$$\boxed{\partial_t (\rho E_k) + \nabla \cdot [(\rho E_k \mathbf{I} + p\mathbf{I} - \boldsymbol{\tau}) \cdot \mathbf{v}] - p\, \nabla \cdot \mathbf{v} = -\boldsymbol{\tau} : D.}$$

Interpretation:

- $\rho E_k = \frac{1}{2} \rho |\mathbf{v}|^2$ is the kinetic energy density;
- $\nabla \cdot \mathbf{v} = \frac{1}{V} \frac{dV}{dt}$ describes local volume change rate;
- $p \nabla \cdot \mathbf{v}$ represents the power exerted by volumetric compression or expansion;
- The term $2\mu |D_s|^2$ is the rate of kinetic energy dissipated by viscous shear stresses;
- The term $2\zeta |D_b|^2$ accounts for dissipation due to volumetric (bulk) compression or expansion;
- Both terms on the right-hand side represent irreversible conversion of kinetic energy into internal energy (heat), in accordance with the second law of thermodynamics.

Incompressible Case: When $\nabla \cdot \mathbf{v} = 0$, the bulk dissipation term vanishes, and we have:

$$\partial_t (\rho E_k) + \nabla \cdot [(\rho E_k \mathbf{I} + p\mathbf{I} - \boldsymbol{\tau}) \cdot \mathbf{v}] = -2\mu |D_s|^2.$$

This reflects the net decay of kinetic energy purely due to shear viscosity.

3.3.2 Entropy Production and the Clausius–Duhem Inequality

We begin by subtracting the kinetic energy equation from the total energy equation:

$$\partial_t(\rho E) + \nabla \cdot [(\rho E + p)\mathbf{v}] = \nabla \cdot (\boldsymbol{\tau} \cdot \mathbf{v} - \mathbf{q}) + \rho r,$$

which yields the equation for internal energy:

$$\partial_t(\rho U) + \nabla \cdot (\rho U \mathbf{v}) = -p\, \nabla \cdot \mathbf{v} - \nabla \cdot \mathbf{q} + \boldsymbol{\tau} : D + \rho r.$$

Interpretation:

- ρU is the internal energy density;
- $-p\, \nabla \cdot \mathbf{v}$ represents mechanical work done by the surrounding fluid;
- $-\nabla \cdot \mathbf{q}$ accounts for energy transport due to heat conduction;
- $\boldsymbol{\tau} : D$ is the energy input due to viscous dissipation — corresponding to the heat lost from kinetic energy;
- ρr is the external heat source.

From the continuity equation, this can be written in material form:

$$\rho \frac{dU}{dt} = -p\, \nabla \cdot \mathbf{v} - \nabla \cdot \mathbf{q} + \boldsymbol{\tau} : D + \rho r.$$

From the first law of thermodynamics,

$$dU = T\, dS - p\, dV,$$

we obtain:

$$\rho \frac{dU}{dt} = \rho T \frac{dS}{dt} - p \nabla \cdot \mathbf{v}.$$

Substituting this into the energy equation gives:

$$\rho T \frac{dS}{dt} = -\nabla \cdot \mathbf{q} + \boldsymbol{\tau} : D + \rho r,$$

or

$$\rho \frac{dS}{dt} = -\frac{\nabla \cdot \mathbf{q}}{T} + \frac{1}{T} \boldsymbol{\tau} : D + \frac{\rho r}{T}.$$

To obtain the conservative form, we use:

$$\frac{\nabla \cdot \mathbf{q}}{T} = \nabla \cdot \left(\frac{\mathbf{q}}{T} \right) + \frac{1}{T^2} \mathbf{q} \cdot \nabla T,$$

and add $S(\partial_t \rho + \nabla \cdot (\rho \mathbf{v})) = 0$ to get:

$$\partial_t(\rho S) + \nabla \cdot (\rho S \mathbf{v}) + \nabla \cdot \left(\frac{\mathbf{q}}{T} \right) - \frac{\rho r}{T} = \frac{\rho r_d}{T},$$

where the entropy production rate r_d is defined as

$$\frac{\rho r_d}{T} := -\frac{1}{T^2} \mathbf{q} \cdot \nabla T + \frac{1}{T} \boldsymbol{\tau} : D.$$

Interpretation: This equation expresses the local entropy balance in a viscous, heat-conducting fluid. The left-hand side is written in conservative form, while the right-hand side represents entropy production.

- The quantity $\dfrac{\mathbf{q}}{T}$ is the entropy flux vector, representing the entropy transported by heat conduction. The term $\nabla \cdot (\mathbf{q}/T)$ is the net entropy outflow due to thermal diffusion.
- The term $\frac{\rho r}{T}$ is the entropy input rate from external heat sources.
- The term $-\frac{1}{T^2}\mathbf{q} \cdot \nabla T$ represents entropy production due to heat conduction. Under Fourier's law $\mathbf{q} = -\kappa \nabla T$ with $\kappa > 0$, this term becomes

$$\frac{\kappa}{T^2}|\nabla T|^2 > 0.$$

- The term $\frac{1}{T}\boldsymbol{\tau} : D$ is the entropy production due to viscous dissipation. For Newtonian fluids with $\mu, \zeta \geq 0$, it is also non-negative.
- The total entropy production rate is

$$\rho r_d = \kappa \frac{|\nabla T|^2}{T} + 2\mu |D_s|^2 + 2\zeta |D_b|^2 \geq 0.$$

Theorem 3.1 (Clausius–Duhem Inequality: Differential Form)**.** *Let ρr_d denote the local entropy production rate due to irreversible processes. Then the second law of thermodynamics is expressed as:*

$$\boxed{\partial_t(\rho S) + \nabla \cdot (\rho S \mathbf{v}) + \nabla \cdot \left(\frac{\mathbf{q}}{T}\right) - \frac{\rho r}{T} = \frac{\rho r_d}{T}.}$$

Under the Newtonian constitutive laws with Fourier heat conduction, the entropy production rate satisfies:

$$\boxed{\rho r_d = \kappa \frac{|\nabla T|^2}{T} + 2\mu |D_s|^2 + 2\zeta |D_b|^2 \geq 0,}$$

which holds if and only if the transport coefficients obey:

$$\boxed{\kappa \geq 0, \quad \mu \geq 0, \quad \zeta \geq 0.}$$

Homework

1. Consider incompressible Newtonian flows with the no-slip boundary condition:

$$\mathbf{v} = 0 \quad \text{on } \partial\Omega.$$

   Define the normal viscous stress as $\boldsymbol{\tau}_N := \boldsymbol{\tau} \cdot \boldsymbol{\nu}$. Show that $\boldsymbol{\tau}_N = 0$ on the boundary.

2. Derive the entropy production formula in the Lagrangian coordinate system.

Remark

1. Consider the heat equation $c_v T_t = \nabla \cdot (\kappa \nabla T)$. Dividing by T and integrating over Ω yields:

$$\begin{aligned}\int_\Omega c_v \frac{T_t}{T}\, d\mathbf{x} &= \int_\Omega \frac{1}{T} \nabla \cdot (\kappa \nabla T)\, d\mathbf{x} \\ &= \int_\Omega \frac{\kappa}{T^2} |\nabla T|^2\, d\mathbf{x} > 0.\end{aligned}$$

   Thus, defining the specific entropy $s := c_v \log T$, we obtain

$$\frac{d}{dt} \int_\Omega s\, d\mathbf{x} > 0.$$

Remark In the variational (Lagrangian or Hamiltonian) formulation of fluid mechanics, the internal energy is given by

$$\mathcal{U} = \int \rho\, U(S, V)\, dV,$$

where U is the specific internal energy, S the specific entropy, and V the specific volume. This formulation assumes that the entropy S is constant along particle trajectories, i.e., $dS/dt = 0$. Under this assumption, the thermodynamic pressure is given by

$$p = -\left(\frac{\partial U}{\partial V}\right)_S.$$

In viscous flows, however, entropy is no longer conserved: internal friction leads to entropy production, and $dS/dt > 0$. As a result, the variational principle is no longer directly applicable. Despite this, one typically continues to use the same pressure formula $p = -(\partial U/\partial V)_S$.

This is justified by the *local equilibrium assumption*: even in the presence of viscosity, it is assumed that each fluid element is locally near thermodynamic equilibrium, so a thermodynamic pressure p can still be defined as a state function of the local density ρ and entropy S. In the Navier–Stokes equations, the Cauchy stress tensor is decomposed as

$$\boldsymbol{\sigma} = -p\, \mathbf{I} + \boldsymbol{\tau},$$

where p is the thermodynamic pressure and $\boldsymbol{\tau}$ is the viscous stress tensor. In this framework, the total stress accounts for both equilibrium (pressure) and non-equilibrium (viscous) effects. Although the entropy evolves due to viscous dissipation and heat conduction, the pressure remains defined via the thermodynamic relation at each point in time and space.

Even in the limit of large viscosity, where viscous stresses dominate the dynamics, the thermodynamic pressure p remains a valid and useful quantity representing the isotropic part of the stress tensor.

3.4 Dimensional Analysis

3.4.1 Nondimensional Compressible Navier-Stokes Equations

The compressible Navier-Stokes equations are:

$$\underbrace{\partial_t \rho}_{\text{(mass change rate)}} + \underbrace{\nabla \cdot (\rho \mathbf{v})}_{\text{(mass convection)}} = 0, \tag{3.13}$$

$$\underbrace{\partial_t (\rho \mathbf{v})}_{\text{(inertia)}} + \underbrace{\nabla \cdot (\rho \mathbf{v} \otimes \mathbf{v})}_{\text{(momentum convection)}} = \underbrace{-\nabla p}_{\text{(pressure gradient)}} + \underbrace{\nabla \cdot \boldsymbol{\tau}}_{\text{(viscous stress)}}, \tag{3.14}$$

$$\underbrace{\partial_t E}_{\text{(rate of energy change)}} + \underbrace{\nabla \cdot [(E+p)\mathbf{v}]}_{\text{(energy convection + pressure work)}} = \underbrace{\nabla \cdot (\boldsymbol{\tau} \cdot \mathbf{v})}_{\text{(viscous work)}} - \underbrace{\nabla \cdot \mathbf{q}}_{\text{(heat conduction)}}. \tag{3.15}$$

We now carry out a dimensional analysis of the compressible Navier–Stokes equations using the following **basic characteristic scales**:

- L: characteristic length,
- t_{char}: characteristic time,
- V: characteristic velocity,
- ρ_0: characteristic density,
- T_0: characteristic temperature.

We use these basic characteristic scales to define the following reference quantities, based on thermodynamic relations and dimensional analysis:

- $c_0 = \sqrt{\gamma R T_0}$: reference sound speed,
- $p_0 = \rho_0 c_0^2$: reference pressure,
- $E_0 = \rho_0 V^2$: reference total energy density,
- $\tau_0 = \dfrac{\mu V}{L^2}$: reference viscous stress,
- $q_0 = \dfrac{\kappa(\gamma - 1) T_0}{L}$: reference heat flux.

We define the nondimensional variables:

$$\mathbf{x}^* = \frac{\mathbf{x}}{L}, \qquad t^* = \frac{t}{t_{\text{char}}}, \qquad \mathbf{v}^* = \frac{\mathbf{v}}{V}, \qquad \rho^* = \frac{\rho}{\rho_0},$$
$$p^* = \frac{p}{p_0}, \qquad E^* = \frac{E}{E_0}, \qquad \boldsymbol{\tau}^* = \frac{\boldsymbol{\tau}}{\tau_0}, \qquad \mathbf{q}^* = \frac{\mathbf{q}}{q_0}.$$

Substituting these nondimensional variables into the dimensional Navier–Stokes equations, we obtain:

$$\left[\frac{\rho_0}{t_{\text{char}}}\right] \partial_{t^*} \rho^* + \left[\frac{\rho_0 V}{L}\right] \nabla^* \cdot (\rho^* \mathbf{v}^*) = 0,$$

$$\left[\frac{\rho_0 V}{t_{\text{char}}}\right]\partial_{t^*}(\rho^*\mathbf{v}^*)+\left[\frac{\rho_0 V^2}{L}\right]\nabla^*\cdot(\rho^*\mathbf{v}^*\otimes\mathbf{v}^*)=-\left[\frac{p_0}{L}\right]\nabla^* p^*+\left[\frac{\tau_0}{L}\right]\nabla^*\cdot\boldsymbol{\tau}^*,$$

$$\left[\frac{E_0}{t_{\text{char}}}\right]\partial_{t^*}E^*+\left[\frac{E_0 V}{L}\right]\nabla^*\cdot\left[\left(E^*+\left[\frac{p_0}{E_0}\right]p^*\right)\mathbf{v}^*\right]=\left[\frac{\tau_0 V}{L}\right]\nabla^*\cdot(\boldsymbol{\tau}^*\cdot\mathbf{v}^*)-\left[\frac{q_0}{L}\right]\nabla^*\cdot\mathbf{q}^*.$$

We normalize the coefficients of the convection terms to be 1 by introducing the following dimensionless parameters Batchelor (1967); White (2006):

$$\text{St}=\frac{L}{V t_{\text{char}}},\qquad \text{Ma}=\frac{V}{c_0},\qquad \text{Re}=\frac{\rho_0 V L}{\mu},\qquad \text{Pr}=\frac{c_p\mu}{\kappa},\qquad \zeta^*=\frac{\zeta}{\mu}.$$

This yields the following dimensionless form of the compressible Navier–Stokes equations:

$$\text{St}\cdot\partial_{t^*}\rho^*+\nabla^*\cdot(\rho^*\mathbf{v}^*)=0, \tag{3.16}$$

$$\text{St}\cdot\partial_{t^*}(\rho^*\mathbf{v}^*)+\nabla^*\cdot(\rho^*\mathbf{v}^*\otimes\mathbf{v}^*)=-\frac{1}{\text{Ma}^2}\nabla^* p^*+\frac{1}{\text{Re}}\nabla^*\cdot\boldsymbol{\tau}^*, \tag{3.17}$$

$$\text{St}\cdot\partial_{t^*}E^*+\nabla^*\cdot\left[\left(E^*+\frac{1}{\text{Ma}^2}p^*\right)\mathbf{v}^*\right]=\frac{1}{\text{Re}}\nabla^*\cdot(\boldsymbol{\tau}^*\cdot\mathbf{v}^*)-\frac{1}{\text{Re}\cdot\text{Pr}\cdot\text{Ma}^2}\nabla^*\cdot\mathbf{q}^*, \tag{3.18}$$

with

$$\boldsymbol{\tau}^*=\left(\nabla^*\mathbf{v}^*+(\nabla^*\mathbf{v}^*)^T-\tfrac{2}{3}(\nabla^*\cdot\mathbf{v}^*)\mathbb{I}\right)+\zeta^*(\nabla^*\cdot\mathbf{v}^*)\mathbb{I},$$

$$\mathbf{q}^*=-\nabla^* T^*.$$

We now compute the dimensionless coefficient in front of the heat conduction term. It is given by the ratio between the scale of heat flux and the scale of energy flux:

$$\frac{q_0/L}{E_0 V/L}.$$

Choosing

$$q_0=\frac{\kappa(\gamma-1)T_0}{L},\quad E_0=\rho_0 V^2,$$

we obtain

$$\frac{q_0/L}{E_0 V/L}=\frac{(\gamma-1)\kappa T_0}{\rho_0 V^3 L}.$$

Now, using the identities

$$\kappa=\frac{c_p\mu}{\text{Pr}},\quad \mu=\frac{\rho_0 V L}{\text{Re}},\quad T_0=\frac{c_0^2}{\gamma R},$$

we compute

$$\frac{\kappa T_0}{\rho_0 V^3 L}=\frac{c_p\mu T_0}{\text{Pr}\cdot\rho_0 V^3 L}=\frac{c_p}{\text{Pr}}\cdot\frac{1}{\text{Re}}\cdot\frac{T_0}{V^2}=\frac{c_p}{\gamma R}\cdot\frac{1}{\text{Pr}\cdot\text{Re}\cdot\text{Ma}^2}.$$

Since $c_p=\dfrac{\gamma R}{\gamma-1}$, we find:

$$\frac{c_p}{\gamma R}=\frac{1}{\gamma-1}.$$

Therefore, the coefficient becomes

$$\frac{(\gamma-1)\kappa T_0}{\rho_0 V^3 L}=\frac{1}{\text{Re}\cdot\text{Pr}\cdot\text{Ma}^2}.$$

3.4.2 Physical Interpretation of Dimensionless Parameters

$\mathrm{St} \ll 1$ (Quasi-steady flow): The flow evolves slowly compared to the convection time scale. Time derivatives are negligible, and the system is approximately steady. This regime is relevant for slowly varying or slowly driven flows.

$\mathrm{St} \gg 1$ (Rapidly unsteady flow): Unsteady effects dominate over convective transport. This regime arises when the characteristic time scale of the flow is much shorter than the convective time scale L/V, such as in rapidly oscillating flows, sudden accelerations, or shock formation. In the dimensionless equations, the Strouhal number St multiplies all time-derivative terms. When $\mathrm{St} \gg 1$, the governing equations become highly sensitive to unsteadiness.

Physically, high Strouhal number flows exhibit temporally rich dynamics and often undergo bifurcations from steady to unsteady patterns. A classical example is *vortex shedding* behind a bluff body, such as a circular cylinder: as the flow speed increases and St grows, the initially steady wake becomes unstable and transitions to a periodic vortex street. Further increase may lead to quasiperiodicity or chaotic behavior.

The phenomenon was first studied experimentally by Vincent Strouhal in 1878, who measured the frequency of tones generated by wires vibrating in an air stream[†]. The theoretical explanation of the alternating vortex pattern was later developed by Theodore von Kármán, now known as the von Kármán vortex street.

This regime is essential in studying dynamic instabilities, flow-induced vibrations, aeroacoustics, and time-dependent propulsion systems.

$\mathrm{Re} \ll 1$ (Creeping or Stokes flow): Viscous forces dominate over inertial forces. This occurs when the Reynolds number $\mathrm{Re} = \rho_0 V L/\mu$ is small, meaning momentum diffusion overwhelms advection. The resulting flow is smooth, laminar, and highly damped.

In this regime, the inertial terms in the momentum equation are negligible, and the flow is governed by the *Stokes equations*:

$$-\nabla p + \nabla \cdot \boldsymbol{\tau} = \mathbf{0}, \qquad \nabla \cdot \mathbf{v} = 0,$$

where $\boldsymbol{\tau} = \mu(\nabla \mathbf{v} + \nabla \mathbf{v}^T)$ is the viscous stress tensor. These equations are linear and elliptic, making them much more tractable than the full Navier–Stokes system.

Stokes flow is *reversible* and lacks flow separation or turbulence. It is typical in:

- Microfluidics and lab-on-a-chip devices,
- Flow through porous media,
- Lubrication theory,
- Slow sedimentation or motion of small organisms (e.g., bacteria swimming).

Because the flow adjusts instantaneously to external forces, time-dependent effects are often negligible unless the Strouhal number is large. As $\mathrm{Re} \to 0$, the dimensionless Navier–Stokes equations reduce to:

$$-\nabla^* p^* + \nabla^* \cdot \boldsymbol{\tau}^* = \mathbf{0}, \qquad \nabla^* \cdot \mathbf{v}^* = 0,$$

[†]V. Strouhal, "Über eine besondere Art der Tonerregung," *Annalen der Physik*, vol. 241, no. 10, pp. 216–251, 1878.

defining the nondimensional Stokes flow.

$\mathrm{Re} \gg 1$ (Inviscid or turbulent flow): Inertial forces dominate over viscous forces. This regime arises when the Reynolds number $\mathrm{Re} = \rho_0 V L/\mu$ is large, indicating that momentum is transported primarily by advection rather than viscous diffusion.

Since the viscous term in the dimensionless equations is multiplied by $1/\mathrm{Re}$, it becomes negligible as $\mathrm{Re} \to \infty$. The flow is then approximately governed by the *inviscid Euler equations*:

$$\partial_t(\rho \mathbf{v}) + \nabla \cdot (\rho \mathbf{v} \otimes \mathbf{v}) = -\nabla p.$$

The Euler equations admit discontinuous weak solutions. Shocks are characterized by jumps in pressure p, normal velocity $\mathbf{v}_n$, and entropy S; contact discontinuities involve jumps in density ρ and tangential velocity $\mathbf{v}_t$, while maintaining continuity of p and $\mathbf{v}_n$.

Although viscosity is small, it plays a crucial role near discontinuities: shocks and contact discontinuities are regularized into thin internal layers whose thickness is controlled by viscous and thermal effects. Moreover, viscous forces cannot be neglected near solid boundaries or in thin shear layers. This gives rise to *boundary layers*, in which velocity transitions rapidly from the no-slip condition at the wall to the inviscid outer flow. The typical boundary layer thickness scales like $\delta \sim L/\sqrt{\mathrm{Re}}$.

At sufficiently high Re, these viscous layers may become unstable, leading to *transition to turbulence*, characterized by vortex stretching, chaotic motion, and enhanced mixing. High Reynolds number flows are typical in aerodynamics (e.g., airflow over wings), geophysical flows (e.g., ocean and atmospheric currents), and industrial applications (e.g., pipeline transport, combustion).

Thus, while the bulk flow may be well-approximated as inviscid, accurate modeling requires special treatment of near-wall viscous effects and turbulent stresses.

$\mathrm{Ma} \ll 1$ (Low Mach number): Flow speed is much less than the sound speed. Pressure adjusts nearly instantaneously, and density variations are negligible—leading to incompressible or nearly incompressible behavior. This can be justified as follows: from the momentum equation, small Mach number implies that the pressure gradient scales like $\nabla p \sim \mathcal{O}(\mathrm{Ma}^2)$, so pressure is nearly uniform. Using the ideal gas law $p = \rho R T$, we take the gradient:

$$\nabla p = R(T \nabla \rho + \rho \nabla T).$$

If $\nabla p \approx 0$, then $T\nabla\rho + \rho\nabla T \approx 0$. In the isothermal case ($\nabla T = 0$), this directly implies $\nabla \rho \approx 0$. More generally, if $\nabla T = \mathcal{O}(\mathrm{Ma}^2)$, then $\nabla \rho = \mathcal{O}(\mathrm{Ma}^2)$ as well. Therefore, in the limit $\mathrm{Ma} \to 0$, density becomes nearly constant and the incompressibility condition $\nabla \cdot \mathbf{v} \approx 0$ follows.

$\mathrm{Ma} \gg 1$ (High Mach number): High Mach number flows arise in **supersonic and hypersonic aerodynamics**, such as around high-speed jets, shock tubes, reentry vehicles, and astrophysical jets. Classical theories such as the Rankine–Hugoniot conditions and Prandtl–Meyer expansions describe their structure and transitions.

$\mathrm{Pr} \ll 1$ (High thermal diffusivity): The Prandtl number $\mathrm{Pr} = \mu c_p/\kappa$ compares the rate of momentum diffusion (viscosity) to thermal diffusion (conductivity). When $\mathrm{Pr} \ll 1$, the thermal diffusivity

κ is much larger than the kinematic viscosity $\nu = \mu/\rho$. As a result, heat spreads through the fluid much faster than momentum.

This has a major impact on boundary layer structure. In forced convection problems, the thermal boundary layer — the region over which temperature adjusts — becomes much *thicker* than the velocity boundary layer. That is,

$$\delta_T \gg \delta_v,$$

where δ_T and δ_v are the characteristic thicknesses of the thermal and velocity boundary layers, respectively.

Physically, this means that temperature gradients are relatively mild compared to sharp velocity gradients near walls or solid surfaces. As a result, heat conduction dominates over convection in the near-wall region. This behavior is typical of low-Prandtl-number fluids such as **liquid metals** (e.g., mercury, sodium, lead–bismuth eutectic), which are often used in nuclear cooling systems and metallurgical processes.

In such flows, care must be taken when modeling the thermal field: simple boundary-layer approximations for velocity may no longer be valid for temperature, and additional transport effects may arise from conduction-dominated diffusion.

$\mathrm{Pr} \gg 1$ (Low thermal diffusivity): The Prandtl number $\mathrm{Pr} = \mu c_p/\kappa$ compares the rate of momentum diffusion (viscous effects) to thermal diffusion (heat conduction). When $\mathrm{Pr} \gg 1$, the thermal diffusivity κ is small compared to the kinematic viscosity $\nu = \mu/\rho$, meaning that heat diffuses slowly relative to momentum.

In this regime, the velocity adjusts quickly due to high viscosity, while temperature gradients persist longer and are confined to thinner regions near the wall. Consequently, the thermal boundary layer is much *thinner* than the velocity boundary layer:

$$\delta_T \ll \delta_v.$$

This implies that temperature varies sharply across a narrow thermal layer near surfaces, whereas velocity transitions more gradually. Convective heat transport dominates over conductive heat diffusion, and accurate resolution of the near-wall temperature profile becomes critical.

Such behavior is typical in fluids with high viscosity and low thermal conductivity, including **oils, glycerin, and molten polymers**. In these fluids, thermal inertia is large, and it takes more time for heat to penetrate the bulk.

In practical applications like lubrication, cooling of viscous materials, and food processing, models must resolve fine thermal gradients to accurately predict heat transfer, especially in wall-bounded flows.

Chapter 4

Flow Invariants for Inviscid Fluid Flows

4.1 Introduction

In this chapter, we consider inviscid fluid flows. The governing equation is the Euler equation. In the preceding chapter, we established that the entropy S remains invariant along the trajectory of a fluid parcel. In this chapter, we explore additional flow invariants, focusing on those associated with energy and vorticity dynamics. The key theoretical frameworks include the Bernoulli principle and Kelvin's circulation theorem Batchelor (1967); Majda and Bertozzi (2002).

4.1.1 The Euler Equation in Lamb Form

We begin with the Euler equation for a fluid subject to a conservative body force (see equation (2.3)):

$$\frac{\partial \mathbf{v}}{\partial t} + \mathbf{v} \cdot \nabla \mathbf{v} + \frac{1}{\rho} \nabla p = \frac{\mathbf{f}}{\rho} = -\nabla \Phi,$$

where $\mathbf{f}$ is the body force per unit mass and Φ is a scalar potential function. A classical example is gravity, where $\Phi = gx^3$ in Cartesian coordinates.

The central idea of this chapter is to decompose each term in the Euler equation into a "potential part" and a "rotation part." Using a vector identity, the convection term can be decomposed as

$$\mathbf{v} \cdot \nabla \mathbf{v} = \underbrace{\nabla \left(\frac{1}{2} |\mathbf{v}|^2 \right)}_{\text{potential}} + \underbrace{(\nabla \times \mathbf{v}) \times \mathbf{v}}_{\text{rotation}} = \nabla \left(\frac{1}{2} |\mathbf{v}|^2 \right) + \boldsymbol{\omega} \times \mathbf{v},$$

where $\boldsymbol{\omega} := \nabla \times \mathbf{v}$ denotes the vorticity.

By Gibbs' relation, the pressure gradient can be expressed as

$$\frac{1}{\rho} \nabla p = \nabla h - T \nabla S,$$

where h denotes the specific enthalpy. Substituting this into the momentum equation, we arrive at the so-called *Lamb form* of the Euler equation:

$$\boxed{\partial_t \mathbf{v} + \boldsymbol{\omega} \times \mathbf{v} + \nabla H = T \nabla S,} \tag{4.1}$$

where

$$H = \left(\frac{1}{2}|\mathbf{v}|^2 + h + \Phi \right)$$

represents the total head (sum of kinetic, enthalpy, and potential energy per unit mass).

This formulation reveals that fluid acceleration consists of three fundamental contributions:

(i) A *vorticity force* $\boldsymbol{\omega} \times \mathbf{v}$, accounting for rotational effects,

(ii) A *conservative force* $\nabla \left(\frac{1}{2}|\mathbf{v}|^2 + h + \Phi \right)$, associated with energy gradients,

(iii) A *buoyancy force* $T\nabla S$, driven by entropy variations.

By taking the inner product of the Euler equation with the velocity field $\mathbf{v}$, we eliminate the rotational contribution, leading to the conservation of the quantity H along streamlines for steady flows — the essence of the Bernoulli principle. Alternatively, taking the *curl* of the Lamb form removes the conservative part and yields an evolution equation for the vorticity, from which the circulation theorem arises.

These fundamental ideas will be developed systematically in the next two sections.

We now begin with the derivation of the Bernoulli principle under various physical scenarios.

Historical Remark

1. The vorticity-based reformulation of the Euler equations, often referred to as the *Lamb form*, was systematically presented by Horace Lamb in his classical treatise *Hydrodynamics* Lamb (1932b). The underlying concept of vorticity and its role in fluid motion had already been recognized earlier, notably by Hermann von Helmholtz in his seminal 1858 work on vortex dynamics. However, it was Lamb who organized and formalized the modern presentation, making the Lamb form a standard and influential tool in fluid dynamics.

2. This Lamb form of the Euler equation is also referred to as *Fridman's equation* in some texts Kochin et al. (1964).

3. The term $\mathbf{v} \times \boldsymbol{\omega}$ is often called the *vortex force*, a term attributed to Prandtl Saffman (1992).

4.2 Bernoulli Principle

4.2.1 Introduction

The Bernoulli principle is a cornerstone of classical fluid dynamics, originally formulated by Daniel Bernoulli in the 18th century. It expresses a balance between kinetic energy, potential energy, and pressure along the trajectories of fluid parcels in steady, inviscid flows.

In modern terms, the Bernoulli principle can be derived directly from the Euler equations of motion under suitable thermodynamic assumptions. In particular, when the flow is *isentropic* (i.e., each fluid parcel conserves its entropy) and the body force is conservative, an energy-like quantity

$$H := \frac{1}{2}|\mathbf{v}|^2 + h + \Phi$$

is conserved along streamlines, where $\mathbf{v}$ is the velocity field, h is the specific enthalpy, and Φ is the external potential (e.g., gravitational potential).

This chapter first presents the general derivation of the Bernoulli invariant for steady isentropic flows, then systematically explores important special cases: barotropic flows, incompressible constant-density flows, and irrotational flows. The section concludes with physical interpretations and practical applications of the Bernoulli principle in classical and geophysical fluid dynamics.

4.2.2 Bernoulli Principle for Steady Isentropic Flows

Theorem 4.1 (Bernoulli Principle)**.** *For steady, inviscid, isentropic flows under a conservative body force $-\rho\nabla\Phi$, the quantity*

$$H := \frac{1}{2}|\mathbf{v}|^2 + h + \Phi \tag{4.2}$$

remains constant along every streamline (i.e., along the integral curves of the velocity field $\mathbf{v}$) in smooth regions of the flow.

Proof. For steady flows, the time derivative vanishes, $\partial_t \mathbf{v} = 0$. The Euler equation reduces to the Crocco relation **?**:

$$\boldsymbol{\omega} \times \mathbf{v} + \nabla H = T\nabla S.$$

Taking the inner product with $\mathbf{v}$ yields:

$$\mathbf{v} \cdot \nabla H = T\,\mathbf{v} \cdot \nabla S = 0,$$

along the integral curves of $\mathbf{v}$. The last equality follows because the flow is steady and isentropic, implying $\mathbf{v} \cdot \nabla S = 0$. Thus, the directional derivative of H along $\mathbf{v}$ vanishes, indicating that H remains constant along streamlines. □

Remarks

1. The Bernoulli theorem provides an algebraic relation between the kinematic variable $\mathbf{v}$, the thermodynamic variable h, and the external potential Φ.

2. This result is often used to derive simplified pressure-velocity relationships in steady flows such as pipe flows, wind tunnels, or inviscid jets.

3. In steady isentropic flows, the Bernoulli quantity H is constant along streamlines, but not necessarily across different streamlines unless the flow is also irrotational.

4. Note that the Bernoulli principle is derived purely from the momentum equation — no explicit use of the energy conservation law is made. The derivation is analogous to the conservation of mechanical energy in classical mechanics. *

5. In the presence of discontinuities, such as shock waves, the isentropic condition holds only in smooth regions; entropy typically exhibits a discontinuous jump across shocks.

*Compare with classical mechanics: For a particle of mass m subject to a conservative force $-\nabla\Phi(\mathbf{x})$, Newton's second law gives $m\ddot{\mathbf{x}} = -\nabla\Phi$. Multiplying by $\dot{\mathbf{x}}$ and integrating yields conservation of mechanical energy:

$$\frac{d}{dt}\left(\frac{1}{2}m|\dot{\mathbf{x}}|^2 + \Phi\right) = 0,$$

along particle trajectories.

4.2.3 Special Cases of the Bernoulli Principle

We now examine several important special cases of the Bernoulli principle for steady flows.

Barotropic Flows

- In a barotropic flow, the pressure is a function of density alone:

$$p = p(\rho).$$

  Since entropy is effectively constant along particle paths, the pressure gradient term $\frac{1}{\rho}\nabla p$ in the Euler equation is indeed a gradient of the enthalpy:

$$\frac{1}{\rho}\nabla p = \nabla h(\rho), \quad h(\rho) = \int \frac{p'(\rho)}{\rho}\, d\rho.$$

  The Euler equation in Lamb form is reduced to

$$\boxed{\partial_t \mathbf{v} + \boldsymbol{\omega} \times \mathbf{v} + \nabla H = 0.} \tag{4.3}$$

  The Bernoulli quantity

$$H = \frac{1}{2}|\mathbf{v}|^2 + h(\rho) + \Phi$$

  remains constant along streamlines.

- For steady barotropic flows, the equation becomes:

$$\boldsymbol{\omega} \times \mathbf{v} + \nabla H = 0. \tag{4.4}$$

  We observe that H remains constant along the integral curve of $\mathbf{v}$. Similarly, applying the same procedure, we derive:

$$\boldsymbol{\omega} \cdot \nabla H = 0.$$

  This implies that H also remains constant along the integral of $\boldsymbol{\omega}$, referred to as the vortex filament.

Examples of Barotropic Flows

- **Isentropic flows with uniform entropy:** For an ideal gas with $p = A\rho^\gamma$ (A, γ constants), pressure is purely a function of density when entropy is spatially constant.

- **Isothermal flows of an ideal gas:** When temperature T is constant, the equation of state simplifies to $p = \rho RT$, so pressure is directly proportional to density.

- **Simplified models in atmospheric or oceanic flows:** In some stratified models, barotropic approximations are used to simplify vertical density variations.

Incompressible Constant-Density Flows

For incompressible flows with constant density $\rho = \text{const}$, the specific enthalpy reduces to

$$h = \frac{p}{\rho}.$$

Thus, the Bernoulli invariant simplifies to:

$$H = \frac{1}{2}|\mathbf{v}|^2 + \frac{p}{\rho} + \Phi = \text{constant along streamlines.}$$

Examples of Incompressible Constant-Density Flows

- **Liquid water flows at moderate speeds:** Water is nearly incompressible under everyday flow conditions (e.g., rivers, pipelines, hydraulic systems).
- **Low-Mach number gas flows:** When the Mach number $M = \frac{|\mathbf{v}|}{c}$ (flow speed over sound speed) satisfies $M \ll 1$, density variations are negligible and the flow can be treated as incompressible.
- **Ocean currents:** Large-scale ocean flows, where temperature and salinity variations are weak, are often modeled as incompressible with nearly constant density.
- **Many laboratory experiments:** Fluid tank experiments, wind tunnel tests at low speeds, and pipe flow studies typically assume constant density.

Irrotational Barotropic Flows

If a barotropic flow is additionally irrotational, i.e., $\nabla \times \mathbf{v} = 0$, then equation (4.4) reduces to

$$\nabla H = 0.$$

In this case, the Bernoulli quantity H is constant throughout the entire fluid domain, not just along streamlines.

Thus, in steady, irrotational, barotropic flows, we have

$$\frac{1}{2}|\mathbf{v}|^2 + h + \Phi = \text{constant everywhere.}$$

This property is foundational for potential flow theory and many classical results in aerodynamics.

Theorem 4.2 (Bernoulli Principle for Steady Irrotational Flows)**.** *In a steady, irrotational, batropic flow under a conservative body force* $\mathbf{f} = -\frac{1}{\rho}\nabla\Phi$*, the Bernoulli quantity*

$$H := \frac{1}{2}|\mathbf{v}|^2 + h + \Phi$$

is constant throughout the entire flow domain.

When a flow is irrotational, incompressible with constant density ρ*, the Bernoulli invariant simplifies to*

$$\frac{1}{2}|\mathbf{v}|^2 + \frac{p}{\rho} + \Phi = \textit{constant everywhere.}$$

Remarks

1. In constant-density flows, the Bernoulli principle provides a direct *algebraic relationship* between pressure, velocity, and potential energy without needing an explicit equation of state.

2. This version of Bernoulli's law is widely applied in classical hydraulics, aerodynamics, and many incompressible flow analyses.

3. The assumption $\rho = \text{const}$ is essential; if ρ varies, the expression $\nabla(p/\rho)$ would not simply replace $\frac{1}{\rho}\nabla p$.

4.2.4 Bernoulli Principle for Unsteady Irrotational Flow

Assume the fluid is inviscid and irrotational, so the velocity field admits a scalar potential:

$$\mathbf{v} = \nabla\varphi,$$

where φ is the velocity potential.[†] We also assume the body force is conservative, i.e.,

$$\mathbf{f} = -\nabla\Phi,$$

for some potential Φ (e.g., gravitational potential). We start from the unsteady Euler equation:

$$\partial_t \mathbf{v} + \nabla\left(\frac{1}{2}|\mathbf{v}|^2\right) + \frac{1}{\rho}\nabla p = -\nabla\Phi.$$

Substituting $\mathbf{v} = \nabla\varphi$, we obtain:

$$\nabla\left(\partial_t\varphi + \frac{1}{2}|\nabla\varphi|^2 + \frac{p}{\rho} + \Phi\right) = 0.$$

Therefore, the expression inside the gradient must be spatially constant:

$$\boxed{\partial_t\varphi + \frac{1}{2}|\nabla\varphi|^2 + h + \Phi = C(t),}$$

where h is the specific enthalpy, satisfying $dh = \frac{1}{\rho}dp$.

Special Case: Incompressible Constant-Density Flow. If the fluid is incompressible and of constant density ρ, then $h = \frac{p}{\rho}$, and the Bernoulli equation becomes:

$$\boxed{\partial_t\varphi + \frac{1}{2}|\nabla\varphi|^2 + \frac{p}{\rho} + \Phi = C(t).}$$

[†]The existence of φ is guaranteed locally. However, global existence of φ on a domain Ω requires that Ω is simply connected.

Example: Potential Flow Around an Accelerating Sphere

Consider an incompressible, irrotational flow around a rigid sphere of radius R that moves with a prescribed time-dependent velocity $\mathbf{U}(t)$. The velocity potential in the fluid is given by:

$$\varphi(\mathbf{x}, t) = -\frac{1}{2} R^3 \frac{\mathbf{x} \cdot \dot{\mathbf{U}}(t)}{|\mathbf{x}|^3} + \mathbf{U}(t) \cdot \mathbf{x},$$

and the pressure field can be found by substituting into Bernoulli's equation:

$$\frac{p}{\rho} = C(t) - \partial_t \varphi - \frac{1}{2} |\nabla \varphi|^2.$$

This is used to compute the added mass effect in unsteady flows and to analyze pressure distribution in flow-induced motion.

4.2.5 Applications of Bernoulli Principle

1. **Vortex Center Has Low Pressure:**
   - Typically, the center of a vortex exhibits higher rotational speed, resulting in lower pressure at the center according to Bernoulli's principle.
2. **Effect of Strong Winds:**
   - In strong winds, the reduced external pressure makes it more difficult to inhale and breathe.
3. **Pitot Tube for Measuring Wind Speed:**
   (See Pitot Tube, Wikipedia and Video demonstration.)
   - The Pitot tube utilizes Bernoulli's principle to measure wind speed. The basic relation between pressures is:
     $$\frac{1}{2} v^2 + \frac{p_s}{\rho} = \frac{p_t}{\rho},$$
     where p_t is the total (stagnation) pressure, and p_s is the static pressure. Thus, the wind speed v can be determined by:
     $$v = \sqrt{\frac{2(p_t - p_s)}{\rho}} = \sqrt{\frac{2\rho_m g h}{\rho}},$$
     where ρ_m is the density of mercury (in the manometer), and ρ is the density of the gas.
4. **Venturi Effect**

   The Venturi effect refers to the phenomenon where the pressure of a fluid decreases as its speed increases when flowing through a constricted section of a pipe.

   Applying Bernoulli's principle between two points in a streamline:

   $$\frac{1}{2}\rho v_1^2 + p_1 = \frac{1}{2}\rho v_2^2 + p_2,$$

   where:

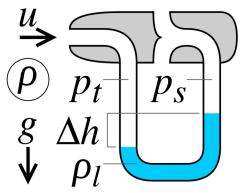


Figure 4.1: Pitot tube setup. Credit: Cmglee, CC BY-SA 4.0, `https://commons.wikimedia.org/w/index.php?curid=74391265`

- v_1, p_1 are the speed and pressure at the wider section,
- v_2, p_2 are the speed and pressure at the narrower section.

Since the flow rate must be conserved ($v_2 > v_1$ in the narrower section), the pressure must decrease ($p_2 < p_1$).

The Venturi effect has important engineering applications, including flow measurement devices (Venturi meters), carburetors, and atomizers.

5. **Torricelli's Law**

   The Torricelli's law states that the speed v of a fluid exiting an orifice under gravity from a tank is given by:

   $$v = \sqrt{2gh},$$

   where:

   - g is the acceleration due to gravity,
   - h is the vertical distance from the fluid surface to the orifice.

   This result can be derived by applying Bernoulli's principle between the fluid surface (where $v \approx 0$) and the exit point.

   Torricelli's law is foundational in fluid dynamics and is used in modeling jet flows, tank draining problems, and hydraulic systems.

6. **Further Applications:** For further examples, see: *Milne-Thomson, Theoretical Hydrodynamics.*

4.3 Vorticity and Circulation Theorem

4.3.1 Motivation and Definition of Circulation

In the early development of fluid mechanics, circulation emerged as a central concept for several key reasons:

- **Characterizing Fluid Rotation:** Circulation provides a means to measure the rotation of a fluid over a finite loop, facilitating the analysis of rotational motion without relying solely on local derivatives of the velocity field.

- **Conservation Laws:** Cauchy, Helmholtz, and Kelvin demonstrated that in ideal, inviscid flows, the circulation around a material loop is conserved. This fundamental conservation law simplifies the study of vortex motion and flow structures.
- **Applications to Aerodynamics:** Later developments, particularly the Kutta–Joukowski theorem, connected circulation directly to lift generation in airfoils, making circulation an essential quantity in the understanding of flight.
- **Mathematical Simplicity:** Before the advent of modern differential geometry, circulation, defined as an integral quantity, offered a tractable and intuitive method for analyzing complex flows compared to purely differential formulations.

Thus, circulation bridges local vorticity dynamics with global flow behavior, providing deep insights into both theoretical and applied fluid dynamics.

With this historical perspective in mind, we now introduce the formal definition of circulation in fluid dynamics.

Definition 4.3 (Circulation)**.** Given a closed curve C in the fluid region, the *circulation* of the flow field $\mathbf{v}$ along C is defined by:

$$\Gamma := \int_C \mathbf{v} \cdot d\mathbf{x},$$

where $d\mathbf{x}$ is the infinitesimal line element along C.

We shall take two complementary approaches. The first examines how the circulation around a material loop evolves along the flow. The second investigates the evolution of the vorticity field itself. These two perspectives are equivalent and are linked through Stokes' theorem.

4.3.2 Circulation Theorems

In this section, we introduce three important circulation theorems:

- The first concerns *baroclinic flows*, where circulation is not conserved due to the presence of a buoyancy (baroclinic) source term.
- The second concerns *barotropic flows*, where circulation is conserved because there is no baroclinic generation of vorticity.
- The third concerns *incompressible constant-density flows*, where circulation is again conserved under the same reasoning.

Thus, the conservation or non-conservation of circulation depends critically on the thermodynamic properties of the flow, specifically whether the pressure is a function solely of density (barotropic) or also of other variables such as entropy or temperature (baroclinic).

Circulation Evolution Formula for Baroclinic Flows

Definition 4.4 (Baroclinic Flow)**.** A flow is said to be *baroclinic* if it is not barotropic; that is, the pressure p depends on variables beyond just density ρ, such as entropy S or temperature T:

$$p = p(\rho, S) \quad \text{or} \quad p = p(\rho, T).$$

Let C_0 be a closed material curve parametrized by arc length s:

$$C_0 = \{X(s) \,|\, 0 \le s \le L\}, \quad X(0) = X(L).$$

The advected curve at time t is:

$$C(t) = \{\mathbf{x}(t, X(s)) \,|\, 0 \le s \le L\}.$$

The circulation around $C(t)$ is defined by:

$$\Gamma(t) = \int_{C(t)} \mathbf{v}(t,\mathbf{x}) \cdot d\mathbf{x} = \int_0^L \mathbf{v}(t, \mathbf{x}(t, X(s))) \cdot \frac{\partial \mathbf{x}(t, X(s))}{\partial s}\, ds.$$

Theorem 4.5 (Circulation Evolution for Baroclinic Flows)**.** *For baroclinic flows under a conservative body force, the circulation around a material loop evolves according to:*

$$\boxed{\frac{d}{dt}\int_{C(t)} \mathbf{v}(t,\mathbf{x}) \cdot d\mathbf{x} = -\int_{C(t)} \frac{1}{\rho}\nabla p \cdot d\mathbf{x} = \int_{C(t)} T\nabla S \cdot d\mathbf{x}.} \tag{4.5}$$

Proof. 1. Taking the time derivative of $\Gamma(t)$ gives:

$$\begin{aligned}
\frac{d}{dt}\Gamma(t) &= \int_0^L \left(\frac{D\mathbf{v}}{Dt} \cdot \frac{\partial \mathbf{x}}{\partial s} + \mathbf{v} \cdot \frac{D}{Dt}\left(\frac{\partial \mathbf{x}}{\partial s}\right)\right) ds \\
&= \int_0^L \left(\frac{D\mathbf{v}}{Dt} \cdot \frac{\partial \mathbf{x}}{\partial s} + \mathbf{v} \cdot \frac{\partial}{\partial s}\frac{D\mathbf{x}}{Dt}\right) ds \\
&= \int_0^L \left(\frac{D\mathbf{v}}{Dt} \cdot \frac{\partial \mathbf{x}}{\partial s} + \mathbf{v} \cdot \frac{\partial \mathbf{v}}{\partial s}\right) ds,
\end{aligned}$$

where we used the commutation of derivatives under smoothness assumptions.

2. Integrating the second term by parts (and using periodicity, since C_0 is a closed curve):

$$\int_0^L \mathbf{v} \cdot \frac{\partial \mathbf{v}}{\partial s}\, ds = \frac{1}{2}\left[|\mathbf{v}|^2\right]_0^L = 0,$$

since $\mathbf{v}(0) = \mathbf{v}(L)$ on a closed loop.

Thus:

$$\frac{d}{dt}\Gamma(t) = \int_0^L \frac{D\mathbf{v}}{Dt} \cdot \frac{\partial \mathbf{x}}{\partial s}\, ds = \int_{C(t)} \frac{D\mathbf{v}}{Dt} \cdot d\mathbf{x}.$$

3. Substituting the Euler equation:

$$\frac{D\mathbf{v}}{Dt} = -\frac{1}{\rho}\nabla p - \nabla\Phi,$$

we find:

$$\frac{d}{dt}\Gamma(t) = -\int_{C(t)} \left(\frac{1}{\rho}\nabla p + \nabla\Phi\right) \cdot d\mathbf{x}.$$

Since Φ is a scalar potential and $C(t)$ is closed, we have:

$$\int_{C(t)} \nabla\Phi \cdot d\mathbf{x} = 0,$$

hence:

$$\frac{d}{dt}\Gamma(t) = -\int_{C(t)} \frac{1}{\rho}\nabla p \cdot d\mathbf{x}.$$

4. Finally, using the thermodynamic identity:

$$\frac{1}{\rho}\nabla p = \nabla h - T\nabla S,$$

where h is the specific enthalpy, we observe that ∇h is a gradient field and integrates to zero around a closed loop. Thus:

$$\frac{d}{dt}\Gamma(t) = -\int_{C(t)} \frac{1}{\rho}\nabla p \cdot d\mathbf{x} = \int_{C(t)} T\nabla S \cdot d\mathbf{x}.$$

□

Remarks

1. Baroclinic effects are significant in atmospheric and oceanographic flows, where variations in temperature and salinity create density stratifications independent of pressure. Examples include cyclogenesis in meteorology and internal wave generation in the oceans.

2. The baroclinic source term

$$\int_{C(t)} T(t,\mathbf{x})\nabla S(t,\mathbf{x}) \cdot d\mathbf{x}$$

is a line integral in the physical domain, measuring the thermal input along the closed material curve $C(t)$. This integral can be interpreted geometrically by mapping $C(t)$ into the thermodynamic (T, S) plane.

Define the image curve $\tilde{C}(t)$ on the (T, S)-plane as:

$$\tilde{C}(t) := \{(T(t,\mathbf{x}(t,X(s))),\, S(t,\mathbf{x}(t,X(s)))) \mid 0 \le s \le L\}.$$

Parametrize this curve using S as the independent variable. Then the circulation source can be represented as a line integral on the thermo-plane:

$$\int_{\tilde{C}(t)} T\, dS,$$

which equals the signed area enclosed by the curve $\tilde{C}(t)$ in the (S, T) plane.

3. Using Gibbs' thermodynamic relation:

$$dU = T\, dS - p\, dV,$$

we note that since dU is an exact differential, its integral over a closed loop vanishes:

$$\int_{\tilde{C}(t)} dU = 0.$$

Thus, the integral $\int_{\tilde{C}(t)} T\,dS$ is equivalent to:

$$\int_{\tilde{C}(t)} T\,dS = \int_{\hat{C}(t)} p\,dV = -\int_{\hat{C}(t)} V\,dp,$$

where $\hat{C}(t)$ is the image of $C(t)$ under the map $\mathbf{x} \mapsto (p(\mathbf{x}), V(\mathbf{x}))$, and the integral $\int p\,dV$ represents the area enclosed by $\hat{C}(t)$ in the p-V thermodynamic plane.

4. The generation of circulation is directly linked to the misalignment of temperature and entropy gradients. In contrast, circulation is conserved when these gradients are aligned, as in the special cases of barotropic and isentropic flows. This leads to the two circulation-conserving corollaries that follow.

Circulation Theorem for Barotropic Flows

Theorem 4.6 (Kelvin's Circulation Theorem Thomson (1869))**.** *In a barotropic, inviscid flow under a conservative body force, the circulation around a closed material loop is conserved:*

$$\boxed{\frac{d}{dt}\Gamma(t) = 0,} \quad \textit{where} \quad \Gamma(t) = \int_{C(t)} \mathbf{v}(t,\mathbf{x}) \cdot d\mathbf{x}.$$

Proof. Let us start from the general circulation evolution formula:

$$\frac{d}{dt}\Gamma(t) = -\int_{C(t)} \frac{1}{\rho}\nabla p \cdot d\mathbf{x}.$$

For barotropic fluids where $p = p(\rho)$, we can define a specific enthalpy $h(\rho)$ such that

$$dh = \frac{1}{\rho}dp, \quad \text{thus} \quad \nabla h = \frac{1}{\rho}\nabla p. \tag{4.6}$$

Therefore:

$$\frac{d}{dt}\Gamma(t) = -\int_{C(t)} \nabla h \cdot d\mathbf{x} = 0,$$

because the line integral of a gradient field around any closed loop vanishes. □

Circulation Theorem for Incompressible Constant-Density Flows

Theorem 4.7 (Circulation Conservation in Constant-Density Incompressible Flows Lamb (1932b))**.** *In an inviscid, incompressible flow with constant density and under a conservative body force, the circulation around any closed material loop is conserved:*

$$\boxed{\frac{d}{dt}\Gamma(t) = 0,} \quad \textit{where} \quad \Gamma(t) = \int_{C(t)} \mathbf{v}(t,\mathbf{x}) \cdot d\mathbf{x}.$$

Proof. From the general circulation evolution formula:

$$\frac{d}{dt}\Gamma(t) = -\int_{C(t)} \frac{1}{\rho}\nabla p \cdot d\mathbf{x},$$

if ρ is constant, then the integrant in the right-hand side is a gradient field, thus its line integral around any closed loop vanishes. □

Remarks

- Constant-density incompressible flows are the classical setting for many laboratory and engineering fluid problems.
- The conservation of circulation in this case is especially relevant in low-Mach number flows, pipe flows, and classical vortex dynamics.

4.3.3 Vorticity Transport Equation

Vorticity Transport Equation in Integral Form The circulation measures the tendency of the fluid to rotate around C. By Stokes' theorem, we have

$$\int_C \mathbf{v} \cdot d\mathbf{x} = \int_\Sigma (\nabla \times \mathbf{v}) \cdot \boldsymbol{\nu}\, dS, \tag{4.7}$$

where Σ is any surface bounded by C, and $\boldsymbol{\nu}$ is the unit normal to Σ. The vector field

$$\boldsymbol{\omega} := \nabla \times \mathbf{v}$$

is called the *vorticity*. The integral

$$\int_\Sigma \boldsymbol{\omega} \cdot \boldsymbol{\nu}\, dS$$

is called the vorticity flux through the surface Σ. Thus, circulation is the vorticity flux through any surface bounded by C.

The circulation evolution equation can be equivalently expressed as an evolution equation of the vorticity with the helps of the Stokes' theorem.

Theorem 4.8 (Vorticity Transport Equation in Integral Form)**.** *For baroclinic flows under a conservative force field, the vorticity flux satisfies the following evolution integral equation:*

$$\frac{d}{dt}\int_{\Sigma(t)} \boldsymbol{\omega} \cdot \boldsymbol{\nu}\, dS_t = \int_{\Sigma(t)} \nabla T \times \nabla S \cdot \boldsymbol{\nu} dS_t, \tag{4.8}$$

Here, $\Sigma(t) = \varphi_t(\Sigma)$ is its image of a material surface Σ under the flow map φ_t at time t, and $\boldsymbol{\nu}$ is the unit normal vector to $\Sigma(t)$.

Proof. Let $C = \partial\Sigma$ be the boundary of the material surface Σ. It is a closed curve. The curve $C(t) = \varphi_t(C) = \partial\varphi_t(\Sigma) = \partial\Sigma(t)$. We apply the Stokes' Theorem to (4.5). The left-hand side gives

$$\frac{d}{dt}\int_{C(t)} \mathbf{v} \cdot d\mathbf{x} = \frac{d}{dt}\int_{\Sigma(t)} (\nabla \times \mathbf{v}) \cdot \boldsymbol{\nu} dS_t.$$

The right-hand side is

$$\int_{C(t)} T\nabla S \cdot d\mathbf{x} = \int_{\Sigma(t)} \nabla \times (T\nabla S) \cdot \boldsymbol{\nu} dS_t = \int_{\Sigma(t)} (\nabla T \times \nabla S) \cdot \boldsymbol{\nu} dS_t.$$

This gives (4.13). □

Corollary 4.9. *For barotropic flows or incompressible, constant-density flows under a conservative force field, the vorticity flux is invariant under the flow. More precisely, if Σ is a closed material surface and $\Sigma(t) = \varphi_t(\Sigma)$ is its image under the flow map at time t, then*

$$\frac{d}{dt} \int_{\Sigma(t)} \boldsymbol{\omega} \cdot \boldsymbol{\nu} \, dS_t = 0, \tag{4.9}$$

where $\boldsymbol{\nu}$ is the unit normal vector to $\Sigma(t)$.

Vorticity Transport Equation in Differential Form In this subsection, we derive the vorticity transport equation directly from the Euler equation. We assume that the specific body force is conservative.

1. We start from the Euler equation in Lamb form (4.1):

   $$\partial_t \mathbf{v} + \boldsymbol{\omega} \times \mathbf{v} + \nabla H = T\nabla S,$$

   where $H := \frac{1}{2}|\mathbf{v}|^2 + h + \Phi$ is the Bernoulli quantity. This vorticity-based reformulation emphasizes the role of vorticity in momentum transport and provides a natural framework for deriving the vorticity equation.

2. Taking the *curl* (i.e., $\nabla\times$) of this equation eliminates the gradient terms and yields:

   $$\boxed{\partial_t \boldsymbol{\omega} + \mathbf{v} \cdot \nabla \boldsymbol{\omega} - (\boldsymbol{\omega} \cdot \nabla)\mathbf{v} + \boldsymbol{\omega}(\nabla \cdot \mathbf{v}) = \nabla T \times \nabla S.} \tag{4.10}$$

   This is the vorticity transport equation in Eulerian coordinates.

3. In the derivation, we used the following vector calculus identities:

   $$\nabla \times (\boldsymbol{\omega} \times \mathbf{v}) = (\mathbf{v} \cdot \nabla)\boldsymbol{\omega} - (\boldsymbol{\omega} \cdot \nabla)\mathbf{v} + \boldsymbol{\omega}(\nabla \cdot \mathbf{v}) - \mathbf{v}(\nabla \cdot \boldsymbol{\omega}),$$
   $$\nabla \cdot \boldsymbol{\omega} = \nabla \cdot (\nabla \times \mathbf{v}) = 0,$$
   $$\nabla \times (T\nabla S) = \nabla T \times \nabla S + T\nabla \times (\nabla S) = \nabla T \times \nabla S.$$

4. Alternatively, starting from Gibbs' relation:

   $$\nabla U = T\nabla S - p\nabla V,$$

   and taking the *curl* of both sides:

   $$\nabla \times \nabla U = 0 = \nabla T \times \nabla S - \nabla p \times \nabla V,$$

   we obtain:

   $$\nabla p \times \nabla V = \nabla T \times \nabla S,$$

   so the vorticity equation (4.10) can equivalently be written as:

   $$\boxed{\partial_t \boldsymbol{\omega} + \mathbf{v} \cdot \nabla \boldsymbol{\omega} - (\boldsymbol{\omega} \cdot \nabla)\mathbf{v} + \boldsymbol{\omega}(\nabla \cdot \mathbf{v}) = \nabla p \times \nabla V.} \tag{4.11}$$

5. Each term in the vorticity equation has a physical interpretation:
   - $\mathbf{v} \cdot \nabla \boldsymbol{\omega}$: the *advection term*, representing transport of vorticity,
   - $(\boldsymbol{\omega} \cdot \nabla)\mathbf{v}$: the *vortex stretching* or deformation term,
   - $\boldsymbol{\omega}(\nabla \cdot \mathbf{v})$: the *vorticity amplification* due to volumetric expansion or compression,
   - $\nabla T \times \nabla S$ or $\nabla p \times \nabla V$: the *baroclinic generation* of vorticity.
6. When the temperature and entropy gradients are not aligned, their cross product $\nabla T \times \nabla S$ is nonzero, leading to the generation of vorticity via the baroclinic term in the vorticity equation.
7. Baroclinic generation of vorticity plays a central role in the formation of large-scale structures in the atmosphere, such as cyclones and frontal systems, where sharp gradients in temperature and entropy naturally occur Vallis (2017).
8. For barotropic flows under a conservative body force, the thermodynamic area element vanishes, and the vorticity equation simplifies to:
$$\boxed{\partial_t \boldsymbol{\omega} + \mathbf{v} \cdot \nabla \boldsymbol{\omega} - (\boldsymbol{\omega} \cdot \nabla)\mathbf{v} + \boldsymbol{\omega}(\nabla \cdot \mathbf{v}) = 0.} \tag{4.12}$$
   This is the vorticity transport equation for barotropic flows, and it leads directly to the circulation conservation theorem.

Homeworks Let $\boldsymbol{\omega} := \nabla \times \mathbf{v}$, show the following identities in vector calculus:

1. $\mathbf{v} \cdot \nabla \mathbf{v} = \nabla \left(\frac{1}{2}|\mathbf{v}|^2\right) + \boldsymbol{\omega} \times \mathbf{v}$.
2. $\nabla \times (\boldsymbol{\omega} \times \mathbf{v}) = \boldsymbol{\omega}(\nabla \cdot \mathbf{v}) - \mathbf{v}(\nabla \cdot \boldsymbol{\omega}) + (\mathbf{v} \cdot \nabla)\boldsymbol{\omega} - \boldsymbol{\omega} \cdot \nabla \mathbf{v}$
3. $\nabla \cdot \nabla \times \mathbf{v} = 0$
4. $\nabla \times (V \nabla p) = \nabla V \times \nabla p + V \nabla \times (\nabla p) = \nabla V \times \nabla p$.

Vorticity Transport Equation in Terms of Lie Derivatives

1. There is a natural way to write the integral form of the vorticity transport equation (4.13):
$$\frac{d}{dt} \int_{\Sigma(t)} \boldsymbol{\omega} \cdot \boldsymbol{\nu} \, dS_t = \int_{\Sigma(t)} \nabla T \times \nabla S \cdot \boldsymbol{\nu} dS_t, \tag{4.13}$$
   in terms of the Lie derivative in differential geometry. Namely,
$$\boxed{\partial_t \tilde{\omega} + \mathcal{L}_{\mathbf{v}} \tilde{\omega} = dT \wedge dS.} \tag{4.14}$$
   The notations in this formula are illustrated below.
2. We define the vorticity 2-form $\tilde{\omega}$ by:
$$\tilde{\omega} = \boldsymbol{\omega} \cdot \boldsymbol{\nu} \, dS = \omega^1 \, dx^2 \wedge dx^3 + \omega^2 \, dx^3 \wedge dx^1 + \omega^3 \, dx^1 \wedge dx^2,$$
   where $\boldsymbol{\omega} = (\omega^1, \omega^2, \omega^3)^T$ is the vorticity vector field.
   Our goals are:

(i) To express the time-derivative of an integral of $\tilde{\omega}$ as an integral of the Lie derivative of $\tilde{\omega}$:

$$\frac{d}{dt}\int_{\Sigma(t)} \tilde{\omega} = \int_{\Sigma(t)} (\partial_t + \mathcal{L}_{\mathbf{v}})\,\tilde{\omega}$$

where $\mathcal{L}_{\mathbf{v}}$ is the Lie derivative along the velocity field $\mathbf{v}$.

(ii) To show

$$\int_{\Sigma(t)} dT \wedge dS = \int_{\Sigma(t)} \nabla T \times \nabla S \cdot \boldsymbol{\nu} dS_t.$$

These two imply (4.14).

3. We show (i).

(a) We express this integral back at the initial time (i.e., over $\Sigma(0)$ in the material coordinates) to bring the time derivative inside the integral:

$$\frac{d}{dt}\int_{\Sigma(t)} \tilde{\omega} = \frac{d}{dt}\int_{\Sigma(0)} \varphi_t^*\tilde{\omega} = \int_{\Sigma(0)} \frac{d}{dt}\varphi_t^*\tilde{\omega}.$$

After differentiation in t with fixed X, we pull the integral back again to time t. We get:

$$\int_{\Sigma(0)} \frac{d}{dt}\varphi_t^*\tilde{\omega} = \int_{\Sigma(0)} \varphi_t^*\,(\partial_t + \mathcal{L}_{\mathbf{v}})\,\tilde{\omega} = \int_{\Sigma(t)} (\partial_t + \mathcal{L}_{\mathbf{v}})\,\tilde{\omega},$$

where $\mathcal{L}_{\mathbf{v}}$ is the Lie derivative along the velocity field $\mathbf{v}$. Indeed, the first equality is the definition of the Lie derivative.

We explain these steps below. For details, see the Appendix.

(b) The pullback $\varphi_t^*\tilde{\omega}$ is a 2-form at time 0, defined by:

$$\begin{aligned}\varphi_t^*\tilde{\omega}(t,X) = {}& \omega^1(t,\mathbf{x}(t,X))\,dx^2(t,X)\wedge dx^3(t,X)\\ &+ \omega^2(t,\mathbf{x}(t,X))\,dx^3(t,X)\wedge dx^1(t,X)\\ &+ \omega^3(t,\mathbf{x}(t,X))\,dx^1(t,X)\wedge dx^2(t,X),\end{aligned}$$

where $\mathbf{x}(t,X)$ is the position at time t of the particle initially located at X.

(c) Let d_t denote differentiation with respect to t at fixed X (the material derivative). Computing $d_t\varphi_t^*\tilde{\omega}$ yields:

$$\begin{aligned}d_t\varphi_t^*\tilde{\omega} = {}& (d_t\omega^1)\,dx^2\wedge dx^3 + (d_t\omega^2)\,dx^3\wedge dx^1 + (d_t\omega^3)\,dx^1\wedge dx^2\\ &+ \omega^1\,d_t(dx^2\wedge dx^3) + \omega^2\,d_t(dx^3\wedge dx^1) + \omega^3\,d_t(dx^1\wedge dx^2).\end{aligned}$$

Carrying out the expansion, we find:

$$d_t\varphi_t^*\tilde{\omega} = \varphi_t^*\left\{\theta^1\,dx^2\wedge dx^3 + \theta^2\,dx^3\wedge dx^1 + \theta^3\,dx^1\wedge dx^2\right\} := \varphi_t^*\tilde{\theta},$$

where the components θ^i are given by:

$$\theta^i = \partial_t\omega^i + v^k\frac{\partial\omega^i}{\partial x^k} + \omega^i\frac{\partial v^k}{\partial x^k} - \omega^k\frac{\partial v^i}{\partial x^k}.$$

Letting $\boldsymbol{\theta} = (\theta^1, \theta^2, \theta^3)^T$, the material evolution equation for the vorticity vector can be expressed in vector form as:

$$\boldsymbol{\theta} = \partial_t \boldsymbol{\omega} + (\mathbf{v} \cdot \nabla)\boldsymbol{\omega} + \boldsymbol{\omega}(\nabla \cdot \mathbf{v}) - (\nabla \mathbf{v})\boldsymbol{\omega}. \tag{4.15}$$

Let $\boldsymbol{\theta} = (\theta^1, \theta^2, \theta^3)^T$. In vector form,

$$\boxed{\boldsymbol{\theta} = \partial_t \boldsymbol{\omega} + \mathbf{v} \cdot \nabla \boldsymbol{\omega} + \boldsymbol{\omega} \nabla \cdot \mathbf{v} - (\nabla \mathbf{v})\boldsymbol{\omega}.} \tag{4.16}$$

(d) Note that the connection between the integral of a 2-form $\tilde{\theta}$ and a surface integral for a flux vector θ is

$$\int \tilde{\theta} = \int \boldsymbol{\theta} \cdot \boldsymbol{\nu} dS$$

Let us define the time-dependent Lie derivative $(\partial_t + \mathcal{L}_{\mathbf{v}})$ of $\tilde{\omega}$ by

$$d_t \varphi_t^* \tilde{\omega} = \varphi_t^* \left(\partial_t + \mathcal{L}_{\mathbf{v}}\right) \tilde{\omega}.$$

Thus, we get

$$\int_{\Sigma(t)} \left(\partial_t + \mathcal{L}_{\mathbf{v}}\right) \tilde{\omega} = \int_{\Sigma(t)} [\partial_t \boldsymbol{\omega} + \mathbf{v} \cdot \nabla \boldsymbol{\omega} + \boldsymbol{\omega} \nabla \cdot \mathbf{v} - (\nabla \mathbf{v})\boldsymbol{\omega}] \cdot \boldsymbol{\nu} dS$$

4. We show (ii): The baroclinic source term is [‡]

$$\begin{aligned} dT \wedge dS &= \left(T_{x^1} dx^1 + T_{x^2} dx^2 + T_{x^3} dx^3\right) \wedge \left(S_{x^1} dx^1 + S_{x^2} dx^2 + S_{x^3} dx^3\right) \\ &= \frac{\partial(T,S)}{\partial(x^2,x^3)} dx^2 \wedge dx^3 + \frac{\partial(T,S)}{\partial(x^3,x^1)} dx^3 \wedge dx^1 + \frac{\partial(T,S)}{\partial(x^1,x^2)} dx^1 \wedge dx^2 \\ &= \nabla T \times \nabla S \cdot (dx^2 \wedge dx^3, dx^3 \wedge dx^1, dx^1 \wedge dx^2) \\ &= \nabla T \times \nabla S \cdot \boldsymbol{\nu} dS_t \end{aligned}$$

Remarks

- When the flow is barotropic ($p = p(\rho)$), the baroclinic term vanishes: $dp \wedge dV = 0$. Thus, $\tilde{\omega}$ is conserved along the flow, i.e.,

  $$\partial_t \tilde{\omega} + \mathcal{L}_{\mathbf{v}} \tilde{\omega} = 0.$$

  This is equivalent to saying that vorticity is *frozen into the fluid*.

- The Lie derivative formulation emphasizes that the vorticity 2-form evolves by pure transport and deformation by the flow, except where baroclinic effects are present.

- This geometric structure underlies many modern theories of vortex dynamics, including the Cauchy invariants and modern geometric hydrodynamics.

[‡]The Jacobian $\frac{\partial(T,S)}{\partial(x^2,x^3)} := T_{x^2} S_{x^3} - T_{x^3} S_{x^2}$

4.3.4 Helmholtz's Vorticity Equation

The vorticity transport equation admits an alternative formulation, known as *Helmholtz's vorticity equation*, which governs the evolution of the vorticity per unit mass.

Recall the general vorticity equation:

$$\partial_t \boldsymbol{\omega} + \mathbf{v} \cdot \nabla \boldsymbol{\omega} - (\boldsymbol{\omega} \cdot \nabla)\mathbf{v} + \boldsymbol{\omega}(\nabla \cdot \mathbf{v}) = \nabla p \times \nabla V,$$

where $V = 1/\rho$ is the specific volume.

To eliminate the amplification term $\boldsymbol{\omega}(\nabla \cdot \mathbf{v})$, we use the continuity equation in the form:

$$\partial_t V + \mathbf{v} \cdot \nabla V = V(\nabla \cdot \mathbf{v}).$$

Multiplying the vorticity equation by V and adding $\boldsymbol{\omega}$ times the continuity equation yields the evolution equation for $V\boldsymbol{\omega}$:

$$\partial_t (V\boldsymbol{\omega}) + \mathbf{v} \cdot \nabla (V\boldsymbol{\omega}) - (V\boldsymbol{\omega} \cdot \nabla)\mathbf{v} = V \nabla p \times \nabla V.$$

Equivalently, in terms of density $\rho = 1/V$, we obtain the Helmholtz vorticity equation for the vorticity per unit mass:

$$\frac{D}{Dt}\left(\frac{\boldsymbol{\omega}}{\rho}\right) - \left(\frac{\boldsymbol{\omega}}{\rho} \cdot \nabla\right)\mathbf{v} = \frac{1}{\rho^3} \nabla\rho \times \nabla p. \tag{4.17}$$

Interpretation

- The right-hand side $\frac{1}{\rho^3}\nabla\rho \times \nabla p$ in (4.17) is called the *baroclinic torque* or *buoyancy source*. It represents the generation of vorticity due to misaligned pressure and density gradients.
- For barotropic flows (i.e., $p = p(\rho)$), this term vanishes. Note that the second term on the left-hand side of (4.17) can be expressed as a matrix-vector product:

  $$\left(\frac{\boldsymbol{\omega}}{\rho} \cdot \nabla\right)\mathbf{v} = (\nabla \mathbf{v})\left(\frac{\boldsymbol{\omega}}{\rho}\right),$$

  so that:

  $$\frac{D}{Dt}\left(\frac{\boldsymbol{\omega}}{\rho}\right) = (\nabla \mathbf{v})\left(\frac{\boldsymbol{\omega}}{\rho}\right).$$

  This equation resembles the evolution equation for the deformation tensor F:

  $$\dot{F} = (\nabla \mathbf{v})F,$$

  which shows that $\boldsymbol{\omega}/\rho$ evolves like a material tangent vector transported by the deformation field.
- This leads to the following classical result, known as Helmholtz's vorticity theorem.

Theorem 4.10 (Helmholtz Vorticity Theorem)**.** *For barotropic flows under a conservative body force, the vorticity per unit mass is transported as a material vector:*

$$\frac{d}{dt}\left(\frac{\boldsymbol{\omega}}{\rho}\right) = (\nabla \mathbf{v})\left(\frac{\boldsymbol{\omega}}{\rho}\right). \tag{4.18}$$

In particular, along a particle path, we have:

$$\boxed{\frac{\boldsymbol{\omega}}{\rho}(t, \mathbf{x}(t, X)) = \frac{\partial \mathbf{x}(t, X)}{\partial X} \frac{\boldsymbol{\omega}}{\rho}(0, X),} \tag{4.19}$$

where $\mathbf{x}(t, X)$ is the flow map. Thus, $\boldsymbol{\omega}/\rho$ evolves like a tangent vector along the flow.

Proof. From equation (4.17), the evolution of $\boldsymbol{\omega}/\rho$ satisfies:

$$\frac{d}{dt}\left(\frac{\boldsymbol{\omega}}{\rho}\right) = (\nabla \mathbf{v})\left(\frac{\boldsymbol{\omega}}{\rho}\right)$$

in the barotropic case, where the right-hand side reduces due to $\nabla\rho \times \nabla p = 0$.

Let $\mathbf{x}(t, X)$ denote the flow map, and define $F(t, X) := \frac{\partial \mathbf{x}(t,X)}{\partial X}$ as the deformation gradient tensor. It satisfies:

$$\frac{d}{dt}F = (\nabla \mathbf{v}) \cdot F, \quad F(0, X) = I.$$

Now define:

$$\zeta(t, X) := \frac{\boldsymbol{\omega}}{\rho}(t, \mathbf{x}(t, X)),$$

which satisfies:

$$\frac{d}{dt}\zeta(t, X) = (\nabla \mathbf{v})(t, \mathbf{x}(t, X))\zeta(t, X),$$

the same equation satisfied by $F\zeta_0(X)$.

Therefore, by uniqueness of solutions to linear ODEs, we have:

$$\zeta(t, X) = F(t, X)\zeta_0(X),$$

or equivalently,

$$\frac{\boldsymbol{\omega}}{\rho}(t, \mathbf{x}(t, X)) = \frac{\partial \mathbf{x}(t, X)}{\partial X} \frac{\boldsymbol{\omega}}{\rho}(0, X).$$

□

Corollary 4.11 (Persistence of Irrotationality)**.** *For barotropic or incompressible flows under a conservative body force, if the vorticity vanishes initially, i.e., $\boldsymbol{\omega}(0) \equiv 0$, then $\boldsymbol{\omega}(t) \equiv 0$ for all future time.*

In other words, an initially irrotational flow remains irrotational for all time.

Proof. This follows directly from the Helmholtz vorticity theorem. In such flows, vorticity is transported by the flow but not generated internally. Hence, if the flow is initially irrotational, it remains irrotational at all later times. □

Vortex Filament

A *vortex filament* (or *vortex line*) is a curve whose tangent vector is aligned with the vorticity field $\boldsymbol{\omega}$. That is, a smooth curve $\boldsymbol{\gamma}(s)$ is a vortex filament if:

$$\frac{d\boldsymbol{\gamma}}{ds} \parallel \boldsymbol{\omega}(\gamma(s)),$$

i.e., the curve $\boldsymbol{\gamma}$ is an integral curve of $\boldsymbol{\omega}$. The term "vortex filament" emphasizes its physical structure, while "vortex line" emphasizes its geometric role.

A *vortex tube* is defined as a family of neighboring vortex filaments forming a tubular region. These structures are fundamental in classical and modern fluid dynamics, appearing in contexts such as turbulence, jet cores, and vortex rings.

Theorem 4.12 (Helmholtz Vortex Line Theorem)**.** *In an inviscid, barotropic flow under a conservative body force, vortex filaments are transported by the flow. That is, the image of a vortex filament under the flow map* $\mathbf{x}(t, X)$ *remains a vortex filament at later times.*

Proof. Let us define the vortex filament to be the integral curve of the vorticity field $\boldsymbol{\omega}$. Let $X(\alpha)$ be a vortex filament at $t = 0$. That is,

$$\frac{dX}{d\alpha} = \frac{\boldsymbol{\omega}(X, 0)}{\rho(X, 0)}.$$

Let us investigate this line following the flow $\mathbf{x}(t, X(\alpha))$. Its tangent is

$$\begin{aligned} \frac{d}{d\alpha}\mathbf{x}(t, X(\alpha)) &= \frac{\partial \mathbf{x}}{\partial X}\frac{dX}{d\alpha} \\ &= \frac{\partial \mathbf{x}}{\partial X}\frac{\boldsymbol{\omega}}{\rho}(0) \\ &= \frac{\boldsymbol{\omega}}{\rho}(t). \qquad \because (4.19) \end{aligned}$$

This shows that the vortex filament stays as a vortex filament. Thus, a vortex filament flows with the fluid flow. □

4.3.5 Potential Vorticity

- Ertel (1942) derived an alternative form of the vorticity evolution equation, in which the buoyancy and vortex stretching terms are removed. This formulation is especially useful in rotating stratified fluid dynamics. The key idea is to introduce a freely advected thermodynamic parameter, denoted by λ, satisfying two properties:
  - $\nabla\lambda \cdot (\nabla V \times \nabla p) = 0$,
  - λ is materially conserved:
$$\partial_t \lambda + \mathbf{v} \cdot \nabla\lambda = 0.$$
- Typical examples of such a function λ include:
  - The entropy S,
  - The potential temperature θ:
$$\theta := T\left(\frac{p_0}{p}\right)^{R/c_p} = T\left(\frac{p_0}{p}\right)^{(\gamma-1)/\gamma},$$
where p_0 is a reference pressure, usually 1,000 hPa (1,000 mb). (The standard atmosphere, denoted atm, is defined as 1,013.25 hPa.)

- Taking the dot product of the Helmholtz vorticity equation with $\nabla\lambda$, the baroclinic source term vanishes because it lies in the thermodynamic plane, and there are only two independent thermodynamic variables. Thus, we isolate a scalar conservation law.

- **Potential Vorticity** is then defined by:

$$q := \frac{\boldsymbol{\omega} \cdot \nabla\lambda}{\rho} = \frac{\nabla \cdot (\lambda\boldsymbol{\omega})}{\rho} \qquad (\text{since } \nabla \cdot \boldsymbol{\omega} = 0).$$

  This scalar quantity is called the *potential vorticity* associated with the advected scalar λ.

Ertel's Theorem: *The potential vorticity q is materially conserved along particle trajectories:*

$$\boxed{\frac{Dq}{Dt} = 0.}$$

That is, q is invariant along the trajectory of a fluid parcel.

Proof. 1. Let us rewrite the Helmholtz vorticity equation (4.17) as

$$\frac{D}{Dt}\zeta - \zeta \cdot \nabla\mathbf{v} = V\nabla V \times \nabla p. \tag{4.20}$$

   where $\zeta := V\boldsymbol{\omega} = \boldsymbol{\omega}/\rho$.

2. We take ∇ to the free advection equation of λ:

$$\begin{aligned} 0 &= \nabla\left(\partial_t\lambda + \mathbf{v} \cdot \nabla\lambda\right) \\ &= \partial_t(\nabla\lambda) + (\nabla\mathbf{v}) \cdot (\nabla\lambda) + \mathbf{v} \cdot \nabla(\nabla\lambda) \\ &= \frac{D}{Dt}(\nabla\lambda) + (\nabla\mathbf{v}) \cdot (\nabla\lambda) \end{aligned} \tag{4.21}$$

3. We take

$$\nabla\lambda \cdot (4.20) + \zeta \cdot (4.21),$$

   Using $\nabla\lambda \cdot (\nabla V \times \nabla p) = 0$, we get

$$\nabla\lambda \cdot \frac{D}{Dt}\zeta + \zeta \cdot \frac{D}{Dt}(\nabla\lambda) = 0.$$

   Thus,

$$\frac{D}{Dt}\left(\zeta \cdot \nabla\lambda\right) = 0.$$

□

Remarks

The concept of *potential temperature*, denoted by θ, dates back to the 19th century and was originally introduced as a way to describe the thermodynamic state of a dry air parcel under adiabatic compression or expansion. It is defined by

$$\theta := T \left(\frac{p_0}{p} \right)^{R/c_p},$$

where T is the absolute temperature, p is the local pressure, p_0 is a reference pressure, and R/c_p is the ratio of the gas constant to specific heat at constant pressure.

Because θ remains constant along the trajectory of a dry, adiabatically moving air parcel, it naturally serves as a materially conserved scalar. In the 20th century, Ertel (1942) used such scalars, including θ, to define what is now called *potential vorticity* (PV). This provided a powerful unification of thermodynamic and dynamic properties of the flow.

In modern geophysical fluid dynamics, θ is one of the most widely used thermodynamic tracers for PV analysis. Its role is particularly prominent in diagnosing large-scale atmospheric phenomena, including the development of Rossby waves, baroclinic instability, and tropopause dynamics.

For detailed treatments, see Holton and Hakim Holton and Hakim (2012), and Vallis Vallis (2017).

The Ertel Theorem can also be derived from the relabeling symmetry of the Euler equation by the Noether's Theorem. See Salmon,1988 Salmon (1998).

4.3.6 Summary

Helmholtz's laws of vortex motion

The following summaries the classical results for barotropic flows derived by Helmholtz (1858):

- **Persistence of Irrotationality:** If the initial flow is irrotational (i.e., $\boldsymbol{\omega} \equiv 0$), it remains irrotational at all times.
- **Vortex Filaments Are Frozen-In:** Vortex lines are transported with the fluid — particles initially lying along a vortex line remain so.
- **Conservation of Vortex Flux:** The flux of vorticity through a vortex tube remains constant in time.

Material Transports are According to the Lie Derivatives

The PV q is a 0-form, the vorticity per unit mass $\boldsymbol{\omega}/\rho$ is a *vector*, while the vorticity flux $\tilde{\omega}$ is a 2-form. Their Lie derivatives are:

- 0-form, such as a PV q:
$$(\partial_t + \mathcal{L}_{\mathbf{v}})q = \partial_t + \mathbf{v} \cdot \nabla q = \frac{D}{Dt} q.$$
- A vector such as $\zeta = \boldsymbol{\omega}/\rho$:
$$(\partial_t + \mathcal{L}_{\mathbf{v}})\zeta = \frac{D}{Dt}\zeta - \zeta \cdot \nabla \mathbf{v}.$$

- A 2-form vorticity flux $\tilde{\omega}$:

$$(\partial_t + \mathcal{L}_{\mathbf{v}})\tilde{\omega} = (\partial_t \boldsymbol{\omega} + \mathbf{v} \cdot \nabla \boldsymbol{\omega} - (\boldsymbol{\omega} \cdot \nabla)\mathbf{v} + \boldsymbol{\omega}(\nabla \cdot \mathbf{v})) \cdot \boldsymbol{\nu} dS.$$

Historical Remark

The concept of circulation conservation has deep historical roots. Early ideas were introduced by Cauchy Cauchy (1815), who developed integral invariants for ideal fluids using Lagrangian particle mappings. Later, Helmholtz Helmholtz (1858) established the fundamental laws of vortex motion, showing that vortex lines are transported by the flow without change of strength in inviscid fluids. Building on these foundations, Lord Kelvin (William Thomson) Thomson (1869) formally stated the circulation theorem: the circulation around a closed material loop is conserved in barotropic, inviscid flows under a conservative body force.

The conservation of circulation along material loops naturally led to the discovery of a related invariant: *potential vorticity*. Rossby Rossby (1939) introduced the concept of potential vorticity in 1939 in the context of large-scale geophysical flows, noting that for adiabatic, inviscid flows on a rotating planet, the relative vorticity divided by the fluid column depth is conserved along particle paths. Later, Ertel Ertel (1942) generalized the idea to arbitrary compressible flows with varying entropy, deriving the conservation of potential vorticity using modern differential calculus.

Thus, the classical circulation theorems of Cauchy, Helmholtz, and Kelvin laid the groundwork for the profound role of potential vorticity in modern geophysical fluid dynamics.

4.4 Vorticity Equation for Viscous Fluid Flows

Vorticity equation for compressible viscous flows From (**??**), the momentum equation can also expressed as

$$\left(\mathbf{v}_t + \boldsymbol{\omega} \times \mathbf{v} + \nabla(\frac{1}{2}|\mathbf{v}|^2)\right) + \frac{\nabla p}{\rho} = \frac{\nabla \cdot \boldsymbol{\tau}}{\rho}, \tag{4.22}$$

By taking *curl* on this equation, we obtain the vorticity equation for incompressible viscous flows:

$$\partial_t \boldsymbol{\omega} + \mathbf{v} \cdot \nabla \boldsymbol{\omega} - (\boldsymbol{\omega} \cdot \nabla)\,\mathbf{v} + \boldsymbol{\omega}\,(\nabla \cdot \mathbf{v}) = \frac{1}{\rho^2}\nabla\rho \times \nabla p + \nabla \times \left(\frac{\nabla \cdot \boldsymbol{\tau}}{\rho}\right). \tag{4.23}$$

In the case of incompressible flows, we have

$$\partial_t \boldsymbol{\omega} + \mathbf{v} \cdot \nabla \boldsymbol{\omega} - (\boldsymbol{\omega} \cdot \nabla)\,\mathbf{v} + \boldsymbol{\omega}\,(\nabla \cdot \mathbf{v}) = \mu \triangle \boldsymbol{\omega}. \tag{4.24}$$

Note that the bulk viscosity does not effect the diffusion of the vortices.

Chapter 5

Variational and Hamiltonian Fluid Mechanics

5.1 Introduction and Main Ideas

The purpose of this chapter is to formulate ideal fluid motion from the viewpoint of variational and Hamiltonian mechanics. We begin with the material description of a compressible fluid. The fundamental unknown is the motion

$$\varphi_t : \widehat{M} \longrightarrow M_t, \qquad \mathbf{x} = \mathbf{x}(t, X) = \varphi_t(X),$$

where $X \in \widehat{M}$ is the material label and $\mathbf{x} \in M_t$ is the current spatial position. The Eulerian fields are induced from the material motion by

$$\mathbf{v}(t, \mathbf{x}(t, X)) = \partial_t \mathbf{x}(t, X),$$

$$\rho(t, \mathbf{x}(t, X))J(t, X) = \rho_0(X), \qquad S(t, \mathbf{x}(t, X)) = S_0(X),$$

where

$$F(t, X) = \nabla_X \mathbf{x}(t, X), \qquad J(t, X) = \det F(t, X).$$

Thus mass and entropy are not imposed afterward; they are transported by the motion itself.

Hamilton's principle in material coordinates gives the compressible Euler equations by varying the flow map $\mathbf{x}(t, X)$. Passing to the material momentum

$$\mathbf{p}(t, X) = \rho_0(X)\partial_t \mathbf{x}(t, X)$$

then gives a canonical Hamiltonian system on the material phase space. This canonical formulation carries the usual symplectic structure and the Lagrangian Poisson bracket. In this sense the material motion of an ideal fluid is a Hamiltonian flow.

The Eulerian description is obtained by reduction. The variables

$$\mathbf{v}(t, x), \qquad \rho(t, x), \qquad S(t, x)$$

are not independent fields: they arise from the same material motion. For this reason the admissible Eulerian variations have the dynamically accessible form

$$\delta\mathbf{v} = \partial_t \mathbf{w} + [\mathbf{v}, \mathbf{w}], \qquad \delta\rho = -\nabla \cdot (\rho\mathbf{w}), \qquad \delta S = -\mathbf{w} \cdot \nabla S.$$

These variations lead to the Euler–Poincare equations for compressible fluids.

Noether's theorem is one of the central principles of the chapter. Spatial translations, rotations, and time translations give the familiar conservation of linear momentum, angular momentum, and energy. The more fluid-specific symmetry is particle relabelling: the material labels may be changed without changing the physical motion. This right symmetry of the material action is the geometric source of Kelvin's circulation theorem and Ertel's potential vorticity theorem.

The Clebsch representation is introduced after the relabelling symmetry has been explained. In this way it is not merely an ansatz for the velocity; it is an Eulerian multiplier representation of advected labels and constraints. For compressible flow the extended Clebsch form is

$$\mathbf{v} = \nabla\varphi + \eta\nabla S + \zeta\nabla a,$$

where S and a are advected scalars. Finally, reducing the canonical material Poisson structure gives the noncanonical Eulerian Poisson bracket. Its degeneracy leads naturally to Casimirs and advected invariants.

The chapter is organized as follows. We first derive the equations from Hamilton's principle in material coordinates. We then pass to the canonical Hamiltonian form and the Lagrangian Poisson bracket. After that we develop Eulerian reduction, dynamically accessible variations, and the Euler–Poincare equations. Noether's theorem is then used to connect symmetries with invariants, especially relabelling symmetry with Kelvin's and Ertel's theorems. The Clebsch representation is discussed next, followed by the Eulerian Poisson structure and its Casimirs.

5.2 Hamilton's Principle in Material Coordinates

5.2.1 The Motion Map and Material Variables

We consider a compressible inviscid fluid occupying a reference material manifold $\widehat{M}$. A fluid particle is labelled by $X \in \widehat{M}$, and its position at time t is

$$\mathbf{x} = \mathbf{x}(t, X) = \varphi_t(X).$$

The deformation gradient and its Jacobian are

$$F(t, X) = \nabla_X \mathbf{x}(t, X), \qquad J(t, X) = \det F(t, X).$$

The material density and entropy are denoted by

$$\rho_0(X), \qquad S_0(X).$$

The corresponding Eulerian density and entropy are defined by

$$\rho(t, \mathbf{x}(t, X))J(t, X) = \rho_0(X), \qquad S(t, \mathbf{x}(t, X)) = S_0(X).$$

The Eulerian velocity is

$$\mathbf{v}(t, \mathbf{x}(t, X)) = \partial_t \mathbf{x}(t, X).$$

We use $\Omega^k(M)$ for the space of k-differential forms on a manifold M. To avoid conflict with this notation, the spatial fluid domain is denoted by M_t rather than by Ω.

5.2.2 The Material Action

For an ideal compressible fluid, the specific internal energy is written as

$$U = U(S, V), \qquad V = \frac{1}{\rho}.$$

Since

$$V(t, \mathbf{x}(t, X)) = \frac{1}{\rho(t, \mathbf{x}(t, X))} = \frac{J(t, X)}{\rho_0(X)},$$

the action in material coordinates is

$$\mathcal{A}[\mathbf{x}] = \int_{t_0}^{t_1} \int_{\widehat{M}} \left[\frac{1}{2} \rho_0(X) |\partial_t \mathbf{x}(t, X)|^2 - \rho_0(X) U \left(S_0(X), \frac{J(t, X)}{\rho_0(X)} \right) \right] dX \, dt. \tag{5.1}$$

Hamilton's principle states that

$$\delta \mathcal{A} = 0$$

for variations $\delta \mathbf{x}(t, X)$ vanishing at the temporal endpoints.

5.2.3 First Variation of the Action

Let

$$\mathbf{x}^\varepsilon(t, X)$$

be a one-parameter family of motions with $\mathbf{x}^0 = \mathbf{x}$. We write

$$\delta \mathbf{x}(t, X) = \left. \frac{d}{d\varepsilon} \right|_{\varepsilon=0} \mathbf{x}^\varepsilon(t, X).$$

The induced variations of the deformation gradient and of the Jacobian are

$$\delta F = \nabla_X \delta \mathbf{x}, \qquad \delta J = J F^{-T} : \delta F.$$

Since

$$V = \frac{J}{\rho_0},$$

we have

$$\delta V = \frac{\delta J}{\rho_0}.$$

Using the thermodynamic relation

$$p = -\frac{\partial U}{\partial V},$$

the variation of the internal energy term is

$$\begin{aligned} \delta \left[\rho_0 U \left(S_0, \frac{J}{\rho_0} \right) \right] &= \rho_0 \frac{\partial U}{\partial V} \, \delta \left(\frac{J}{\rho_0} \right) \\ &= -p \, \delta J \\ &= -p J F^{-T} : \delta F. \end{aligned}$$

Therefore, if

$$W(F) = \rho_0 U\left(S_0, \frac{\det F}{\rho_0}\right),$$

then

$$\frac{\partial W}{\partial F} = -pJF^{-T}.$$

We denote this first Piola–Kirchhoff stress by

$$P := \frac{\partial W}{\partial F} = -pJF^{-T}.$$

The first variation of the action is

$$\delta\mathcal{A} = \int_{t_0}^{t_1} \int_{\widehat{M}} \left[\rho_0 \partial_t \mathbf{x} \cdot \partial_t \delta\mathbf{x} - P : \nabla_X \delta\mathbf{x}\right] dX\, dt.$$

Integrating by parts in time and in the material coordinate gives

$$\delta\mathcal{A} = \int_{t_0}^{t_1} \int_{\widehat{M}} \left[-\rho_0 \partial_{tt}\mathbf{x} + \nabla_X \cdot P\right] \cdot \delta\mathbf{x}\, dX\, dt,$$

where the temporal endpoint terms vanish because $\delta\mathbf{x}(t_0, X) = \delta\mathbf{x}(t_1, X) = 0$. Boundary terms on $\partial\widehat{M}$ vanish under the usual fixed-boundary or natural boundary assumptions.

5.2.4 Euler–Lagrange Equations in Material Coordinates

Hamilton's principle therefore gives

$$\boxed{\rho_0(X)\partial_{tt}\mathbf{x}(t, X) = \nabla_X \cdot P(t, X), \qquad P = -pJF^{-T}.} \tag{5.2}$$

This is the equation of motion in material coordinates. It has the same form as the material equation of elasticity, but here the stress is the fluid stress determined by the internal energy through the pressure.

5.2.5 Recovery of the Compressible Euler Equations

We now transform (5.2) back to Eulerian variables. The material acceleration satisfies

$$\partial_{tt}\mathbf{x}(t, X) = \left(\partial_t \mathbf{v} + \mathbf{v} \cdot \nabla_{\mathbf{x}} \mathbf{v}\right)(t, \mathbf{x}(t, X)).$$

The Cauchy stress $\boldsymbol{\sigma}$ is related to the first Piola–Kirchhoff stress by

$$\boldsymbol{\sigma} = J^{-1} P F^T.$$

Since $P = -pJF^{-T}$, we obtain

$$\boldsymbol{\sigma} = -pI.$$

Using the Piola transformation, the material equation becomes

$$\rho\left(\partial_t \mathbf{v} + \mathbf{v} \cdot \nabla_{\mathbf{x}} \mathbf{v}\right) = \nabla_{\mathbf{x}} \cdot \boldsymbol{\sigma} = -\nabla_{\mathbf{x}} p.$$

Thus Hamilton's principle recovers the compressible Euler momentum equation

$$\boxed{\rho\left(\partial_t \mathbf{v} + \mathbf{v}\cdot\nabla_{\mathbf{x}}\mathbf{v}\right) = -\nabla_{\mathbf{x}} p.} \tag{5.3}$$

Together with the transported mass and entropy equations

$$\partial_t \rho + \nabla_{\mathbf{x}}\cdot(\rho\mathbf{v}) = 0, \qquad \partial_t S + \mathbf{v}\cdot\nabla_{\mathbf{x}} S = 0,$$

this gives the compressible adiabatic Euler system.

5.3 Canonical Form and Lagrangian Poisson Structure

5.3.1 Material Momentum and Legendre Transform

The material Lagrangian associated with (5.1) is

$$L[\mathbf{x}, \partial_t \mathbf{x}] = \int_{\widehat{M}} \left[\frac{1}{2}\rho_0 |\partial_t \mathbf{x}|^2 - \rho_0 U\left(S_0, \frac{J}{\rho_0}\right)\right] dX.$$

The canonical momentum conjugate to $\mathbf{x}(t, X)$ is

$$\boxed{\mathbf{p}(t, X) = \frac{\delta L}{\delta(\partial_t \mathbf{x})} = \rho_0(X)\partial_t \mathbf{x}(t, X).} \tag{5.4}$$

Thus

$$\partial_t \mathbf{x} = \frac{\mathbf{p}}{\rho_0}.$$

The Legendre transform gives the material Hamiltonian

$$\boxed{H[\mathbf{x}, \mathbf{p}] = \int_{\widehat{M}} \frac{|\mathbf{p}|^2}{2\rho_0}\, dX + \int_{\widehat{M}} \rho_0 U\left(S_0, \frac{J}{\rho_0}\right) dX.} \tag{5.5}$$

This Hamiltonian is the total kinetic plus internal energy written in material variables.

5.3.2 Canonical Hamiltonian Equations

The Hamiltonian equations in material coordinates are

$$\boxed{\partial_t \mathbf{x} = \frac{\delta H}{\delta \mathbf{p}}, \qquad \partial_t \mathbf{p} = -\frac{\delta H}{\delta \mathbf{x}}.} \tag{5.6}$$

The first equation gives $\partial_t \mathbf{x} = \mathbf{p}/\rho_0$. The second equation is equivalent to

$$\rho_0 \partial_{tt}\mathbf{x} = \nabla_X \cdot P,$$

and hence to the material Euler–Lagrange equation (5.2).

5.3.3 Canonical Symplectic Form

The material phase space consists of pairs $(\mathbf{x}, \mathbf{p})$. A tangent vector to the phase space at $(\mathbf{x}, \mathbf{p})$ is a pair

$$(\mathbf{V}, \mathbf{\Pi}),$$

where $\mathbf{V}$ is a variation of the configuration $\mathbf{x}$ and $\mathbf{\Pi}$ is a variation of the momentum $\mathbf{p}$.

In this subsection, the symbol δ denotes exterior differentiation on the infinite-dimensional phase space. Thus $\delta\mathbf{x}$ and $\delta\mathbf{p}$ are phase-space one-forms, analogous to dq^i and dp_i in finite-dimensional Hamiltonian mechanics. They act by

$$\delta\mathbf{x}(\mathbf{V}, \mathbf{\Pi}) = \mathbf{V}, \qquad \delta\mathbf{p}(\mathbf{V}, \mathbf{\Pi}) = \mathbf{\Pi}.$$

The canonical one-form is

$$\Theta = \int_{\widehat{M}} \mathbf{p}(X) \cdot \delta\mathbf{x}(X)\, dX.$$

The canonical symplectic form is

$$\Omega_L = -\delta\Theta.$$

Formally this gives

$$\boxed{\Omega_L = \int_{\widehat{M}} \delta\mathbf{x}(X) \wedge \delta\mathbf{p}(X)\, dX.} \tag{5.7}$$

Here the wedge product is the antisymmetric product of phase-space one-forms. A tangent vector to the phase space at $(\mathbf{x}, \mathbf{p})$ is a pair

$$(\mathbf{V}, \mathbf{\Pi}),$$

where $\mathbf{V}$ is a variation of the configuration $\mathbf{x}$ and $\mathbf{\Pi}$ is a variation of the momentum $\mathbf{p}$. The phase-space one-forms $\delta\mathbf{x}$ and $\delta\mathbf{p}$ act by

$$\delta\mathbf{x}(\mathbf{V}, \mathbf{\Pi}) = \mathbf{V}, \qquad \delta\mathbf{p}(\mathbf{V}, \mathbf{\Pi}) = \mathbf{\Pi}.$$

Thus, if $(\mathbf{V}, \mathbf{\Pi})$ and $(\mathbf{W}, \mathbf{\Sigma})$ are two tangent vectors to the phase space, then

$$\Omega_L\big((\mathbf{V}, \mathbf{\Pi}), (\mathbf{W}, \mathbf{\Sigma})\big) = \int_{\widehat{M}} (\mathbf{V} \cdot \mathbf{\Sigma} - \mathbf{W} \cdot \mathbf{\Pi})\, dX.$$

This is the infinite-dimensional analogue of

$$\omega = dq^i \wedge dp_i.$$

Thus the material fluid motion is a Hamiltonian flow preserving Ω_L.

5.3.4 Hamiltonian Vector Fields and the Poisson Bracket

Let $F = F[\mathbf{x}, \mathbf{p}]$ be a functional on the material phase space. Its differential is defined by

$$dF(\mathbf{V}, \mathbf{\Pi}) = \frac{d}{d\varepsilon}\bigg|_{\varepsilon=0} F[\mathbf{x} + \varepsilon\mathbf{V}, \mathbf{p} + \varepsilon\mathbf{\Pi}].$$

We write this differential in variational form as

$$dF(\mathbf{V}, \mathbf{\Pi}) = \int_{\widehat{M}} \left(\frac{\delta F}{\delta \mathbf{x}} \cdot \mathbf{V} + \frac{\delta F}{\delta \mathbf{p}} \cdot \mathbf{\Pi} \right) dX.$$

Thus $\delta F/\delta \mathbf{x}$ and $\delta F/\delta \mathbf{p}$ are variational derivatives. Geometrically they are components of the one-form dF. In the Euclidean setting we identify vectors and covectors by the usual dot product, which is why they are written as vector-valued functions.

The Hamiltonian vector field X_F associated with F is defined by

$$\iota_{X_F} \Omega_L = dF,$$

or equivalently,

$$\Omega_L(X_F, Y) = dF(Y)$$

for every tangent vector Y to the phase space. Write

$$X_F = (\mathbf{V}_F, \mathbf{\Pi}_F).$$

Using the formula for Ω_L, we have, for every $Y = (\mathbf{W}, \mathbf{\Sigma})$,

$$\Omega_L(X_F, Y) = \int_{\widehat{M}} (\mathbf{V}_F \cdot \mathbf{\Sigma} - \mathbf{W} \cdot \mathbf{\Pi}_F)\, dX,$$
$$dF(Y) = \int_{\widehat{M}} \left(\frac{\delta F}{\delta \mathbf{x}} \cdot \mathbf{W} + \frac{\delta F}{\delta \mathbf{p}} \cdot \mathbf{\Sigma} \right) dX.$$

Since this holds for arbitrary $\mathbf{W}$ and $\mathbf{\Sigma}$, we obtain

$$\mathbf{V}_F = \frac{\delta F}{\delta \mathbf{p}}, \qquad \mathbf{\Pi}_F = -\frac{\delta F}{\delta \mathbf{x}}.$$

Therefore

$$X_F = \left(\frac{\delta F}{\delta \mathbf{p}}, -\frac{\delta F}{\delta \mathbf{x}} \right).$$

Taking $F = H$, the Hamiltonian evolution is the flow generated by X_H:

$$\frac{d}{dt}(\mathbf{x}, \mathbf{p}) = X_H(\mathbf{x}, \mathbf{p}).$$

Hence

$$\dot{\mathbf{x}} = \frac{\delta H}{\delta \mathbf{p}}, \qquad \dot{\mathbf{p}} = -\frac{\delta H}{\delta \mathbf{x}}.$$

These are the canonical Hamiltonian equations in material coordinates.

5.3.5 The Lagrangian Poisson Bracket

The Poisson bracket of two functionals F and G is defined by

$$\{F, G\}_L = dF(X_G).$$

Equivalently,

$$\{F, G\}_L = \Omega_L(X_G, X_F).$$

Using the expression for Hamiltonian vector fields, this gives

$$\boxed{\{F,G\}_L = \int_{\widehat{M}} \left(\frac{\delta F}{\delta \mathbf{x}} \cdot \frac{\delta G}{\delta \mathbf{p}} - \frac{\delta G}{\delta \mathbf{x}} \cdot \frac{\delta F}{\delta \mathbf{p}} \right) dX.} \tag{5.8}$$

For any functional $F[\mathbf{x}, \mathbf{p}]$, its evolution is

$$\frac{dF}{dt} = \{F, H\}_L.$$

Taking $F = \mathbf{x}$ and $F = \mathbf{p}$ gives the canonical equations (5.6).

5.3.6 Advantages of the Hamiltonian Viewpoint

The Hamiltonian formulation gives more than another derivation of the Euler equations. It identifies the material motion of an ideal fluid as a Hamiltonian flow on the phase space with coordinates $(\mathbf{x}, \mathbf{p})$. The Hamiltonian is the total energy,

$$H[\mathbf{x}, \mathbf{p}] = \int_{\widehat{M}} \frac{|\mathbf{p}|^2}{2\rho_0} \, dX + \int_{\widehat{M}} \rho_0 U \left(S_0, \frac{J}{\rho_0} \right) dX.$$

If the Hamiltonian has no explicit time dependence, then

$$\frac{dH}{dt} = \{H, H\}_L = 0.$$

Thus energy conservation follows immediately from the antisymmetry of the Poisson bracket.

A second advantage is geometric. The Hamiltonian flow preserves the canonical symplectic form:

$$(\Phi_t)^* \Omega_L = \Omega_L,$$

where Φ_t denotes the flow map on phase space. This is the infinite-dimensional analogue of the preservation of $dq^i \wedge dp_i$ in finite-dimensional mechanics. Formally, it also corresponds to a Liouville-type preservation of phase-space volume.

A third advantage is that conservation laws are tied systematically to symmetry through Noether's theorem. Spatial translation symmetry gives linear momentum conservation, rotational symmetry gives angular momentum conservation, and time translation symmetry gives energy conservation. For fluids there is an additional and deeper symmetry: particle relabelling of the material manifold. This symmetry leads to the circulation and potential-vorticity invariants discussed below.

Finally, the material Hamiltonian formulation explains why the Eulerian Hamiltonian structure is noncanonical. The variables $(\mathbf{x}, \mathbf{p})$ are canonical coordinates on the material phase space, but the Eulerian variables

$$\mathbf{m} = \rho \mathbf{v}, \qquad \rho, \qquad S$$

are reduced variables. Passing from material to Eulerian variables removes the particle labels. As a result, the Eulerian Poisson bracket is no longer canonical and becomes degenerate. This degeneracy is responsible for the appearance of Casimirs.

5.4 Eulerian Reduction and Dynamically Accessible Variations

The material formulation uses the particle map $\mathbf{x}(t, X)$ as the fundamental variable. In Eulerian coordinates, however, the basic fields are

$$\mathbf{v}(t, \mathbf{x}), \qquad \rho(t, \mathbf{x}), \qquad S(t, \mathbf{x}),$$

where $\mathbf{x} \in M_t$. These fields are not independent. They are induced from the same material motion by

$$\mathbf{v}(t, \mathbf{x}(t, X)) = \partial_t \mathbf{x}(t, X),$$
$$\rho(t, \mathbf{x}(t, X))J(t, X) = \rho_0(X), \qquad S(t, \mathbf{x}(t, X)) = S_0(X).$$

The passage from the material variables to these Eulerian fields is called Eulerian reduction.

5.4.1 The Reduced Lagrangian

The material Lagrangian can be written in Eulerian variables as

$$l[\mathbf{v}, \rho, S] = \int_{M_t} \left[\frac{1}{2}\rho|\mathbf{v}|^2 - \rho U\left(S, \frac{1}{\rho}\right) \right] d\mathbf{x}.$$

Thus the action becomes

$$\mathcal{A} = \int_{t_0}^{t_1} l[\mathbf{v}, \rho, S]\, dt.$$

Although this action is expressed in Eulerian variables, the variations of $\mathbf{v}$, ρ, and S are not arbitrary. They must come from variations of the underlying material motion.

5.4.2 Eulerian Variation Field

Let $\mathbf{x}^\varepsilon(t, X)$ be a variation of the material motion and define

$$\delta\mathbf{x}(t, X) = \left.\frac{d}{d\varepsilon}\right|_{\varepsilon=0} \mathbf{x}^\varepsilon(t, X).$$

The corresponding Eulerian variation field is

$$\mathbf{w}(t, \mathbf{x}(t, X)) = \delta\mathbf{x}(t, X).$$

Thus $\mathbf{w}(t, \mathbf{x})$ is the Eulerian representation of the virtual displacement of particles.

The variation of the Eulerian velocity is obtained by differentiating

$$\mathbf{v}^\varepsilon(t, \mathbf{x}^\varepsilon(t, X)) = \partial_t \mathbf{x}^\varepsilon(t, X).$$

Taking the ε-derivative at $\varepsilon = 0$ gives

$$\delta\mathbf{v}(t, \mathbf{x}(t, X)) + (\mathbf{w} \cdot \nabla)\mathbf{v}(t, \mathbf{x}(t, X)) = \partial_t \mathbf{w}(t, \mathbf{x}(t, X)) + (\mathbf{v} \cdot \nabla)\mathbf{w}(t, \mathbf{x}(t, X)).$$

Therefore

$$\delta\mathbf{v} = \partial_t \mathbf{w} + \mathbf{v} \cdot \nabla\mathbf{w} - \mathbf{w} \cdot \nabla\mathbf{v}.$$

Using the Lie bracket of vector fields,

$$[\mathbf{v}, \mathbf{w}] = \mathbf{v} \cdot \nabla\mathbf{w} - \mathbf{w} \cdot \nabla\mathbf{v},$$

we obtain

$$\boxed{\delta\mathbf{v} = \partial_t \mathbf{w} + [\mathbf{v}, \mathbf{w}].} \tag{5.9}$$

5.4.3 Variations of Density and Entropy

The variations of ρ and S are also induced by variations of the material motion. More precisely, let

$$\mathbf{x}^\varepsilon(t, X)$$

be a family of motions, and let

$$\rho^\varepsilon(t, \mathbf{x}), \qquad S^\varepsilon(t, \mathbf{x})$$

be the corresponding Eulerian density and entropy. The variations are not arbitrary: for each ε, the transported quantities must satisfy

$$\rho^\varepsilon(t, \mathbf{x}^\varepsilon(t, X))J^\varepsilon(t, X) = \rho_0(X),$$

and

$$S^\varepsilon(t, \mathbf{x}^\varepsilon(t, X)) = S_0(X),$$

where

$$J^\varepsilon(t, X) = \det \nabla_X \mathbf{x}^\varepsilon(t, X).$$

Define the Eulerian variation field by

$$\mathbf{w}(t, \mathbf{x}(t, X)) = \left.\frac{d}{d\varepsilon}\right|_{\varepsilon=0} \mathbf{x}^\varepsilon(t, X).$$

We first vary the mass constraint

$$\rho^\varepsilon(t, \mathbf{x}^\varepsilon(t, X))J^\varepsilon(t, X) = \rho_0(X).$$

Differentiating with respect to ε at $\varepsilon = 0$ gives

$$(\delta\rho + \mathbf{w} \cdot \nabla\rho)\, J + \rho\, \delta J = 0.$$

Since

$$\delta J = J\nabla \cdot \mathbf{w},$$

we obtain

$$\delta\rho + \mathbf{w} \cdot \nabla\rho + \rho\nabla \cdot \mathbf{w} = 0.$$

Therefore

$$\boxed{\delta\rho = -\nabla \cdot (\rho\mathbf{w}).} \tag{5.10}$$

Similarly, entropy is transported by the motion:

$$S^\varepsilon(t, \mathbf{x}^\varepsilon(t, X)) = S_0(X).$$

Differentiating with respect to ε at $\varepsilon = 0$ gives

$$\delta S + \mathbf{w} \cdot \nabla S = 0.$$

Hence

$$\boxed{\delta S = -\mathbf{w} \cdot \nabla S.} \tag{5.11}$$

The three formulas

$$\delta\mathbf{v} = \partial_t\mathbf{w} + [\mathbf{v}, \mathbf{w}], \qquad \delta\rho = -\nabla \cdot (\rho\mathbf{w}), \qquad \delta S = -\mathbf{w} \cdot \nabla S$$

are called dynamically accessible variations. They are "accessible" because they are precisely the Eulerian variations induced by variations of the material flow map. Thus, in the Eulerian variational principle, $\mathbf{v}$, ρ, and S cannot be varied independently.

5.4.4 Eulerian Form of Hamilton's Principle

Hamilton's principle in Eulerian variables is therefore

$$\delta \int_{t_0}^{t_1} l[\mathbf{v}, \rho, S]\, dt = 0,$$

where

$$l[\mathbf{v}, \rho, S] = \int_{M_t} \left[\frac{1}{2}\rho|\mathbf{v}|^2 - \rho U\left(S, \frac{1}{\rho}\right) \right] d\mathbf{x},$$

and the variations are constrained by

$$\delta\mathbf{v} = \partial_t \mathbf{w} + [\mathbf{v}, \mathbf{w}], \qquad \delta\rho = -\nabla \cdot (\rho\mathbf{w}), \qquad \delta S = -\mathbf{w} \cdot \nabla S.$$

The variation field $\mathbf{w}$ is assumed to vanish at the temporal endpoints:

$$\mathbf{w}(t_0, \mathbf{x}) = \mathbf{w}(t_1, \mathbf{x}) = 0.$$

This is the Eulerian reduced form of Hamilton's principle. It is the starting point for the Euler–Poincare equations.

5.5 The Euler–Poincare Equations

The Eulerian variational principle obtained above has the form

$$\delta \int_{t_0}^{t_1} l[\mathbf{v}, \rho, S]\, dt = 0,$$

where the variations are dynamically accessible:

$$\delta\mathbf{v} = \partial_t \mathbf{w} + [\mathbf{v}, \mathbf{w}], \qquad \delta\rho = -\nabla \cdot (\rho\mathbf{w}), \qquad \delta S = -\mathbf{w} \cdot \nabla S.$$

We now compute the resulting Eulerian equation.

Let

$$l = l[\mathbf{v}, \rho, S]$$

be a reduced Lagrangian. Its first variation is written as

$$\delta l = \int_{M_t} \left(\frac{\delta l}{\delta \mathbf{v}} \cdot \delta\mathbf{v} + \frac{\delta l}{\delta \rho}\, \delta\rho + \frac{\delta l}{\delta S}\, \delta S \right) d\mathbf{x}.$$

Substituting the dynamically accessible variations gives

$$\begin{aligned} \delta l = &\int_{M_t} \frac{\delta l}{\delta \mathbf{v}} \cdot (\partial_t \mathbf{w} + [\mathbf{v}, \mathbf{w}])\, d\mathbf{x} \\ &- \int_{M_t} \frac{\delta l}{\delta \rho} \nabla \cdot (\rho\mathbf{w})\, d\mathbf{x} - \int_{M_t} \frac{\delta l}{\delta S} \mathbf{w} \cdot \nabla S\, d\mathbf{x}. \end{aligned}$$

After integration by parts in time and space, and using $\mathbf{w}(t_0, \mathbf{x}) = \mathbf{w}(t_1, \mathbf{x}) = 0$, we obtain

$$0 = \delta \int_{t_0}^{t_1} l\, dt = \int_{t_0}^{t_1} \int_{M_t} \left[-\partial_t \frac{\delta l}{\delta \mathbf{v}} - \mathrm{ad}^*_{\mathbf{v}} \frac{\delta l}{\delta \mathbf{v}} + \rho \nabla \frac{\delta l}{\delta \rho} - \frac{\delta l}{\delta S} \nabla S \right] \cdot \mathbf{w}\, d\mathbf{x}\, dt.$$

Since $\mathbf{w}$ is arbitrary, the Euler–Poincare equation is

$$\boxed{\partial_t \frac{\delta l}{\delta \mathbf{v}} + \mathrm{ad}^*_{\mathbf{v}} \frac{\delta l}{\delta \mathbf{v}} = \rho \nabla \frac{\delta l}{\delta \rho} - \frac{\delta l}{\delta S} \nabla S.} \tag{5.12}$$

Here $\mathrm{ad}^*_{\mathbf{v}}$ denotes the coadjoint operator associated with the vector field $\mathbf{v}$. We now recall its definition and fix the sign convention used in this chapter. Let

$$\mathbf{m} = \frac{\delta l}{\delta \mathbf{v}}.$$

Then

$$\int_{M_t} \mathbf{m} \cdot \delta \mathbf{v} \, d\mathbf{x} = \int_{M_t} \mathbf{m} \cdot (\partial_t \mathbf{w} + [\mathbf{v}, \mathbf{w}]) \, d\mathbf{x}.$$

Integrating the first term by parts in time gives

$$\int_{M_t} \mathbf{m} \cdot \partial_t \mathbf{w} \, d\mathbf{x} = - \int_{M_t} \partial_t \mathbf{m} \cdot \mathbf{w} \, d\mathbf{x},$$

where the endpoint terms vanish because $\mathbf{w}(t_0, \mathbf{x}) = \mathbf{w}(t_1, \mathbf{x}) = 0$.

For the Lie bracket term, we define $\mathrm{ad}^*_{\mathbf{v}}$ by

$$- \int_{M_t} \mathbf{m} \cdot [\mathbf{v}, \mathbf{w}] \, d\mathbf{x} = \int_{M_t} \mathrm{ad}^*_{\mathbf{v}} \, \mathbf{m} \cdot \mathbf{w} \, d\mathbf{x}.$$

Equivalently,

$$-\mathbf{m} \cdot [\mathbf{v}, \mathbf{w}] = \mathrm{ad}^*_{\mathbf{v}} \, \mathbf{m} \cdot \mathbf{w} \quad \text{after integration over } M_t.$$

In components,

$$[\mathbf{v}, \mathbf{w}]^i = v^j \partial_j w^i - w^j \partial_j v^i.$$

Hence

$$\begin{aligned} - \int_{M_t} m_i [\mathbf{v}, \mathbf{w}]^i \, d\mathbf{x} &= - \int_{M_t} m_i \left(v^j \partial_j w^i - w^j \partial_j v^i \right) \, d\mathbf{x} \\ &= \int_{M_t} \left[\partial_j (m_i v^j) + m_j \partial_i v^j \right] w^i \, d\mathbf{x}. \end{aligned}$$

Therefore

$$\boxed{(\mathrm{ad}^*_{\mathbf{v}} \, \mathbf{m})_i = \partial_j (m_i v^j) + m_j \partial_i v^j.} \tag{5.13}$$

In vector notation,

$$\mathrm{ad}^*_{\mathbf{v}} \, \mathbf{m} = \nabla \cdot (\mathbf{v} \otimes \mathbf{m}) + (\nabla \mathbf{v})^T \mathbf{m}.$$

Here $\mathrm{ad}^*_{\mathbf{v}}$ is the formal adjoint of the Lie bracket operator. In vector notation, if $\mathbf{m}$ is a one-form density, then

$$\mathrm{ad}^*_{\mathbf{v}} \, \mathbf{m} = \nabla \cdot (\mathbf{v} \otimes \mathbf{m}) + (\nabla \mathbf{v})^T \mathbf{m}.$$

Equivalently, in components,

$$(\mathrm{ad}^*_{\mathbf{v}} \, \mathbf{m})_i = \partial_j (v^j m_i) + m_j \partial_i v^j.$$

5.5.1 Application to Compressible Ideal Fluids

For the compressible ideal fluid,

$$l[\mathbf{v}, \rho, S] = \int_{M_t} \left[\frac{1}{2}\rho|\mathbf{v}|^2 - \rho U\left(S, \frac{1}{\rho}\right) \right] d\mathbf{x}.$$

The variational derivatives are

$$\frac{\delta l}{\delta \mathbf{v}} = \rho\mathbf{v} = \mathbf{m},$$
$$\frac{\delta l}{\delta S} = -\rho U_S = -\rho T,$$

where

$$T = \frac{\partial U}{\partial S}.$$

To compute $\delta l/\delta\rho$, write

$$V = \frac{1}{\rho}, \qquad p = -\frac{\partial U}{\partial V}.$$

Then

$$\begin{aligned}\frac{\delta l}{\delta \rho} &= \frac{1}{2}|\mathbf{v}|^2 - U(S,V) - \rho U_V \frac{\partial V}{\partial \rho} \\ &= \frac{1}{2}|\mathbf{v}|^2 - U(S,V) - \rho(-p)\left(-\frac{1}{\rho^2}\right) \\ &= \frac{1}{2}|\mathbf{v}|^2 - U(S,V) - \frac{p}{\rho}.\end{aligned}$$

Thus

$$\frac{\delta l}{\delta \rho} = \frac{1}{2}|\mathbf{v}|^2 - h, \qquad h = U + \frac{p}{\rho}.$$

Substituting these derivatives into (5.12) gives

$$\partial_t \mathbf{m} + \mathrm{ad}^*_{\mathbf{v}}\, \mathbf{m} = \rho\nabla\left(\frac{1}{2}|\mathbf{v}|^2 - h\right) + \rho T\nabla S.$$

Since $\mathbf{m} = \rho\mathbf{v}$, this equation is equivalent to

$$\rho\left(\partial_t \mathbf{v} + \mathbf{v}\cdot\nabla\mathbf{v}\right) = -\rho\nabla h + \rho T\nabla S.$$

Using the thermodynamic identity

$$dh = T\, dS + \frac{1}{\rho}\, dp,$$

we obtain

$$-\rho\nabla h + \rho T\nabla S = -\nabla p.$$

Therefore the Euler–Poincare equation becomes

$$\boxed{\rho\left(\partial_t \mathbf{v} + \mathbf{v}\cdot\nabla\mathbf{v}\right) = -\nabla p.} \tag{5.14}$$

Together with

$$\partial_t \rho + \nabla\cdot(\rho\mathbf{v}) = 0, \qquad \partial_t S + \mathbf{v}\cdot\nabla S = 0,$$

this recovers the compressible adiabatic Euler system.

5.5.2 Meaning of the Euler–Poincare Form

The Euler–Poincare equation is not a new fluid equation. It is the Eulerian form of Hamilton's principle after reduction by particle labels. Its importance is structural. It tells us that the Eulerian velocity, density, and entropy must be varied in a coordinated way, because they all come from the same underlying material motion.

Thus the passage

$$\mathbf{x}(t, X) \quad \longrightarrow \quad (\mathbf{v}, \rho, S)$$

has two consequences. First, the variational principle becomes an Eulerian variational principle with dynamically accessible variations. Second, the canonical material Hamiltonian structure will become a noncanonical Eulerian Hamiltonian structure. Both features come from the same reduction process.

5.6 Noether's Theorem: Symmetry and Invariants

The variational formulation gives a systematic relation between symmetries and conservation laws. This relation is Noether's theorem. In this chapter we use it in a concrete form adapted to material fluid mechanics.

Suppose the material action

$$\mathcal{A}[\mathbf{x}] = \int_{t_0}^{t_1} L[\mathbf{x}, \dot{\mathbf{x}}]\, dt$$

is unchanged under a one-parameter family of transformations

$$\mathbf{x}(t, X) \mapsto \mathbf{x}^\varepsilon(t, X), \qquad \mathbf{x}^0(t, X) = \mathbf{x}(t, X).$$

The infinitesimal generator of this transformation is

$$\mathbf{Z}(t, X) = \left.\frac{d}{d\varepsilon}\right|_{\varepsilon=0} \mathbf{x}^\varepsilon(t, X).$$

If the transformation leaves the Lagrangian invariant, then Noether's theorem states that

$$\boxed{I_{\mathbf{Z}}(t) = \int_{\widehat{M}} \mathbf{p}(t, X) \cdot \mathbf{Z}(t, X)\, dX} \tag{5.15}$$

is conserved:

$$\frac{d}{dt} I_{\mathbf{Z}}(t) = 0.$$

Here

$$\mathbf{p}(t, X) = \frac{\delta L}{\delta \dot{\mathbf{x}}}(t, X)$$

is the material momentum. Thus the rule is simple:

$$\boxed{\text{infinitesimal symmetry } \mathbf{Z} \quad \Longrightarrow \quad \text{conserved quantity } \int_{\widehat{M}} \mathbf{p} \cdot \mathbf{Z}\, dX.}$$

We give the short proof, since it explains why the momentum appears in the conserved quantity. Invariance of the Lagrangian gives

$$\frac{d}{d\varepsilon}\bigg|_{\varepsilon=0} L[\mathbf{x}^\varepsilon, \dot{\mathbf{x}}^\varepsilon] = 0.$$

By the chain rule,

$$0 = \int_{\widehat{M}} \left(\frac{\delta L}{\delta \mathbf{x}} \cdot \mathbf{Z} + \frac{\delta L}{\delta \dot{\mathbf{x}}} \cdot \dot{\mathbf{Z}} \right) dX.$$

Along a solution of the Euler–Lagrange equation,

$$\frac{\delta L}{\delta \mathbf{x}} = \frac{d}{dt} \frac{\delta L}{\delta \dot{\mathbf{x}}}.$$

Therefore

$$\begin{aligned} 0 &= \int_{\widehat{M}} \left[\frac{d}{dt} \left(\frac{\delta L}{\delta \dot{\mathbf{x}}} \right) \cdot \mathbf{Z} + \frac{\delta L}{\delta \dot{\mathbf{x}}} \cdot \dot{\mathbf{Z}} \right] dX \\ &= \frac{d}{dt} \int_{\widehat{M}} \frac{\delta L}{\delta \dot{\mathbf{x}}} \cdot \mathbf{Z} \, dX. \end{aligned}$$

Since

$$\mathbf{p} = \frac{\delta L}{\delta \dot{\mathbf{x}}},$$

we obtain

$$\frac{d}{dt} \int_{\widehat{M}} \mathbf{p}(t, X) \cdot \mathbf{Z}(t, X) \, dX = 0.$$

This proves (5.15).

We now apply this rule to three concrete symmetries: translations, rotations, and particle relabelling.

5.6.1 Spatial Symmetries and Classical Conservation Laws

First consider spatial translations. For a fixed constant vector $\mathbf{a}$, define

$$\mathbf{x}^\varepsilon(t, X) = \mathbf{x}(t, X) + \varepsilon \mathbf{a}.$$

The infinitesimal generator is

$$\mathbf{Z}(t, X) = \mathbf{a}.$$

If the Lagrangian is invariant under translations, then Noether's theorem gives

$$I_{\mathbf{a}}(t) = \int_{\widehat{M}} \mathbf{p}(t, X) \cdot \mathbf{a} \, dX.$$

Since $\mathbf{a}$ is arbitrary, this is equivalent to conservation of total linear momentum:

$$\boxed{\mathbf{P} = \int_{\widehat{M}} \mathbf{p}(t, X) \, dX = \int_{M_t} \rho \mathbf{v} \, d\mathbf{x}, \qquad \frac{d\mathbf{P}}{dt} = 0.} \tag{5.16}$$

Next consider rotations. Let $\mathbf{a}$ be a fixed vector and rotate the configuration infinitesimally around the axis $\mathbf{a}$:

$$\mathbf{x}^\varepsilon(t,X) = \mathbf{x}(t,X) + \varepsilon\,\mathbf{a}\times\mathbf{x}(t,X) + O(\varepsilon^2).$$

The infinitesimal generator is

$$\mathbf{Z}(t,X) = \mathbf{a}\times\mathbf{x}(t,X).$$

If the Lagrangian is invariant under rotations, Noether's theorem gives

$$\begin{aligned} I_{\mathbf{a}}(t) &= \int_{\widehat{M}} \mathbf{p}\cdot(\mathbf{a}\times\mathbf{x})\,dX \\ &= \mathbf{a}\cdot\int_{\widehat{M}} \mathbf{x}\times\mathbf{p}\,dX. \end{aligned}$$

Since $\mathbf{a}$ is arbitrary, the total angular momentum is conserved:

$$\boxed{\mathbf{L} = \int_{\widehat{M}} \mathbf{x}(t,X)\times\mathbf{p}(t,X)\,dX = \int_{M_t} \mathbf{x}\times\rho\mathbf{v}\,d\mathbf{x}, \qquad \frac{d\mathbf{L}}{dt} = 0.} \tag{5.17}$$

Finally, invariance under time translation gives energy conservation. If the Lagrangian has no explicit dependence on t, then

$$\boxed{E = H[\mathbf{x},\mathbf{p}], \qquad \frac{dE}{dt} = 0.} \tag{5.18}$$

The same rule applies to relabelling symmetry. The difference is that translations and rotations move the physical position $\mathbf{x}$, while relabelling changes the material label X.

5.6.2 Particle Relabelling Symmetry and Fluid Invariants

Fluid mechanics has another symmetry that does not occur in finite-dimensional particle mechanics in the same way. The material coordinate X is a label attached to a fluid particle. The physical motion is the set of particle trajectories in space, not the particular names assigned to the particles. Therefore one may change labels without changing the physical flow.

A relabelling is a diffeomorphism

$$\psi : \widehat{M} \to \widehat{M}.$$

It acts on the material motion from the right:

$$\varphi_t \mapsto \varphi_t \circ \psi.$$

Equivalently,

$$\mathbf{x}(t,X) \mapsto \mathbf{x}(t,\psi(X)).$$

For a compressible adiabatic fluid, not every diffeomorphism of $\widehat{M}$ is an admissible relabelling. The relabelling must preserve the material mass form and the material entropy distribution:

$$\boxed{\psi^*(\rho_0\,dX) = \rho_0\,dX, \qquad S_0\circ\psi = S_0.} \tag{5.19}$$

Infinitesimally, if $\mathbf{W}(X)$ is the generator of the relabelling, then

$$\boxed{\nabla_X\cdot(\rho_0\mathbf{W}) = 0, \qquad \mathbf{W}\cdot\nabla_X S_0 = 0.} \tag{5.20}$$

Thus $\mathbf{W}$ preserves both the mass distribution and the entropy labels.

We now apply Noether's theorem to this right symmetry. Let ψ_ε be a one-parameter family of relabellings with

$$\left.\frac{d}{d\varepsilon}\right|_{\varepsilon=0} \psi_\varepsilon(X) = \mathbf{W}(X).$$

The induced variation of the motion is

$$\delta\mathbf{x}(t,X) = \left.\frac{d}{d\varepsilon}\right|_{\varepsilon=0} \mathbf{x}(t,\psi_\varepsilon(X)) = \nabla_X \mathbf{x}(t,X)\mathbf{W}(X).$$

Therefore the Noether quantity is

$$\int_{\widehat{M}} \frac{\delta L}{\delta \dot{\mathbf{x}}} \cdot \delta\mathbf{x}\, dX = \int_{\widehat{M}} \mathbf{p}(t,X) \cdot \nabla_X \mathbf{x}(t,X)\mathbf{W}(X)\, dX.$$

Since

$$\mathbf{p} = \rho_0 \dot{\mathbf{x}}, \qquad \mathbf{v}(t,\mathbf{x}(t,X)) = \dot{\mathbf{x}}(t,X),$$

this can be written in terms of the pullback of the Eulerian velocity one-form

$$v = \mathbf{v} \cdot d\mathbf{x}.$$

Thus the relabelling Noether invariant is

$$\boxed{I_{\mathbf{W}}(t) = \int_{\widehat{M}} \rho_0(X) \left(\varphi_t^* v\right)_X (\mathbf{W}(X))\, dX, \qquad \frac{d}{dt} I_{\mathbf{W}}(t) = 0.} \tag{5.21}$$

This is the material form of the Noether invariant associated with particle relabelling.

Formula (5.21) contains Kelvin's theorem as a special case. If $\mathbf{W}$ is chosen to be concentrated in a thin material tube around a closed material curve γ_0, and tangent to that curve, then the invariant reduces, after division by the cross-sectional mass, to

$$\oint_{\gamma_0} \varphi_t^* v = \oint_{\gamma_t} \mathbf{v} \cdot d\mathbf{x}, \qquad \gamma_t = \varphi_t(\gamma_0).$$

Thus Kelvin circulation is the loop version of the relabelling Noether invariant. The direct Kelvin formula was derived in Chapter 4; here the point is its variational origin.

For non-isentropic flow, the relabelling generator must also satisfy

$$\mathbf{W} \cdot \nabla_X S_0 = 0.$$

Thus $\mathbf{W}$ is tangent to the material entropy surfaces.

In three dimensions, the two infinitesimal relabelling conditions (5.20) can be represented locally in a useful form. The first condition says that the vector field $\rho_0\mathbf{W}$ is divergence free in material coordinates. The second says that $\mathbf{W}$ is tangent to the level surfaces of S_0. A convenient local way to satisfy both conditions is to introduce another material label $a_0(X)$ and set

$$\boxed{\rho_0 \mathbf{W} = \nabla_X a_0 \times \nabla_X S_0.} \tag{5.22}$$

Indeed,

$$\nabla_X \cdot (\nabla_X a_0 \times \nabla_X S_0) = 0,$$

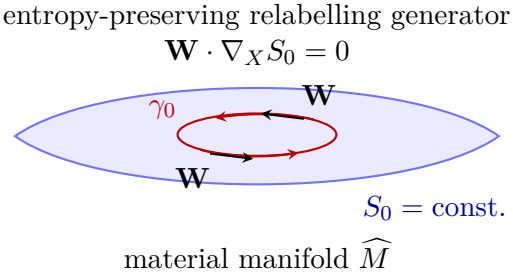


Figure 5.1: A relabelling generator $\mathbf{W}$ tangent to a closed material curve γ_0 lying on an entropy surface $S_0 = \text{const.}$. Such generators preserve the material entropy distribution and lead, through Noether's theorem, to circulation and potential-vorticity invariants.

because

$$\nabla_X a_0 \times \nabla_X S_0 = \nabla_X \times (a_0 \nabla_X S_0),$$

and the divergence of a curl is zero. Also,

$$\mathbf{W} \cdot \nabla_X S_0 = \frac{1}{\rho_0} (\nabla_X a_0 \times \nabla_X S_0) \cdot \nabla_X S_0 = 0.$$

Substituting (5.22) into (5.21) gives

$$I_{\mathbf{W}}(t) = \int_{\widehat{M}} (\varphi_t^* v) \, (\nabla_X a_0 \times \nabla_X S_0) \, dX.$$

Now pass to Eulerian variables. Define the advected labels

$$a(t, \mathbf{x}(t, X)) = a_0(X), \qquad S(t, \mathbf{x}(t, X)) = S_0(X).$$

Then

$$D_t a = 0, \qquad D_t S = 0.$$

The material vector

$$\frac{1}{\rho_0} \nabla_X a_0 \times \nabla_X S_0$$

pushes forward to the Eulerian vector field

$$\frac{1}{\rho} \nabla a \times \nabla S.$$

Therefore the Noether invariant becomes

$$I_{\mathbf{W}}(t) = \int_{M_t} \mathbf{v} \cdot (\nabla a \times \nabla S) \, d\mathbf{x}.$$

Using integration by parts, and assuming either suitable boundary conditions or compact support, we obtain

$$\begin{aligned} \int_{M_t} \mathbf{v} \cdot (\nabla a \times \nabla S) \, d\mathbf{x} &= \int_{M_t} a \, \nabla S \cdot (\nabla \times \mathbf{v}) \, d\mathbf{x} \\ &= \int_{M_t} a \, \boldsymbol{\omega} \cdot \nabla S \, d\mathbf{x} \\ &= \int_{M_t} \rho a \left(\frac{\boldsymbol{\omega} \cdot \nabla S}{\rho} \right) \, d\mathbf{x}. \end{aligned}$$

Thus the relabelling Noether invariant takes the Eulerian form

$$\boxed{I_{\mathbf{W}}(t) = \int_{M_t} \rho a q \, d\mathbf{x}, \qquad q = \frac{\boldsymbol{\omega} \cdot \nabla S}{\rho}.} \tag{5.23}$$

Since a is an arbitrary advected label, the conservation of these integrals is the variational origin of Ertel's theorem

$$D_t q = 0.$$

The direct verification of $D_t q = 0$ from the vorticity equation was given in Chapter 4. Here the point is different: potential vorticity appears as the Eulerian density of a Noether invariant associated with entropy-preserving particle relabelling.

Thus Kelvin circulation and Ertel potential vorticity are Eulerian expressions of the same underlying material relabelling symmetry. This interpretation is important for the rest of the chapter. The Clebsch representation introduced next makes the advected labels explicit in an Eulerian variational principle. Later, in the Eulerian Hamiltonian formulation, the same relabelling structure appears as degeneracy of the noncanonical Poisson bracket and gives rise to Casimirs.

5.7 Clebsch Representation

The Eulerian variational principle in the preceding sections used dynamically accessible variations. These variations are constrained because the Eulerian fields $\mathbf{v}$, ρ, and S come from an underlying material motion. The Clebsch representation gives another way to encode the same constraints. Instead of restricting the variations directly, one introduces Lagrange multipliers for the transport equations. The multipliers then become Clebsch potentials.

5.7.1 Clebsch Ansatz and Variational Meaning

Clebsch originally introduced potential representations of velocity, such as

$$\mathbf{v} = \nabla\phi + \alpha\nabla\beta.$$

In modern variational language, such formulas arise naturally from constrained Eulerian actions. The advected quantities play the role of labels, and their Lagrange multipliers appear in the velocity representation.

For a compressible adiabatic fluid, the most useful local form is the extended Clebsch representation

$$\boxed{\mathbf{v} = \nabla\varphi + \eta\nabla S + \zeta\nabla a.} \tag{5.24}$$

Here S is the entropy, a is an additional advected label, and η, ζ are conjugate multiplier fields. The scalar a is often called a Lin label.

5.7.2 Herivel–Lin Constrained Variations

We now derive (5.24) from an Eulerian constrained variational principle. Consider the action

$$\begin{aligned}\mathcal{A} = \int_{t_0}^{t_1} \int_{M_t} \Big\{ &\frac{1}{2}\rho|\mathbf{v}|^2 - \rho U\left(S, \frac{1}{\rho}\right) \\ &+ \varphi\left[\partial_t \rho + \nabla\cdot(\rho\mathbf{v})\right] \\ &- \rho\eta\left[\partial_t S + \mathbf{v}\cdot\nabla S\right] \\ &- \rho\zeta\left[\partial_t a + \mathbf{v}\cdot\nabla a\right] \Big\}\, d\mathbf{x}\, dt.\end{aligned}$$

The multiplier φ enforces mass conservation, η enforces entropy advection, and ζ enforces the advection of the Lin label a.

Variation with respect to φ, η, and ζ gives

$$\partial_t \rho + \nabla\cdot(\rho\mathbf{v}) = 0,$$

$$\partial_t S + \mathbf{v}\cdot\nabla S = 0, \qquad \partial_t a + \mathbf{v}\cdot\nabla a = 0.$$

Thus

$$D_t S = 0, \qquad D_t a = 0.$$

Now vary the action with respect to $\mathbf{v}$. The terms containing $\mathbf{v}$ are

$$\frac{1}{2}\rho|\mathbf{v}|^2 + \varphi\nabla\cdot(\rho\mathbf{v}) - \rho\eta\,\mathbf{v}\cdot\nabla S - \rho\zeta\,\mathbf{v}\cdot\nabla a.$$

Using integration by parts,

$$\int_{M_t} \varphi\nabla\cdot(\rho\,\delta\mathbf{v})\, d\mathbf{x} = -\int_{M_t} \rho\nabla\varphi\cdot\delta\mathbf{v}\, d\mathbf{x},$$

up to boundary terms. Therefore the $\mathbf{v}$-variation gives

$$\rho\mathbf{v} - \rho\nabla\varphi - \rho\eta\nabla S - \rho\zeta\nabla a = 0.$$

Hence

$$\mathbf{v} = \nabla\varphi + \eta\nabla S + \zeta\nabla a.$$

This is the extended Clebsch representation.

5.7.3 Why Lin Labels Are Needed

If we omit the Lin label a, the constrained action gives only

$$\mathbf{v} = \nabla\varphi + \eta\nabla S.$$

Then

$$\nabla\times\mathbf{v} = \nabla\eta\times\nabla S.$$

Thus the vorticity is restricted by the entropy field. In particular, if S is constant, this representation reduces to potential flow:

$$\nabla\times\mathbf{v} = 0.$$

This is too restrictive for general fluid motion.

The additional advected label a supplies the missing material-label information. With

$$\mathbf{v} = \nabla\varphi + \eta\nabla S + \zeta\nabla a,$$

the vorticity becomes

$$\boldsymbol{\omega} = \nabla \times \mathbf{v} = \nabla\eta \times \nabla S + \nabla\zeta \times \nabla a.$$

The second term carries vorticity associated with the advected Lin label. Thus the Clebsch representation is closely related to the relabelling symmetry discussed above: it keeps track of advected labels inside an Eulerian variational principle.

5.7.4 Evolution Equations for the Clebsch Variables

The remaining variations give evolution equations for the multipliers. Variation with respect to ρ gives

$$\partial_t\varphi + \mathbf{v}\cdot\nabla\varphi = \frac{1}{2}|\mathbf{v}|^2 - U - \frac{p}{\rho}.$$

Equivalently,

$$D_t\varphi = \frac{1}{2}|\mathbf{v}|^2 - h, \qquad h = U + \frac{p}{\rho}.$$

Variation with respect to S gives

$$D_t\eta = T,$$

where

$$T = \frac{\partial U}{\partial S}.$$

Variation with respect to a gives

$$D_t\zeta = 0.$$

Together with

$$D_t S = 0, \qquad D_t a = 0,$$

we obtain the Clebsch system

$$\boxed{\begin{aligned} \mathbf{v} &= \nabla\varphi + \eta\nabla S + \zeta\nabla a, \\ D_t S = 0, &\qquad D_t a = 0, \\ D_t\eta = T, &\qquad D_t\zeta = 0, \\ D_t\varphi &= \frac{1}{2}|\mathbf{v}|^2 - h. \end{aligned}} \tag{5.25}$$

These equations imply the compressible Euler momentum equation. Indeed, differentiate

$$\mathbf{v} = \nabla\varphi + \eta\nabla S + \zeta\nabla a$$

materially. Using

$$\frac{D}{Dt}\nabla f = \nabla(D_t f) - (\nabla\mathbf{v})^T\nabla f,$$

we find

$$\frac{D\mathbf{v}}{Dt} = \nabla(D_t\varphi) + (D_t\eta)\nabla S + \eta\nabla(D_t S) + (D_t\zeta)\nabla a + \zeta\nabla(D_t a) - (\nabla\mathbf{v})^T\mathbf{v}.$$

Since

$$(\nabla\mathbf{v})^T\mathbf{v} = \nabla\left(\frac{1}{2}|\mathbf{v}|^2\right),$$

and using the Clebsch system above, we obtain

$$\begin{aligned}\frac{D\mathbf{v}}{Dt} &= \nabla\left(\frac{1}{2}|\mathbf{v}|^2 - h\right) + T\nabla S - \nabla\left(\frac{1}{2}|\mathbf{v}|^2\right)\\ &= -\nabla h + T\nabla S.\end{aligned}$$

Using the thermodynamic identity

$$dh = T\,dS + \frac{1}{\rho}\,dp,$$

this becomes

$$\frac{D\mathbf{v}}{Dt} = -\frac{1}{\rho}\nabla p.$$

Thus the Clebsch system recovers the Euler momentum equation.

5.7.5 Geometric Interpretation and Local Validity

The extended Clebsch representation may also be understood through the modified velocity

$$\widetilde{\mathbf{v}} = \mathbf{v} - \eta\nabla S.$$

Then

$$\nabla\times\widetilde{\mathbf{v}} = \boldsymbol{\omega} - \nabla\eta\times\nabla S.$$

For smooth flows, this modified vorticity is transported by the motion. The local existence of Clebsch potentials is a form of the Darboux–Pfaff theorem. To see the idea, let

$$\widetilde{v} = \widetilde{\mathbf{v}}\cdot d\mathbf{x}$$

be the one-form associated with the modified velocity. Its exterior derivative

$$d\widetilde{v}$$

is the modified vorticity two-form. Locally, a two-form of rank two can be written in Darboux form

$$d\widetilde{v} = d\zeta\wedge da.$$

In vector notation this corresponds to

$$\nabla\times\widetilde{\mathbf{v}} = \nabla\zeta\times\nabla a.$$

Consequently,

$$d(\widetilde{v} - \zeta\,da) = 0.$$

By the Poincare lemma, on a simply connected coordinate neighborhood there exists a scalar function φ such that

$$\widetilde{v} - \zeta\, da = d\varphi.$$

Therefore

$$\widetilde{v} = d\varphi + \zeta\, da,$$

or, in vector notation,

$$\widetilde{\mathbf{v}} = \nabla\varphi + \zeta\nabla a.$$

Since

$$\mathbf{v} = \widetilde{\mathbf{v}} + \eta\nabla S,$$

we obtain the local extended Clebsch representation

$$\mathbf{v} = \nabla\varphi + \eta\nabla S + \zeta\nabla a.$$

This construction is local. Globally defined single-valued Clebsch potentials may fail to exist when the spatial domain has nontrivial topology, when the vorticity has linked or knotted structures, or when the helicity is nonzero. In such cases one may need multiple Clebsch charts, multivalued potentials, or a more general geometric formulation. For the variational structure, however, the local representation already reveals the important point: Clebsch variables are an Eulerian way to encode advected labels and relabelling information.

5.8 Eulerian Poisson Structure

We now return to the Hamiltonian viewpoint. In material coordinates the phase variables $(\mathbf{x}, \mathbf{p})$ are canonical, and the Poisson bracket is the canonical Lagrangian bracket. In Eulerian coordinates the natural variables are

$$\mathbf{m} = \rho\mathbf{v}, \qquad \rho, \qquad S.$$

These variables are obtained from $(\mathbf{x}, \mathbf{p})$ by reduction. As a result, the Eulerian Poisson bracket is no longer canonical. It is a noncanonical bracket whose degeneracy is responsible for Casimirs.

For the Hamiltonian formulation it is convenient to use the entropy density

$$\eta = \rho S$$

instead of the specific entropy S. Thus the Eulerian variables are

$$(\mathbf{m}, \rho, \eta).$$

The Hamiltonian is the total energy

$$\boxed{H[\mathbf{m}, \rho, \eta] = \int_{M_t} \left[\frac{|\mathbf{m}|^2}{2\rho} + \rho U\left(\frac{\eta}{\rho}, \frac{1}{\rho}\right) \right] d\mathbf{x}.} \tag{5.26}$$

Here

$$S = \frac{\eta}{\rho}.$$

5.8.1 Variational Derivatives of the Hamiltonian

The variational derivatives of H are

$$\frac{\delta H}{\delta \mathbf{m}} = \frac{\mathbf{m}}{\rho} = \mathbf{v}.$$

To compute the derivatives with respect to ρ and η, write

$$S = \frac{\eta}{\rho}, \qquad V = \frac{1}{\rho}.$$

Then

$$H = \int_{M_t} \left[\frac{|\mathbf{m}|^2}{2\rho} + \rho U(S, V) \right] d\mathbf{x}.$$

Using

$$T = U_S, \qquad p = -U_V,$$

one obtains

$$\frac{\delta H}{\delta \eta} = T,$$

and

$$\frac{\delta H}{\delta \rho} = -\frac{1}{2}|\mathbf{v}|^2 + U + \frac{p}{\rho} - TS.$$

Equivalently,

$$\frac{\delta H}{\delta \rho} = -\frac{1}{2}|\mathbf{v}|^2 + h - TS, \qquad h = U + \frac{p}{\rho}.$$

5.8.2 From the Lagrangian Bracket to the Eulerian Bracket

The Eulerian bracket is obtained by reducing the canonical Lagrangian bracket. The canonical variables are

$$(\mathbf{x}(X), \mathbf{p}(X)),$$

with bracket

$$\{F, G\}_L = \int_{\widehat{M}} \left(\frac{\delta F}{\delta \mathbf{x}} \cdot \frac{\delta G}{\delta \mathbf{p}} - \frac{\delta G}{\delta \mathbf{x}} \cdot \frac{\delta F}{\delta \mathbf{p}} \right) dX.$$

The Eulerian variables are obtained from the material variables by

$$\mathbf{m}(\mathbf{x}) = \int_{\widehat{M}} \mathbf{p}(X) \delta(\mathbf{x} - \mathbf{x}(X))\, dX,$$

$$\rho(\mathbf{x}) = \int_{\widehat{M}} \rho_0(X) \delta(\mathbf{x} - \mathbf{x}(X))\, dX,$$

and

$$\eta(\mathbf{x}) = \int_{\widehat{M}} \eta_0(X) \delta(\mathbf{x} - \mathbf{x}(X))\, dX, \qquad \eta_0 = \rho_0 S_0.$$

These formulas simply say that material momentum, mass, and entropy density are pushed forward by the motion.

Let $F = F[\mathbf{m}, \rho, \eta]$ be an Eulerian functional. When it is regarded as a functional of $(\mathbf{x}, \mathbf{p})$ through the above push-forward formulas, its variation has two contributions. A variation of $\mathbf{p}$ gives

$$\frac{\delta F}{\delta \mathbf{p}}(X) = \frac{\delta F}{\delta \mathbf{m}}(\mathbf{x}(X)).$$

A variation of $\mathbf{x}$ moves the delta functions and gives

$$\frac{\delta F}{\delta \mathbf{x}}(X) = -\Big[(\nabla \frac{\delta F}{\delta \mathbf{m}})^T \mathbf{m} + \rho \nabla \frac{\delta F}{\delta \rho} + \eta \nabla \frac{\delta F}{\delta \eta}\Big]_{\mathbf{x}=\mathbf{x}(X)}.$$

Equivalently, in weak form,

$$\delta F = \int_{\widehat{M}} \frac{\delta F}{\delta \mathbf{m}}(\mathbf{x}(X)) \cdot \delta \mathbf{p}(X)\, dX - \int_{\widehat{M}} \Big[(\nabla \frac{\delta F}{\delta \mathbf{m}})^T \mathbf{m} + \rho \nabla \frac{\delta F}{\delta \rho} + \eta \nabla \frac{\delta F}{\delta \eta}\Big]_{\mathbf{x}=\mathbf{x}(X)} \cdot \delta \mathbf{x}(X)\, dX.$$

Substituting these chain-rule formulas for F and G into the canonical bracket $\{F, G\}_L$, and then changing variables from X to $\mathbf{x}$, gives the Eulerian reduced bracket below.

5.8.3 The Noncanonical Poisson Bracket

For functionals $F = F[\mathbf{m}, \rho, \eta]$ and $G = G[\mathbf{m}, \rho, \eta]$, the Eulerian noncanonical Poisson bracket is

$$\boxed{\begin{aligned} \{F, G\}_E = & -\int_{M_t} \mathbf{m} \cdot \left[\frac{\delta F}{\delta \mathbf{m}}, \frac{\delta G}{\delta \mathbf{m}}\right] d\mathbf{x} \\ & -\int_{M_t} \rho \left(\frac{\delta F}{\delta \mathbf{m}} \cdot \nabla \frac{\delta G}{\delta \rho} - \frac{\delta G}{\delta \mathbf{m}} \cdot \nabla \frac{\delta F}{\delta \rho}\right) d\mathbf{x} \\ & -\int_{M_t} \eta \left(\frac{\delta F}{\delta \mathbf{m}} \cdot \nabla \frac{\delta G}{\delta \eta} - \frac{\delta G}{\delta \mathbf{m}} \cdot \nabla \frac{\delta F}{\delta \eta}\right) d\mathbf{x}. \end{aligned}} \tag{5.27}$$

Here

$$[\mathbf{u}, \mathbf{w}] = \mathbf{u} \cdot \nabla \mathbf{w} - \mathbf{w} \cdot \nabla \mathbf{u}$$

is the Lie bracket of vector fields.

This bracket is noncanonical because $(\mathbf{m}, \rho, \eta)$ are not canonical position-momentum variables. They are reduced variables obtained from $(\mathbf{x}, \mathbf{p})$ by forgetting the particle labels. The same loss of label information is responsible for the degeneracy of the bracket and hence for the Casimirs discussed below.

This bracket is the reduced form of the canonical material bracket. The minus sign in the first term reflects the convention used for the right-invariant relabelling reduction. It is noncanonical because the Eulerian variables $(\mathbf{m}, \rho, \eta)$ are not canonical position-momentum coordinates.

5.8.4 Hamiltonian Form of the Compressible Euler Equations

The Hamiltonian evolution is

$$\frac{dF}{dt} = \{F, H\}_E$$

for every functional $F[\mathbf{m}, \rho, \eta]$. Taking F successively to test $\mathbf{m}$, ρ, and η, one obtains

$$\boxed{\begin{aligned} \partial_t \mathbf{m} &= -\operatorname{ad}^*_{\mathbf{v}} \mathbf{m} - \rho \nabla \frac{\delta H}{\delta \rho} - \eta \nabla \frac{\delta H}{\delta \eta}, \\ \partial_t \rho &= -\nabla \cdot (\rho \mathbf{v}), \\ \partial_t \eta &= -\nabla \cdot (\eta \mathbf{v}). \end{aligned}} \tag{5.28}$$

Since

$$\eta = \rho S,$$

the last two equations imply

$$\partial_t S + \mathbf{v} \cdot \nabla S = 0.$$

It remains to check the momentum equation. Using

$$\frac{\delta H}{\delta \rho} = -\frac{1}{2}|\mathbf{v}|^2 + h - TS, \qquad \frac{\delta H}{\delta \eta} = T,$$

we have

$$\rho \nabla \frac{\delta H}{\delta \rho} + \eta \nabla \frac{\delta H}{\delta \eta} = \rho \nabla \left(-\frac{1}{2}|\mathbf{v}|^2 + h - TS \right) + \rho S \nabla T.$$

Since

$$\nabla(TS) = T \nabla S + S \nabla T,$$

this becomes

$$\rho \nabla \frac{\delta H}{\delta \rho} + \eta \nabla \frac{\delta H}{\delta \eta} = -\rho \nabla \left(\frac{1}{2}|\mathbf{v}|^2 \right) + \rho \nabla h - \rho T \nabla S.$$

Using

$$dh = T\, dS + \frac{1}{\rho}\, dp,$$

we obtain

$$\rho \nabla h - \rho T \nabla S = \nabla p.$$

Thus

$$\rho \nabla \frac{\delta H}{\delta \rho} + \eta \nabla \frac{\delta H}{\delta \eta} = -\rho \nabla \left(\frac{1}{2}|\mathbf{v}|^2 \right) + \nabla p.$$

Substitution into the first equation of (5.28) gives the compressible Euler momentum equation

$$\rho \left(\partial_t \mathbf{v} + \mathbf{v} \cdot \nabla \mathbf{v} \right) = -\nabla p.$$

The Eulerian bracket therefore reproduces the same equations obtained from Hamilton's principle and from the Euler–Poincare formulation. Its importance is that it reveals the reduced Hamiltonian structure of the Eulerian variables.

5.9 Casimirs and Advected Invariants

The Eulerian Poisson bracket is noncanonical and degenerate. Degeneracy means that there are nontrivial functionals $C[\mathbf{m}, \rho, \eta]$ satisfying

$$\{C, F\}_E = 0$$

for every functional F. Such functionals are called Casimirs. They are conserved for every Hamiltonian, not because of the particular energy, but because of the structure of the Poisson bracket itself.

5.9.1 Entropy Casimirs

The simplest Casimirs come from entropy advection. Let

$$S = \frac{\eta}{\rho}.$$

For any smooth function f, define

$$\boxed{C_f[\rho, \eta] = \int_{M_t} \rho\, f(S)\, d\mathbf{x} = \int_{M_t} \rho\, f\left(\frac{\eta}{\rho}\right)\, d\mathbf{x}.} \tag{5.29}$$

We show that C_f is a Casimir.

First compute its variational derivatives:

$$\frac{\delta C_f}{\delta \mathbf{m}} = 0.$$

Since

$$S = \frac{\eta}{\rho},$$

we have

$$\delta S = \frac{\delta \eta}{\rho} - \frac{\eta}{\rho^2}\delta\rho = \frac{1}{\rho}\delta\eta - \frac{S}{\rho}\delta\rho.$$

Thus

$$\begin{aligned}\delta C_f &= \int_{M_t} \left[f(S)\delta\rho + \rho f'(S)\delta S\right]\, d\mathbf{x} \\ &= \int_{M_t} \left[f(S) - S f'(S)\right]\delta\rho\, d\mathbf{x} + \int_{M_t} f'(S)\delta\eta\, d\mathbf{x}.\end{aligned}$$

Therefore

$$\frac{\delta C_f}{\delta \rho} = f(S) - S f'(S), \qquad \frac{\delta C_f}{\delta \eta} = f'(S).$$

Now insert these into the Eulerian bracket. Since $\delta C_f/\delta\mathbf{m} = 0$, only the terms involving $\delta F/\delta\mathbf{m}$ remain:

$$\{C_f, F\}_E = \int_{M_t} \rho \frac{\delta F}{\delta \mathbf{m}} \cdot \nabla \frac{\delta C_f}{\delta \rho}\, d\mathbf{x} + \int_{M_t} \eta \frac{\delta F}{\delta \mathbf{m}} \cdot \nabla \frac{\delta C_f}{\delta \eta}\, d\mathbf{x}.$$

Using $\eta = \rho S$, this becomes

$$\{C_f, F\}_E = \int_{M_t} \rho \frac{\delta F}{\delta \mathbf{m}} \cdot \left[\nabla\left(f - Sf'\right) + S\nabla f'\right]\, d\mathbf{x}.$$

But

$$\nabla\left(f - Sf'\right) = -Sf''(S)\nabla S, \qquad S\nabla f' = Sf''(S)\nabla S.$$

The two terms cancel. Hence

$$\{C_f, F\}_E = 0$$

for every F. Therefore C_f is a Casimir.

These Casimirs express the fact that entropy is advected by the flow. The distribution of entropy among fluid particles is preserved.

5.9.2 Potential-Vorticity Casimirs

In three-dimensional non-isentropic flow, Ertel's potential vorticity

$$q = \frac{\boldsymbol{\omega} \cdot \nabla S}{\rho}$$

is also advected:

$$D_t q = 0.$$

Therefore functionals of the form

$$\boxed{C_f[\mathbf{m}, \rho, \eta] = \int_{M_t} \rho\, f(S, q)\, d\mathbf{x}} \tag{5.30}$$

are conserved, under suitable boundary conditions. These are the potential-vorticity Casimirs.

The reason is again advective. Since

$$D_t S = 0, \qquad D_t q = 0,$$

we have

$$D_t f(S, q) = 0.$$

Together with mass conservation,

$$\partial_t \rho + \nabla \cdot (\rho \mathbf{v}) = 0,$$

this implies

$$\partial_t(\rho f(S, q)) + \nabla \cdot (\rho f(S, q)\mathbf{v}) = 0.$$

Integrating over the fluid domain gives

$$\frac{d}{dt} \int_{M_t} \rho f(S, q)\, d\mathbf{x} = 0.$$

Thus (5.30) is conserved.

From the Hamiltonian viewpoint, these conservation laws reflect the degeneracy of the Eulerian Poisson bracket. From the variational viewpoint, they are the Eulerian remnants of particle relabelling symmetry.

5.9.3 Relation to Relabelling Symmetry

The appearance of Casimirs is not accidental. In material coordinates, the Hamiltonian structure is canonical and nondegenerate. After reduction to Eulerian variables, the particle labels are no longer explicit. The noncanonical bracket remembers this lost label information through its degeneracy.

Entropy Casimirs record the preservation of the material entropy distribution. Potential-vorticity Casimirs record the deeper relabelling invariants associated with entropy-preserving rearrangements of material labels. Thus the same structure appears in three forms:

$$\begin{aligned} \text{material relabelling symmetry} &\implies \text{Noether invariants,} \\ \text{Eulerian reduction} &\implies \text{noncanonical Poisson bracket,} \\ \text{degeneracy of the bracket} &\implies \text{Casimirs.} \end{aligned}$$

This closes the circle connecting Hamilton's principle, Noether's theorem, Clebsch variables, and the Eulerian Hamiltonian structure.

5.10 Summary and Further Reading

In this chapter we developed the variational and Hamiltonian formulation of compressible ideal fluids. The starting point was Hamilton's principle in material coordinates, where the basic unknown is the motion

$$\varphi_t : \widehat{M} \to M_t, \qquad \mathbf{x} = \mathbf{x}(t, X).$$

The material action gives the compressible Euler equations by variation of the flow map. Passing to the canonical momentum

$$\mathbf{p} = \rho_0 \dot{\mathbf{x}}$$

puts the system into canonical Hamiltonian form. Thus, in material coordinates, ideal fluid motion is a Hamiltonian flow preserving the canonical symplectic structure.

We then passed from material variables to Eulerian variables:

$$(\mathbf{x}, \mathbf{p}) \quad \longrightarrow \quad (\mathbf{v}, \rho, S) \quad \text{or} \quad (\mathbf{m}, \rho, \eta).$$

This reduction explains why Eulerian variations are dynamically accessible rather than arbitrary:

$$\delta\mathbf{v} = \partial_t \mathbf{w} + [\mathbf{v}, \mathbf{w}], \qquad \delta\rho = -\nabla \cdot (\rho \mathbf{w}), \qquad \delta S = -\mathbf{w} \cdot \nabla S.$$

It also explains why the Eulerian Poisson bracket is noncanonical and degenerate.

A central role was played by Noether's theorem. Spatial symmetries give the classical conservation laws of linear momentum, angular momentum, and energy. The special symmetry of fluids is particle relabelling: the physical motion does not depend on how fluid particles are named. This right symmetry of the material action gives the circulation and potential-vorticity invariants. In particular, Ertel's potential vorticity

$$q = \frac{\boldsymbol{\omega} \cdot \nabla S}{\rho}$$

appears as the Eulerian expression of a relabelling Noether invariant.

The Clebsch representation gives another view of the same structure. By introducing Lagrange multipliers for mass, entropy, and label advection, one obtains the local representation

$$\mathbf{v} = \nabla\varphi + \eta \nabla S + \zeta \nabla a.$$

Thus Clebsch variables encode advected labels directly in an Eulerian variational principle. Finally, the degeneracy of the Eulerian Poisson bracket leads to Casimirs, such as entropy Casimirs

$$C_f = \int_{M_t} \rho f(S)\, d\mathbf{x}$$

and potential-vorticity Casimirs

$$C_f = \int_{M_t} \rho f(S, q)\, d\mathbf{x}.$$

These are the Hamiltonian remnants of the relabelling symmetry.

Historical remarks. Variational ideas in fluid mechanics go back to Clebsch's work on potential representations of fluid velocity (Clebsch, 1859) and to the classical mechanics of Lagrange (Lagrange, 1788). Arnold's geometric interpretation of ideal incompressible flow as geodesic motion on a diffeomorphism group profoundly influenced the modern viewpoint (Arnold, 1966). The variational derivations of Herivel, Lin, and Seliger–Whitham clarified the role of advected constraints, particle labels, and Clebsch variables in ideal fluid mechanics (Herivel, 1955; Lin, 1963; Seliger and Whitham, 1968). The Euler–Poincare and Hamiltonian reduction viewpoints were later developed systematically in geometric mechanics (Abraham and Marsden, 1978; Marsden and Ratiu, 1994; Holm et al., 1998). The noncanonical Hamiltonian brackets for fluids and plasmas were developed by Morrison and others, and they explain the appearance of Casimirs and advected invariants (Morrison, 1982, 1998, 2006).

Further reading. For classical fluid mechanics and vorticity dynamics, see Batchelor (1967), Lamb (1932a), and Saffman (1992). For variational principles and Clebsch variables, see Herivel (1955), Lin (1963), Seliger and Whitham (1968), and Salmon (1988). For the geometric and Hamiltonian formulation, see Arnold (1966), Abraham and Marsden (1978), Marsden and Ratiu (1994), Holm et al. (1998), and Morrison (1998). For applications to geophysical fluid dynamics and potential vorticity, see Salmon (1988) and Vallis (2017).

Chapter 6

Flow Decomposition, Topology, and Applications

6.1 Introduction

The preceding chapter explained how circulation and vorticity evolve. We now ask the complementary question: what information determines the velocity? In a bounded fluid domain, the answer involves divergence, vorticity, normal boundary velocity, and finitely many global circulations. The boundary conditions are essential to this statement.

Throughout the bounded-domain discussion, $M \subset \mathbb{R}^3$ is connected with smooth boundary, $\boldsymbol{\nu}$ is its outward unit normal, and all fields are sufficiently regular for the calculations below. The same decomposition will be used for compressible and incompressible flows:

$$\mathbf{v} = \operatorname{grad} \varphi + \operatorname{curl} \boldsymbol{\psi} + \mathbf{h}.$$

The potential part carries divergence and normal boundary velocity. The vortical part carries vorticity and has zero normal boundary velocity. The harmonic part is both divergence-free and curl-free, is tangent to the boundary, and carries the remaining circulation information. The three components are orthogonal in the ordinary L^2 inner product.

We first recall the whole-space Helmholtz decomposition, then construct the boundary-adapted Hodge decomposition and explain its relation to the Hodge–Morrey–Friedrichs theorem. We combine topology and harmonic flow examples before discussing compressible and incompressible applications and the evolution of the components. The chapter prepares for irrotational flows and vortex dynamics in the following chapters. A central distinction is that Kelvin circulation around a material loop and the coefficient of a fixed harmonic basis are different quantities; conservation of the former does not generally imply constancy of the latter (Yin et al., 2023).

6.2 Helmholtz Decomposition in Euclidean Space

We begin with the classical Helmholtz decomposition in $\mathbb{R}^3$. Let $\mathbf{v}$ be a sufficiently smooth vector field that decays rapidly enough at infinity. Then $\mathbf{v}$ can be decomposed into an irrotational part and a solenoidal part:

$$\boxed{\mathbf{v} = \operatorname{grad} \varphi + \operatorname{curl} \boldsymbol{\psi}.} \tag{6.1}$$

Here

$$\operatorname{curl}(\operatorname{grad}\varphi) = 0, \qquad \operatorname{div}(\operatorname{curl}\boldsymbol{\psi}) = 0.$$

Thus $\operatorname{grad}\varphi$ is curl-free and $\operatorname{curl}\boldsymbol{\psi}$ is divergence-free.

Taking divergence in (6.1) gives

$$\Delta\varphi = \operatorname{div}\mathbf{v}.$$

Thus the scalar potential φ is determined by the divergence of $\mathbf{v}$. Taking curl gives

$$\operatorname{curl}(\operatorname{curl}\boldsymbol{\psi}) = \operatorname{curl}\mathbf{v}.$$

Therefore the vector potential $\boldsymbol{\psi}$ is determined by the vorticity

$$\boldsymbol{\omega} = \operatorname{curl}\mathbf{v}.$$

This already suggests the fluid interpretation:

$$\begin{aligned} \operatorname{grad}\varphi &: \text{ compressive or potential part,} \\ \operatorname{curl}\boldsymbol{\psi} &: \text{ vortical or solenoidal part.} \end{aligned}$$

The potential part carries the divergence:

$$\operatorname{div}\mathbf{v} = \Delta\varphi,$$

while the solenoidal part carries the vorticity:

$$\boldsymbol{\omega} = \operatorname{curl}(\operatorname{curl}\boldsymbol{\psi}).$$

Integral representation in $\mathbb{R}^3$. On the whole space, the decomposition can be written using Newtonian potentials. Let

$$G(\mathbf{x},\mathbf{y}) = \frac{1}{4\pi|\mathbf{x}-\mathbf{y}|}$$

be the fundamental solution of $-\Delta$ in $\mathbb{R}^3$. Formally,

$$\varphi(\mathbf{x}) = -\int_{\mathbb{R}^3} G(\mathbf{x},\mathbf{y})\ \operatorname{div}\mathbf{v}(\mathbf{y})\,d\mathbf{y}.$$

The vortical part can be reconstructed from vorticity by the Biot–Savart operator:

$$\operatorname{curl}\boldsymbol{\psi}(\mathbf{x}) = \frac{1}{4\pi}\int_{\mathbb{R}^3} \frac{\boldsymbol{\omega}(\mathbf{y})\times(\mathbf{x}-\mathbf{y})}{|\mathbf{x}-\mathbf{y}|^3}\,d\mathbf{y}.$$

This formula shows directly that the solenoidal component is determined by the vorticity, provided the domain is the whole space and the velocity decays suitably at infinity.

Why domains with boundary are different. The whole-space decomposition hides two important issues. First, in a bounded domain one must impose boundary conditions. Second, in a multiply connected domain, a vector field may have zero divergence and zero curl but still fail to vanish. This missing piece is the harmonic component.

Thus, on a general domain M, the correct decomposition is not merely

$$\mathbf{v} = \operatorname{grad}\varphi + \operatorname{curl}\boldsymbol{\psi},$$

but rather

$$\mathbf{v} = \operatorname{grad}\varphi + \operatorname{curl}\boldsymbol{\psi} + \mathbf{h}.$$

The next section explains this refined decomposition.

6.3 The Hodge–Morrey–Friedrichs Decomposition and Reconstruction

6.3.1 The Hodge–Morrey–Friedrichs Theorem

The classical Helmholtz decomposition separates a vector field in $\mathbb{R}^3$ into gradient and curl components, under suitable decay conditions at infinity. On a bounded domain, boundary conditions and topology must also be taken into account. The Hodge–Morrey–Friedrichs theorem provides the corresponding orthogonal decompositions. We use the following form, adapted to fluid velocity reconstruction (Schwarz, 1995).

Theorem: boundary-adapted orthogonal decomposition. Let $M \subset \mathbb{R}^3$ be a bounded, connected domain with smooth boundary ∂M, and let $\boldsymbol{\nu}$ denote the outward unit normal. Every sufficiently smooth vector field $\mathbf{v}$ on $\overline{M}$ admits a decomposition

$$\boxed{\mathbf{v} = \operatorname{grad}\varphi + \operatorname{curl}\boldsymbol{\psi} + \mathbf{h}.} \tag{6.2}$$

The three vector-field components are uniquely determined and mutually orthogonal in $L^2(M;\mathbb{R}^3)$. They have the following properties.

1. **Potential gradient component:** $\operatorname{grad}\varphi$**.**

   The scalar potential satisfies

   $$\begin{aligned} \Delta\varphi &= \operatorname{div}\mathbf{v} \quad \text{in } M, \\ \partial_\nu\varphi &= \mathbf{v}\cdot\boldsymbol{\nu} \quad \text{on } \partial M. \end{aligned} \tag{6.3}$$

   It is unique up to an additive constant, which may be fixed by

   $$\int_M \varphi \, d\mathbf{x} = 0.$$

   This component is curl-free and carries both the divergence and the normal boundary velocity:

   $$\operatorname{curl}(\operatorname{grad}\varphi) = 0, \qquad (\operatorname{grad}\varphi)\cdot\boldsymbol{\nu} = \mathbf{v}\cdot\boldsymbol{\nu} \quad \text{on } \partial M.$$

   No Dirichlet condition is imposed on φ.

2. **Curl component:** $\operatorname{curl}\boldsymbol{\psi}$**.**

   The vector potential can be chosen to satisfy

   $$\begin{aligned} \operatorname{curl}(\operatorname{curl}\boldsymbol{\psi}) &= \operatorname{curl}\mathbf{v} \quad && \text{in } M, \\ \operatorname{div}\boldsymbol{\psi} &= 0 && \text{in } M, \\ \boldsymbol{\psi}\times\boldsymbol{\nu} &= 0 && \text{on } \partial M. \end{aligned} \tag{6.4}$$

   Here $\operatorname{div}\boldsymbol{\psi} = 0$ is the Coulomb gauge, and the boundary condition means that $\boldsymbol{\psi}$ is normal to the boundary. Its curl satisfies

   $$\operatorname{div}(\operatorname{curl}\boldsymbol{\psi}) = 0, \qquad (\operatorname{curl}\boldsymbol{\psi})\cdot\boldsymbol{\nu} = 0 \quad \text{on } \partial M.$$

   Thus this component carries the vorticity and contributes no normal boundary velocity.

The curl component is unique, although its vector potential need not be. Under the Coulomb gauge, the remaining ambiguity can be removed by requiring

$$\boldsymbol{\psi} \perp \mathcal{H}^1_D(M),$$

where

$$\mathcal{H}^1_D(M) = \{\mathbf{k} : \operatorname{div}\mathbf{k} = 0, \quad \operatorname{curl}\mathbf{k} = 0, \quad \mathbf{k}\times\boldsymbol{\nu} = 0 \text{ on } \partial M\}.$$

3. **Harmonic component: h.**

   The harmonic field satisfies

$$\begin{aligned} \operatorname{div}\mathbf{h} &= 0 \quad \text{in } M, \\ \operatorname{curl}\mathbf{h} &= 0 \quad \text{in } M, \\ \mathbf{h}\cdot\boldsymbol{\nu} &= 0 \quad \text{on } \partial M. \end{aligned} \tag{6.5}$$

   It belongs to the finite-dimensional Neumann harmonic space

$$\mathcal{H}^1_N(M) = \{\mathbf{h} : \operatorname{div}\mathbf{h} = 0, \quad \operatorname{curl}\mathbf{h} = 0, \quad \mathbf{h}\cdot\boldsymbol{\nu} = 0 \text{ on } \partial M\}.$$

   Its dimension is the first Betti number $b_1(M)$. This component carries the global circulation information not determined by divergence, vorticity, and normal boundary velocity.

The orthogonality asserted in the theorem is

$$\int_M \operatorname{grad}\varphi\cdot\operatorname{curl}\boldsymbol{\psi}\,d\mathbf{x} = 0, \qquad \int_M \operatorname{grad}\varphi\cdot\mathbf{h}\,d\mathbf{x} = 0, \qquad \int_M \operatorname{curl}\boldsymbol{\psi}\cdot\mathbf{h}\,d\mathbf{x} = 0.$$

No boundary condition on the original field $\mathbf{v}$ is required.

Function-space formulation and boundary convention. The natural space for a square-integrable vector potential with square-integrable curl is

$$H(\operatorname{curl}; M) = \left\{\boldsymbol{\psi} \in L^2(M;\mathbb{R}^3) : \operatorname{curl}\boldsymbol{\psi} \in L^2(M;\mathbb{R}^3)\right\},$$

where the curl is understood in the distributional sense. Its norm is

$$\|\boldsymbol{\psi}\|^2_{H(\operatorname{curl};M)} = \|\boldsymbol{\psi}\|^2_{L^2(M)} + \|\operatorname{curl}\boldsymbol{\psi}\|^2_{L^2(M)}.$$

Fields in this space possess a tangential boundary trace in the Sobolev trace sense, although they need not possess pointwise boundary values.

To follow the differential-form convention, define the operator curl_N by

$$\begin{aligned} D(\operatorname{curl}_N) &= \{\boldsymbol{\psi} \in H(\operatorname{curl}; M) : \boldsymbol{\psi}\times\boldsymbol{\nu} = 0 \text{ on } \partial M\}, \\ \operatorname{curl}_N\boldsymbol{\psi} &= \operatorname{curl}\boldsymbol{\psi}. \end{aligned}$$

The boundary condition is understood through the tangential trace. Thus $\boldsymbol{\psi}$ is normal to the boundary when it is smooth. In standard vector Sobolev notation, $D(\operatorname{curl}_N)$ is also denoted $H_0(\operatorname{curl}; M)$.

The range of this operator is

$$\operatorname{im}(\operatorname{curl}_N) = \{\operatorname{curl}\boldsymbol{\psi} : \boldsymbol{\psi} \in D(\operatorname{curl}_N)\}.$$

The Coulomb gauge is not part of this domain definition; it is an additional condition used to select a vector potential representing a given curl component.

The orthogonal decomposition extends to arbitrary L^2 vector fields:

$$\boxed{\begin{aligned} L^2(M;\mathbb{R}^3) = {} & \operatorname{grad} H^1(M) \\ & \oplus \operatorname{im}(\operatorname{curl}_N) \oplus \mathcal{H}^1_N(M). \end{aligned}} \tag{6.6}$$

For this formulation, derivatives and boundary traces are understood weakly. In particular, the scalar potential is characterized by

$$\int_M \operatorname{grad}\varphi \cdot \operatorname{grad} q \, d\mathbf{x} = \int_M \mathbf{v} \cdot \operatorname{grad} q \, d\mathbf{x} \qquad \text{for every } q \in H^1(M),$$

together with the mean-zero normalization.

6.3.2 The Scalar potential φ

We seek φ such that the remainder

$$\mathbf{w} = \mathbf{v} - \operatorname{grad}\varphi$$

is divergence-free and tangent to the boundary. This gives

$$\boxed{\begin{aligned} \Delta\varphi &= \operatorname{div}\mathbf{v} \quad \text{in } M, \\ \partial_\nu\varphi &= \mathbf{v}\cdot\boldsymbol{\nu} \quad \text{on } \partial M, \\ \int_M \varphi \, d\mathbf{x} &= 0. \end{aligned}} \tag{6.7}$$

The compatibility condition

$$\int_M \operatorname{div}\mathbf{v} \, d\mathbf{x} = \int_{\partial M} \mathbf{v}\cdot\boldsymbol{\nu} \, dS$$

is exactly the divergence theorem. If divergence and boundary velocity are prescribed independently as reconstruction data, they must satisfy this condition.

The resulting $\mathbf{w} := \mathbf{v} - \nabla\varphi$ satisfies

$$\nabla\cdot\mathbf{w} = 0, \qquad \mathbf{w}\cdot\boldsymbol{\nu} = 0.$$

Thus the decomposition does not require an a priori boundary condition on the original field.

6.3.3 Vector Potential and Gauge

The solenoidal remainder is further split as

$$\mathbf{w} = \operatorname{curl}\boldsymbol{\psi} + \mathbf{h}, \qquad \mathbf{h} \in \mathcal{H}^1_N(M).$$

Its vorticity determines the curl component through

$$\boxed{\operatorname{curl}(\operatorname{curl}\boldsymbol{\psi}) = \boldsymbol{\omega}, \qquad \boldsymbol{\omega} = \operatorname{curl}\mathbf{v}, \qquad \boldsymbol{\psi}\times\boldsymbol{\nu} = 0 \text{ on } \partial M.} \tag{6.8}$$

A variational formulation is

$$\begin{aligned}\int_M (\operatorname{curl}\boldsymbol{\psi})\cdot(\operatorname{curl}\boldsymbol{\eta})\,d\mathbf{x}\\ = \int_M \mathbf{w}\cdot(\operatorname{curl}\boldsymbol{\eta})\,d\mathbf{x} \quad \text{for every } \boldsymbol{\eta}\in H_0(\operatorname{curl};M).\end{aligned} \tag{6.9}$$

It determines $\operatorname{curl}\boldsymbol{\psi}$ uniquely, with $\boldsymbol{\psi}$ understood modulo the curl-free kernel. For smooth compatible vorticity, the right-hand side can also be written $\int_M \boldsymbol{\omega}\cdot\boldsymbol{\eta}\,d\mathbf{x}$.

The identity

$$\operatorname{curl}(\operatorname{curl}\boldsymbol{\psi}) = \operatorname{grad}(\operatorname{div}\boldsymbol{\psi}) - \Delta\boldsymbol{\psi}$$

suggests the Coulomb gauge $\operatorname{div}\boldsymbol{\psi}=0$. With this gauge the equations become

$$\boxed{\begin{aligned} -\Delta\boldsymbol{\psi} &= \boldsymbol{\omega} && \text{in } M,\\ \operatorname{div}\boldsymbol{\psi} &= 0 && \text{in } M,\\ \boldsymbol{\psi}\times\boldsymbol{\nu} &= 0 && \text{on } \partial M.\end{aligned}} \tag{6.10}$$

These are a constrained vector problem, not three independent scalar Dirichlet problems. For a smooth solution, the divergence constraint also holds at the boundary. The remaining gauge kernel is

$$\mathcal{H}^1_D(M) = \{\mathbf{k} : \operatorname{div}\mathbf{k} = \operatorname{curl}\mathbf{k} = 0,\ \mathbf{k}\times\boldsymbol{\nu} = 0 \text{ on } \partial M\}.$$

It can be removed by requiring $\boldsymbol{\psi}\perp\mathcal{H}^1_D(M)$. This normalization fixes the potential; it does not transfer any velocity to $\mathbf{h}$.

Vorticity supplied independently must satisfy the conditions for being a curl: it is divergence-free and has zero flux through every closed two-cycle in M. Data obtained as $\operatorname{curl}\mathbf{v}$ automatically satisfy these constraints. Vorticity alone determines the curl component in this chosen orthogonal reconstruction; it does not determine $\operatorname{grad}\varphi$ or $\mathbf{h}$.

6.3.4 Boundary Conditions and Orthogonality

Green's identity gives

$$\int_M \operatorname{grad}\varphi\cdot\mathbf{w}\,d\mathbf{x} = -\int_M \varphi\operatorname{div}\mathbf{w}\,d\mathbf{x} + \int_{\partial M}\varphi\mathbf{w}\cdot\boldsymbol{\nu}\,dS. \tag{6.11}$$

Thus the gradient of any H^1 scalar is orthogonal to every divergence-free field with zero normal trace. This proves orthogonality of the potential component to both remaining terms without imposing $\varphi=0$ on the boundary.

For the curl component the correct identity is

$$\begin{aligned}\int_M (\operatorname{curl}\boldsymbol{\psi})\cdot\mathbf{w}\,d\mathbf{x} = &\int_M \boldsymbol{\psi}\cdot(\operatorname{curl}\mathbf{w})\,d\mathbf{x}\\ &+\int_{\partial M}(\boldsymbol{\psi}\times\mathbf{w})\cdot\boldsymbol{\nu}\,dS.\end{aligned} \tag{6.12}$$

Taking $\mathbf{w}=\mathbf{h}$ makes the volume term vanish; the boundary term vanishes because $\boldsymbol{\psi}\times\boldsymbol{\nu}=0$. Moreover,

$$(\operatorname{curl}\boldsymbol{\psi})\cdot\boldsymbol{\nu} = 0 \quad \text{on } \partial M.$$

For smooth fields this follows from the surface curl identity or Stokes' theorem applied to every boundary patch.

Consequently,

$$\|\mathbf{v}\|_{L^2}^2 = \|\operatorname{grad}\varphi\|_{L^2}^2 + \|\operatorname{curl}\boldsymbol{\psi}\|_{L^2}^2 + \|\mathbf{h}\|_{L^2}^2.$$

This is a geometric L^2 identity. In a compressible fluid with variable density, it does not imply orthogonality in the density-weighted kinetic energy $\frac{1}{2}\int_M \rho|\mathbf{v}|^2\,d\mathbf{x}$.

6.3.5 Relation to the Four-Component Theorem

The Hodge–Morrey–Friedrichs theorem also provides a decomposition with a Dirichlet scalar potential and an unrestricted harmonic remainder. In vector notation, its Neumann harmonic refinement is

$$\mathbf{v} = \operatorname{grad}\varphi_D + \operatorname{curl}\boldsymbol{\psi} + \operatorname{grad}\phi_h + \mathbf{h}, \qquad \varphi_D|_{\partial M} = 0, \quad \Delta\phi_h = 0, \tag{6.13}$$

with $\mathbf{h} \in \mathcal{H}_N^1(M)$. All four terms are orthogonal. This is the degree-one vector version of Corollary 11.15 in Albert Chern's notes, November 2020; see also Schwarz (1995). Regrouping the two gradient terms gives

$$\varphi = \varphi_D + \phi_h,$$

and recovers (6.2). Their separate scalar problems are

$$\begin{aligned} &\Delta\varphi_D = \operatorname{div}\mathbf{v}, \quad \varphi_D|_{\partial M} = 0, \\ &\Delta\phi_h = 0, \qquad\qquad \partial_\nu\phi_h = \mathbf{v}\cdot\boldsymbol{\nu} - \partial_\nu\varphi_D. \end{aligned}$$

Thus $\operatorname{grad}\varphi_D$ reflects divergence, while $\operatorname{grad}\phi_h$ supplies the remaining normal boundary data.

If these two gradients are not regrouped, the three-term expression with $\operatorname{grad}\varphi_D$ must retain the full harmonic remainder $\operatorname{grad}\phi_h + \mathbf{h}$, which generally has nonzero normal trace and is not a finite-dimensional space. One cannot impose both $\varphi = 0$ and $\mathbf{h}\cdot\boldsymbol{\nu} = 0$ in the three-component fluid decomposition for an arbitrary velocity.

The alternative refinement uses coexact harmonic fields and $\mathcal{H}_D^1(M)$. It is useful for flux obstructions and vector potentials, but is not needed as a second velocity formulation here. We use (6.2) consistently from now on.

6.4 Harmonic Fields, Topology, and Examples

6.4.1 Circulation, Cohomology, and Harmonic Coefficients

A curl-free field is locally a gradient, but it need not have a global single-valued potential. The obstruction is its circulation around homology cycles. For closed one-forms,

$$H_{\mathrm{dR}}^1(M) = \frac{\{\text{closed one-forms}\}}{\{\text{exact one-forms}\}}, \qquad \mathcal{H}_N^1(M) \simeq H_{\mathrm{dR}}^1(M).$$

Thus $g = \dim\mathcal{H}_N^1(M) = b_1(M)$ is the number of independent real circulation classes. Choose representative loops $\gamma_1, \ldots, \gamma_g$ and a harmonic basis normalized by

$$\oint_{\gamma_i} \mathbf{h}_j \cdot d\mathbf{x} = \delta_{ij}.$$

Write

$$\mathbf{h} = \sum_{j=1}^{g} c_j \mathbf{h}_j, \qquad \Gamma_i = \oint_{\gamma_i} \mathbf{v} \cdot d\mathbf{x}. \tag{6.14}$$

The exact gradient has zero circulation, but the curl component generally does not. Hence

$$\boxed{c_i = \Gamma_i - \oint_{\gamma_i} \operatorname{curl} \boldsymbol{\psi} \cdot d\mathbf{x}.} \tag{6.15}$$

Only for a pure harmonic flow, or a reconstruction whose vortical part has zero periods on these loops, can one identify c_i with Γ_i. For a velocity with nonzero vorticity, circulation need not depend only on the homology class of the loop; the representatives must therefore be specified. It is the closed harmonic one-form, not the full rotational velocity one-form, that represents a de Rham class.

Alternatively choose an L^2-orthonormal harmonic basis. Then

$$c_i = \int_M \mathbf{v} \cdot \mathbf{h}_i \, d\mathbf{x}.$$

Such a basis need not be circulation-normalized. For the latter basis, define the positive-definite Gram matrix

$$\mathsf{G}_{ij} = \int_M \mathbf{h}_i \cdot \mathbf{h}_j \, d\mathbf{x}.$$

The projection coefficients satisfy $\sum_j \mathsf{G}_{ij} c_j = \int_M \mathbf{v} \cdot \mathbf{h}_i \, d\mathbf{x}$.

6.4.2 Handles, Cavities, and Flux

In three dimensions, loop topology and cavity topology play different roles. Homology $H_1(M;\mathbb{R})$ describes independent loop classes, whereas $H_2(M;\mathbb{R})$ describes closed surface classes. The latter can detect nonzero flux of a divergence-free field. Hodge theory and Poincaré–Lefschetz duality give

$$\dim \mathcal{H}^1_N(M) = b_1(M), \qquad \dim \mathcal{H}^1_D(M) = b_2(M).$$

For a bounded oriented three-dimensional domain, the duality is

$$H^k(M;\mathbb{R}) \simeq H_{3-k}(M, \partial M;\mathbb{R}), \qquad H^k(M, \partial M;\mathbb{R}) \simeq H_{3-k}(M;\mathbb{R}).$$

A loop through a handle is dual to a relative surface cutting across it. A cavity sphere is dual to a relative path joining boundary components. A relative cycle is allowed to have its boundary on ∂M. These distinctions explain why simply connected does not mean devoid of all topological flux information.

For example, a spherical shell has $b_1 = 0$ and $b_2 = 1$. Its radial field

$$\frac{C}{r^2}\mathbf{e}_r = \operatorname{grad}\left(-\frac{C}{r}\right)$$

is divergence-free and curl-free but has nonzero normal velocity and nonzero flux through an intermediate sphere. In the fluid decomposition it belongs to the potential component, not to $\mathbf{h}$. In particular, cavities do not require an additional tangential harmonic term when normal boundary velocity is already assigned to φ.

6.4.3 Pure Harmonic Circulation: Annulus and Multiple Obstacles

A pure harmonic flow in our convention satisfies

$$\mathbf{v} = \mathbf{h}, \qquad \operatorname{div} \mathbf{h} = \operatorname{curl} \mathbf{h} = 0, \qquad \mathbf{h} \cdot \boldsymbol{\nu} = 0.$$

A useful two-dimensional illustration is the bounded annulus

$$M = \{(r, \theta) : R_1 < r < R_2\}, \qquad \mathbf{h} = \frac{\Gamma}{2\pi r} \mathbf{e}_\theta.$$

It has zero divergence and vorticity, is tangent to both circles, and has circulation Γ around the hole. It has no single-valued scalar potential. A bounded planar domain with N disjoint interior obstacles has N such independent harmonic circulation fields. For a pure harmonic flow,

$$\mathbf{v} = \sum_{j=1}^{N} \Gamma_j \mathbf{h}_j$$

in a circulation-normalized basis. For a rotational flow one must use (6.15) instead.

This bounded-domain example avoids the additional conditions at infinity needed for planar exterior flows. In particular, a nonzero total circulation produces a $1/r$ far field and generally infinite L^2 energy in a two-dimensional exterior domain.

6.4.4 A Solid Torus and Exterior Domains

A bounded solid torus has $b_1 = 1$ and $b_2 = 0$. There is a unique circulation-normalized tangential harmonic field $\mathbf{h}_1$, and

$$\mathbf{h} = c_1 \mathbf{h}_1, \qquad c_1 = \Gamma_1 - \oint_{\gamma_1} \operatorname{curl} \boldsymbol{\psi} \cdot d\mathbf{x}.$$

This is a genuinely three-dimensional harmonic circulation mode.

The exterior of a solid torus also has an independent loop class linking the obstacle. A corresponding decaying harmonic circulation field exists with suitable conditions at infinity. By contrast, the exterior of a ball has no loop obstruction and no such harmonic circulation mode. Exterior decompositions additionally require a specified decay or far-field condition; the bounded-domain L^2 theorem cannot be applied without this qualification.

In particular, classical uniform flow past a sphere has a nonzero velocity at infinity. Its potential is determined partly by that far-field data, and the full velocity is not in L^2 of the exterior domain. It should not be treated as an example of the bounded-domain homogeneous projection problem.

6.4.5 Constant Harmonic Flows on a Periodic Domain

On the flat periodic domain

$$\mathbb{T}^3 = (\mathbb{R}/L_1\mathbb{Z}) \times (\mathbb{R}/L_2\mathbb{Z}) \times (\mathbb{R}/L_3\mathbb{Z}),$$

there is no boundary. With periodic potentials the harmonic fields are constant:

$$\mathbf{h} = U_1 \mathbf{e}_1 + U_2 \mathbf{e}_2 + U_3 \mathbf{e}_3, \qquad \mathbf{h} = \frac{1}{|\mathbb{T}^3|} \int_{\mathbb{T}^3} \mathbf{v} \, d\mathbf{x}.$$

For a pure harmonic flow, the periods are $\Gamma_i = U_i L_i$. For a general flow, a periodic curl can contribute circulation along a chosen fundamental loop, even though its spatial mean is zero. The three mean velocities are therefore the natural orthogonal harmonic coefficients on the periodic box.

6.5 Applications to Incompressible and Compressible Flow

6.5.1 Fixed Impermeable Boundaries

For a fixed impermeable wall, $\mathbf{v} \cdot \boldsymbol{\nu} = 0$. In incompressible flow, (6.7) gives

$$\Delta\varphi = 0, \qquad \partial_\nu \varphi = 0.$$

Integration by parts shows $\operatorname{grad}\varphi = 0$, so

$$\boxed{\mathbf{v} = \operatorname{curl}\boldsymbol{\psi} + \mathbf{h} \quad \text{for incompressible impermeable flow.}} \tag{6.16}$$

If $b_1(M) = 0$, the tangential harmonic term also vanishes. Vorticity then determines the velocity through the chosen boundary-compatible curl reconstruction.

For compressible flow, mass conservation gives, where $\rho > 0$,

$$\partial_t \rho + \operatorname{div}(\rho \mathbf{v}) = 0, \qquad \operatorname{div}\mathbf{v} = -\frac{D}{Dt}\log\rho.$$

Thus φ solves a generally nonhomogeneous Poisson equation with homogeneous Neumann boundary condition. It represents compression and expansion. The other two components remain solenoidal and tangent. The decomposition is kinematic and is the same in both fluid regimes; the governing equations determine its time-dependent data.

6.5.2 Nonzero Normal Velocity and Viscous Walls

With prescribed normal velocity, including inflow, outflow, or a moving wall, the scalar condition is always $\partial_\nu\varphi = \mathbf{v}\cdot\boldsymbol{\nu}$. Even incompressible flow may then have a nonzero harmonic potential component. For moving domains, this reconstruction applies at each instant, but time differentiation must also account for changes of the domain and its projection spaces.

The Hodge decomposition enforces the assigned normal boundary velocity; it does not independently impose viscous no-slip. At a stationary no-slip wall,

$$\mathbf{v} = 0 \quad \Longrightarrow \quad \partial_\nu\varphi = 0, \qquad (\operatorname{curl}\boldsymbol{\psi} + \mathbf{h})_\tau = -(\operatorname{grad}\varphi)_\tau.$$

Here the subscript τ denotes tangential projection. In incompressible flow $\operatorname{grad}\varphi = 0$, so the tangential components of the curl and harmonic parts must cancel. These constraints couple vorticity, harmonic coefficients, and wall vorticity generation. They are not independent arbitrary boundary values for all potentials.

6.5.3 The Pressure Projection

For a fixed impermeable boundary, let

$$P\mathbf{v} = \mathbf{v} - \operatorname{grad}\varphi = \operatorname{curl}\boldsymbol{\psi} + \mathbf{h}$$

be the Leray projection onto divergence-free fields with zero normal trace. This projection retains the harmonic component. For constant-density incompressible Euler flow,

$$\partial_t\mathbf{v} + (\mathbf{v}\cdot\nabla)\mathbf{v} = -\frac{1}{\rho}\operatorname{grad} p, \qquad \partial_t\mathbf{v} = -P((\mathbf{v}\cdot\nabla)\mathbf{v}).$$

The scalar projection problem supplies the pressure correction needed to preserve incompressibility and impermeability. A viscous projection method must additionally enforce the tangential wall condition; the normal projection alone does not enforce no-slip.

In compressible flow the gradient component is a physical velocity component and must not be discarded. Moreover, $\rho^{-1}\operatorname{grad} p$ is generally not an ordinary gradient when density varies. The incompressible pressure projection is therefore not a replacement for the compressible momentum and continuity equations. Around a uniform resting state, the linearized equations separate potential acoustic motion from solenoidal motion; this interpretation need not remain an uncoupled split for nonlinear or nonuniform flows.

6.6 Evolution of the Decomposed Components

We now work on a fixed domain, so the harmonic basis and orthogonal projection spaces do not depend on time. For inviscid compressible flow without body forces, the momentum equation in enthalpy form is

$$\frac{D\mathbf{v}}{Dt} = -\operatorname{grad} h + T\operatorname{grad} S, \qquad h = U + \frac{p}{\rho}.$$

Thus, with $\boldsymbol{\omega} = \operatorname{curl}\mathbf{v}$,

$$\partial_t\mathbf{v} = -\operatorname{grad}\left(h + \frac{1}{2}|\mathbf{v}|^2\right) + \mathbf{v}\times\boldsymbol{\omega} + T\operatorname{grad} S. \tag{6.17}$$

For constant-density incompressible flow the pressure replaces the thermodynamic enthalpy term, and the same projection arguments apply with the corresponding force terms.

6.6.1 Vorticity and the Potential Component

Taking curl yields

$$\boxed{\partial_t\boldsymbol{\omega} = \operatorname{curl}(\mathbf{v}\times\boldsymbol{\omega}) + \operatorname{grad} T\times\operatorname{grad} S.} \tag{6.18}$$

The baroclinic term vanishes for barotropic flow or uniform entropy. Vorticity determines $\operatorname{curl}\boldsymbol{\psi}$ at each time through (6.8), including its boundary convention and the gauge needed for $\boldsymbol{\psi}$.

The scalar component is reconstructed simultaneously from (6.7). Equivalently, if $\partial_t\mathbf{v} = \mathbf{F}$, then on a fixed domain

$$\Delta(\partial_t\varphi) = \operatorname{div}\mathbf{F}, \qquad \partial_\nu(\partial_t\varphi) = \mathbf{F}\cdot\boldsymbol{\nu}, \qquad \int_M \partial_t\varphi\, d\mathbf{x} = 0.$$

These are projection identities, not closed evolution equations for the components separately: $\mathbf{F}$, the thermodynamic variables, and the vorticity transport all depend on the full coupled fluid state.

6.6.2 Harmonic Evolution by Projection

Write $\mathbf{h}(t) = \sum_j c_j(t)\mathbf{h}_j$ in a fixed harmonic basis. Since each $\mathbf{h}_i$ is divergence-free and tangent to the boundary,

$$\int_M \operatorname{grad} B \cdot \mathbf{h}_i \, d\mathbf{x} = 0 \quad \text{for every single-valued scalar } B.$$

Taking the inner product of (6.17) with $\mathbf{h}_i$ gives

$$\boxed{\sum_{j=1}^{g} \mathsf{G}_{ij}\dot{c}_j = \int_M (\mathbf{v} \times \boldsymbol{\omega} + T \operatorname{grad} S) \cdot \mathbf{h}_i \, d\mathbf{x}.} \tag{6.19}$$

For an L^2-orthonormal basis this reduces to

$$\dot{c}_i = \int_M (\mathbf{v} \times \boldsymbol{\omega} + T \operatorname{grad} S) \cdot \mathbf{h}_i \, d\mathbf{x}.$$

Even in barotropic flow the first term need not vanish. A fixed-domain harmonic projection is therefore generally time-dependent. For a pure irrotational barotropic flow the projected right-hand side vanishes, so its harmonic coefficients are constant under these assumptions.

If a viscous acceleration $\rho^{-1} \operatorname{div} \boldsymbol{\sigma}$ is added to the momentum equation, its harmonic projection must also be added. For constant-density incompressible Navier–Stokes flow with constant kinematic viscosity ν, this contribution is

$$\nu \int_M \Delta\mathbf{v} \cdot \mathbf{h}_i \, d\mathbf{x}.$$

It need not vanish just because $\Delta\mathbf{h}_i = 0$: integration by parts retains boundary terms. Wall stresses can change the harmonic component.

6.6.3 Kelvin Circulation and the Distinction Between Coefficients

For a material loop $\gamma_i(t)$ transported by the inviscid flow, Kelvin's theorem gives

$$\boxed{\frac{d}{dt} \oint_{\gamma_i(t)} \mathbf{v} \cdot d\mathbf{x} = \oint_{\gamma_i(t)} T \operatorname{grad} S \cdot d\mathbf{x}.} \tag{6.20}$$

This is a material circulation equation, not an equation asserting that $\dot{c}_i = 0$. If the material loops start from the representatives used to normalize the harmonic basis, their homology classes remain the same under a smooth flow, and each harmonic field has unchanged periods on them. Therefore

$$c_i(t) = \oint_{\gamma_i(t)} \mathbf{v} \cdot d\mathbf{x} - \oint_{\gamma_i(t)} \operatorname{curl} \boldsymbol{\psi} \cdot d\mathbf{x}.$$

Conservation of the first integral does not prevent changes in the second. This reconciles Kelvin's theorem with (6.19).

If the representatives γ_i are instead kept fixed in space, then (6.17) gives

$$\frac{d\Gamma_i}{dt} = \oint_{\gamma_i} (\mathbf{v} \times \boldsymbol{\omega} + T \operatorname{grad} S) \cdot d\mathbf{x}.$$

The extra $\mathbf{v} \times \boldsymbol{\omega}$ term distinguishes fixed-loop circulation from material circulation. Both descriptions are consistent when the corresponding loop convention is retained.

6.6.4 Reconstruction at Each Time

The bounded-domain reconstruction data are

$$\boxed{\operatorname{div}\mathbf{v}, \qquad \mathbf{v}\cdot\boldsymbol{\nu}\big|_{\partial M}, \qquad \boldsymbol{\omega}, \qquad \Gamma_1,\dots,\Gamma_g.}$$

First solve (6.7); next reconstruct the curl component using its boundary condition and gauge; finally determine c_i by (6.15). Instead of prescribing Γ_i, one may evolve the projection coefficients using (6.19). The data must satisfy the divergence and vorticity compatibility conditions stated earlier. This reconstruction does not close compressible dynamics without the mass and thermodynamic equations, nor viscous dynamics without the physical wall conditions.

6.7 Clebsch Representation and Hodge Decomposition

The Hodge decomposition is a global linear decomposition tied to a metric and boundary conditions. It reconstructs velocity from divergence, vorticity, boundary velocity, and harmonic data. Clebsch representation has a different purpose: it expresses velocity through advected labels and their variational multipliers. A local non-isentropic form is

$$\mathbf{v} = \operatorname{grad}\phi + \eta\operatorname{grad}S + \zeta\operatorname{grad}a,$$

where S and a are advected and η, ζ are conjugate multiplier fields. Its curl is

$$\boldsymbol{\omega} = \operatorname{grad}\eta\times\operatorname{grad}S + \operatorname{grad}\zeta\times\operatorname{grad}a.$$

Each cross product has the geometry of intersecting level surfaces; with two terms, their sum need not be tangent to the intersection of any one specified pair of these surfaces.

The Clebsch gradient $\operatorname{grad}\phi$ is not generally the orthogonal Hodge gradient $\operatorname{grad}\varphi$. Nor need the other Clebsch terms be solenoidal or orthogonal. Clebsch variables are useful for relabeling symmetry and Hamiltonian formulations, whereas Hodge variables organize elliptic reconstruction and projection.

Global single-valued representations require additional hypotheses. In the single-pair form $\mathbf{v} = \operatorname{grad}\phi + \zeta\operatorname{grad}a$, helicity becomes a boundary integral; under conditions that make it vanish, nonzero helicity obstructs such a global representation. That obstruction should not be applied without qualification to representations with additional pairs or different boundary data. Multiple charts, extra pairs, or multivalued potentials may be needed. Hodge decomposition instead retains the topology explicitly in $\mathbf{h}$ (Arnold and Khesin, 1998).

6.8 Summary, Further Reading, and the Next Chapters

The working fluid decomposition is

$$\mathbf{v} = \operatorname{grad}\varphi + \operatorname{curl}\boldsymbol{\psi} + \mathbf{h}, \qquad \boldsymbol{\psi}\times\boldsymbol{\nu} = 0, \quad \mathbf{h}\cdot\boldsymbol{\nu} = 0.$$

Its scalar potential solves a Neumann problem; the vortical component is the boundary-adapted curl reconstruction; and $\mathbf{h}$ belongs to the finite-dimensional tangential harmonic space. This is

a regrouping of the four-component Hodge–Morrey–Friedrichs decomposition, valid for both compressible and incompressible velocities. Keeping the four components separate is useful when distinguishing divergence-driven potential motion from harmonic potential motion driven by boundary data.

For incompressible flow at a fixed impermeable wall, the potential component vanishes. For compressible flow it generally remains, and for nonzero normal boundary velocity it can remain even in incompressible flow. Viscous no-slip supplies additional tangential constraints. Harmonic coefficients are obtained by projection or by subtracting vortical circulation from total circulation; Kelvin's theorem concerns material loops and does not generally freeze these coefficients.

The next chapter develops irrotational flows, including boundary-driven potential flows and harmonic circulations. The chapter after that treats vortex dynamics. In each setting, velocity reconstruction requires the boundary and far-field information appropriate to the domain, as well as any surviving harmonic circulation data.

Historical remarks. Helmholtz's work on vortex motion is an early source of the vector calculus viewpoint (**?**). Hodge developed the theory of harmonic forms (Hodge, 1941), while Friedrichs and Morrey clarified the role of boundaries (Friedrichs, 1955; Morrey, 1956). In fluid mechanics these ideas underlie pressure projection, potential theory, and vorticity reconstruction. Fluid cohomology makes the remaining topological degrees of freedom explicit (Yin et al., 2023).

Further reading. For classical fluid mechanics, see Batchelor (1967) and Lamb (1932a); for vorticity and vortex dynamics, see **?** and Majda and Bertozzi (2002). For Hodge theory with boundary, see Schwarz (1995); for geometric fluid mechanics, see Arnold and Khesin (1998). Discrete exterior calculus and geometric computational viewpoints are developed in Desbrun et al. (2005), Crane (2023), and Wang et al. (2023). For fluid cohomology and related structure-preserving computational formulations, see Yin et al. (2023) and Nabizadeh et al. (2024).

Chapter 7

Irrotational Flows

7.1 Introduction

In the preceding chapter we decomposed a velocity field into three geometric parts:

$$\mathbf{v} = \operatorname{grad}\varphi + \operatorname{curl}\boldsymbol{\psi} + \mathbf{h}.$$

The first term is the potential part, the second is the vortical part, and the third is the harmonic or topological circulation part. In this chapter we study the non-vortical part of the flow. Thus the main condition is

$$\operatorname{curl}\mathbf{v} = 0.$$

Such flows are called *irrotational flows*. They form the classical setting of potential theory in fluid mechanics.

If the domain is simply connected, the condition

$$\operatorname{curl}\mathbf{v} = 0$$

implies that there exists a single-valued scalar function φ such that

$$\mathbf{v} = \operatorname{grad}\varphi.$$

The function φ is called the velocity potential. In this case the flow is a potential flow in the strict sense.

On a multiply connected domain, however, an irrotational velocity field need not be the gradient of a single-valued potential. There may be nonzero circulation around holes, obstacles, or handles. In Hodge-theoretic language, one writes

$$\mathbf{v} = \operatorname{grad}\varphi + \mathbf{h},$$

where

$$\operatorname{div}\mathbf{h} = 0, \qquad \operatorname{curl}\mathbf{h} = 0.$$

The field $\mathbf{h}$ is the harmonic circulation part. It is invisible to both divergence and curl, but it is detected by circulation integrals

$$\oint_\gamma \mathbf{h}\cdot d\mathbf{x}.$$

Equivalently, one may absorb $\mathbf{h}$ into a multivalued potential. For example, in the exterior of a circular cylinder,

$$\frac{\Gamma}{2\pi r}\mathbf{e}_\theta = \operatorname{grad}\left(\frac{\Gamma}{2\pi}\theta\right),$$

but the function θ is multivalued.

Thus, in this chapter, irrotational flow means more than the local formula $\mathbf{v} = \operatorname{grad}\varphi$. It also includes the global harmonic circulation fields allowed by the topology of the fluid domain. The distinction is important in classical examples such as flow around a cylinder with circulation, where the topological circulation produces lift.

7.1.1 Why Irrotational Flows Form a Natural Class

Irrotational flow is not only a simplifying assumption. Under important physical hypotheses, it is preserved by the fluid evolution.

In Chapter **??**, we proved the persistence of irrotationality: for barotropic or incompressible inviscid flows under a conservative body force, if

$$\boldsymbol{\omega}(0) = \operatorname{curl}\mathbf{v}(0) = 0,$$

then

$$\boldsymbol{\omega}(t) = 0$$

for all later times for which the smooth solution exists.

Thus an initially irrotational flow remains irrotational. Consequently, for these flows the velocity can be represented locally by a potential,

$$\mathbf{v} = \operatorname{grad}\varphi.$$

In a multiply connected domain, one must also allow harmonic circulation fields, so that

$$\mathbf{v} = \operatorname{grad}\varphi + \mathbf{h}, \qquad \operatorname{curl}\mathbf{h} = 0, \qquad \operatorname{div}\mathbf{h} = 0.$$

This is the main reason for studying irrotational flows as a separate class. They arise naturally from the dynamics, not merely from an artificial restriction. Potential theory then gives a powerful way to compute the velocity, pressure, force, and circulation effects.

There are also important mechanisms that can destroy irrotationality. In nonbarotropic compressible flow, the baroclinic term

$$\frac{1}{\rho^2}\nabla\rho \times \nabla p$$

may generate vorticity. Vorticity may also be produced by viscosity near solid boundaries, by vortex sheets, by shock interactions, or by imposed circulation. These mechanisms lead naturally to vortex dynamics, which is the subject of the next chapter.

7.1.2 Incompressible Irrotational Flow

If the flow is both irrotational and incompressible, then

$$\operatorname{curl}\mathbf{v} = 0, \qquad \operatorname{div}\mathbf{v} = 0.$$

In a simply connected domain this gives

$$\mathbf{v} = \operatorname{grad} \varphi, \qquad \Delta \varphi = 0.$$

Hence incompressible irrotational flow is governed by harmonic potential theory.

In a multiply connected domain, the more precise representation is

$$\mathbf{v} = \operatorname{grad} \varphi + \mathbf{h}, \qquad \Delta \varphi = 0,$$

where $\mathbf{h}$ is the harmonic circulation part. The potential $\operatorname{grad} \varphi$ is used to satisfy boundary conditions, far-field conditions, imposed sources and sinks, or body motion. The harmonic field $\mathbf{h}$ records the topological circulation data.

Therefore one should distinguish two related notions:

$$\boxed{\text{harmonic potential flow: } \mathbf{v} = \operatorname{grad} \varphi, \quad \Delta \varphi = 0,}$$

and

$$\boxed{\text{harmonic circulation flow: } \mathbf{v} = \mathbf{h}, \quad \operatorname{div} \mathbf{h} = 0, \quad \operatorname{curl} \mathbf{h} = 0.}$$

Both are incompressible and irrotational. The second one is the finite-dimensional topological part of the velocity.

7.1.3 Steady and Unsteady Potential Flows

Irrotational and incompressible flow does not have to be steady. For example,

$$\mathbf{v}(t, \mathbf{x}) = U(t)\mathbf{e}_x$$

is incompressible and irrotational for every t, with potential

$$\varphi(t, \mathbf{x}) = U(t)x.$$

It is unsteady whenever $U'(t) \neq 0$.

Thus we shall study both steady and unsteady potential flows. In the steady case, many classical examples can be constructed from harmonic functions: uniform flows, sources and sinks, doublets, flow around cylinders, and flow around spheres. In the unsteady case, the velocity potential depends on time and the pressure is obtained from the unsteady Bernoulli equation.

The harmonic circulation part behaves differently. For a free inviscid barotropic flow in a fixed domain, Kelvin's theorem implies that the circulation variables are conserved. Thus a pure harmonic circulation flow is steady unless circulation is changed by boundary forcing, viscosity, baroclinic effects, or moving boundaries.

7.2 Steady Incompressible Potential Flows

We now give several classical steady incompressible potential flows. The important point is that nontrivial examples do not arise from the equation alone. If the fluid occupies the whole space $\mathbb{R}^d$ and the velocity is smooth, irrotational, incompressible, and decays suitably at infinity, then the flow is trivial. Indeed, in a simply connected domain,

$$\mathbf{v} = \operatorname{grad} \varphi, \qquad \Delta \varphi = 0.$$

If $\operatorname{grad}\varphi \to 0$ at infinity, then under standard decay conditions φ is constant, and hence

$$\mathbf{v} = 0.$$

Thus classical potential flows become nontrivial because of boundary conditions, far-field conditions, singularities, or topology. Typical situations include:

solid bodies:	$\mathbf{v} \cdot \boldsymbol{\nu} = 0$ on the body surface,
moving bodies:	$\mathbf{v} \cdot \boldsymbol{\nu} = \mathbf{U} \cdot \boldsymbol{\nu}$ on the body surface,
far-field flow:	$\mathbf{v} \to \mathbf{U}_\infty$ as $\lvert\mathbf{x}\rvert \to \infty$,
sources and sinks:	$\operatorname{div}\mathbf{v}$ has prescribed singularities,
circulation:	$\displaystyle\oint_{\gamma_j} \mathbf{v} \cdot d\mathbf{x} = \Gamma_j.$

In this sense, potential flow is a boundary-value problem. The geometry of the domain and the imposed boundary data are part of the physical model.

In this section the velocity has the form

$$\mathbf{v} = \operatorname{grad}\varphi + \mathbf{h},$$

where

$$\Delta\varphi = 0, \qquad \operatorname{div}\mathbf{h} = 0, \qquad \operatorname{curl}\mathbf{h} = 0.$$

The term $\operatorname{grad}\varphi$ is the harmonic potential part, while $\mathbf{h}$ is the harmonic circulation part. The potential part is determined by boundary conditions, far-field conditions, or singularities such as sources and sinks. The harmonic circulation part is determined by the topology of the domain and by prescribed circulations around noncontractible loops.

In simply connected domains, $\mathbf{h}$ is absent under the usual boundary conditions. In multiply connected domains, $\mathbf{h}$ records circulation around holes or obstacles. Once φ and $\mathbf{h}$ are determined, the velocity is known, and the pressure is obtained from Bernoulli's law.

These examples are classical because they reduce the fluid problem to potential theory. Once φ is found, the velocity is obtained by differentiation, and the pressure is obtained from Bernoulli's law.

7.2.1 Uniform Flow

The simplest potential flow is uniform flow:

$$\mathbf{v} = U\mathbf{e}_x,$$

where U is a constant. A velocity potential is

$$\varphi(\mathbf{x}) = Ux.$$

Then

$$\operatorname{grad}\varphi = U\mathbf{e}_x, \qquad \Delta\varphi = 0.$$

Thus uniform flow is incompressible and irrotational:

$$\operatorname{div}\mathbf{v} = 0, \qquad \operatorname{curl}\mathbf{v} = 0.$$

Although this example is elementary, it is important as a far-field condition. For example, in exterior flow around a body one often imposes

$$\mathbf{v}(\mathbf{x}) \to U\mathbf{e}_x \quad \text{as } \lvert\mathbf{x}\rvert \to \infty.$$

7.2.2 Source and Sink

In three dimensions, a point source at the origin has potential

$$\varphi(\mathbf{x}) = -\frac{Q}{4\pi|\mathbf{x}|},$$

where Q is the source strength. The velocity is

$$\mathbf{v} = \operatorname{grad}\varphi = \frac{Q}{4\pi}\frac{\mathbf{x}}{|\mathbf{x}|^3}.$$

For $\mathbf{x} \neq 0$,

$$\Delta\varphi = 0, \qquad \operatorname{div}\mathbf{v} = 0, \qquad \operatorname{curl}\mathbf{v} = 0.$$

At the origin, the divergence has a singular source:

$$\operatorname{div}\mathbf{v} = Q\delta_0$$

in the distributional sense.

If $Q > 0$, fluid is emitted from the origin; if $Q < 0$, the flow is a sink. Sources and sinks are idealized singular solutions. They are useful as building blocks for more complicated potential flows.

7.2.3 Doublet Flow

A doublet is obtained by placing a source and a sink close together and letting their separation tend to zero while keeping the dipole strength fixed. The resulting flow pattern is analogous to the field of a magnetic dipole: fluid appears to emerge from one side of the singularity and return on the other side, with streamlines bending around the origin. If the doublet is oriented in the direction of a constant vector $\mathbf{a}$, the three-dimensional potential is

$$\varphi(\mathbf{x}) = \frac{\mathbf{a}\cdot\mathbf{x}}{4\pi|\mathbf{x}|^3}.$$

Away from the origin,

$$\Delta\varphi = 0.$$

Thus

$$\mathbf{v} = \operatorname{grad}\varphi$$

is incompressible and irrotational away from the singularity.

Doublets are important because they can be combined with uniform flow to construct potential flows around solid bodies, such as a sphere.

7.2.4 Flow Around a Circular Cylinder

Consider two-dimensional uniform flow around a circular cylinder of radius a. The exterior domain is

$$M = \{(r,\theta) : r > a\}.$$

The potential

$$\varphi(r,\theta) = U\left(r + \frac{a^2}{r}\right)\cos\theta$$

satisfies

$$\Delta\varphi = 0 \quad \text{for } r > a.$$

The velocity is

$$\mathbf{v} = \operatorname{grad}\varphi.$$

In polar coordinates,

$$v_r = \frac{\partial\varphi}{\partial r} = U\left(1 - \frac{a^2}{r^2}\right)\cos\theta,$$

and

$$v_\theta = \frac{1}{r}\frac{\partial\varphi}{\partial\theta} = -U\left(1 + \frac{a^2}{r^2}\right)\sin\theta.$$

On the cylinder surface $r = a$,

$$v_r(a,\theta) = 0.$$

Thus the no-through boundary condition is satisfied:

$$\mathbf{v}\cdot\boldsymbol{\nu} = 0 \quad \text{on } r = a.$$

At infinity,

$$\mathbf{v} \to U\mathbf{e}_x.$$

This is the classical incompressible potential flow around a cylinder.

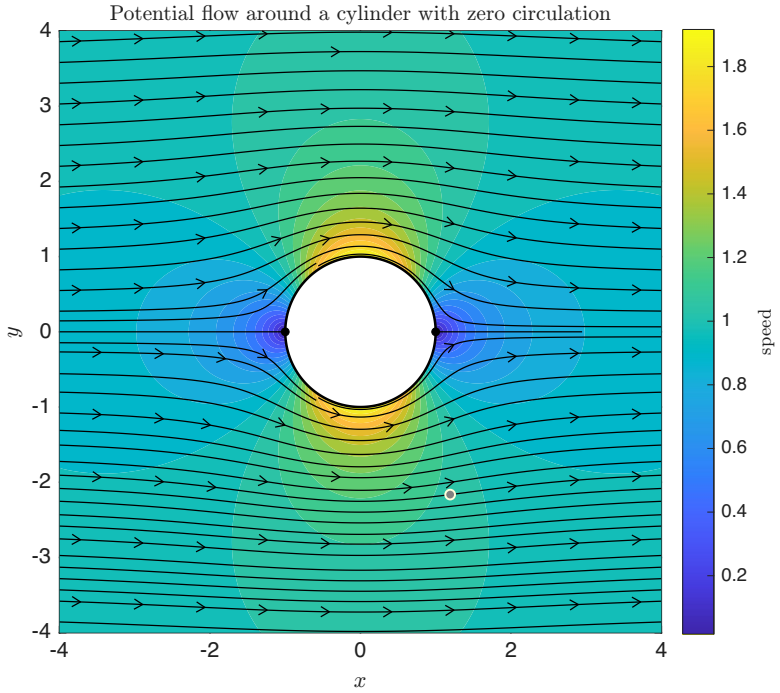


Figure 7.1: Steady incompressible potential flow around a circular cylinder with zero circulation. The cylinder boundary is a streamline, and the stagnation points occur at the front and rear of the cylinder.

7.2.5 Flow Around a Cylinder with Circulation

Because the exterior of a cylinder is multiply connected, one may add a harmonic circulation field

$$\mathbf{h} = \frac{\Gamma}{2\pi r}\mathbf{e}_\theta.$$

This field satisfies

$$\operatorname{div}\mathbf{h} = 0, \qquad \operatorname{curl}\mathbf{h} = 0 \quad \text{for } r > a,$$

and

$$\mathbf{h}\cdot\boldsymbol{\nu} = 0 \quad \text{on } r = a.$$

However, it has nonzero circulation around the cylinder:

$$\oint_{r=R} \mathbf{h}\cdot d\mathbf{x} = \Gamma, \qquad R > a.$$

Therefore the most general irrotational incompressible flow around the cylinder with prescribed uniform velocity at infinity and circulation Γ is

$$\mathbf{v} = \operatorname{grad}\varphi + \frac{\Gamma}{2\pi r}\mathbf{e}_\theta,$$

where

$$\varphi(r,\theta) = U\left(r + \frac{a^2}{r}\right)\cos\theta.$$

The tangential velocity on the cylinder is

$$v_\theta(a,\theta) = -2U\sin\theta + \frac{\Gamma}{2\pi a}.$$

The circulation changes the pressure distribution around the cylinder. This is the origin of the Kutta–Joukowski lift formula discussed later.

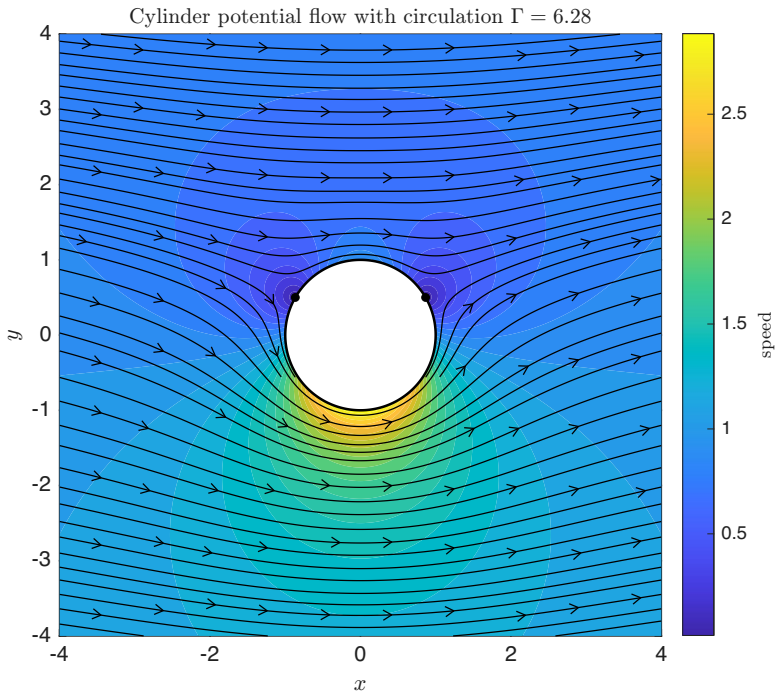


Figure 7.2: Steady incompressible potential flow around a circular cylinder with circulation. The velocity is the sum of the zero-circulation potential flow and the harmonic circulation field $\Gamma(2\pi r)^{-1}\mathbf{e}_\theta$. The circulation shifts the stagnation points and changes the pressure distribution around the cylinder.

7.2.6 Flow Around a Sphere

Consider uniform flow with speed U in the z-direction around a sphere of radius a. The exterior domain is

$$r > a.$$

The potential is

$$\varphi(r,\theta) = U\left(r + \frac{a^3}{2r^2}\right)\cos\theta,$$

where θ is the polar angle measured from the positive z-axis. The velocity is

$$\mathbf{v} = \operatorname{grad}\varphi.$$

This potential satisfies

$$\Delta\varphi = 0 \quad \text{for } r > a,$$

and the no-through boundary condition

$$\mathbf{v}\cdot\boldsymbol{\nu} = 0 \quad \text{on } r = a.$$

At infinity,

$$\mathbf{v} \to U\mathbf{e}_z.$$

Thus this is the incompressible irrotational flow around a sphere.

Unlike the exterior of a circular cylinder in two dimensions, the exterior of a ball in three dimensions has no harmonic circulation degree of freedom of the same type. The flow around a sphere is therefore a harmonic potential flow, but it does not contain a topological circulation component.

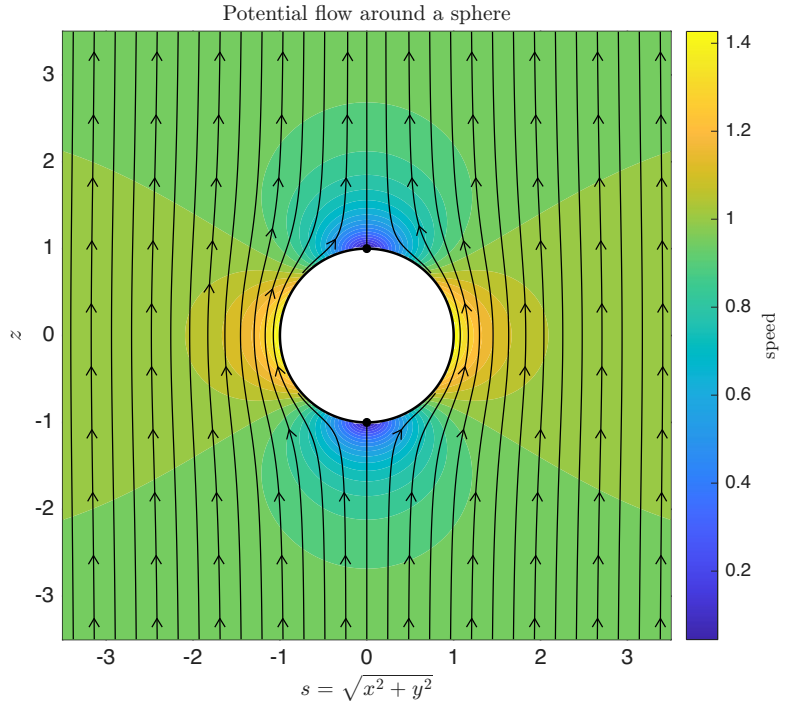


Figure 7.3: Meridional cross-section of steady incompressible potential flow around a sphere. The far-field flow is in the positive z-direction, and the sphere boundary is a streamline with two stagnation points at the front and rear.

Remark 7.1. The exterior of a sphere in $\mathbb{R}^3$ has no harmonic circulation part of the cylinder type. Indeed,

$$M = \mathbb{R}^3 \setminus \overline{B_a(0)}$$

is simply connected, so every closed loop in M can be contracted to a point without crossing the sphere. Consequently there is no nontrivial first cohomology contribution:

$$\mathcal{H}^1(M) = 0.$$

Under the usual decay and impermeability conditions, the harmonic circulation part is therefore absent:

$$\mathbf{h} = 0.$$

Thus the flow around a sphere is a harmonic potential flow,

$$\mathbf{v} = \operatorname{grad} \varphi, \qquad \Delta\varphi = 0,$$

but it has no additional topological circulation degree of freedom.

This is different from the two-dimensional exterior of a cylinder, where

$$\mathbb{R}^2 \setminus \overline{B_a(0)}$$

is not simply connected and admits the harmonic circulation field

$$\mathbf{h} = \frac{\Gamma}{2\pi r}\mathbf{e}_\theta.$$

For a nontrivial harmonic circulation field in three dimensions, one needs a domain with handles, such as the exterior of a solid torus.

7.2.7 Flow Outside a Solid Torus

Let T be a solid torus in $\mathbb{R}^3$, and let

$$M = \mathbb{R}^3 \setminus \overline{T}$$

be the fluid domain outside the torus. This domain is multiply connected. There is one basic noncontractible loop: a loop γ in the fluid domain that links the solid torus once. Such a loop cannot be contracted to a point without crossing the solid torus.

Topologically,

$$\dim H^1(M) = 1.$$

Therefore the harmonic circulation space is one-dimensional. There exists a harmonic vector field $\mathbf{h}_T$ satisfying

$$\operatorname{div} \mathbf{h}_T = 0, \qquad \operatorname{curl} \mathbf{h}_T = 0, \qquad \mathbf{h}_T \cdot \boldsymbol{\nu} = 0 \quad \text{on } \partial M,$$

and normalized by

$$\oint_\gamma \mathbf{h}_T \cdot d\mathbf{x} = 1.$$

Here γ is any loop in the fluid domain linking the solid torus once. Then any harmonic circulation component has the form

$$\mathbf{h} = \Gamma \mathbf{h}_T,$$

where

$$\Gamma = \oint_\gamma \mathbf{v} \cdot d\mathbf{x}$$

is the circulation around the torus.

The field $\mathbf{h}_T$ is the three-dimensional analogue of the harmonic circulation field

$$\frac{1}{2\pi r}\mathbf{e}_\theta$$

around a circular cylinder in two dimensions. In the torus case, however, there is usually no simple elementary formula for $\mathbf{h}_T$. It is obtained as the solution of a boundary-value problem:

$$\operatorname{div} \mathbf{h}_T = 0, \qquad \operatorname{curl} \mathbf{h}_T = 0 \quad \text{in } M,$$

$$\mathbf{h}_T \cdot \boldsymbol{\nu} = 0 \quad \text{on } \partial M,$$

together with the normalization

$$\oint_\gamma \mathbf{h}_T \cdot d\mathbf{x} = 1$$

and suitable decay at infinity.

Equivalently, $\mathbf{h}_T$ is the harmonic representative of the generator of $H^1(M)$. Thus the role of topology is concrete: one independent handle of the obstacle gives one independent harmonic circulation variable.

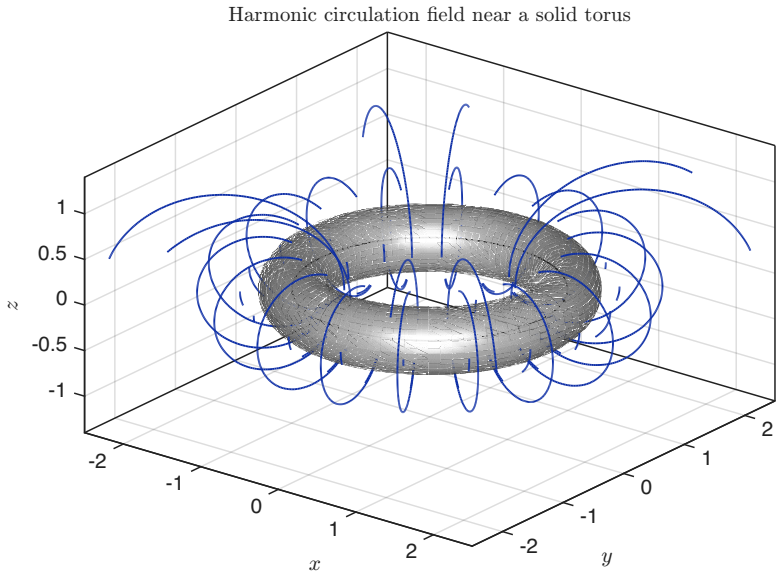


Figure 7.4: A model harmonic circulation field near a solid torus. The field is visualized using the Biot–Savart field of a circular current loop along the core of the torus. Outside the core loop it is divergence-free and curl-free, and it represents the harmonic circulation associated with loops linking the torus.

7.2.8 Harmonic Flow on a Three-Dimensional Periodic Box

Consider the three-dimensional periodic box

$$M = \mathbb{T}^3 = \mathbb{R}^3/(L_1\mathbb{Z} \times L_2\mathbb{Z} \times L_3\mathbb{Z}).$$

Since the three coordinate directions are periodic, there are three independent noncontractible loops:

$$\gamma_1, \qquad \gamma_2, \qquad \gamma_3,$$

where γ_i goes once around the i-th periodic direction.

The harmonic vector fields on $\mathbb{T}^3$ are precisely the constant vector fields:

$$\mathbf{h} = U_1\mathbf{e}_1 + U_2\mathbf{e}_2 + U_3\mathbf{e}_3.$$

Indeed,

$$\operatorname{div}\mathbf{h} = 0, \qquad \operatorname{curl}\mathbf{h} = 0.$$

Thus

$$\mathcal{H}^1(\mathbb{T}^3) = \operatorname{span}\{\mathbf{e}_1, \mathbf{e}_2, \mathbf{e}_3\},$$

and

$$\dim \mathcal{H}^1(\mathbb{T}^3) = 3.$$

The circulations around the three periodic directions are

$$\Gamma_i = \oint_{\gamma_i} \mathbf{h} \cdot d\mathbf{x} = U_i L_i, \qquad i = 1, 2, 3.$$

Thus the constants U_i are determined by the circulation data:

$$U_i = \frac{\Gamma_i}{L_i}.$$

This example shows that the harmonic component need not look like a swirling flow around an obstacle. On a periodic box, the harmonic part is simply a constant background flow:

$$\mathbf{h} = \frac{\Gamma_1}{L_1}\mathbf{e}_1 + \frac{\Gamma_2}{L_2}\mathbf{e}_2 + \frac{\Gamma_3}{L_3}\mathbf{e}_3.$$

Equivalently, it is the spatial mean of the velocity:

$$\mathbf{h} = \langle \mathbf{v} \rangle = \frac{1}{|M|} \int_M \mathbf{v}\, d\mathbf{x}.$$

For instance, if

$$\Gamma_1 = UL_1, \qquad \Gamma_2 = \Gamma_3 = 0,$$

then

$$\mathbf{h} = U\mathbf{e}_1.$$

This is a pure harmonic flow: it is incompressible, irrotational, and nontrivial because of the periodic topology of the domain.

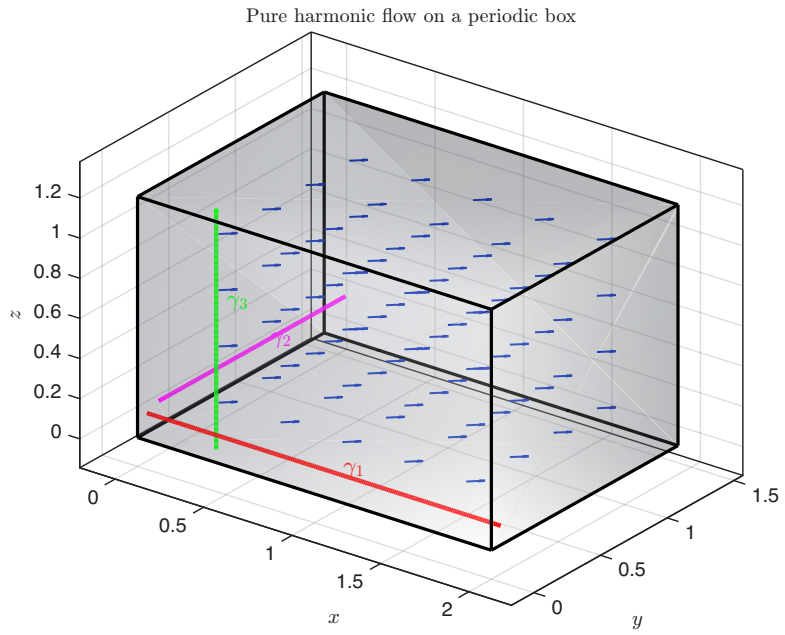


Figure 7.5: Pure harmonic flow on a three-dimensional periodic box. The harmonic vector field is a constant background flow, representing the three independent circulation degrees of freedom along the periodic directions.

7.2.9 Summary: Topology and Harmonic Circulation

The preceding examples show that incompressible irrotational flow has two different sources of nontrivial behavior. The first is the harmonic potential part

$$\operatorname{grad}\varphi, \qquad \Delta\varphi = 0,$$

which is determined by boundary conditions, far-field conditions, moving bodies, sources, sinks, or doublets. The second is the harmonic circulation part

$$\mathbf{h}, \qquad \operatorname{div}\mathbf{h} = 0, \qquad \operatorname{curl}\mathbf{h} = 0,$$

which is determined by the topology of the domain.

If the domain has independent noncontractible loops

$$\gamma_1, \dots, \gamma_g,$$

then the harmonic circulation space is finite-dimensional:

$$\dim \mathcal{H}^1(M) = g.$$

One may choose harmonic fields

$$\mathbf{h}_1, \dots, \mathbf{h}_g$$

normalized by

$$\oint_{\gamma_i} \mathbf{h}_j \cdot d\mathbf{x} = \delta_{ij}.$$

Then

$$\mathbf{h} = \sum_{j=1}^{g} \Gamma_j \mathbf{h}_j, \qquad \Gamma_j = \oint_{\gamma_j} \mathbf{v} \cdot d\mathbf{x}.$$

Thus the decomposition of an incompressible irrotational flow is

$$\mathbf{v} = \operatorname{grad} \varphi + \sum_{j=1}^{g} \Gamma_j \mathbf{h}_j, \qquad \Delta\varphi = 0.$$

The potential part handles boundary and far-field data. The harmonic part records circulation around holes, handles, obstacles, or periodic directions.

For example:

$$\begin{aligned}
\text{exterior of a sphere in } \mathbb{R}^3 &\quad : \quad \mathcal{H}^1(M) = 0, \\
\text{exterior of a cylinder in } \mathbb{R}^2 &\quad : \quad \dim \mathcal{H}^1(M) = 1, \\
\text{exterior of a solid torus in } \mathbb{R}^3 &\quad : \quad \dim \mathcal{H}^1(M) = 1, \\
\text{three-dimensional periodic box } \mathbb{T}^3 &\quad : \quad \dim \mathcal{H}^1(M) = 3.
\end{aligned}$$

This point is easy to miss in classical potential flow. A flow may have zero divergence and zero curl in the fluid region and still be physically nontrivial because it carries global circulation. The harmonic part is therefore the topological part of irrotational flow.

7.2.10 Time Dependence of Harmonic Circulation

The harmonic circulation part may be written as

$$\mathbf{h}(t, \mathbf{x}) = \sum_{j=1}^{g} \Gamma_j(t) \mathbf{h}_j(\mathbf{x}),$$

where

$$\oint_{\gamma_i} \mathbf{h}_j \cdot d\mathbf{x} = \delta_{ij}.$$

At each fixed time, $\mathbf{h}(t, \cdot)$ is divergence-free and curl-free:

$$\operatorname{div} \mathbf{h} = 0, \qquad \operatorname{curl} \mathbf{h} = 0.$$

Thus one may formally construct time-dependent harmonic flows by allowing the circulation coefficients $\Gamma_j(t)$ to vary.

However, for a free inviscid barotropic Euler flow in a fixed domain, the circulation coefficients are conserved. Indeed, Kelvin's circulation theorem gives

$$\frac{d}{dt} \oint_{\gamma_j(t)} \mathbf{v} \cdot d\mathbf{x} = 0.$$

Therefore

$$\frac{d}{dt} \Gamma_j(t) = 0, \qquad j = 1, \dots, g.$$

In this case the harmonic circulation part is steady:

$$\mathbf{h}(t, \mathbf{x}) = \mathbf{h}(0, \mathbf{x}).$$

Equivalently, in the incompressible Euler equation, if

$$\mathbf{v}(t, \mathbf{x}) = \mathbf{h}(t, \mathbf{x})$$

is purely harmonic, then

$$\partial_t \mathbf{h} + \mathbf{h} \cdot \nabla \mathbf{h} = -\operatorname{grad} p.$$

Since

$$\operatorname{curl} \mathbf{h} = 0,$$

we have

$$\mathbf{h} \cdot \nabla \mathbf{h} = \operatorname{grad}\left(\frac{1}{2}|\mathbf{h}|^2\right).$$

Hence

$$\partial_t \mathbf{h} = -\operatorname{grad}\left(p + \frac{1}{2}|\mathbf{h}|^2\right).$$

But $\partial_t \mathbf{h}$ is again harmonic, while the right-hand side is an exact gradient. Under the Hodge decomposition, the only harmonic circulation field that is also an exact gradient is zero. Therefore

$$\partial_t \mathbf{h} = 0.$$

Thus pure harmonic Euler flows are steady under free inviscid barotropic evolution in a fixed domain. Time-dependent harmonic circulation requires external mechanisms, such as boundary forcing, moving boundaries, viscosity, baroclinic circulation generation, or imposed circulation control.

7.3 Unsteady Incompressible Potential Flows

We now consider unsteady incompressible irrotational flows. The velocity still has the form

$$\mathbf{v} = \operatorname{grad} \varphi + \mathbf{h},$$

and incompressibility gives

$$\Delta \varphi = 0.$$

The difference is that the potential may depend on time:

$$\varphi = \varphi(t, \mathbf{x}).$$

Thus the velocity field may be unsteady even though it remains irrotational and incompressible at each fixed time.

The harmonic circulation part may also be written in time-dependent form,

$$\mathbf{h}(t, \mathbf{x}) = \sum_{j=1}^{g} \Gamma_j(t) \mathbf{h}_j(\mathbf{x}).$$

However, for a free inviscid barotropic Euler flow in a fixed domain, Kelvin's theorem implies that the circulation coefficients Γ_j are constant. Hence time-dependent harmonic circulation requires forcing, moving boundaries, viscosity, baroclinic effects, or imposed circulation control. In contrast, the harmonic potential part $\operatorname{grad} \varphi(t, \mathbf{x})$ may be unsteady because of time-dependent boundary motion or far-field forcing.

7.3.1 Unsteady Bernoulli Equation

For incompressible irrotational Euler flow, let

$$\mathbf{v} = \operatorname{grad} \varphi.$$

The Euler equation is

$$\partial_t \mathbf{v} + \mathbf{v} \cdot \nabla \mathbf{v} = -\frac{1}{\rho} \operatorname{grad} p - \operatorname{grad} \Phi,$$

where Φ is an external potential. Since

$$\mathbf{v} = \operatorname{grad} \varphi,$$

we have

$$\partial_t \mathbf{v} = \operatorname{grad}(\partial_t \varphi),$$

and

$$\mathbf{v} \cdot \nabla \mathbf{v} = \operatorname{grad} \left(\frac{1}{2} |\operatorname{grad} \varphi|^2 \right).$$

Therefore

$$\operatorname{grad} \left(\partial_t \varphi + \frac{1}{2} |\operatorname{grad} \varphi|^2 + \frac{p}{\rho} + \Phi \right) = 0.$$

Hence

$$\boxed{\partial_t \varphi + \frac{1}{2} |\operatorname{grad} \varphi|^2 + \frac{p}{\rho} + \Phi = C(t).} \tag{7.1}$$

The function $C(t)$ can be absorbed into the potential by replacing φ with

$$\varphi - \int_0^t C(s)\, ds.$$

Thus one often writes

$$p = p_0 - \rho \left(\partial_t \varphi + \frac{1}{2} |\operatorname{grad} \varphi|^2 + \Phi \right).$$

This equation is important because it shows how unsteady potential flow produces pressure forces even when the flow remains irrotational.

7.3.2 Accelerating Uniform Flow

The simplest unsteady potential flow is an accelerating uniform flow:

$$\mathbf{v}(t, \mathbf{x}) = U(t) \mathbf{e}_x.$$

A velocity potential is

$$\varphi(t, \mathbf{x}) = U(t) x.$$

Then

$$\Delta \varphi = 0, \qquad \operatorname{grad} \varphi = U(t) \mathbf{e}_x.$$

The flow is incompressible and irrotational for every t, but it is unsteady if $U'(t) \neq 0$.

If $\Phi = 0$, the unsteady Bernoulli equation gives

$$p = C(t) - \rho\left(U'(t)x + \frac{1}{2}U(t)^2\right).$$

The spatial pressure gradient is therefore

$$\operatorname{grad} p = -\rho U'(t)\mathbf{e}_x.$$

Thus an accelerating potential flow requires a pressure gradient in the direction opposite to the acceleration.

7.3.3 Accelerating Flow Around a Cylinder

Consider the potential flow around a circular cylinder with a time-dependent far-field speed $U(t)$. The potential is

$$\varphi(t, r, \theta) = U(t)\left(r + \frac{a^2}{r}\right)\cos\theta.$$

For each fixed t,

$$\Delta\varphi = 0 \quad \text{for } r > a,$$

and the no-through boundary condition

$$\frac{\partial\varphi}{\partial r} = 0 \quad \text{on } r = a$$

is satisfied.

The velocity is

$$\mathbf{v}(t, r, \theta) = \operatorname{grad}\varphi(t, r, \theta).$$

The pressure is obtained from

$$p = C(t) - \rho\left(\partial_t\varphi + \frac{1}{2}|\operatorname{grad}\varphi|^2\right).$$

The term $\partial_t\varphi$ is absent in steady potential flow, but it is essential in unsteady motion. It is responsible for the added-mass force: accelerating the cylinder relative to the fluid requires accelerating some surrounding fluid as well.

7.3.4 Accelerating Flow Around a Sphere

The same idea applies to a sphere. If the far-field speed in the z-direction is $U(t)$, then

$$\varphi(t, r, \theta) = U(t)\left(r + \frac{a^3}{2r^2}\right)\cos\theta.$$

Again,

$$\Delta\varphi = 0 \quad \text{for } r > a,$$

and the no-through boundary condition is satisfied on the sphere:

$$\mathbf{v} \cdot \boldsymbol{\nu} = 0 \quad \text{on } r = a.$$

The unsteady Bernoulli equation gives the pressure. The force associated with the $\partial_t\varphi$ term is the classical added-mass force for a sphere. This is one of the simplest examples where unsteady potential flow has direct mechanical consequences.

7.3.5 Time-Dependent Circulation

In a multiply connected domain, one may write

$$\mathbf{v}(t,\mathbf{x}) = \operatorname{grad}\varphi(t,\mathbf{x}) + \sum_{j=1}^{g} \Gamma_j(t)\mathbf{h}_j(\mathbf{x}).$$

At each fixed time, this flow is irrotational and incompressible if

$$\Delta\varphi = 0, \qquad \operatorname{div}\mathbf{h}_j = 0, \qquad \operatorname{curl}\mathbf{h}_j = 0.$$

However, for inviscid barotropic Euler flow in a fixed domain, Kelvin's theorem gives

$$\Gamma_j'(t) = 0.$$

Therefore time-dependent circulation cannot occur freely in such a flow. It must be produced by some external mechanism, such as boundary forcing, viscosity, moving boundaries, imposed circulation, or baroclinic generation.

For example, in the exterior of a cylinder one may formally write

$$\mathbf{h}(t,r,\theta) = \frac{\Gamma(t)}{2\pi r}\mathbf{e}_\theta.$$

This field is divergence-free and curl-free for every fixed time. But if it is to satisfy the free inviscid barotropic Euler equations in a fixed domain, then Kelvin's theorem forces

$$\Gamma(t) = \text{constant}.$$

Thus time-dependent circulation is a forced phenomenon, not a free harmonic Euler motion.

7.4 Forces and Momentum in Potential Flow

Potential flow is not only a method for finding velocity fields. It also gives a direct way to compute pressure forces on solid bodies. Once the velocity potential is known, Bernoulli's equation determines the pressure, and the pressure determines the force:

$$\mathbf{F} = -\int_{\partial B} p\,\boldsymbol{\nu}\,dS,$$

where ∂B is the surface of the solid body and $\boldsymbol{\nu}$ is the unit normal pointing from the body into the fluid.

This section discusses several classical mechanical consequences of potential flow: d'Alembert's paradox, lift from circulation, and added mass. These examples show that the potential and harmonic parts of an irrotational flow have direct physical effects.

7.4.1 Pressure from Bernoulli's Law

For steady incompressible inviscid potential flow, Bernoulli's law gives

$$\frac{1}{2}|\mathbf{v}|^2 + \frac{p}{\rho} + \Phi = C.$$

If $\Phi = 0$, then

$$p = C - \frac{1}{2}\rho|\mathbf{v}|^2.$$

Thus regions of high speed correspond to lower pressure.

For unsteady potential flow,

$$\mathbf{v} = \operatorname{grad}\varphi,$$

the pressure is determined by

$$p = C(t) - \rho\left(\partial_t\varphi + \frac{1}{2}|\operatorname{grad}\varphi|^2 + \Phi\right).$$

The additional term $\partial_t\varphi$ is responsible for many unsteady force effects, including added mass.

7.4.2 Force on a Solid Body

Let B be a solid body with boundary ∂B. The force exerted by the fluid pressure on the body is

$$\mathbf{F} = -\int_{\partial B} p\,\boldsymbol{\nu}\,dS.$$

The moment about the origin is

$$\mathbf{M} = -\int_{\partial B} \mathbf{x}\times p\boldsymbol{\nu}\,dS.$$

Thus, once the potential flow is known, the force and moment are obtained by integrating the pressure over the body surface.

In steady potential flow, this calculation often leads to surprising results. In particular, for steady incompressible inviscid flow around a closed body with no circulation and suitable symmetry, the drag force vanishes. This is d'Alembert's paradox.

7.4.3 D'Alembert's Paradox

Consider steady incompressible inviscid potential flow around a solid body in an unbounded domain. Since the flow is irrotational and inviscid, there is no viscosity and no boundary layer. For many classical body shapes, the pressure distribution is symmetric in the direction of motion. The result is zero drag:

$$D = 0.$$

For example, in potential flow around a circular cylinder with zero circulation, the pressure is symmetric between the front and rear halves of the cylinder. Hence the net drag vanishes. Similarly, potential flow around a sphere gives zero drag.

This conclusion contradicts everyday experience, where bodies moving through fluids experience drag. The resolution is that real fluids have viscosity. Viscosity produces boundary layers, separation, and wakes. The wake breaks the front–back symmetry of the pressure distribution and produces drag. Thus d'Alembert's paradox shows both the power and the limitation of inviscid potential flow.

7.4.4 Kutta–Joukowski Lift and Circulation

We now discuss one of the most important mechanical consequences of circulation in potential flow: lift. Consider first the classical two-dimensional potential flow around a circular cylinder of radius a. The velocity is

$$\mathbf{v} = \operatorname{grad}\varphi + \frac{\Gamma}{2\pi r}\mathbf{e}_\theta,$$

where

$$\varphi(r,\theta) = U\left(r + \frac{a^2}{r}\right)\cos\theta.$$

The second term is the harmonic circulation field. It is divergence-free and curl-free in the fluid domain $r > a$, but it has circulation

$$\oint_{r=R} \mathbf{v}\cdot d\mathbf{x} = \Gamma.$$

On the cylinder surface $r = a$, the radial velocity vanishes and the tangential velocity is

$$v_\theta(a,\theta) = -2U\sin\theta + \frac{\Gamma}{2\pi a}.$$

For steady incompressible potential flow, Bernoulli's law gives

$$p + \frac{1}{2}\rho|\mathbf{v}|^2 = p_\infty + \frac{1}{2}\rho U^2.$$

Hence, on $r = a$,

$$p(a,\theta) = p_\infty + \frac{1}{2}\rho U^2 - \frac{1}{2}\rho v_\theta(a,\theta)^2.$$

The pressure force per unit length exerted by the fluid on the cylinder is

$$\mathbf{F}' = -a\int_0^{2\pi} p(a,\theta)\mathbf{e}_r\, d\theta,$$

where

$$\mathbf{e}_r = (\cos\theta, \sin\theta).$$

The vertical component is

$$F_y' = -a\int_0^{2\pi} p(a,\theta)\sin\theta\, d\theta.$$

The constant terms in $p(a,\theta)$ give no contribution. Thus

$$F_y' = \frac{1}{2}\rho a\int_0^{2\pi} v_\theta(a,\theta)^2\sin\theta\, d\theta.$$

Substituting

$$v_\theta(a,\theta) = -2U\sin\theta + \frac{\Gamma}{2\pi a},$$

we obtain

$$v_\theta(a,\theta)^2 = 4U^2\sin^2\theta - \frac{4U\Gamma}{2\pi a}\sin\theta + \left(\frac{\Gamma}{2\pi a}\right)^2.$$

Multiplying by $\sin\theta$ and integrating from 0 to 2π, the first and third terms vanish:

$$\int_0^{2\pi} \sin^3\theta\, d\theta = 0, \qquad \int_0^{2\pi} \sin\theta\, d\theta = 0.$$

The middle term gives

$$F_y' = \frac{1}{2}\rho a \left(-\frac{4U\Gamma}{2\pi a}\right) \int_0^{2\pi} \sin^2\theta\, d\theta.$$

Since

$$\int_0^{2\pi} \sin^2\theta\, d\theta = \pi,$$

we obtain

$$F_y' = -\rho U \Gamma.$$

Thus, with the convention

$$\mathbf{U}_\infty = U\mathbf{e}_x, \qquad \mathbf{\Gamma} = \Gamma\mathbf{e}_z,$$

the lift force per unit span is

$$\boxed{\mathbf{L}' = \rho\, \mathbf{U}_\infty \times \mathbf{\Gamma}.} \tag{7.2}$$

In magnitude,

$$\boxed{L' = \rho U |\Gamma|.} \tag{7.3}$$

With the orientation used here, positive counterclockwise circulation gives downward lift, while negative clockwise circulation gives upward lift.

Remark 1: The formula is not special to a cylinder. The Kutta–Joukowski theorem holds much more generally for steady two-dimensional incompressible inviscid flow around a body. The lift per unit span depends only on the far-field velocity and the circulation:

$$\mathbf{L}' = \rho\, \mathbf{U}_\infty \times \mathbf{\Gamma}.$$

The detailed geometry of the body does not appear explicitly in the formula. The geometry affects the lift indirectly by determining which value of Γ is physically realized.

Remark 2: The circulation looks like a hidden vortex. For the cylinder, the harmonic circulation field is

$$\frac{\Gamma}{2\pi r}\mathbf{e}_\theta.$$

It is curl-free in the fluid domain $r > a$. However, if it is extended to the whole plane in the sense of distributions, then

$$\operatorname{curl}\left(\frac{\Gamma}{2\pi r}\mathbf{e}_\theta\right) = \Gamma\delta_0.$$

Thus the exterior circulation field behaves as if a point vortex of strength Γ were hidden inside the cylinder. More generally, circulation around a body may be interpreted as vorticity enclosed by the body. This is one way to see why lift is closely connected to vortex dynamics.

Remark 3: How is Γ determined? In the circular-cylinder potential flow, Γ is a free parameter. The no-through boundary condition

$$\mathbf{v} \cdot \boldsymbol{\nu} = 0 \quad \text{on } r = a$$

is satisfied for every value of Γ. Since the cylinder has no sharp trailing edge, there is no Kutta condition to select a unique circulation.

For a cylinder, circulation must be prescribed initially or generated by additional physics. For example:

initial circulation	Γ is conserved by Kelvin's theorem,
rotating cylinder	Γ is generated by viscous interaction with the wall,
boundary actuation	Γ is imposed by external forcing,
viscous startup	Γ may be associated with boundary layers and vortex shedding.

A rotating cylinder with circulation experiences lift; this is the Magnus effect.

Remark 4: The Kutta condition for an airfoil. For an airfoil with a sharp trailing edge, the circulation is not arbitrary. Potential theory again gives a one-parameter family of solutions, but most choices of Γ produce an unphysical singular behavior at the trailing edge. The Kutta condition selects the circulation by requiring that the flow leave the trailing edge smoothly, with finite velocity.

Thus the logic for an airfoil is:

$$\text{Kutta condition} \quad \Longrightarrow \quad \Gamma,$$

and then

$$\text{Kutta–Joukowski theorem} \quad \Longrightarrow \quad \mathbf{L}' = \rho\, \mathbf{U}_\infty \times \boldsymbol{\Gamma}.$$

Conclusion. The lift in potential flow is produced by circulation. In the fluid region the circulation field may be irrotational, but topologically it represents vorticity enclosed by the body. Thus even in an irrotational-flow chapter, lift already reveals the central role of vortices. This provides a natural bridge to the next chapter on vortex dynamics.

7.4.5 Added Mass

Unsteady potential flow reveals another important mechanical effect: added mass. When a solid body accelerates through an ideal fluid, it must also accelerate some surrounding fluid. Therefore the force required to accelerate the body is larger than the force required in vacuum.

For example, consider a sphere of radius a accelerating through an incompressible inviscid fluid at rest at infinity. The force associated with the unsteady potential flow has the form

$$\mathbf{F}_{\text{fluid}} = -m_a \dot{\mathbf{U}},$$

where $\mathbf{U}(t)$ is the velocity of the sphere and

$$m_a = \frac{1}{2}\rho \frac{4}{3}\pi a^3$$

is the added mass of a sphere. Thus the added mass is one half of the mass of the displaced fluid.

For a circular cylinder moving perpendicular to its axis, the added mass per unit length is

$$m_a' = \rho\pi a^2.$$

These formulas are classical consequences of unsteady potential flow.

7.4.6 Impulse and Unsteady Motion

Momentum and impulse provide another way to understand forces in irrotational and vortical flows. In potential flow, the fluid velocity is determined by boundary motion and far-field conditions. The resulting pressure force can often be interpreted as the rate of change of a fluid impulse or added momentum.

For irrotational flow around a moving body, the added-mass force is one example of this principle: changing the body's velocity changes the potential flow around it, and hence changes the fluid momentum associated with the motion.

In the next chapter, impulse will reappear in vortex dynamics. There it is often expressed in terms of vorticity, for example through quantities of the form

$$\int \mathbf{x} \times \boldsymbol{\omega}\, d\mathbf{x}.$$

This is consistent with the vortex interpretation of circulation discussed above. In the cylinder example, the exterior flow is irrotational, but the nonzero circulation behaves as if a point vortex were hidden inside the solid body. The lift force is therefore already a sign that force and momentum can be encoded by vorticity, even when the vorticity is excluded from the fluid region itself.

Thus potential-flow mechanics and vortex mechanics are two complementary ways of relating fluid motion to force and momentum. Potential flow computes forces from the pressure field determined by Bernoulli's law, whereas vortex dynamics expresses forces and impulse in terms of vorticity, circulation, and their spatial distribution.

7.5 Compressible Potential Flows

We now turn to compressible potential flow. The velocity is represented by a velocity potential,

$$\mathbf{v} = \operatorname{grad} \varphi,$$

while the density is allowed to vary. Thus the equation for φ is no longer simply Laplace's equation. Instead, the continuity equation couples the potential to the density.

The main point is that compressible potential flow leads to a nonlinear potential equation. In the subsonic regime this equation is elliptic and resembles the incompressible potential equation. In transonic or supersonic regimes, the equation may change type and shocks may appear. In this chapter we emphasize the smooth subsonic theory and only briefly indicate what changes in transonic and supersonic flow.

7.5.1 Isentropic Compressible Potential Flow Equation

Consider an inviscid compressible flow satisfying the Euler equations

$$\partial_t \rho + \operatorname{div}(\rho \mathbf{v}) = 0,$$

and

$$\partial_t \mathbf{v} + \mathbf{v} \cdot \nabla \mathbf{v} = -\frac{1}{\rho} \operatorname{grad} p.$$

Assume the flow is potential:

$$\mathbf{v} = \operatorname{grad} \varphi.$$

Assume also that the flow is *isentropic*, so that

$$p = p(\rho).$$

Let the specific enthalpy h be defined by

$$dh = \frac{1}{\rho}\, dp.$$

Then the momentum equation becomes

$$\operatorname{grad}\left(\partial_t \varphi + \frac{1}{2} |\operatorname{grad} \varphi|^2 + h(\rho)\right) = 0.$$

After absorbing a function of time into φ, we obtain the Bernoulli relation

$$\boxed{\partial_t \varphi + \frac{1}{2} |\operatorname{grad} \varphi|^2 + h(\rho) = 0.} \tag{7.4}$$

If h is invertible, this relation determines ρ as a function of

$$-\partial_t \varphi - \frac{1}{2} |\operatorname{grad} \varphi|^2.$$

Write

$$\rho = H\left(-\partial_t \varphi - \frac{1}{2} |\operatorname{grad} \varphi|^2\right).$$

Substituting this into the continuity equation gives the compressible potential-flow equation:

$$\boxed{\partial_t H\left(-\partial_t \varphi - \frac{1}{2} |\operatorname{grad} \varphi|^2\right) + \operatorname{div}\left[H\left(-\partial_t \varphi - \frac{1}{2} |\operatorname{grad} \varphi|^2\right) \operatorname{grad} \varphi\right] = 0.} \tag{7.5}$$

This equation replaces Laplace's equation in compressible potential flow.

7.5.2 Polytropic Gas

For a polytropic gas,

$$p = K\rho^\gamma, \qquad \gamma > 1.$$

Then

$$dh = \frac{1}{\rho}\, dp = K\gamma\rho^{\gamma-2}\, d\rho,$$

and hence

$$h(\rho) = \frac{K\gamma}{\gamma-1}\rho^{\gamma-1}.$$

The Bernoulli relation becomes

$$\partial_t\varphi + \frac{1}{2}|\operatorname{grad}\varphi|^2 + \frac{K\gamma}{\gamma-1}\rho^{\gamma-1} = 0.$$

Therefore

$$\rho = \left[\frac{\gamma-1}{K\gamma}\left(-\partial_t\varphi - \frac{1}{2}|\operatorname{grad}\varphi|^2\right)\right]^{1/(\gamma-1)}.$$

This gives the explicit function H:

$$H(s) = \left(\frac{\gamma-1}{K\gamma}s\right)^{1/(\gamma-1)}.$$

7.5.3 Steady Isentropic Compressible Potential Flow

For steady flow,

$$\partial_t\varphi = 0.$$

Bernoulli's relation becomes

$$\frac{1}{2}|\operatorname{grad}\varphi|^2 + h(\rho) = B,$$

where B is a Bernoulli constant. Thus

$$\rho = \rho(|\operatorname{grad}\varphi|).$$

The continuity equation becomes

$$\boxed{\operatorname{div}\left(\rho(|\operatorname{grad}\varphi|)\operatorname{grad}\varphi\right) = 0.} \tag{7.6}$$

This is the steady compressible potential-flow equation.

When the velocity is small compared with the sound speed, the density varies little and the equation approaches

$$\Delta\varphi = 0.$$

Thus incompressible potential flow appears as the low-Mach-number limit of compressible potential flow.

7.5.4 Subsonic Potential Flow

The mathematical type of the steady compressible potential equation depends on the Mach number

$$M = \frac{|\mathbf{v}|}{c},$$

where the sound speed c is defined by

$$c^2 = \frac{dp}{d\rho}.$$

In the subsonic regime,

$$M < 1,$$

the steady potential-flow equation is elliptic. This is why subsonic compressible potential flow still resembles incompressible potential theory. One can impose boundary conditions such as

$$\operatorname{grad}\varphi \cdot \boldsymbol{\nu} = 0 \quad \text{on a solid wall,}$$

and far-field conditions such as

$$\operatorname{grad}\varphi \to \mathbf{U}_\infty \quad \text{as } |\mathbf{x}| \to \infty.$$

Thus subsonic compressible potential flow provides a nonlinear elliptic theory for smooth irrotational gas flow.

7.5.5 Small Perturbations and Acoustic Limit

Compressible potential flow also contains acoustic waves. Consider small perturbations around a uniform rest state:

$$\rho = \rho_0 + \rho', \qquad \mathbf{v} = \operatorname{grad}\varphi,$$

where ρ' and $\operatorname{grad}\varphi$ are small. Linearizing the continuity equation gives

$$\partial_t \rho' + \rho_0 \Delta\varphi = 0.$$

Linearizing Bernoulli's relation gives

$$\partial_t \varphi + \frac{c_0^2}{\rho_0}\rho' = 0,$$

where

$$c_0^2 = p'(\rho_0)$$

is the sound speed squared at the reference state. Eliminating ρ' yields

$$\partial_{tt}\varphi - c_0^2 \Delta\varphi = 0.$$

Thus small-amplitude compressible potential flow reduces to the acoustic wave equation.

This gives another interpretation of the potential part of the velocity: in compressible flow, it carries acoustic or compressive motion.

7.5.6 Nozzle and Jet Examples

Compressible potential flow is useful for idealized nozzle and jet problems. For steady isentropic potential flow, the governing equation is

$$\operatorname{div}\left(\rho(|\operatorname{grad}\varphi|)\operatorname{grad}\varphi\right) = 0.$$

In a nozzle, the boundary condition is the no-through condition along the wall:

$$\operatorname{grad}\varphi \cdot \boldsymbol{\nu} = 0.$$

The geometry of the nozzle changes the speed

$$|\operatorname{grad}\varphi|$$

and hence the density through Bernoulli's relation.

A smooth subsonic jet may also be modeled approximately by compressible potential flow near the nozzle exit. However, a real jet usually has a velocity jump relative to the surrounding fluid. In an ideal inviscid description, this jump is a vortex sheet; in a viscous flow, it becomes a shear layer. Therefore the potential-flow description is valid only before vorticity, shear-layer instability, and mixing become dominant.

This observation prepares the transition to vortex dynamics: the interface between a jet and its surroundings is one of the simplest places where irrotational flow breaks down and vorticity becomes essential.

Subsonic regime. For steady compressible potential flow, the equation has the form

$$\operatorname{div}\left[\rho(|\operatorname{grad}\varphi|)\operatorname{grad}\varphi\right] = 0.$$

The character of this equation depends on the Mach number

$$M = \frac{|\mathbf{v}|}{c},$$

where

$$c^2 = \frac{dp}{d\rho}$$

is the square of the sound speed. In the subsonic regime,

$$M < 1,$$

the equation is elliptic. This is the compressible analogue of the elliptic potential equation

$$\Delta\varphi = 0$$

for incompressible potential flow.

Thus subsonic potential flow belongs naturally in the present chapter: it is a smooth elliptic theory of the potential component of the velocity. When

$$M > 1,$$

the equation becomes hyperbolic, and mixed subsonic–supersonic flows may develop shocks. Those phenomena require weak solutions and entropy conditions, so they are not treated here.

7.5.7 Remarks on Transonic and Supersonic Flows

When the Mach number exceeds one,

$$M > 1,$$

the steady compressible potential equation becomes hyperbolic. In the transonic regime, where both subsonic and supersonic regions are present, the equation is of mixed type. Shocks may form, and entropy conditions are needed to select physically relevant weak solutions.

These phenomena are central in compressible gas dynamics, but they go beyond the main scope of this chapter. Here the purpose is to show how irrotational flow extends from harmonic potential theory to nonlinear compressible potential theory. A deeper treatment of transonic flow, supersonic flow, and shocks requires additional tools and will be discussed elsewhere.

7.6 Transition to Vortex Dynamics

Irrotational flow describes the non-vortical part of fluid motion:

$$\mathbf{v} = \operatorname{grad}\varphi + \mathbf{h}, \qquad \operatorname{curl}\mathbf{v} = 0 \quad \text{in the fluid region.}$$

It explains many important phenomena, including potential flow around bodies, harmonic circulation, lift, added mass, and compressible potential flow. However, it cannot describe flows in which vorticity is present in the fluid region:

$$\boldsymbol{\omega} = \operatorname{curl}\mathbf{v} \neq 0.$$

Such vortical flows arise in many ways: through velocity jumps, shear layers, no-slip boundary layers, starting vortices, wakes, and vortex roll-up. For example, an idealized jet may be regarded as a potential flow separated from the ambient fluid by a vortex sheet. In real fluids this sheet is smoothed into a shear layer, which may become unstable and roll up into vortices.

Thus potential flow describes the ideal exterior motion once circulation is known, while vortex dynamics explains how vorticity and circulation are generated, transported, stretched, and organized. This is the subject of the next chapter.

7.7 Summary and Further Reading

The main point of this chapter is that irrotational flow is the non-vortical part of fluid motion. In simply connected domains, an irrotational velocity field is represented by a scalar potential:

$$\mathbf{v} = \operatorname{grad}\varphi.$$

If the flow is incompressible, then

$$\Delta\varphi = 0.$$

Thus incompressible irrotational flow is governed by harmonic potential theory.

In multiply connected domains, irrotational flow may also contain harmonic circulation:

$$\mathbf{v} = \operatorname{grad}\varphi + \mathbf{h}.$$

The potential part satisfies boundary and far-field conditions. The harmonic part records circulation around holes, obstacles, handles, or periodic directions:

$$\Gamma_j = \oint_{\gamma_j} \mathbf{v} \cdot d\mathbf{x}.$$

This topological circulation may have direct mechanical consequences, most notably lift.

Classical potential-flow examples include uniform flow, sources and sinks, doublets, flow around a cylinder, flow around a cylinder with circulation, and flow around a sphere. These examples show how boundary conditions and singularities generate nontrivial harmonic potentials. The cylinder with circulation shows how topology enters through a harmonic circulation field.

The mechanical part of the chapter shows that potential flow can predict pressure forces. Bernoulli's law gives the pressure once the potential is known. Steady potential flow leads to d'Alembert's paradox, while circulation leads to the Kutta–Joukowski lift formula. Unsteady potential flow leads to added mass and impulse.

For compressible potential flow, the velocity is still written as

$$\mathbf{v} = \operatorname{grad} \varphi,$$

but the density is variable. In the isentropic case, Bernoulli's relation determines ρ from φ, and the continuity equation becomes a nonlinear potential equation. Subsonic compressible potential flow remains elliptic, while transonic and supersonic regimes require additional ideas.

The limitations of irrotational flow lead naturally to vortex dynamics. Velocity jumps, shear layers, vortex sheets, starting vortices, wakes, and vortex rings cannot be described by potential theory alone. They require the vorticity equation and the Hamiltonian/geometric structure of vortex motion, which are the subject of the next chapter.

For classical potential flow, see Batchelor (1967), Lamb (1932a), and Milne-Thomson (1968). For aerodynamics, lift, and the Kutta–Joukowski theorem, see **?**, Acheson (1990), and Anderson (2002). For compressible potential flow and gas dynamics, see Courant and Friedrichs (1948), Landau and Lifshitz (1987), and Liepmann and Roshko (1957). For the relation between potential flow, topology, and Hodge decomposition, see Arnold and Khesin (1998) and Schwarz (1995).

Chapter 8

Vortex Dynamics and Applications

8.1 Introduction: From Irrotational Flow to Vortex Dynamics

In the preceding chapter, we studied irrotational flows. In such flows the velocity has the form

$$\mathbf{v} = \operatorname{grad} \varphi + \mathbf{h}.$$

The potential part $\operatorname{grad} \varphi$ is determined by boundary conditions, far-field conditions, sources, sinks, or body motion. The harmonic part $\mathbf{h}$ carries the topological circulation of the domain. It is curl-free in the fluid region, but it may have nonzero circulation around noncontractible loops:

$$\oint_\gamma \mathbf{h} \cdot d\mathbf{x} \neq 0.$$

This harmonic circulation is responsible for effects such as the lift in potential flow around a cylinder.

The present chapter studies the general case, where the flow is rotational:

$$\boldsymbol{\omega} = \operatorname{curl} \mathbf{v} \neq 0.$$

Now circulation is carried by vorticity inside the fluid itself. The main object is no longer only the potential φ or the harmonic field $\mathbf{h}$, but the vorticity field $\boldsymbol{\omega}$ and the vortex structures it forms.

Vorticity carries circulation, induces velocity, transports impulse, and produces force. Thus the main theme of this chapter is:

vortex dynamics explains how circulation becomes motion, impulse, and force.

Vorticity appears in many idealized and physical forms:

point vortices	vorticity concentrated at isolated points in two dimensions,
vortex patches	regions of nonzero vorticity with sharp boundaries,
vortex sheets	tangential velocity jumps and singular vorticity,
vortex filaments	thin vortex tubes concentrated near curves in three dimensions,
vortex rings	closed vortex tubes moving through fluid,
shear layers	large velocity gradients across an interface,
boundary layers	vorticity generated by no-slip walls,
wakes	vorticity shed behind bodies,
turbulence	complex stretching and interaction of vorticity.

The examples are the main objects of the chapter. Hamiltonian structure is the theory that explains their organization. Point vortices, vortex patches, vortex sheets, filaments, rings, wakes, and coherent vortices are concrete fluid structures. Hamiltonian and geometric ideas explain why their motion has conserved quantities, impulse, circulation, topology, and force laws.

The Hodge decomposition also remains important. Since

$$\mathbf{v} = \operatorname{grad}\varphi + \operatorname{curl}\boldsymbol{\psi} + \mathbf{h},$$

the vorticity detects the vortical component

$$\operatorname{curl}\boldsymbol{\psi},$$

but it does not determine the potential or harmonic parts. Therefore velocity reconstruction from vorticity must still respect boundary conditions and harmonic circulation data.

8.2 What Is a Vortex?

We start with a velocity vector field

$$\mathbf{v} = \mathbf{v}(t, \mathbf{x}).$$

Its vorticity is defined by

$$\boldsymbol{\omega} = \operatorname{curl}\mathbf{v} = \nabla \times \mathbf{v}.$$

The vorticity measures the local rotational content of the flow. A vortex is a region or structure in which this rotational content is organized in a coherent way. Depending on the model, a vortex may appear as a vortex tube, a vortex patch, a vortex sheet, a vortex filament, or a vortex ring.

8.2.1 Vortex Lines and Vortex Tubes

Fix a time t. A vortex line is an integral curve of the vorticity field. Thus a curve

$$s \mapsto \boldsymbol{\gamma}(s)$$

is a vortex line if

$$\frac{d\boldsymbol{\gamma}}{ds}(s) = \lambda(s)\boldsymbol{\omega}(t, \boldsymbol{\gamma}(s))$$

for some scalar function $\lambda(s)$. Equivalently,

$$\frac{d\boldsymbol{\gamma}}{ds}(s) \parallel \boldsymbol{\omega}(t, \boldsymbol{\gamma}(s)).$$

Thus vortex lines are to vorticity what streamlines are to velocity.

A vortex tube is obtained by taking a closed curve C and drawing all vortex lines passing through points of C. The resulting surface is tangent to the vorticity field. If A is a cross-section of the tube, the vortex strength, or circulation, is

$$\Gamma = \int_A \boldsymbol{\omega} \cdot \boldsymbol{\nu}\, dS.$$

By Stokes' theorem,

$$\Gamma = \oint_{\partial A} \mathbf{v} \cdot d\mathbf{x}.$$

Thus the strength of a vortex tube is the circulation around its cross-section.

In an ideal barotropic flow, Helmholtz's vortex theorem implies that vortex tubes move with the fluid and preserve their strength. Therefore, if a vortex tube is stretched, its cross-sectional area decreases and the vorticity magnitude increases. This is the geometric meaning of vortex stretching.

Vortex lines and tubes cannot end inside a fluid. Since

$$\operatorname{div} \boldsymbol{\omega} = 0,$$

vorticity has no sources or sinks. Therefore vortex lines cannot begin or end at an interior point of the fluid. A vortex line must satisfy one of the following alternatives:

form a closed loop	such as a ring,
meet the boundary	such as a solid wall or free surface,
extend to infinity	in an unbounded domain.

The same statement applies to vortex tubes. A vortex tube cannot terminate in the interior of the fluid. It must either close on itself, meet the boundary, or extend to infinity.

8.2.2 Vortex Filaments

A vortex filament is a thin vortex tube whose core radius is small compared with its length scale of bending. One idealizes the vorticity as being concentrated near a space curve

$$\mathbf{x} = \boldsymbol{\gamma}(s),$$

where s is an arclength parameter. In this idealization, the filament carries a circulation strength Γ, and the vorticity is concentrated along the curve.

Since a vortex filament is the thin-core limit of a vortex tube, it cannot have a free endpoint in the interior of the fluid. It must either form a closed loop, such as a vortex ring, meet the boundary of the fluid domain, or extend to infinity.

A useful formal expression is

$$\boldsymbol{\omega}(\mathbf{x}) = \Gamma \int \frac{d\boldsymbol{\gamma}}{ds}(s)\delta(\mathbf{x} - \boldsymbol{\gamma}(s))\, ds.$$

This formula says that the vorticity is tangent to the filament and is supported on the curve.

In three dimensions, vortex filaments are central in the study of vortex rings, knotted vortices, and thin coherent structures. In two dimensions, a thin vortex tube perpendicular to the plane appears as a point vortex. Thus the point vortex is the two-dimensional reduction of a vortex filament:

$$\text{vortex filament in three dimensions} \quad \longrightarrow \quad \text{point vortex in two dimensions.}$$

8.2.3 Vortex Patches

In two-dimensional flow, the velocity has the form

$$\mathbf{v} = (u, v),$$

and the vorticity is a scalar:

$$\omega = \partial_x v - \partial_y u.$$

A vortex patch is a region in which the vorticity is approximately constant and concentrated on a bounded set. The idealized form is

$$\omega(\mathbf{x}) = \omega_0 \chi_D(\mathbf{x}),$$

where D is a bounded region in the plane and χ_D is its characteristic function.

The strength of the patch is its total circulation:

$$\Gamma = \int_{\mathbb{R}^2} \omega(\mathbf{x})\, d\mathbf{x} = \omega_0 |D|.$$

Here $|D|$ denotes the area of the patch.

A vortex patch is therefore a distributed version of a point vortex. A point vortex concentrates the circulation at one point, while a vortex patch spreads the circulation over a finite region:

$$\Gamma \delta_{\mathbf{x}_0} \quad \text{versus} \quad \omega_0 \chi_D.$$

The boundary ∂D is the contour of the patch. Later we shall see that, for two-dimensional incompressible inviscid flow, the dynamics of a vortex patch can be described by the motion of this contour.

8.2.4 Vortex Sheets

A vortex sheet is an idealized surface across which the tangential velocity jumps. Let Σ be an oriented surface with unit normal $\boldsymbol{\nu}$. The velocity has two limiting values on the two sides of the sheet:

$$\mathbf{v}_+, \qquad \mathbf{v}_-.$$

For an inviscid sheet, the normal velocity is continuous,

$$\mathbf{v}_+ \cdot \boldsymbol{\nu} = \mathbf{v}_- \cdot \boldsymbol{\nu},$$

so that fluid does not pass through the sheet. However, the tangential velocity may jump:

$$\mathbf{v}_{+,\parallel} \neq \mathbf{v}_{-,\parallel}.$$

The strength of the vortex sheet is the tangential velocity jump. It is convenient to write it as the vector

$$\boldsymbol{\gamma} = \boldsymbol{\nu} \times (\mathbf{v}_+ - \mathbf{v}_-).$$

Thus $\boldsymbol{\gamma}$ is tangent to Σ.

The vorticity is concentrated on the sheet. In a distributional sense, one may write

$$\boldsymbol{\omega} = \boldsymbol{\gamma}\, \delta_\Sigma,$$

where δ_Σ is the surface delta distribution supported on Σ. Thus a vortex sheet is a singular vortex structure.

In two dimensions, a vortex sheet is supported on a curve. If the sheet is parametrized by

$$\mathbf{x} = \mathbf{x}(\alpha),$$

then its strength is a scalar density $\gamma(\alpha)$, and the vorticity is concentrated on the curve:

$$\omega = \gamma(\alpha)\,\delta_\Sigma.$$

Equivalently, the circulation along a portion of the sheet is obtained by integrating the sheet strength:

$$\Gamma_{[\alpha_1,\alpha_2]} = \int_{\alpha_1}^{\alpha_2} \gamma(\alpha)\,d\alpha.$$

Vortex sheets arise as idealizations of thin shear layers, jet boundaries, separated wakes, and free interfaces with tangential velocity jumps. Later we shall see that vortex sheets are closely related to the Kelvin–Helmholtz instability and vortex roll-up.

8.3 Vorticity Dynamics Laws

The vorticity equations were derived in Chapter **??**. Here we recall them as the starting point of vortex dynamics. The purpose is not to rederive the equations, but to interpret what they say about the motion, growth, and organization of vortices.

8.3.1 Recall of the Vorticity Laws

For inviscid compressible flow, the vorticity satisfies

$$\boxed{D_t\boldsymbol{\omega} = \boldsymbol{\omega}\cdot\nabla\mathbf{v} - \boldsymbol{\omega}\,\operatorname{div}\mathbf{v} + \frac{1}{\rho^2}\nabla\rho\times\nabla p.} \tag{8.1}$$

Equivalently, using the continuity equation, the specific vorticity satisfies

$$\boxed{D_t\left(\frac{\boldsymbol{\omega}}{\rho}\right) = \left(\frac{\boldsymbol{\omega}}{\rho}\right)\cdot\nabla\mathbf{v} + \frac{1}{\rho^3}\nabla\rho\times\nabla p.} \tag{8.2}$$

These two equations contain the main mechanisms of vortex dynamics.

The term

$$\boldsymbol{\omega}\cdot\nabla\mathbf{v}$$

is the vortex stretching and tilting term. It describes how the velocity gradient changes the direction and magnitude of vorticity.

The term

$$-\boldsymbol{\omega}\,\operatorname{div}\mathbf{v}$$

is the compressibility contribution. Expansion weakens vorticity, while compression strengthens it.

The term

$$\frac{1}{\rho^2}\nabla\rho\times\nabla p$$

is the baroclinic generation term. It creates vorticity when the density and pressure gradients are not parallel.

For barotropic flow,

$$p = p(\rho),$$

the pressure and density gradients are parallel:

$$\nabla p \parallel \nabla \rho.$$

Hence

$$\nabla \rho \times \nabla p = 0,$$

and the baroclinic term vanishes. The specific vorticity equation becomes

$$\boxed{D_t \left(\frac{\boldsymbol{\omega}}{\rho} \right) = \left(\frac{\boldsymbol{\omega}}{\rho} \right) \cdot \nabla \mathbf{v}.} \tag{8.3}$$

This says that specific vorticity is transported and stretched like a material line element.

For incompressible flow,

$$\rho = \text{constant}, \qquad \operatorname{div} \mathbf{v} = 0,$$

we obtain

$$\boxed{D_t \boldsymbol{\omega} = \boldsymbol{\omega} \cdot \nabla \mathbf{v}.} \tag{8.4}$$

Thus three-dimensional incompressible vortex dynamics is governed by transport and stretching.

In two-dimensional incompressible flow,

$$\mathbf{v} = (u, v, 0), \qquad \boldsymbol{\omega} = (0, 0, \omega),$$

and the stretching term vanishes:

$$\boldsymbol{\omega} \cdot \nabla \mathbf{v} = 0.$$

Therefore

$$\boxed{D_t \omega = 0.} \tag{8.5}$$

Thus two-dimensional vorticity is transported as a scalar.

The contrast between two and three dimensions is fundamental:

$$\begin{aligned} \text{two dimensions} \quad &: \quad D_t \omega = 0, \\ \text{three dimensions} \quad &: \quad D_t \boldsymbol{\omega} = \boldsymbol{\omega} \cdot \nabla \mathbf{v}. \end{aligned}$$

In two dimensions, vortices move and deform but their scalar vorticity values are preserved along particle paths. In three dimensions, vortices move, tilt, stretch, and may intensify.

8.3.2 Consequences for Vortex Structures

We now interpret these equations for the vortex structures introduced above.

Vortex lines and vortex tubes. In ideal barotropic flow, the equation

$$D_t\left(\frac{\boldsymbol{\omega}}{\rho}\right) = \left(\frac{\boldsymbol{\omega}}{\rho}\right) \cdot \nabla \mathbf{v}$$

says that the specific vorticity is transported like a material line element. Thus vortex lines move with the fluid. A material curve that is initially tangent to $\boldsymbol{\omega}$ remains tangent to $\boldsymbol{\omega}$.

For a vortex tube, the circulation around a cross-section is conserved:

$$\Gamma = \int_A \boldsymbol{\omega} \cdot \boldsymbol{\nu}\, dS = \oint_{\partial A} \mathbf{v} \cdot d\mathbf{x}.$$

If the tube is stretched, the cross-sectional area decreases. Since the circulation is preserved, the vorticity magnitude increases. This is the basic mechanism of vortex stretching.

Vortex filaments. A vortex filament is the thin-core limit of a vortex tube. The same principle applies: the filament is transported by the flow, and its circulation strength Γ is preserved in ideal barotropic motion. Because

$$\operatorname{div} \boldsymbol{\omega} = 0,$$

a filament cannot end freely inside the fluid. It must form a closed loop, end on a boundary, or extend to infinity.

Point vortices. In two-dimensional incompressible flow,

$$D_t \omega = 0.$$

Thus vorticity is transported as a scalar. If the vorticity is concentrated at isolated points,

$$\omega = \sum_{j=1}^{N} \Gamma_j \delta_{\mathbf{x}_j},$$

then the strengths Γ_j are conserved. The point vortices move with the velocity induced by the other vortices. This gives a finite-dimensional model of vortex dynamics.

Vortex patches. For a vortex patch,

$$\omega = \omega_0 \chi_{D(t)},$$

the equation

$$D_t \omega = 0$$

implies that the vorticity value ω_0 is preserved. The patch is transported by the flow, so the main dynamics is the evolution of the boundary $\partial D(t)$. This is why two-dimensional vortex patch motion can be formulated as contour dynamics.

Vortex sheets. A vortex sheet is a singular concentration of vorticity on a curve or surface. In two dimensions, one may write formally

$$\omega = \gamma(\alpha)\delta_{\Sigma}.$$

The vorticity equation implies that the sheet is transported by the induced velocity, while the sheet strength evolves according to the jump conditions across the sheet. Vortex sheets are typically unstable; small perturbations may grow through the Kelvin–Helmholtz instability and roll up into spiral vortex structures.

Baroclinic generation. The above transport picture is modified when

$$\nabla\rho \times \nabla p \neq 0.$$

Then vorticity can be created in the fluid interior. This is important in compressible, stratified, and thermally driven flows. In such cases vortex dynamics is not only the motion of pre-existing vorticity; it also includes the generation of new vorticity by thermodynamic inhomogeneity.

These consequences explain why vortex dynamics naturally separates into two parts. First, one studies how vorticity is transported, stretched, and generated. Second, one studies how vorticity determines the velocity that moves it. The latter is the problem of velocity reconstruction from vorticity.

8.4 Velocity Reconstruction from Vorticity

Vorticity is not the same thing as velocity. To evolve a vortex, one must recover the velocity field induced by the vorticity, subject to boundary conditions and circulation constraints.

8.4.1 Biot–Savart Law in Free Space

In $\mathbb{R}^3$, for an incompressible velocity field decaying at infinity, the velocity can be reconstructed from vorticity by the Biot–Savart law:

$$\mathbf{v}(\mathbf{x}) = \frac{1}{4\pi}\int_{\mathbb{R}^3} \frac{\boldsymbol{\omega}(\mathbf{y}) \times (\mathbf{x}-\mathbf{y})}{|\mathbf{x}-\mathbf{y}|^3}\, d\mathbf{y}.$$

We recall why this formula appears. For incompressible flow,

$$\operatorname{div}\mathbf{v} = 0, \qquad \operatorname{curl}\mathbf{v} = \boldsymbol{\omega}.$$

Choose a vector potential $\boldsymbol{\psi}$ such that

$$\mathbf{v} = \operatorname{curl}\boldsymbol{\psi}, \qquad \operatorname{div}\boldsymbol{\psi} = 0.$$

Then

$$\boldsymbol{\omega} = \operatorname{curl}\mathbf{v} = \operatorname{curl}(\operatorname{curl}\boldsymbol{\psi}) = \operatorname{grad}(\operatorname{div}\boldsymbol{\psi}) - \Delta\boldsymbol{\psi} = -\Delta\boldsymbol{\psi}.$$

Thus

$$-\Delta\boldsymbol{\psi} = \boldsymbol{\omega}.$$

Using the Newtonian potential in $\mathbb{R}^3$,

$$G(\mathbf{x},\mathbf{y}) = \frac{1}{4\pi|\mathbf{x}-\mathbf{y}|},$$

we obtain

$$\boldsymbol{\psi}(\mathbf{x}) = \int_{\mathbb{R}^3} G(\mathbf{x},\mathbf{y})\boldsymbol{\omega}(\mathbf{y})\,d\mathbf{y}.$$

Taking curl in $\mathbf{x}$ gives the Biot–Savart law:

$$\mathbf{v}(\mathbf{x}) = \operatorname{curl}_{\mathbf{x}} \boldsymbol{\psi}(\mathbf{x}) = \frac{1}{4\pi}\int_{\mathbb{R}^3} \frac{\boldsymbol{\omega}(\mathbf{y})\times(\mathbf{x}-\mathbf{y})}{|\mathbf{x}-\mathbf{y}|^3}\,d\mathbf{y}.$$

In two dimensions, if

$$\omega = \partial_x v_2 - \partial_y v_1,$$

then one writes

$$\mathbf{v} = \nabla^\perp \psi, \qquad -\Delta\psi = \omega.$$

Thus vorticity determines the stream function, and hence the velocity, once boundary conditions are specified.

For example, if

$$\omega(\mathbf{x}) = \Gamma\delta(\mathbf{x}-\mathbf{x}_0),$$

then

$$-\Delta\psi = \Gamma\delta(\mathbf{x}-\mathbf{x}_0).$$

Since

$$-\Delta\left(-\frac{1}{2\pi}\log|\mathbf{x}-\mathbf{x}_0|\right) = \delta(\mathbf{x}-\mathbf{x}_0),$$

we may take

$$\psi(\mathbf{x}) = -\frac{\Gamma}{2\pi}\log|\mathbf{x}-\mathbf{x}_0|.$$

Therefore

$$\mathbf{v}(\mathbf{x}) = \nabla^\perp\psi(\mathbf{x}) = \frac{\Gamma}{2\pi}\frac{(\mathbf{x}-\mathbf{x}_0)^\perp}{|\mathbf{x}-\mathbf{x}_0|^2}.$$

This is the velocity field of a point vortex.

8.4.2 Boundary-Compatible Reconstruction

Boundary correction. On a bounded or multiply connected domain, free-space Biot–Savart reconstruction is not enough. Suppose a velocity field must satisfy the impermeability condition

$$\mathbf{v}\cdot\boldsymbol{\nu} = 0 \quad \text{on } \partial M.$$

Starting from the vorticity $\boldsymbol{\omega}$, one may first construct a velocity $\mathbf{v}_{\boldsymbol{\omega}}$ satisfying

$$\operatorname{curl}\mathbf{v}_{\boldsymbol{\omega}} = \boldsymbol{\omega}, \qquad \operatorname{div}\mathbf{v}_{\boldsymbol{\omega}} = 0,$$

for example by a Biot–Savart or vector-potential construction. However, $\mathbf{v}_{\boldsymbol{\omega}}$ will usually not satisfy the boundary condition

$$\mathbf{v}_{\boldsymbol{\omega}} \cdot \boldsymbol{\nu} = 0 \quad \text{on } \partial M.$$

We therefore correct it by adding a potential part and a harmonic part:

$$\mathbf{v} = \mathbf{v}_{\boldsymbol{\omega}} + \operatorname{grad} \varphi + \mathbf{h}.$$

The potential φ is chosen to enforce the normal boundary condition. For an impermeable fixed boundary, since the harmonic fields will be chosen to satisfy $\mathbf{h} \cdot \boldsymbol{\nu} = 0$, we impose

$$\frac{\partial \varphi}{\partial \boldsymbol{\nu}} = -\mathbf{v}_{\boldsymbol{\omega}} \cdot \boldsymbol{\nu} \quad \text{on } \partial M.$$

In the incompressible case,

$$\operatorname{div} \mathbf{v} = 0,$$

so φ satisfies

$$\Delta \varphi = 0 \quad \text{in } M,$$

together with the above Neumann boundary condition.

Harmonic circulation. If the domain is multiply connected, this still does not determine the full velocity. One must also prescribe the harmonic circulation part. Let

$$\gamma_1, \dots, \gamma_g$$

be a basis of noncontractible loops in M. Choose harmonic fields $\mathbf{h}_1, \dots, \mathbf{h}_g$ satisfying

$$\operatorname{div} \mathbf{h}_j = 0, \qquad \operatorname{curl} \mathbf{h}_j = 0 \quad \text{in } M,$$

$$\mathbf{h}_j \cdot \boldsymbol{\nu} = 0 \quad \text{on } \partial M,$$

and normalized by

$$\oint_{\gamma_i} \mathbf{h}_j \cdot d\mathbf{x} = \delta_{ij}.$$

Then

$$\mathbf{h} = \sum_{j=1}^{g} \Gamma_j \mathbf{h}_j,$$

where the circulation constants are

$$\Gamma_j = \oint_{\gamma_j} \mathbf{v} \cdot d\mathbf{x}.$$

Thus the reconstruction data are

$$\boldsymbol{\omega}, \qquad \Gamma_1, \dots, \Gamma_g, \qquad \text{boundary conditions.}$$

The constants Γ_j are not determined by the vorticity. They are topological circulation data. In ideal barotropic flow, they are determined by the initial condition and are conserved by Kelvin's theorem.

With this convention, the harmonic fields already satisfy the homogeneous normal boundary condition. The potential correction $\operatorname{grad} \varphi$ is then used only to fix the normal boundary condition left over from $\mathbf{v}_{\boldsymbol{\omega}}$.

Compressible and baroclinic flows. The preceding reconstruction is simplest for incompressible flow, where

$$\operatorname{div} \mathbf{v} = 0.$$

For compressible flow, the divergence is generally nonzero:

$$\operatorname{div} \mathbf{v} \neq 0.$$

Thus the potential part is no longer merely a boundary correction. It also carries the compressible part of the motion:

$$\operatorname{div} \mathbf{v} = \Delta\varphi + \operatorname{div} \mathbf{v}_{\boldsymbol{\omega}} + \operatorname{div} \mathbf{h}.$$

If $\mathbf{v}_{\boldsymbol{\omega}}$ and $\mathbf{h}$ are chosen divergence-free, then

$$\Delta\varphi = \operatorname{div} \mathbf{v}.$$

Therefore, in compressible flow, the reconstruction requires not only vorticity and circulation data, but also the divergence of the velocity:

$$\operatorname{curl} \mathbf{v} = \boldsymbol{\omega}, \qquad \operatorname{div} \mathbf{v} = \theta,$$

where

$$\theta = \operatorname{div} \mathbf{v}.$$

The velocity decomposition should then be viewed as

$$\mathbf{v} = \operatorname{grad} \varphi + \mathbf{v}_{\boldsymbol{\omega}} + \mathbf{h},$$

where $\operatorname{grad} \varphi$ contains the compressible part of the motion.

For barotropic ideal flow, the harmonic circulation coefficients

$$\Gamma_j = \oint_{\gamma_j} \mathbf{v} \cdot d\mathbf{x}$$

are conserved along material loops by Kelvin's theorem. In this case the Γ_j are determined by the initial data.

For baroclinic flow, however, the vorticity equation contains the source term

$$\frac{1}{\rho^2} \nabla\rho \times \nabla p.$$

This term can create vorticity in the fluid interior. Correspondingly, circulation around a material loop may change:

$$\frac{d}{dt} \oint_{\gamma(t)} \mathbf{v} \cdot d\mathbf{x} = \oint_{\gamma(t)} T \nabla S \cdot d\mathbf{x}$$

or, equivalently, it may be written in terms of the non-barotropic pressure force. Thus in baroclinic flow the harmonic circulation coefficients Γ_j are not necessarily constant. They must be evolved together with the vorticity, density, and entropy.

Hence, for compressible baroclinic flow, velocity reconstruction requires the data

$$\boldsymbol{\omega}, \qquad \theta = \operatorname{div} \mathbf{v}, \qquad \Gamma_1, \dots, \Gamma_g, \qquad \text{boundary conditions},$$

and the circulation variables Γ_j may evolve in time.

8.5 Vortex Formation and Growth

Vortex dynamics is not only the motion of pre-existing vortices. Vorticity can also be generated, concentrated, stretched, and amplified. Some mechanisms create vorticity in the fluid interior, some concentrate vorticity on interfaces, and some generate vorticity near solid boundaries. After vorticity is present, the flow may transport it, stretch it, roll it up, or organize it into coherent structures.

8.5.1 Generation and Concentration of Vorticity

The main mechanisms of vortex formation can be read from the vorticity equation together with boundary and interface effects. For inviscid compressible flow,

$$D_t\boldsymbol{\omega} = \boldsymbol{\omega}\cdot\nabla\mathbf{v} - \boldsymbol{\omega}\,\operatorname{div}\mathbf{v} + \frac{1}{\rho^2}\nabla\rho\times\nabla p.$$

The last term is a volume source of vorticity. In addition, vorticity may be concentrated on an interface or generated near a no-slip boundary. Schematically, one may think of the sources as

$$\text{volume source} \quad + \quad \text{interface source} \quad + \quad \text{boundary source}.$$

Baroclinic generation. The term

$$\frac{1}{\rho^2}\nabla\rho\times\nabla p$$

is the baroclinic generation term. It vanishes for barotropic flow,

$$p = p(\rho),$$

because then ∇p is parallel to $\nabla\rho$. In nonbarotropic flow, however,

$$\nabla\rho\times\nabla p \neq 0,$$

and vorticity can be generated inside the fluid. This mechanism is important in compressible flow, stratified flow, combustion, shock interactions, and atmospheric and oceanic flows.

Shear layers and vortex sheets. A second mechanism is concentration of vorticity in a thin shear layer. Suppose the tangential velocity changes rapidly across an interface Σ. In the inviscid idealization, this becomes a vortex sheet. If the normal velocity is continuous but the tangential velocity jumps,

$$\mathbf{v}_+\cdot\boldsymbol{\nu} = \mathbf{v}_-\cdot\boldsymbol{\nu}, \qquad \mathbf{v}_{+,\parallel} \neq \mathbf{v}_{-,\parallel},$$

then the vorticity is concentrated on Σ. Formally,

$$\boldsymbol{\omega} = \boldsymbol{\gamma}\,\delta_\Sigma, \qquad \boldsymbol{\gamma} = \boldsymbol{\nu}\times(\mathbf{v}_+ - \mathbf{v}_-).$$

Thus a vortex sheet is an interface-supported vorticity distribution. Jets, mixing layers, and separated wakes often contain such concentrated vorticity.

Viscous boundary generation. A no-slip boundary may be viewed, in the thin-boundary-layer limit, as producing a vortex sheet on the wall. Let $\mathbf{U}_{\partial M}$ be the wall velocity and let $\mathbf{v}_e$ be the limiting outer velocity just outside the boundary layer. The corresponding vortex sheet strength is

$$\boxed{\boldsymbol{\gamma}_{\partial M} = \boldsymbol{\nu} \times (\mathbf{v}_e - \mathbf{U}_{\partial M}).}$$

Thus the boundary vorticity may be represented formally as

$$\boldsymbol{\omega}_{\partial M} = \boldsymbol{\gamma}_{\partial M}\, \delta_{\partial M}.$$

However, this describes the amount of vorticity concentrated near the wall, not the rate at which vorticity is generated. The generation rate is a dynamical quantity. For incompressible Navier–Stokes flow with constant viscosity, the vorticity equation is

$$D_t \boldsymbol{\omega} = \boldsymbol{\omega} \cdot \nabla \mathbf{v} + \nu \Delta \boldsymbol{\omega}.$$

At a no-slip wall, viscosity and the boundary condition create a flux of vorticity from the wall into the fluid. In a schematic distributional notation, one may write

$$D_t \boldsymbol{\omega} = \boldsymbol{\omega} \cdot \nabla \mathbf{v} + \nu \Delta \boldsymbol{\omega} + \boldsymbol{\sigma}_{\partial M}\, \delta_{\partial M},$$

where $\boldsymbol{\sigma}_{\partial M}$ is the boundary vorticity generation rate.

For a fixed impermeable wall, Lighthill's formula relates this rate to the tangential pressure gradient. Up to the convention for the normal orientation, one may write

$$\boxed{\boldsymbol{\sigma}_{\partial M} = \frac{1}{\rho}\, \boldsymbol{\nu} \times \nabla p \quad \text{on } \partial M.}$$

Thus a tangential pressure gradient along the wall produces vorticity at the boundary. In two dimensions this reduces to the scalar statement that the rate of vorticity production is proportional to the pressure gradient along the wall:

$$\sigma_{\partial M} = \frac{1}{\rho} \frac{\partial p}{\partial s},$$

again up to the sign convention for the boundary orientation.

The vortex-sheet strength $\boldsymbol{\gamma}_{\partial M}$ measures the vorticity accumulated across a thin boundary layer. It is determined by the tangential velocity jump:

$$\boldsymbol{\gamma}_{\partial M} = \boldsymbol{\nu} \times (\mathbf{v}_e - \mathbf{U}_{\partial M}).$$

Thus $\boldsymbol{\gamma}_{\partial M}$ answers the question: how much vorticity is contained in the boundary layer?

The vorticity generation rate $\boldsymbol{\sigma}_{\partial M}$ measures how fast vorticity is produced at the wall. For incompressible Navier–Stokes flow with constant density and viscosity, Lighthill's formula gives, up to orientation convention,

$$\boldsymbol{\sigma}_{\partial M} = \frac{1}{\rho} \boldsymbol{\nu} \times \nabla p.$$

Thus $\boldsymbol{\sigma}_{\partial M}$ answers the question: how fast is new vorticity injected from the wall into the fluid?

Shear layers and viscous boundary layers are closely related. A shear layer concentrates vorticity across an interface; a no-slip wall creates a shear layer next to the boundary. In both cases, vorticity becomes organized in a thin region and may later be shed into the flow.

Formation of vortex tubes from a planar boundary. In three-dimensional viscous flow, vortex tubes may be generated from vorticity produced near a solid boundary. Even if the boundary is planar, the no-slip condition creates a thin boundary layer in which the velocity changes rapidly in the direction normal to the wall. This produces vorticity concentrated near the boundary.

For example, suppose the wall is locally given by $z = 0$ and the main flow is approximately in the x-direction:

$$\mathbf{u} \approx (u(z), 0, 0).$$

Then the vorticity is

$$\boldsymbol{\omega} = \nabla \times \mathbf{u} = \left(0, \frac{\partial u}{\partial z}, 0\right),$$

up to sign convention. Thus the shear in the boundary layer generates vorticity parallel to the wall.

This boundary vorticity may subsequently be lifted away from the wall by three-dimensional disturbances, separation, adverse pressure gradients, or instabilities. Once away from the wall, the vorticity is stretched and tilted by the surrounding flow. The originally sheet-like vorticity near the boundary can then roll up into concentrated vortex tubes.

8.5.2 Vortex Stretching and Intensification

In three-dimensional flow, vorticity may grow by stretching. For incompressible inviscid flow,

$$D_t\boldsymbol{\omega} = \boldsymbol{\omega} \cdot \nabla \mathbf{v}.$$

Local stretching mechanism. The term

$$\boldsymbol{\omega} \cdot \nabla \mathbf{v}$$

describes stretching and tilting of vortex lines. In components,

$$(\boldsymbol{\omega} \cdot \nabla \mathbf{v})_i = \omega_j \partial_j v_i.$$

Thus the vorticity vector is acted on by the velocity gradient:

$$D_t\boldsymbol{\omega} = (\nabla \mathbf{v})\boldsymbol{\omega} \qquad \text{for incompressible inviscid flow.}$$

If we freeze the velocity gradient near a particle path and write

$$A = \nabla \mathbf{v}(t_0, \mathbf{x}_0),$$

then the linearized approximation gives

$$\boldsymbol{\omega}(t) \approx e^{(t-t_0)A}\boldsymbol{\omega}(t_0).$$

Thus vorticity is amplified in directions in which the local flow stretches material line elements.

The same matrix $A = \nabla \mathbf{v}$ appears in the equation for the separation between nearby particles. If $\delta\mathbf{x}$ is a small material line element, then

$$D_t(\delta\mathbf{x}) = (\nabla \mathbf{v})\delta\mathbf{x}.$$

Therefore, in the same frozen-gradient approximation,

$$\delta\mathbf{x}(t) \approx e^{(t-t_0)A}\delta\mathbf{x}(t_0).$$

This shows the geometric meaning of vortex stretching: vorticity evolves like a material line element. If the local flow stretches material line elements in one direction, then a vortex line aligned with that direction is stretched as well.

To see the amplification rate, decompose the velocity gradient into its symmetric and antisymmetric parts:

$$\nabla\mathbf{v} = \mathbf{S} + \mathbf{R},$$

where

$$\mathbf{S} = \frac{1}{2}\left(\nabla\mathbf{v} + (\nabla\mathbf{v})^T\right), \qquad \mathbf{R} = \frac{1}{2}\left(\nabla\mathbf{v} - (\nabla\mathbf{v})^T\right).$$

The antisymmetric part $\mathbf{R}$ rotates vectors, while the symmetric part $\mathbf{S}$ changes their length. Let

$$\boldsymbol{\omega} = |\boldsymbol{\omega}|\boldsymbol{\xi}, \qquad |\boldsymbol{\xi}| = 1.$$

Then

$$D_t|\boldsymbol{\omega}| = (\boldsymbol{\xi}\cdot\mathbf{S}\boldsymbol{\xi})|\boldsymbol{\omega}|$$

for incompressible inviscid flow. Hence the instantaneous growth rate of the vorticity magnitude is

$$\boldsymbol{\xi}\cdot\mathbf{S}\boldsymbol{\xi}.$$

If $\lambda_1 \geq \lambda_2 \geq \lambda_3$ are the eigenvalues of $\mathbf{S}$, then

$$\lambda_3 \leq \boldsymbol{\xi}\cdot\mathbf{S}\boldsymbol{\xi} \leq \lambda_1.$$

Thus the strongest local amplification occurs when the vorticity is aligned with the most stretching eigenvector. In that case,

$$|\boldsymbol{\omega}(t)| \approx e^{\lambda_1(t-t_0)}|\boldsymbol{\omega}(t_0)|.$$

For incompressible flow,

$$\operatorname{div}\mathbf{v} = 0,$$

so

$$\operatorname{tr}\mathbf{S} = 0.$$

Thus stretching in one direction must be accompanied by compression in another direction. A vortex tube stretched along its axis becomes thinner in cross-section. Since its circulation is conserved,

$$\Gamma = \int_A \boldsymbol{\omega}\cdot\boldsymbol{\nu}\, dS,$$

a decrease of cross-sectional area forces the vorticity magnitude to increase. This is the geometric mechanism behind vortex intensification in three-dimensional flow.

This mechanism is absent in two-dimensional incompressible flow, where

$$D_t\omega = 0.$$

Therefore vorticity values are transported but not amplified along particle paths. The difference between two and three dimensions is one of the most important distinctions in vortex dynamics.

Vortex stretching is central in three-dimensional turbulence. It transfers motion to smaller scales and can create thin, intense vortex filaments.

8.5.3 Merging, Concentration, and Coherent Structures

Vortices may also grow in an organizational sense. The vorticity magnitude need not increase at every point, but the flow may reorganize vorticity into larger or more coherent structures. This is an important distinction: vortex growth may mean amplification of $|\boldsymbol{\omega}|$, or it may mean the formation of a larger organized vortex from several smaller ones.

Two dimensions. In two-dimensional incompressible flow, vorticity is transported as a scalar:

$$D_t\omega = 0.$$

Thus the value of vorticity along each particle path is preserved. However, the spatial organization of vorticity can change dramatically. Vortices of the same sign tend to rotate around each other. If they are sufficiently close, their outer streamlines interact, the vortices deform, and they may merge into a larger coherent vortex.

For example, two like-signed vortex patches may first rotate around a common center. As their boundaries deform, thin filaments of vorticity may be pulled out from the patches. Part of this filamentary vorticity is carried away, while the main cores may merge into a single larger patch. In this way, the flow separates into a coherent core and fine-scale filamentary vorticity.

This behavior is closely related to the inverse cascade in two-dimensional turbulence. Since vortex stretching is absent in two dimensions, vorticity is not amplified by stretching. Instead, nonlinear advection rearranges vorticity. Small vortices can merge into larger vortices, and energy tends to move toward larger spatial scales, while enstrophy is transferred toward smaller scales through filamentation.

Vortex concentration is another part of this process. Even when the vorticity value is materially conserved, the support of vorticity may be stretched into long thin filaments. These filaments create fine scales in the vorticity field. Thus two-dimensional vortex dynamics has two competing tendencies:

merging of like-signed vortices	formation of larger coherent structures,
filamentation of patch boundaries	creation of fine-scale vorticity structure.

The coherent vortices are the large organized part of the flow, while the filaments form the surrounding fine-scale field.

Three dimensions. In three-dimensional flows, the situation is richer. Vortex filaments and tubes may stretch, bend, twist, and interact. Stretching can increase the vorticity magnitude, while bending and twisting change the geometry of the vortex lines. In viscous flows, nearby vortex tubes may reconnect. This allows the topology of vortex lines to change, which is impossible in smooth ideal flow.

Three-dimensional coherent vortex structures include vortex rings, streamwise vortex tubes, hairpin vortices, braided vortex bundles, and swirling vortex cores. These structures are common in jets, wakes, boundary layers, and turbulent flows. They are coherent because they persist for a significant time compared with the local turnover time and because their motion is organized rather than random.

A useful local time scale is the vortex turnover time

$$\tau_\omega \sim \frac{1}{|\boldsymbol{\omega}|}.$$

A structure may be regarded as coherent when it remains identifiable over several turnover times. In practice, coherent vortices are recognized by large vorticity, swirling motion, pressure minima, or persistent material organization.

These structures carry impulse, momentum, and energy. Therefore they are not only geometric objects. They produce mechanical effects on the surrounding fluid and on solid bodies. Vortex rings propel themselves through the fluid, aircraft wake vortices carry downward momentum, and vortices shed behind a body contribute to drag and unsteady force.

Thus vortex dynamics is not merely the study of the scalar or vector field $\boldsymbol{\omega}$. It is also the study of how vorticity self-organizes into structures that transport momentum, exert forces, and shape the large-scale motion of the fluid.

8.5.4 Summary

The formation and growth of vortices may therefore be summarized as follows:

baroclinicity	creates vorticity in the fluid interior,
shear layers	concentrate vorticity across thin regions,
solid boundaries	generate vorticity through viscous boundary layers,
instability	rolls sheets and layers into vortices,
stretching	amplifies three-dimensional vorticity,
merging	organizes vortices into coherent structures.

8.6 Two-Dimensional Vortex Dynamics

Two-dimensional incompressible vortex dynamics has a special structure: vorticity is a scalar transported by the flow. This makes point vortices, vortex patches, and contour dynamics especially natural.

8.6.1 Point Vortices

A point vortex of strength Γ located at $\mathbf{x}_0$ has vorticity

$$\omega(\mathbf{x}) = \Gamma \delta(\mathbf{x} - \mathbf{x}_0).$$

The induced velocity is

$$\mathbf{v}(\mathbf{x}) = \frac{\Gamma}{2\pi} \frac{(\mathbf{x} - \mathbf{x}_0)^\perp}{|\mathbf{x} - \mathbf{x}_0|^2}.$$

For N point vortices with strengths Γ_i and positions $\mathbf{x}_i$, the equations of motion are

$$\dot{\mathbf{x}}_i = \sum_{j \neq i} \frac{\Gamma_j}{2\pi} \frac{(\mathbf{x}_i - \mathbf{x}_j)^\perp}{|\mathbf{x}_i - \mathbf{x}_j|^2}.$$

This formula is obtained by evaluating at each vortex the velocity induced by all the other vortices. A point vortex does not advect itself. Thus

$$\dot{\mathbf{x}}_i = \sum_{j \neq i} \mathbf{v}_j(\mathbf{x}_i),$$

where

$$\mathbf{v}_j(\mathbf{x}) = \frac{\Gamma_j}{2\pi} \frac{(\mathbf{x} - \mathbf{x}_j)^\perp}{|\mathbf{x} - \mathbf{x}_j|^2}.$$

For two vortices, the motion can be read off explicitly. If

$$\Gamma_1 = \Gamma_2 = \Gamma,$$

then the vortices rotate around their midpoint. If the distance between them is d, each vortex moves with speed

$$V = \frac{\Gamma}{2\pi d}.$$

Since each vortex moves on a circle of radius $d/2$, the angular velocity is

$$\Omega = \frac{V}{d/2} = \frac{\Gamma}{\pi d^2}.$$

If instead

$$\Gamma_1 = \Gamma, \qquad \Gamma_2 = -\Gamma,$$

then the two vortices translate together as a dipole. The translation speed is again

$$V = \frac{\Gamma}{2\pi d},$$

with direction perpendicular to the line joining the vortices.

8.6.2 Hamiltonian Structure of Point Vortices

Point vortices form a finite-dimensional Hamiltonian system. If

$$\mathbf{x}_i = (x_i, y_i),$$

then

$$\Gamma_i \dot{x}_i = \frac{\partial H}{\partial y_i}, \qquad \Gamma_i \dot{y}_i = -\frac{\partial H}{\partial x_i},$$

where

$$H = -\frac{1}{4\pi} \sum_{i \neq j} \Gamma_i \Gamma_j \log |\mathbf{x}_i - \mathbf{x}_j|.$$

This is one of the clearest places where the Hamiltonian structure of fluid motion becomes visible in a finite-dimensional model.

Indeed, differentiating H gives

$$\frac{\partial H}{\partial x_i} = -\frac{1}{2\pi} \sum_{j \neq i} \Gamma_i \Gamma_j \frac{x_i - x_j}{|\mathbf{x}_i - \mathbf{x}_j|^2},$$

and

$$\frac{\partial H}{\partial y_i} = -\frac{1}{2\pi} \sum_{j \neq i} \Gamma_i \Gamma_j \frac{y_i - y_j}{|\mathbf{x}_i - \mathbf{x}_j|^2}.$$

The Hamiltonian equations

$$\Gamma_i \dot{x}_i = \frac{\partial H}{\partial y_i}, \qquad \Gamma_i \dot{y}_i = -\frac{\partial H}{\partial x_i}$$

therefore give

$$\dot{x}_i = -\frac{1}{2\pi} \sum_{j \neq i} \Gamma_j \frac{y_i - y_j}{|\mathbf{x}_i - \mathbf{x}_j|^2},$$

$$\dot{y}_i = \frac{1}{2\pi} \sum_{j \neq i} \Gamma_j \frac{x_i - x_j}{|\mathbf{x}_i - \mathbf{x}_j|^2}.$$

This is exactly

$$\dot{\mathbf{x}}_i = \sum_{j \neq i} \frac{\Gamma_j}{2\pi} \frac{(\mathbf{x}_i - \mathbf{x}_j)^\perp}{|\mathbf{x}_i - \mathbf{x}_j|^2}.$$

Thus point vortex dynamics is a finite-dimensional Hamiltonian reduction of Euler vortex dynamics.

8.6.3 Rotating and Translating Vortex Pairs

The simplest nontrivial point-vortex motions occur for two vortices. Let the vortex positions be

$$\mathbf{x}_1(t), \qquad \mathbf{x}_2(t),$$

with strengths

$$\Gamma_1, \qquad \Gamma_2.$$

In the plane, the velocity induced at $\mathbf{x}_i$ by the other vortex is

$$\dot{\mathbf{x}}_i = \sum_{j \neq i} \frac{\Gamma_j}{2\pi} \frac{(\mathbf{x}_i - \mathbf{x}_j)^\perp}{|\mathbf{x}_i - \mathbf{x}_j|^2}.$$

Thus, for two vortices,

$$\boxed{\dot{\mathbf{x}}_1 = \frac{\Gamma_2}{2\pi} \frac{(\mathbf{x}_1 - \mathbf{x}_2)^\perp}{|\mathbf{x}_1 - \mathbf{x}_2|^2}, \qquad \dot{\mathbf{x}}_2 = \frac{\Gamma_1}{2\pi} \frac{(\mathbf{x}_2 - \mathbf{x}_1)^\perp}{|\mathbf{x}_2 - \mathbf{x}_1|^2}.} \tag{8.6}$$

Let

$$\mathbf{r} = \mathbf{x}_1 - \mathbf{x}_2.$$

Then

$$\dot{\mathbf{r}} = \dot{\mathbf{x}}_1 - \dot{\mathbf{x}}_2 = \frac{\Gamma_1 + \Gamma_2}{2\pi} \frac{\mathbf{r}^\perp}{|\mathbf{r}|^2}.$$

Therefore

$$\frac{d}{dt}|\mathbf{r}|^2 = 2\mathbf{r} \cdot \dot{\mathbf{r}} = \frac{\Gamma_1 + \Gamma_2}{\pi} \frac{\mathbf{r} \cdot \mathbf{r}^\perp}{|\mathbf{r}|^2} = 0.$$

Thus the distance between the two vortices is constant:

$$|\mathbf{r}(t)| = d.$$

Two vortices of the same sign. Assume first that

$$\Gamma_1 = \Gamma_2 = \Gamma.$$

Then

$$\dot{\mathbf{r}} = \frac{\Gamma}{\pi d^2}\mathbf{r}^{\perp}.$$

Hence the relative vector $\mathbf{r}$ rotates with angular velocity

$$\boxed{\Omega = \frac{\Gamma}{\pi d^2}.}$$

Thus

$$\mathbf{r}(t) = R_{\Omega t}\mathbf{r}(0),$$

where R_θ is rotation by angle θ.

The midpoint

$$\mathbf{X} = \frac{\mathbf{x}_1 + \mathbf{x}_2}{2}$$

satisfies

$$\dot{\mathbf{X}} = \frac{1}{2}(\dot{\mathbf{x}}_1 + \dot{\mathbf{x}}_2) = 0.$$

Therefore the midpoint is fixed, and the two vortices rotate around their midpoint. If initially

$$\mathbf{x}_1(0) = \mathbf{X}_0 + \frac{1}{2}\mathbf{r}_0, \qquad \mathbf{x}_2(0) = \mathbf{X}_0 - \frac{1}{2}\mathbf{r}_0,$$

then

$$\boxed{\mathbf{x}_1(t) = \mathbf{X}_0 + \frac{1}{2}R_{\Omega t}\mathbf{r}_0, \qquad \mathbf{x}_2(t) = \mathbf{X}_0 - \frac{1}{2}R_{\Omega t}\mathbf{r}_0.}$$

Thus two equal vortices of the same sign form a rotating vortex pair.

Two vortices of opposite sign. Now assume

$$\Gamma_1 = \Gamma, \qquad \Gamma_2 = -\Gamma.$$

Then

$$\Gamma_1 + \Gamma_2 = 0,$$

and hence

$$\dot{\mathbf{r}} = 0.$$

The separation vector is constant:

$$\mathbf{r}(t) = \mathbf{r}_0.$$

Both vortices move with the same velocity. Indeed,

$$\dot{\mathbf{x}}_1 = -\frac{\Gamma}{2\pi}\frac{\mathbf{r}_0^{\perp}}{d^2},$$

and

$$\dot{\mathbf{x}}_2 = -\frac{\Gamma}{2\pi}\frac{\mathbf{r}_0^{\perp}}{d^2}.$$

Therefore

$$\boxed{\mathbf{x}_1(t) = \mathbf{x}_1(0) + \mathbf{U}_d t, \qquad \mathbf{x}_2(t) = \mathbf{x}_2(0) + \mathbf{U}_d t,}$$

where

$$\boxed{\mathbf{U}_d = -\frac{\Gamma}{2\pi d^2}\mathbf{r}_0^{\perp}.}$$

Thus a pair of equal and opposite vortices translates without changing its shape. This is a vortex dipole.

If

$$\mathbf{r}_0 = d\mathbf{e}_y,$$

then

$$\mathbf{r}_0^{\perp} = -d\mathbf{e}_x,$$

and therefore

$$\mathbf{U}_d = \frac{\Gamma}{2\pi d}\mathbf{e}_x.$$

Hence the dipole translates perpendicular to the line joining the two vortices, with speed

$$\boxed{|\mathbf{U}_d| = \frac{|\Gamma|}{2\pi d}.}$$

This calculation shows two basic coherent motions in vortex dynamics:

$$\Gamma_1 = \Gamma_2 \quad \Longrightarrow \quad \text{rotating pair},$$

whereas

$$\Gamma_1 = -\Gamma_2 \quad \Longrightarrow \quad \text{translating dipole}.$$

Aircraft wake vortices are a physical example of a dipole-like vortex pair in cross-section.

8.6.4 Von Karman Vortex Street

Behind a bluff body, such as a circular cylinder, vortices of alternating sign may be shed periodically into the wake. The resulting pattern is called a von Karman vortex street:

$$+\Gamma,\ -\Gamma,\ +\Gamma,\ -\Gamma, \ldots.$$

It is one of the most important examples of organized vorticity generation in two-dimensional wake flow.

The mechanism is the following. Near the body, viscosity creates vorticity in the boundary layer. When the boundary layer separates, this vorticity is shed into the wake. The two sides of the body generate vorticity of opposite signs. Instead of being shed symmetrically, the vortices often shed alternately:

$$\text{upper side} \quad \Longrightarrow \quad +\Gamma, \qquad \text{lower side} \quad \Longrightarrow \quad -\Gamma.$$

This alternating shedding produces a staggered array of vortices.

A simple idealization is a pair of infinite staggered rows of point vortices. Suppose vortices of strength $+\Gamma$ lie on one row and vortices of strength $-\Gamma$ lie on the other row. Let a be the

streamwise spacing between vortices in each row, and let $2b$ be the vertical distance between the two rows. Then the vortex street has the schematic form

$$\begin{array}{ccccccccc} \cdots & & +\Gamma & & & +\Gamma & & +\Gamma & \cdots \\ & & & -\Gamma & & & -\Gamma & & \cdots \end{array}$$

with the two rows shifted by half a period.

The point-vortex model explains why the street moves as a coherent pattern. Each vortex is transported by the velocity induced by all the other vortices. Although the individual induced velocities are nonlocal, the periodic staggered arrangement can translate downstream approximately as a whole. Thus the von Karman street is a coherent vortex pattern, not merely a random collection of vortices.

The geometry of the staggered arrangement is important. Von Karman showed that a stable point-vortex street requires a special ratio between the cross-stream spacing and the streamwise spacing. In the idealized infinite-row model, the neutral stability condition is

$$\sinh\left(\frac{\pi b}{a}\right) = 1.$$

Hence

$$\frac{b}{a} = \frac{1}{\pi}\sinh^{-1}(1) \approx 0.2805.$$

This number is not meant to be exact for real viscous wakes, but it shows that the stability of the street depends on its geometry.

The shedding frequency is often described by the Strouhal number

$$St = \frac{fD}{U},$$

where f is the shedding frequency, D is the diameter of the body, and U is the incoming flow speed. For flow past a circular cylinder over a wide range of Reynolds numbers, St is approximately of order 0.2. Thus vortex shedding has a characteristic frequency determined by the body size and the incoming velocity.

The von Karman vortex street also has a mechanical effect. Alternating vortex shedding produces an oscillatory lift force on the body. This is why vortex shedding can cause vibration of chimneys, bridge cables, cylinders, and other bluff structures. The wake pattern is therefore not only a visual feature of the flow; it is directly connected to force and momentum exchange.

In summary, the von Karman vortex street illustrates several central themes of vortex dynamics:

boundary generation	vorticity is produced near the body,
separation	vorticity is shed into the wake,
organization	vortices arrange into a staggered pattern,
force	alternating shedding produces unsteady lift.

It is therefore a basic example of how vorticity generation, coherent structure, and fluid force are connected.

8.6.5 Viscous Vortex: Lamb–Oseen Vortex

The Lamb–Oseen vortex is a viscous vortex whose vorticity is Gaussian:

$$\omega_z(r,t) = \frac{\Gamma}{4\pi\nu t}\exp\left(-\frac{r^2}{4\nu t}\right).$$

It describes viscous diffusion of a line vortex.

The tangential velocity is obtained from circulation inside radius r:

$$v_\theta(r,t) = \frac{1}{r}\int_0^r \omega_z(s,t)s\,ds.$$

Substituting the Lamb–Oseen vorticity gives

$$v_\theta(r,t) = \frac{\Gamma}{2\pi r}\left(1-\exp\left(-\frac{r^2}{4\nu t}\right)\right).$$

For small r, the velocity is finite; for large r, it approaches the inviscid point-vortex velocity

$$v_\theta(r,t) \sim \frac{\Gamma}{2\pi r}.$$

8.6.6 Vortex Patches and Contour Dynamics

A circular vortex patch: Rankine vortex

The Rankine vortex has solid-body rotation inside a core and potential vortex motion outside:

$$v_\theta(r) = \begin{cases} \Omega r, & 0 \le r \le a, \\ \dfrac{\Gamma}{2\pi r}, & r > a. \end{cases}$$

It is a simple model of a vortex with a finite core.

The corresponding vorticity is

$$\omega_z = \frac{1}{r}\frac{d}{dr}(rv_\theta).$$

For $r < a$,

$$rv_\theta = \Omega r^2, \qquad \omega_z = 2\Omega.$$

For $r > a$,

$$rv_\theta = \frac{\Gamma}{2\pi}, \qquad \omega_z = 0.$$

Continuity of v_θ at $r = a$ gives

$$\Omega a = \frac{\Gamma}{2\pi a}, \qquad \Gamma = 2\pi\Omega a^2.$$

Thus the Rankine vortex has constant vorticity inside the core and zero vorticity outside.

Stability of a Circular Vortex Patch

The simplest vortex patch is a circular patch, also called the Rankine vortex patch. Let

$$D_0 = B_R(0)$$

and

$$\omega_0(\mathbf{x}) = \Omega_0 \chi_{D_0}(\mathbf{x}),$$

where Ω_0 is constant. The induced velocity is azimuthal:

$$\mathbf{v}(\mathbf{x}) = v_\theta(r)\mathbf{e}_\theta.$$

Inside the patch,

$$v_\theta(r) = \frac{\Omega_0}{2} r, \qquad 0 \le r < R,$$

while outside the patch,

$$v_\theta(r) = \frac{\Omega_0 R^2}{2r}, \qquad r > R.$$

Thus the circular patch rotates rigidly inside and induces the same exterior velocity as a point vortex of circulation

$$\Gamma = \int_{\mathbb{R}^2} \omega_0 \, d\mathbf{x} = \Omega_0 \pi R^2.$$

The circular vortex patch is stable in a strong nonlinear sense. Roughly speaking, if an initial patch is close to a circular patch in area, then it remains close to some circular patch for all time. One convenient way to measure this closeness is the L^1 distance of vorticities. If

$$\omega(0, \mathbf{x}) = \Omega_0 \chi_{D(0)}(\mathbf{x}),$$

then

$$\|\omega(0) - \Omega_0 \chi_{B_R}\|_{L^1} = |\Omega_0| \, |D(0) \triangle B_R|,$$

where

$$D(0) \triangle B_R$$

is the symmetric difference of the two sets.

The nonlinear stability statement may be expressed informally as follows: if

$$|D(0) \triangle B_R|$$

is small, then for all later times there exists a center $\mathbf{a}(t)$ such that

$$|D(t) \triangle B_R(\mathbf{a}(t))|$$

remains small. Equivalently,

$$\omega(t)$$

stays close in L^1 to a translated circular vortex patch.

The reason is that the two-dimensional Euler equation preserves important quantities, including the distribution of vorticity, the energy, the circulation, and the impulse. A circular patch is an energy extremal among patches with fixed area and circulation. These conserved quantities prevent a small perturbation of the circular patch from drifting far away in L^1.

This stability result should be distinguished from pointwise stability of the boundary. The boundary of the patch may deform and oscillate, but the amount of vorticity that leaves a nearly circular region remains controlled in the L^1 or area sense. Thus the circular vortex patch is stable as a vorticity distribution, even though its boundary may support waves and shape oscillations.

Contour dynamics

Contour dynamics provides a Lagrangian formulation of the two-dimensional incompressible Euler equation for piecewise constant vorticity. Instead of discretizing the vorticity throughout the fluid domain, one tracks the interfaces separating regions of constant vorticity.

We first consider an isolated vortex patch in $\mathbb{R}^2$:

$$\omega(t, \mathbf{x}) = \omega_0 \chi_{D(t)}(\mathbf{x}),$$

where ω_0 is constant and $D(t)$ is a bounded region. Throughout this subsection, we use

$$\mathbf{a}^\perp = (-a_2, a_1), \qquad \nabla^\perp = (-\partial_{x_2}, \partial_{x_1}),$$

and orient $\partial D(t)$ counterclockwise, so that the patch lies to the left of its oriented boundary.

Why the patch remains a patch. The Euler vorticity equation is

$$\partial_t \omega + \mathbf{v} \cdot \nabla \omega = 0, \qquad \nabla \cdot \mathbf{v} = 0.$$

If φ_t denotes the fluid flow map, then

$$\omega(t, \varphi_t(\mathbf{x})) = \omega(0, \mathbf{x}).$$

Consequently,

$$D(t) = \varphi_t(D(0)), \qquad \partial D(t) = \varphi_t(\partial D(0)).$$

The vorticity remains equal to ω_0 inside the moving patch and zero outside. Thus the unknown is the geometry of $D(t)$, which is completely determined by its boundary.

This statement is understood in the transport sense: the spatial derivatives of ω are distributions supported on the interface, but the vorticity itself is a bounded function.

From the area integral to a contour integral. The velocity induced by the patch is

$$\mathbf{v}(\mathbf{x}, t) = \frac{\omega_0}{2\pi} \int_{D(t)} \frac{(\mathbf{x} - \mathbf{y})^\perp}{|\mathbf{x} - \mathbf{y}|^2} \, dA_{\mathbf{y}}.$$

Since

$$\nabla_{\mathbf{y}} \log |\mathbf{x} - \mathbf{y}| = -\frac{\mathbf{x} - \mathbf{y}}{|\mathbf{x} - \mathbf{y}|^2},$$

we obtain

$$\mathbf{v}(\mathbf{x}, t) = -\frac{\omega_0}{2\pi} \int_{D(t)} \nabla_{\mathbf{y}}^\perp \log |\mathbf{x} - \mathbf{y}| \, dA_{\mathbf{y}}.$$

Let $\mathbf{n}$ be the outward unit normal and let $\boldsymbol{\tau} = \mathbf{n}^\perp$ be the positively oriented unit tangent. Green's theorem gives

$$\int_{D(t)} \nabla_{\mathbf{y}}^\perp f \, dA_{\mathbf{y}} = \int_{\partial D(t)} f \boldsymbol{\tau} \, ds.$$

Hence

$$\boxed{\mathbf{v}(\mathbf{x}, t) = -\frac{\omega_0}{2\pi} \int_{\partial D(t)} \log \left(\frac{|\mathbf{x} - \mathbf{y}|}{\ell} \right) \boldsymbol{\tau}(\mathbf{y}, t) \, ds_{\mathbf{y}}.}$$

Here $\ell > 0$ is an arbitrary reference length. Its value does not affect the velocity, because

$$\int_{\partial D(t)} \boldsymbol{\tau}\, ds = \int_{\partial D(t)} d\mathbf{y} = \mathbf{0}.$$

When $\mathbf{x}$ belongs to the patch or its boundary, the derivation can be justified by excluding a small disk about $\mathbf{x}$ and then letting its radius tend to zero. The additional boundary contribution vanishes.

Let $\mathbf{z}(\alpha, t)$, $0 \le \alpha < 2\pi$, be a regular periodic parametrization of the contour. Since

$$\boldsymbol{\tau}\, ds = \partial_\beta \mathbf{z}(\beta, t)\, d\beta,$$

the induced velocity becomes

$$\mathbf{v}(\mathbf{x}, t) = -\frac{\omega_0}{2\pi} \int_0^{2\pi} \log\left(\frac{|\mathbf{x} - \mathbf{z}(\beta, t)|}{\ell}\right) \partial_\beta \mathbf{z}(\beta, t)\, d\beta.$$

The contour evolution equation. For material labels α, the boundary particles satisfy

$$\partial_t \mathbf{z}(\alpha, t) = \mathbf{v}(\mathbf{z}(\alpha, t), t).$$

Substitution gives the closed contour equation

$$\boxed{\partial_t \mathbf{z}(\alpha, t) = -\frac{\omega_0}{2\pi} \int_0^{2\pi} \log\left(\frac{|\mathbf{z}(\alpha, t) - \mathbf{z}(\beta, t)|}{\ell}\right) \partial_\beta \mathbf{z}(\beta, t)\, d\beta.}$$

Thus the two-dimensional fluid problem reduces to a nonlocal evolution equation for a curve. Every part of the contour interacts with every other part through the logarithmic kernel.

More generally, one may write

$$\partial_t \mathbf{z} = \mathbf{v}(\mathbf{z}, t) + \lambda(\alpha, t) \partial_\alpha \mathbf{z}.$$

The additional term is tangent to the contour and changes only its parametrization. In particular,

$$\partial_t \mathbf{z} \cdot \mathbf{n} = \mathbf{v} \cdot \mathbf{n}.$$

The normal velocity determines the evolving patch shape, whereas λ can be chosen to improve the distribution of numerical markers. With $\lambda \neq 0$, the parameter labels are generally no longer material labels.

The apparent singularity. For a smooth regular contour,

$$\mathbf{z}(\beta, t) - \mathbf{z}(\alpha, t) = (\beta - \alpha) \partial_\alpha \mathbf{z}(\alpha, t) + O(|\beta - \alpha|^2).$$

Consequently,

$$\log|\mathbf{z}(\alpha, t) - \mathbf{z}(\beta, t)| = \log|\alpha - \beta| + \log|\partial_\alpha \mathbf{z}(\alpha, t)| + O(|\alpha - \beta|).$$

The singularity is logarithmic and locally integrable:

$$\int_0^\delta |\log s|\, ds < \infty.$$

Therefore the contour integral is an ordinary improper integral; a Cauchy principal value is not required for this formula. Nevertheless, numerical quadrature must treat the logarithmic singularity explicitly.

Several patches and nested contours. Suppose the vorticity has the representation

$$\omega(t,\mathbf{x}) = \sum_{j=1}^{M} q_j \chi_{D_j(t)}(\mathbf{x}),$$

where the coefficients q_j are constant. The regions may be disjoint or nested. For nested regions, the coefficients represent successive vorticity increments, rather than the total vorticity in each region.

If $\mathbf{z}_j$ parametrizes ∂D_j counterclockwise, then

$$\mathbf{v}(\mathbf{x},t) = -\frac{1}{2\pi}\sum_{j=1}^{M} q_j \int_0^{2\pi} \log\left(\frac{|\mathbf{x}-\mathbf{z}_j(\beta,t)|}{\ell}\right)\partial_\beta \mathbf{z}_j(\beta,t)\,d\beta.$$

Each contour satisfies

$$\partial_t \mathbf{z}_k(\alpha,t) = \mathbf{v}(\mathbf{z}_k(\alpha,t),t) + \lambda_k(\alpha,t)\partial_\alpha \mathbf{z}_k(\alpha,t).$$

These equations account simultaneously for self-induced deformation and interaction between patches.

For a patch with holes, the boundary formula also applies directly when every boundary component is oriented with the patch on its left: the outer boundary is counterclockwise and the inner boundaries are clockwise.

Conserved quantities and diagnostic checks. Incompressibility implies conservation of patch area:

$$\frac{d}{dt}|D(t)| = \int_{\partial D(t)} \mathbf{v}\cdot\mathbf{n}\,ds = \int_{D(t)} \nabla\cdot\mathbf{v}\,dA = 0.$$

Hence the circulation

$$\Gamma = \omega_0 |D(t)|$$

is constant. The area can be computed directly from the contour:

$$|D(t)| = \frac{1}{2}\int_0^{2\pi} (z_1\partial_\alpha z_2 - z_2\partial_\alpha z_1)\,d\alpha.$$

For isolated patches in the plane, the first vorticity moment and angular impulse,

$$\mathbf{P} = \int_{\mathbb{R}^2} \mathbf{x}\omega(\mathbf{x},t)\,dA, \qquad I = \frac{1}{2}\int_{\mathbb{R}^2} |\mathbf{x}|^2\omega(\mathbf{x},t)\,dA,$$

are also conserved. For a single patch with $\omega_0 \neq 0$, this implies that its centroid is fixed.

A finite Hamiltonian for compactly supported patch vorticity is

$$\mathcal{H} = -\frac{1}{4\pi}\int_{\mathbb{R}^2}\int_{\mathbb{R}^2} \omega(\mathbf{x})\omega(\mathbf{y})\log\left(\frac{|\mathbf{x}-\mathbf{y}|}{\ell}\right)\,dA_{\mathbf{y}}\,dA_{\mathbf{x}}.$$

It is conserved by the exact Euler evolution. When the total circulation is nonzero, the kinetic energy over the entire plane diverges logarithmically at infinity; $\mathcal{H}$ represents the corresponding renormalized interaction energy.

These invariants provide useful diagnostics for a numerical method. They are not automatically preserved by a generic contour discretization and time integrator.

Example: a circular vortex patch. For a disk of radius R centered at the origin, symmetry gives

$$\mathbf{v}(\mathbf{x}) = \begin{cases} \dfrac{\omega_0}{2}\mathbf{x}^\perp, & |\mathbf{x}| \le R, \\ \dfrac{\omega_0 R^2}{2|\mathbf{x}|^2}\mathbf{x}^\perp, & |\mathbf{x}| \ge R. \end{cases}$$

Thus material boundary particles rotate with angular velocity $\omega_0/2$, but the circular patch has no normal boundary motion and its shape remains stationary.

This example distinguishes particle motion from shape evolution: a tangential reparametrization can keep the contour parametrization fixed even though the fluid particles move around the circle.

Numerical implementation. A practical contour-dynamics calculation proceeds as follows:

1. Represent each closed contour by ordered markers and interpolate between them using line segments or smooth curves.

2. Evaluate the contour-induced velocity at each marker. Integrate the local logarithmic contribution analytically or use quadrature designed for logarithmic kernels.

3. Advance the markers with a suitable time integrator.

4. Redistribute or insert markers where curvature is large or neighboring contour segments approach one another.

5. Monitor area, circulation, vorticity moments, and the Hamiltonian to assess numerical accuracy.

With N markers, direct pairwise evaluation typically requires $O(N^2)$ work per velocity evaluation. Fast summation techniques can reduce this cost.

The main advantage is that no interior grid is needed. The main difficulty is filamentation: the contour can stretch into long, thin structures that require increasingly many markers. Redistribution improves resolution but must be performed carefully to avoid artificial changes in area and other invariants.

Relation to smooth vorticity and vortex sheets. A smooth vorticity distribution can be approximated by a sequence of piecewise constant levels. Tracking the interfaces between these levels produces a multi-contour approximation of the Euler evolution.

A vortex patch, however, is not a vortex sheet. In a patch, vorticity is distributed over an area and has a finite jump across the boundary; the induced velocity is continuous across that boundary. A vortex sheet instead has vorticity of the form

$$\omega = \gamma\, \delta_{\mathcal{C}},$$

where $\delta_{\mathcal{C}}$ denotes arclength measure on a curve. Its tangential velocity generally has a jump, and its evolution involves a different singular integral.

A thin patch layer may formally approach a vortex sheet if its thickness tends to zero while its vorticity increases so that the integrated vorticity across the layer remains finite. This is a singular limit, rather than an identification of the two models.

Scope of the formulation. The logarithmic formula above applies to inviscid flow in the whole plane. In a bounded or multiply connected fluid domain, the velocity reconstruction must include the appropriate boundary correction and any required harmonic circulation fields.

For viscous flow, diffusion destroys the piecewise constant patch structure, so boundary tracking alone no longer closes the evolution.

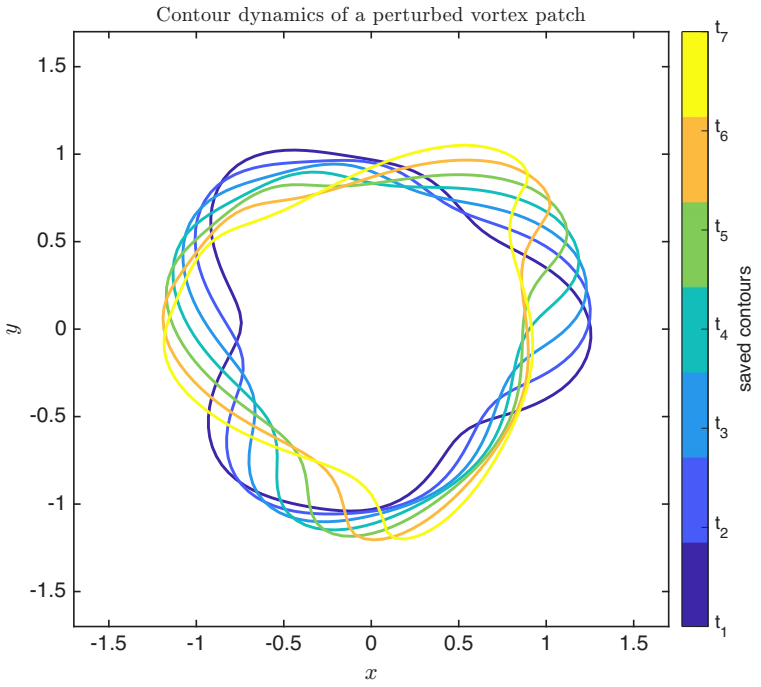


Figure 8.1: Contour dynamics of a perturbed vortex patch. The initial contour is a perturbed circle of the form $r(\theta) = 1 + 0.18\cos(3\theta) + 0.08\cos(5\theta + 0.4)$. The patch has constant vorticity $\omega = \omega_0$ inside the contour and zero vorticity outside. The boundary is transported by the velocity induced by the patch itself. The successive contours show how a vortex patch deforms and develops filamentary structures while preserving its vorticity value.

Kirchhoff Elliptic Vortex Patch

A classical exact solution of vortex patch dynamics is the Kirchhoff elliptic vortex patch. Consider a two-dimensional incompressible inviscid flow. Let the vorticity be constant inside an ellipse and zero outside:

$$\omega(\mathbf{x}) = \omega_0 \chi_D(\mathbf{x}),$$

where

$$D = \left\{ (x, y) : \frac{x^2}{a^2} + \frac{y^2}{b^2} < 1 \right\}.$$

Here a and b are the semi-major and semi-minor axes of the ellipse.

Kirchhoff showed that this patch is an exact solution of the two-dimensional Euler equation. The ellipse does not change its shape. Instead, it rotates rigidly about its center with angular

velocity

$$\boxed{\Omega = \omega_0 \frac{ab}{(a+b)^2}.} \tag{8.7}$$

Thus the boundary of the patch is

$$D(t) = R_{\Omega t} D(0),$$

where $R_{\Omega t}$ denotes rotation by angle Ωt.

This example is important for two reasons. First, it shows that a vortex patch can move coherently without changing its shape. The boundary is transported by the induced velocity, but the induced motion is exactly a rigid rotation of the ellipse. Second, it shows that elongation alone does not necessarily imply filamentation. A uniform elliptic patch is a coherent structure.

The stability of the Kirchhoff ellipse depends on its aspect ratio. Love showed that the elliptic vortex patch is linearly stable only when the aspect ratio is sufficiently small:

$$\frac{a}{b} < 3$$

assuming $a \geq b$.

When the elliptic patch is unstable or strongly perturbed, the boundary no longer remains close to an ellipse. The induced velocity stretches some parts of the contour outward and folds other parts back toward the core. As a result, long thin extensions of vorticity may be pulled away from the main patch. These extensions are often called filaments or finger-like structures. They carry vorticity away from the coherent core and create fine spatial scales in the flow.

Thus filamentation is not a property of the exact Kirchhoff ellipse itself. The exact Kirchhoff ellipse rotates rigidly and preserves its shape. Finger-like structures appear when the patch is sufficiently elongated, unstable, perturbed, or interacting with other vortices. This distinction is important: coherent vortex patches and filamentary vortex patches are two different regimes of the same contour dynamics.

Kirchhoff elliptic vortices are useful idealized models for coherent elliptical vortices observed in geophysical and astrophysical flows. They also provide a benchmark for contour dynamics methods: a numerical method should preserve the rotating elliptic shape when the initial data is an exact Kirchhoff ellipse.

8.6.7 Interaction and Merging of Vortex Patches

Vortex patches do not merely move independently. When two patches of the same sign are close enough, their induced velocities deform each other. The patches may stretch into elongated shapes, develop thin filaments, and eventually merge into a single larger vortex structure. This vortex merging process is one of the basic mechanisms by which coherent vortices form in two-dimensional flows.

The simplest qualitative picture is the following. Two like-signed patches rotate around each other because each patch is advected by the velocity induced by the other. If their separation is large compared with their radii, they behave approximately like two point vortices. If their separation is small, the strain field produced by each patch strongly deforms the other. The boundary becomes elongated, a thin bridge may form, and the two patches can merge.

Thus vortex-patch dynamics contains both coherent motion and filamentation:

$$\text{rotation} \quad \longrightarrow \quad \text{deformation} \quad \longrightarrow \quad \text{filamentation} \quad \longrightarrow \quad \text{merging}.$$

This is one of the reasons vortex patches are useful models for coherent structures. They are simple enough to be described by contour dynamics, but rich enough to show vortex interaction, deformation, and merger.

In two-dimensional turbulence, like-signed vortices tend to merge into larger coherent vortices. This is related to the inverse cascade picture: energy is transferred toward larger scales, while enstrophy is transferred toward smaller scales through the formation of thin vorticity filaments.

8.6.8 Vortex Sheets and Kelvin–Helmholtz Instability

Dynamics of a vortex sheet: Birkhoff–Rott Equation. In two dimensions, a vortex sheet may be represented by a curve

$$\mathbf{z}(\alpha, t)$$

with sheet strength $\gamma(\alpha, t)$. The velocity on the sheet is given formally by a principal-value Biot–Savart integral:

$$\partial_t \mathbf{z}(\alpha, t) = \mathrm{p.\,v.}\, \frac{1}{2\pi} \int \frac{\big(\mathbf{z}(\alpha, t) - \mathbf{z}(\beta, t)\big)^{\perp}}{|\mathbf{z}(\alpha, t) - \mathbf{z}(\beta, t)|^2} \gamma(\beta, t)\, d\beta.$$

This is the Birkhoff–Rott equation.

The equation is singular because the kernel behaves like

$$\frac{1}{|\mathbf{z}(\alpha) - \mathbf{z}(\beta)|}$$

as $\beta \to \alpha$. The principal value removes the leading symmetric singularity, but the resulting evolution remains delicate. This singular character is one reason vortex sheets can develop complicated roll-up and possible singular behavior.

Kelvin-Helmholtz instability. Shear layers and vortex sheets are often unstable. A small perturbation of the interface may grow because the two sides of the sheet move with different tangential velocities. This is the Kelvin–Helmholtz instability.

We illustrate the mechanism by the simplest model. Consider two incompressible inviscid fluids separated by the flat interface

$$y = 0.$$

Assume that the upper and lower fluids move with constant horizontal velocities

$$\mathbf{v}_+ = U_+ \mathbf{e}_x, \qquad y > 0,$$

and

$$\mathbf{v}_- = U_- \mathbf{e}_x, \qquad y < 0.$$

The normal velocity is continuous across the interface, but the tangential velocity jumps if

$$U_+ \neq U_-.$$

Thus the unperturbed interface is a vortex sheet. Its sheet strength is

$$\gamma = U_+ - U_-,$$

up to the sign convention for the normal direction.

Now perturb the interface:

$$y = \eta(t, x),$$

where $|\eta|$ is small. Since the flow is irrotational away from the sheet, we introduce velocity potentials

$$\mathbf{v}_\pm = U_\pm \mathbf{e}_x + \operatorname{grad} \phi_\pm,$$

where

$$\Delta \phi_\pm = 0$$

in the upper and lower half-planes. We look for normal modes of the form

$$\eta(t, x) = \eta_0 e^{ikx+\sigma t}.$$

The corresponding potentials decay away from the interface:

$$\phi_+(t, x, y) = A_+ e^{ikx+\sigma t} e^{-|k|y}, \qquad y > 0,$$

and

$$\phi_-(t, x, y) = A_- e^{ikx+\sigma t} e^{|k|y}, \qquad y < 0.$$

The kinematic boundary condition says that the interface moves with the normal velocity of the fluid:

$$\partial_t \eta + U_\pm \partial_x \eta = \partial_y \phi_\pm \quad \text{at } y = 0.$$

Substituting the normal modes gives

$$(\sigma + ikU_+)\eta_0 = -|k| A_+,$$

and

$$(\sigma + ikU_-)\eta_0 = |k| A_-.$$

The dynamic boundary condition is continuity of pressure across the interface. Linearizing Bernoulli's law gives

$$\partial_t \phi_\pm + U_\pm \partial_x \phi_\pm + \frac{p_\pm}{\rho_\pm} = 0.$$

For equal densities and no surface tension or gravity, pressure continuity therefore gives

$$(\sigma + ikU_+)A_+ = (\sigma + ikU_-)A_-.$$

Using the kinematic relations to eliminate A_+ and A_-, we obtain

$$(\sigma + ikU_+)^2 + (\sigma + ikU_-)^2 = 0.$$

Hence

$$\sigma = -ik\frac{U_+ + U_-}{2} \pm \frac{|k|}{2}(U_+ - U_-).$$

Therefore one branch has positive real part:

$$\boxed{\operatorname{Re} \sigma = \frac{|k|}{2}|U_+ - U_-|.}$$

Thus every wavenumber is unstable in the ideal vortex-sheet model. Shorter waves grow faster, since the growth rate is proportional to $|k|$. This high-wavenumber instability is one reason why the ideal vortex sheet is a singular model.

The imaginary part

$$-k\frac{U_+ + U_-}{2}$$

shows that the disturbance is convected with the mean velocity

$$\frac{U_+ + U_-}{2}.$$

The real part gives the exponential growth:

$$|\eta(t)| \sim e^{\frac{|k|}{2}|U_+ - U_-|t}|\eta(0)|.$$

In real fluids, viscosity, surface tension, density stratification, or a finite-thickness shear layer regularizes the very short waves. Nevertheless the basic mechanism remains: a tangential velocity jump or a strong shear layer amplifies interface perturbations.

As the instability grows beyond the linear regime, the vortex sheet no longer remains nearly flat. The sheet rolls up into spiral structures. This roll-up is one of the basic mechanisms by which coherent vortices are formed from shear. It appears in mixing layers, jets, cloud patterns, wakes, and many free-surface and stratified-flow problems.

Thus the sequence

$$\text{velocity jump} \implies \text{vortex sheet} \implies \text{Kelvin–Helmholtz instability} \implies \text{vortex roll-up}$$

is one of the fundamental pathways from nearly irrotational motion to vortex dynamics.

Jets as vortex sheets. A jet is a flow injected into a surrounding fluid. In the simplest two-dimensional idealization, the jet has a velocity different from the ambient fluid. Suppose the jet occupies a region D and the surrounding fluid occupies the exterior. Across the jet boundary $\Sigma = \partial D$, the normal velocity is continuous,

$$\mathbf{v}_+ \cdot \boldsymbol{\nu} = \mathbf{v}_- \cdot \boldsymbol{\nu},$$

but the tangential velocity may jump:

$$\mathbf{v}_{+,\parallel} \neq \mathbf{v}_{-,\parallel}.$$

Thus the jet boundary is a vortex sheet.

For example, consider a planar jet moving with speed U in the x- direction into a fluid that is initially at rest. Across the upper and lower edges of the jet, the tangential velocity jumps from approximately U to 0. The vortex sheet strength is therefore of size

$$|\gamma| \approx U.$$

The two sides of the jet carry vortex sheets of opposite signs because the outward normals have opposite orientations.

In a real viscous fluid, the velocity does not jump discontinuously. Instead, the transition from the jet velocity to the ambient velocity occurs across a finite-thickness shear layer. The vorticity is then spread across this layer:

$$\omega \approx -\frac{\partial u}{\partial y}$$

for a nearly parallel velocity field

$$\mathbf{v} = (u(y), 0).$$

Thus the ideal vortex sheet is the zero-thickness limit of a viscous shear layer.

The shear layer at the edge of a jet is often unstable. Small disturbances grow through the Kelvin–Helmholtz instability. As the instability becomes nonlinear, the shear layer rolls up into vortices. These vortices entrain ambient fluid, enhance mixing, and organize the jet into coherent vortex structures.

Thus the idealized picture is

jet velocity jump $\Longrightarrow$ vortex sheet $\Longrightarrow$ Kelvin–Helmholtz instability $\Longrightarrow$ vortex roll-up and mixing.

This is one of the most important physical pathways from a nearly potential or piecewise potential flow to a vortical flow.

8.7 Three-Dimensional Vortex Dynamics

Three-dimensional vortex dynamics is different from two-dimensional vortex dynamics because vorticity is a vector. Vortex lines can bend, tilt, and stretch. The stretching term

$$\boldsymbol{\omega} \cdot \nabla \mathbf{v}$$

has no analogue in two-dimensional incompressible flow, and it is the main mechanism by which three-dimensional vorticity can intensify.

8.7.1 Vortex Filaments

A vortex filament is a thin vortex tube concentrated near a space curve

$$\mathbf{x} = \boldsymbol{\gamma}(s, t),$$

where s denotes arclength along the filament. The filament carries a circulation strength Γ. In the singular filament approximation, the vorticity is written formally as

$$\boldsymbol{\omega}(\mathbf{x}, t) = \Gamma \int \frac{\partial \boldsymbol{\gamma}}{\partial s}(s, t)\delta(\mathbf{x} - \boldsymbol{\gamma}(s, t))\, ds.$$

The vorticity is tangent to the filament, and the total circulation around a small loop linking the filament is Γ.

The induced velocity is obtained from the three-dimensional Biot–Savart law:

$$\mathbf{v}(\mathbf{x}, t) = \frac{1}{4\pi} \int_{\mathbb{R}^3} \frac{\boldsymbol{\omega}(\mathbf{y}, t) \times (\mathbf{x} - \mathbf{y})}{|\mathbf{x} - \mathbf{y}|^3}\, d\mathbf{y}.$$

Substituting the filament expression for $\boldsymbol{\omega}$, we obtain the filament Biot–Savart formula

$$\boxed{\mathbf{v}(\mathbf{x},t) = \frac{\Gamma}{4\pi}\int \frac{\frac{\partial \boldsymbol{\gamma}}{\partial s}(s,t)\times(\mathbf{x}-\boldsymbol{\gamma}(s,t))}{|\mathbf{x}-\boldsymbol{\gamma}(s,t)|^3}\,ds.} \tag{8.8}$$

The filament moves with the fluid velocity. Therefore its evolution is

$$\boxed{\frac{\partial \boldsymbol{\gamma}}{\partial t}(s,t) = \mathbf{v}(\boldsymbol{\gamma}(s,t),t).} \tag{8.9}$$

However, the velocity in (8.8) is singular when $\mathbf{x}$ lies on the filament. This singularity reflects the idealization of a finite-core vortex tube by a curve. In practice one either keeps a small core radius or uses an asymptotic approximation.

Stretching of a vortex filament. Let $\delta\mathbf{x}$ be a small material line element tangent to a vortex line. Then

$$D_t(\delta\mathbf{x}) = (\nabla\mathbf{v})\delta\mathbf{x}.$$

For inviscid barotropic flow, the specific vorticity satisfies

$$D_t\left(\frac{\boldsymbol{\omega}}{\rho}\right) = \left(\frac{\boldsymbol{\omega}}{\rho}\right)\cdot\nabla\mathbf{v}.$$

Thus $\boldsymbol{\omega}/\rho$ evolves like a material line element. In incompressible flow this becomes

$$D_t\boldsymbol{\omega} = \boldsymbol{\omega}\cdot\nabla\mathbf{v}.$$

If a vortex filament is stretched, the length element along the filament increases. Since circulation is preserved,

$$\Gamma = \int_A \boldsymbol{\omega}\cdot\boldsymbol{\nu}\,dS,$$

the cross-sectional area of the corresponding vortex tube decreases and the magnitude of vorticity increases.

A local calculation makes this precise. Write

$$\boldsymbol{\omega} = |\boldsymbol{\omega}|\boldsymbol{\xi}, \qquad |\boldsymbol{\xi}| = 1.$$

For incompressible inviscid flow,

$$D_t|\boldsymbol{\omega}| = (\boldsymbol{\xi}\cdot\mathbf{S}\boldsymbol{\xi})|\boldsymbol{\omega}|,$$

where

$$\mathbf{S} = \frac{1}{2}\left(\nabla\mathbf{v} + (\nabla\mathbf{v})^T\right)$$

is the rate-of-strain tensor. Thus the vorticity grows when it is aligned with a stretching direction of the strain tensor.

Interaction of filaments. If two vortex filaments are present, each filament is transported by the velocity induced by all filaments. For filaments

$$\boldsymbol{\gamma}_1(s,t), \qquad \boldsymbol{\gamma}_2(s,t),$$

with strengths Γ_1 and Γ_2, the velocity at a point on $\boldsymbol{\gamma}_1$ contains the contribution

$$\mathbf{v}_{2\to 1} = \frac{\Gamma_2}{4\pi} \int \frac{\frac{\partial \boldsymbol{\gamma}_2}{\partial s'}(s',t) \times (\boldsymbol{\gamma}_1(s,t) - \boldsymbol{\gamma}_2(s',t))}{|\boldsymbol{\gamma}_1(s,t) - \boldsymbol{\gamma}_2(s',t)|^3}\, ds'.$$

This velocity bends and transports the first filament. Similarly, the first filament induces velocity on the second. Filament interaction is therefore nonlocal: every part of a filament influences every other part through the Biot–Savart kernel.

Finite-core regularization. A real vortex tube has a finite core radius a. A common regularized filament model replaces the singular kernel by

$$\frac{\mathbf{r}}{|\mathbf{r}|^3} \quad \text{with} \quad \frac{\mathbf{r}}{(|\mathbf{r}|^2 + a^2)^{3/2}}.$$

Then the filament velocity is approximated by

$$\mathbf{v}(\mathbf{x},t) = \frac{\Gamma}{4\pi} \int \frac{\frac{\partial \boldsymbol{\gamma}}{\partial s}(s,t) \times (\mathbf{x} - \boldsymbol{\gamma}(s,t))}{(|\mathbf{x} - \boldsymbol{\gamma}(s,t)|^2 + a^2)^{3/2}}\, ds.$$

The core radius removes the singularity and represents the fact that the vorticity is distributed over a thin tube rather than concentrated on an exact curve.

This filament model captures several important features of three-dimensional vortex dynamics: self-induced motion, nonlocal filament interaction, stretching, bending, and the concentration of vorticity into thin structures.

Local induction approximation. For a thin vortex filament, the velocity induced by the filament itself is singular in the ideal curve model. If the vortex tube has a small core radius a, then the dominant local contribution comes from the nearby portion of the filament. This leads to the local induction approximation.

Let the filament be parametrized by arclength:

$$\mathbf{x} = \boldsymbol{\gamma}(s,t).$$

Let

$$\mathbf{T} = \frac{\partial \boldsymbol{\gamma}}{\partial s}$$

be the unit tangent. The Frenet–Serret formulas give

$$\frac{\partial \mathbf{T}}{\partial s} = \kappa \mathbf{N}, \qquad \mathbf{B} = \mathbf{T} \times \mathbf{N},$$

where κ is the curvature, $\mathbf{N}$ is the normal vector, and $\mathbf{B}$ is the binormal vector.

The local induction approximation states that the self-induced motion of the filament is mainly in the binormal direction:

$$\boxed{\frac{\partial \boldsymbol{\gamma}}{\partial t} = c\,\kappa \mathbf{B}.} \tag{8.10}$$

Here the constant c depends on the circulation and on the logarithm of the ratio between the macroscopic length scale and the vortex core radius. In a typical asymptotic form,

$$c \sim \frac{\Gamma}{4\pi} \log\left(\frac{\ell}{a}\right),$$

where ℓ is a characteristic radius of curvature or outer length scale.

Thus the filament moves faster where it is more strongly curved. A straight filament has

$$\kappa = 0,$$

and has no local self-induced motion under this approximation. A curved filament moves in the binormal direction.

This approximation reveals a deep relation between vortex dynamics and curve geometry. The equation

$$\partial_t \boldsymbol{\gamma} = c\kappa \mathbf{B}$$

is the binormal curvature flow. Under the Hasimoto transform, it is related to the nonlinear Schrödinger equation. Thus the local motion of a thin vortex filament connects fluid mechanics, differential geometry, and integrable systems.

Hasimoto Transform and the Nonlinear Schrödinger Equation

The local induction approximation gives the binormal curvature flow

$$\boxed{\frac{\partial \boldsymbol{\gamma}}{\partial t} = c\kappa \mathbf{B},} \tag{8.11}$$

where κ is the curvature and $\mathbf{B}$ is the binormal vector of the filament. This equation describes the motion of a vortex filament under its locally induced velocity.

A remarkable observation due to Hasimoto is that this geometric curve equation can be transformed into the nonlinear Schrödinger equation. Let τ denote the torsion of the curve. Define the complex function

$$\boxed{q(s,t) = \kappa(s,t) \exp\left(i \int^s \tau(\sigma,t)\, d\sigma\right).} \tag{8.12}$$

The magnitude of q is the curvature:

$$|q(s,t)| = \kappa(s,t),$$

while the phase records the accumulated torsion.

After a suitable rescaling of time, the binormal curvature flow (8.11) is equivalent to the focusing cubic nonlinear Schrödinger equation

$$\boxed{iq_t + q_{ss} + \frac{1}{2}|q|^2 q = 0.} \tag{8.13}$$

Thus the curvature and torsion of the vortex filament are encoded in a complex wave function q.

This result shows that the local dynamics of a thin vortex filament is not only a fluid-mechanical problem. It is also a geometric and integrable system. Solitary-wave solutions of the nonlinear Schrödinger equation correspond to special traveling or twisting motions of the filament.

The Hasimoto transform is based on the local induction approximation, so it does not describe the full nonlocal Biot–Savart dynamics. Nevertheless, it gives a powerful model for understanding how curvature, torsion, and wave-like distortions propagate along a vortex filament.

8.7.2 Vortex Rings

A vortex ring is a closed vortex tube whose centerline is approximately a circle. It is one of the most important coherent structures in three-dimensional vortex dynamics. Smoke rings, bubble rings, and starting jets all produce vortex rings. Unlike a two-dimensional vortex pair, a vortex ring is a genuinely three-dimensional structure: its vorticity is concentrated around a closed tube, and the ring moves through the fluid under its own induced velocity.

Consider a circular vortex ring of radius R, circulation Γ, and core radius a, with

$$a \ll R.$$

The ring moves along its symmetry axis. This motion can be understood from the local induction approximation. The centerline of the ring is a circle, so its curvature is

$$\kappa = \frac{1}{R}.$$

The binormal vector $\mathbf{B}$ points along the symmetry axis of the ring. Thus the binormal curvature law

$$\partial_t \boldsymbol{\gamma} = c\kappa \mathbf{B}$$

predicts that the ring translates along its axis.

A more detailed asymptotic calculation using the Biot–Savart law gives the self-induced speed

$$\boxed{U \approx \frac{\Gamma}{4\pi R}\left[\log\left(\frac{8R}{a}\right) - C\right].} \tag{8.14}$$

Here C depends on the vorticity distribution inside the core. The main feature is the logarithmic dependence

$$U \sim \frac{\Gamma}{4\pi R}\log\left(\frac{R}{a}\right).$$

Thus a thinner core gives a larger self-induced speed.

The direction of motion is determined by the orientation of the circulation. If the fingers of the right hand follow the vorticity around the ring, then the thumb gives the direction of propagation. This is the same orientation rule as for the magnetic field of a current loop.

A vortex ring also carries hydrodynamic impulse. For a thin circular ring, the impulse is approximately

$$\boxed{\mathbf{I} = \rho\Gamma\pi R^2 \mathbf{B},}$$

where $\mathbf{B}$ is the unit vector along the symmetry axis. This formula shows that a vortex ring transports momentum-like information through the fluid. The ring is therefore not merely a geometric vortex tube; it is a moving coherent structure carrying circulation, impulse, and energy.

The energy of a thin vortex ring has the asymptotic form

$$E \approx \frac{1}{2}\rho\Gamma^2 R\left[\log\left(\frac{8R}{a}\right) - C_E\right],$$

where C_E again depends on the core profile. The same logarithmic factor appears because the velocity field near a thin vortex core is nearly singular.

Vortex rings are important because they are self-propelled. The vorticity in the ring induces a velocity field; this velocity field moves the ring; and the structure persists for a long time when viscosity is small. This makes vortex rings basic examples of coherent structures in three-dimensional vortex dynamics.

They also provide a bridge to the mechanics of force and impulse. A starting jet creates a vortex ring at its front. The formation and motion of the ring are tied to the impulse delivered to the fluid. We will return to this point in the section on impulse, momentum, and forces.

Leapfrogging Vortex Rings

Two coaxial vortex rings with the same orientation can undergo a remarkable motion called leapfrogging. Suppose two vortex rings have the same circulation direction and move along the same symmetry axis. The rear ring is pulled forward by the velocity induced by the front ring. As it contracts, its self-induced speed increases. It may then pass through the front ring. After passing through, it expands and slows down, while the other ring contracts and accelerates. The process may repeat periodically.

The mechanism is based on the dependence of the ring speed on its radius. For a thin vortex ring,

$$U \approx \frac{\Gamma}{4\pi R}\left[\log\left(\frac{8R}{a}\right) - C\right].$$

A smaller ring moves faster. During leapfrogging, the rear ring is deformed into a smaller radius and therefore accelerates. The front ring is expanded and slows down. This exchange allows the rear ring to pass through the front one.

Thus leapfrogging is a nonlinear interaction between two coherent vortex rings:

$$\text{rear ring contracts} \quad \Longrightarrow \quad \text{moves faster} \quad \Longrightarrow \quad \text{passes through front ring.}$$

After the passage, the roles are exchanged.

Leapfrogging vortex rings illustrate the nonlocal character of three-dimensional vortex dynamics. Each ring moves not only by its own self-induced velocity, but also by the velocity induced by the other ring. The phenomenon is a three-dimensional analogue of coherent vortex-pair motion in two dimensions, but with an additional degree of freedom: the ring radius can change.

8.7.3 A 3D Viscous Vortex: Burgers Vortex

The Burgers vortex balances vortex stretching against viscous diffusion. A typical strain field is

$$\mathbf{v}_s = \left(-\frac{\alpha}{2}x, -\frac{\alpha}{2}y, \alpha z\right).$$

Radial inflow concentrates vorticity, axial stretching intensifies it, and viscosity prevents collapse.

For an axisymmetric Burgers vortex, the vorticity has the form

$$\boldsymbol{\omega} = \omega_z(r)\mathbf{e}_z.$$

The steady balance is between radial compression, axial stretching, and viscous diffusion. The vorticity profile is Gaussian:

$$\omega_z(r) = \frac{\Gamma\alpha}{4\pi\nu}\exp\left(-\frac{\alpha r^2}{4\nu}\right).$$

Here $\alpha > 0$ is the strain rate. The characteristic core radius is

$$\delta \sim \sqrt{\frac{\nu}{\alpha}}.$$

Thus stronger stretching produces a thinner and more intense vortex core. This is why Burgers vortex is a local model for small intense vortices in three-dimensional flows.

8.7.4 Swirling Vortices and Tornado-Type Flows

Many intense vortices in nature and engineering are not purely circular motions. They combine swirl, radial inflow, and axial stretching. Tornadoes are the most familiar example, but similar mechanisms also appear in dust devils, bathtub vortices, combustion vortices, and swirling flows in tubes.

We describe the basic local mechanism in cylindrical coordinates

$$(r, \theta, z).$$

A swirling vortex has velocity of the form

$$\mathbf{v} = v_r(r, z)\mathbf{e}_r + v_\theta(r, z)\mathbf{e}_\theta + v_z(r, z)\mathbf{e}_z.$$

The azimuthal velocity v_θ represents rotation. The radial velocity v_r may represent inflow toward the vortex core. The axial velocity v_z may represent upward stretching.

The corresponding vorticity has components

$$\boldsymbol{\omega} = \omega_r\mathbf{e}_r + \omega_\theta\mathbf{e}_\theta + \omega_z\mathbf{e}_z.$$

For an axisymmetric flow with no θ-dependence,

$$\omega_z = \frac{1}{r}\frac{\partial}{\partial r}\left(rv_\theta\right).$$

Thus vertical vorticity is produced by the radial variation of swirl.

The key intensification mechanism is vortex stretching. In incompressible flow,

$$D_t\boldsymbol{\omega} = \boldsymbol{\omega}\cdot\nabla\mathbf{v}.$$

If the vorticity is mainly vertical,

$$\boldsymbol{\omega} \approx \omega_z\mathbf{e}_z,$$

then the stretching term gives approximately

$$D_t\omega_z \approx \omega_z \frac{\partial v_z}{\partial z}.$$

Therefore, if

$$\frac{\partial v_z}{\partial z} > 0,$$

vertical stretching amplifies vertical vorticity:

$$\omega_z(t) \sim \omega_z(0) \exp\left(\int_0^t \frac{\partial v_z}{\partial z}\, ds\right).$$

For incompressible flow,

$$\operatorname{div} \mathbf{v} = 0.$$

In axisymmetric coordinates this means

$$\frac{1}{r}\frac{\partial}{\partial r}(r v_r) + \frac{\partial v_z}{\partial z} = 0.$$

Thus axial stretching,

$$\frac{\partial v_z}{\partial z} > 0,$$

is associated with radial convergence,

$$\frac{1}{r}\frac{\partial}{\partial r}(r v_r) < 0.$$

In physical terms, fluid is drawn inward toward the vortex core and then stretched upward. Conservation of angular momentum also tends to increase the swirl speed as fluid parcels move inward. This is the familiar "spinning faster when pulled inward" effect.

Thus the local tornado-type mechanism may be summarized as

$$\text{rotation} + \text{radial convergence} + \text{axial stretching} \quad \Longrightarrow \quad \text{vorticity intensification}.$$

A simple idealized model is a vortex in an imposed axisymmetric strain field. Suppose

$$v_r = -\frac{\alpha}{2} r, \qquad v_z = \alpha z,$$

with $\alpha > 0$. Then

$$\operatorname{div} \mathbf{v} = \frac{1}{r}\frac{\partial}{\partial r}\left(r\left(-\frac{\alpha}{2} r\right)\right) + \frac{\partial}{\partial z}(\alpha z) = -\alpha + \alpha = 0.$$

This velocity field pulls fluid radially inward and stretches it vertically. If a vertical vortex is placed in this strain field, its vertical vorticity satisfies approximately

$$D_t\omega_z = \alpha \omega_z,$$

so that

$$\omega_z(t) = e^{\alpha t}\omega_z(0)$$

as long as the ideal stretching model remains valid.

In a real viscous flow, stretching is balanced by viscous diffusion and possibly by pressure, buoyancy, surface friction, and turbulence. The Burgers vortex is an idealized example in which axial stretching is balanced by viscous diffusion, producing a steady vortex core. Tornadoes are far more complicated: they involve moist thermodynamics, boundary-layer inflow, surface friction, buoyancy, and interaction with a storm-scale environment. Nevertheless, the local vortex mechanism is the same:

$$\text{inflow concentrates rotation,} \qquad \text{stretching intensifies vorticity.}$$

Thus tornado-type vortices are not merely rotating flows. They are stretching vortices. Their intensity comes from the coupling between swirl, convergence, and axial stretching.

8.7.5 Aircraft Wake Dipoles

A lifting wing leaves behind a pair of trailing vortices. These vortices are among the most familiar examples of coherent vortex structures in three-dimensional flow. They are important in aerodynamics because they carry circulation, impulse, and downward momentum into the wake.

The origin of the wake vortices is the bound circulation around the wing. For a wing producing lift, the flow has a circulation around each airfoil section. Since circulation cannot simply end in the fluid, the bound circulation is connected to trailing vorticity shed from the wing tips and from the spanwise variation of lift. In an idealized picture, a trailing vortex sheet is shed behind the wing. This sheet then rolls up into two dominant counter-rotating vortices.

Thus the sequence is

$$\text{bound circulation on wing} \implies \text{trailing vortex sheet} \implies \text{roll-up} \implies \text{counter-rotating wake vortex pa}$$

Far behind the wing, the wake is often dominated by two long counter-rotating vortex tubes. In a cross-section perpendicular to the flight direction, these appear as a vortex pair of opposite signs. This is the three-dimensional realization of the two-dimensional vortex dipole discussed earlier.

To see the connection, suppose the two vortices have circulations

$$\Gamma \quad \text{and} \quad -\Gamma$$

and are separated by a distance d in the cross-section. The induced velocity of a two-dimensional point-vortex dipole has magnitude

$$U_d = \frac{|\Gamma|}{2\pi d}.$$

Thus a pair of opposite-signed vortices translates in the direction perpendicular to the line joining them. In an aircraft wake, this induced motion is mainly downward. This downward motion is called downwash.

The downwash is directly related to lift. The wing gives downward momentum to the air, and by Newton's third law the air exerts an upward lift force on the wing. The trailing vortex pair is the organized vortical structure that carries this momentum into the far wake.

A useful physical picture is therefore

$$\text{lift} \iff \text{bound circulation} \iff \text{trailing vortices} \iff \text{downwash.}$$

The wake vortices are not merely by-products of lift. They are the vortical signature of the momentum balance that produces lift.

In real aircraft wakes, viscosity, turbulence, stratification, ground effect, and atmospheric disturbances gradually weaken and deform the vortex pair. Nevertheless, the ideal dipole picture captures the leading-order geometry: two counter-rotating vortex tubes induce a downward velocity and transport impulse through the wake.

This example also illustrates the connection between two- and three-dimensional vortex dynamics. In cross-section, the wake resembles a two-dimensional translating dipole. In space, it is a pair of long three-dimensional vortex tubes trailing behind the wing.

8.8 Helicity, Linking, and Knotting

A new feature of three-dimensional vortex dynamics is topology. Vortex lines and vortex tubes can link, twist, writhe, and knot. These possibilities have no direct analogue in two-dimensional vorticity dynamics. The main quantity connecting vortex topology with fluid motion is the helicity

$$\boxed{\mathcal{H} = \int_M \mathbf{v} \cdot \boldsymbol{\omega}\, d\mathbf{x},} \tag{8.15}$$

where

$$\boldsymbol{\omega} = \operatorname{curl} \mathbf{v}.$$

Analytically, helicity measures the alignment between velocity and vorticity. Geometrically, for thin vortex tubes, it measures linking, twisting, and writhing of vortex structures.

8.8.1 Linking Number

Let γ_1 and γ_2 be two disjoint closed oriented curves in $\mathbb{R}^3$. Their linking number is defined by the Gauss linking integral:

$$\boxed{Lk(\gamma_1, \gamma_2) = \frac{1}{4\pi} \int_{\gamma_1} \int_{\gamma_2} \frac{(d\mathbf{x} \times d\mathbf{y}) \cdot (\mathbf{x} - \mathbf{y})}{|\mathbf{x} - \mathbf{y}|^3}.} \tag{8.16}$$

Here $\mathbf{x} \in \gamma_1$ and $\mathbf{y} \in \gamma_2$. The orientation of the two curves determines the sign.

The linking number is an integer. It counts, with sign, how many times one closed curve winds around the other. It is unchanged under smooth deformations as long as the two curves do not cross. Thus it is a topological invariant.

Equivalently, one may compute the linking number from a planar projection. Choose a generic projection direction so that the projected curves have only transverse crossings and no triple intersections. At each crossing between γ_1 and γ_2, assign a sign $+1$ or -1 according to the right-hand rule.

More precisely, suppose the projection is onto the plane with normal $\mathbf{n}$. At a crossing, let $\mathbf{T}_1$ and $\mathbf{T}_2$ be the oriented tangent vectors of the two curves at the crossing point, with the convention that the strand of γ_1 passes over the strand of γ_2. The sign of the crossing is

$$\operatorname{sgn}\left((\mathbf{T}_1 \times \mathbf{T}_2) \cdot \mathbf{n}\right).$$

Thus each crossing contributes either $+1$ or -1.

Then

$$\boxed{Lk(\gamma_1,\gamma_2)=\frac{1}{2}\sum_{\text{crossings between }\gamma_1\text{ and }\gamma_2}\text{sign(crossing)}.}$$

The factor $\frac{1}{2}$ appears because, for two closed curves, the signed crossing count changes by two when one curve winds once around the other.

For example, if the two curves form a positive Hopf link, the projection has two positive crossings:

$$\sum \text{sign(crossing)} = 2,$$

and hence

$$Lk = 1.$$

If the two crossings are negative, then

$$Lk = -1.$$

If the signed crossings cancel, then the linking number is zero.

This crossing-count formula gives a visual interpretation of the Gauss linking integral. The Gauss integral is independent of projection, while the crossing formula is computed from any generic projection and gives the same integer.

8.8.2 Twist, Writhe, and Self-Linking

For a single vortex tube, one needs a notion of internal linking. Choose a centerline

$$\boldsymbol{\gamma}(s)$$

and a unit normal vector field $\mathbf{u}(s)$ along the curve. The displaced curve

$$\boldsymbol{\gamma}_\varepsilon(s)=\boldsymbol{\gamma}(s)+\varepsilon\mathbf{u}(s)$$

may be interpreted as a nearby vortex line inside the tube.

The self-linking number is

$$SL = Lk(\boldsymbol{\gamma},\boldsymbol{\gamma}_\varepsilon).$$

It measures how the nearby vortex line winds around the centerline.

The self-linking number decomposes as

$$\boxed{SL = Tw + Wr.} \tag{8.17}$$

This is the Călugăreanu–White–Fuller formula.

The *twist* measures rotation of the internal direction $\mathbf{u}$ around the centerline. If

$$\mathbf{T}=\frac{d\boldsymbol{\gamma}}{ds}$$

is the unit tangent, then

$$\boxed{Tw=\frac{1}{2\pi}\int(\mathbf{T}\times\mathbf{u})\cdot\frac{d\mathbf{u}}{ds}\,ds.} \tag{8.18}$$

The *writhe* measures how the centerline itself coils in space. It is given by the Gauss-type integral

$$\boxed{Wr(\boldsymbol{\gamma}) = \frac{1}{4\pi}\int_{\boldsymbol{\gamma}}\int_{\boldsymbol{\gamma}} \frac{(d\mathbf{x}\times d\mathbf{y})\cdot(\mathbf{x}-\mathbf{y})}{|\mathbf{x}-\mathbf{y}|^3},} \tag{8.19}$$

understood as a principal value integral.

Thus

linking	:	how two different tubes wind around each other,
twist	:	how vortex lines wind inside one tube,
writhe	:	how the centerline of one tube coils in space.

8.8.3 Knots

A closed vortex filament may also be knotted. Knotting is the topological type of the closed curve itself, for example an unknot, trefoil knot, or figure-eight knot. Knot type is not measured completely by helicity. Different knots may have the same helicity. To distinguish knots one needs additional knot invariants, such as crossing number, the Alexander polynomial, the Jones polynomial, or the knot group.

Thus helicity detects important topological information, but it is not a complete invariant of vortex knotting.

8.8.4 Helicity of Thin Vortex Tubes

Helicity of two closed vortex tubes. Consider thin vortex tubes with centerlines γ_i and circulations Γ_i. If two tubes γ_1 and γ_2 are linked, their mutual helicity is

$$\boxed{\mathcal{H}_{\text{mutual}} = 2\Gamma_1\Gamma_2 Lk(\gamma_1,\gamma_2).} \tag{8.20}$$

Thus two tubes linked once contribute $2\Gamma_1\Gamma_2$ to helicity.

Derivation of the mutual helicity formula. We give a formal derivation for two thin vortex tubes. Let their centerlines be γ_1 and γ_2, and let their circulations be Γ_1 and Γ_2. In the thin-filament approximation, the vorticity is written as

$$\boldsymbol{\omega} = \boldsymbol{\omega}_1 + \boldsymbol{\omega}_2,$$

where

$$\boldsymbol{\omega}_i(\mathbf{x}) = \Gamma_i \int_{\gamma_i} \delta(\mathbf{x}-\mathbf{y}_i)\, d\mathbf{y}_i.$$

Here $d\mathbf{y}_i$ is the oriented line element along γ_i.

Let $\mathbf{v}_i$ be the velocity induced by $\boldsymbol{\omega}_i$, so that

$$\operatorname{curl}\mathbf{v}_i = \boldsymbol{\omega}_i.$$

Then the helicity is

$$\begin{aligned}\mathcal{H} &= \int_M (\mathbf{v}_1 + \mathbf{v}_2) \cdot (\boldsymbol{\omega}_1 + \boldsymbol{\omega}_2)\, d\mathbf{x} \\ &= \int_M \mathbf{v}_1 \cdot \boldsymbol{\omega}_1\, d\mathbf{x} + \int_M \mathbf{v}_2 \cdot \boldsymbol{\omega}_2\, d\mathbf{x} \\ &\quad + \int_M \mathbf{v}_1 \cdot \boldsymbol{\omega}_2\, d\mathbf{x} + \int_M \mathbf{v}_2 \cdot \boldsymbol{\omega}_1\, d\mathbf{x}.\end{aligned}$$

The first two terms are self-helicity terms, depending on the twist and writhe of each tube. The last two terms are the mutual helicity terms.

We compute one of them. Since $\boldsymbol{\omega}_2$ is concentrated on γ_2,

$$\int_M \mathbf{v}_1 \cdot \boldsymbol{\omega}_2\, d\mathbf{x} = \Gamma_2 \int_{\gamma_2} \mathbf{v}_1(\mathbf{y}_2) \cdot d\mathbf{y}_2.$$

The velocity $\mathbf{v}_1$ induced by the first thin filament is given by the Biot–Savart law:

$$\mathbf{v}_1(\mathbf{y}_2) = \frac{\Gamma_1}{4\pi} \int_{\gamma_1} \frac{d\mathbf{y}_1 \times (\mathbf{y}_2 - \mathbf{y}_1)}{|\mathbf{y}_2 - \mathbf{y}_1|^3}.$$

Therefore

$$\int_M \mathbf{v}_1 \cdot \boldsymbol{\omega}_2\, d\mathbf{x} = \frac{\Gamma_1 \Gamma_2}{4\pi} \int_{\gamma_2} \int_{\gamma_1} \frac{[d\mathbf{y}_1 \times (\mathbf{y}_2 - \mathbf{y}_1)] \cdot d\mathbf{y}_2}{|\mathbf{y}_2 - \mathbf{y}_1|^3}.$$

Using the scalar triple product identity,

$$[d\mathbf{y}_1 \times (\mathbf{y}_2 - \mathbf{y}_1)] \cdot d\mathbf{y}_2 = (d\mathbf{y}_1 \times d\mathbf{y}_2) \cdot (\mathbf{y}_2 - \mathbf{y}_1),$$

and changing the sign convention consistently with the definition of the Gauss linking integral, we obtain

$$\int_M \mathbf{v}_1 \cdot \boldsymbol{\omega}_2\, d\mathbf{x} = \Gamma_1 \Gamma_2 Lk(\gamma_1, \gamma_2).$$

Similarly,

$$\int_M \mathbf{v}_2 \cdot \boldsymbol{\omega}_1\, d\mathbf{x} = \Gamma_1 \Gamma_2 Lk(\gamma_1, \gamma_2).$$

Hence the mutual part of the helicity is

$$\begin{aligned}\mathcal{H}_{\text{mutual}} &= \int_M \mathbf{v}_1 \cdot \boldsymbol{\omega}_2\, d\mathbf{x} + \int_M \mathbf{v}_2 \cdot \boldsymbol{\omega}_1\, d\mathbf{x} \\ &= 2\Gamma_1 \Gamma_2 Lk(\gamma_1, \gamma_2).\end{aligned}$$

Thus

$$\boxed{\mathcal{H}_{\text{mutual}} = 2\Gamma_1 \Gamma_2 Lk(\gamma_1, \gamma_2).} \tag{8.21}$$

If the two tubes are linked once and the orientations are positive, then $Lk(\gamma_1, \gamma_2) = 1$, and the mutual helicity is

$$2\Gamma_1 \Gamma_2.$$

Helicity of several thin vortex tubes. For several thin vortex tubes, one has schematically

$$\boxed{\mathcal{H} = 2\sum_{i<j} \Gamma_i \Gamma_j Lk(\gamma_i, \gamma_j) + \sum_i \Gamma_i^2 SL_i.} \tag{8.22}$$

Using

$$SL_i = Tw_i + Wr_i,$$

this becomes

$$\mathcal{H} = 2\sum_{i<j} \Gamma_i \Gamma_j Lk(\gamma_i, \gamma_j) + \sum_i \Gamma_i^2 (Tw_i + Wr_i).$$

The first term records linking between different vortex tubes. The second term records internal topology of each tube.

This formula explains why helicity is not merely the analytic integral

$$\int_M \mathbf{v} \cdot \boldsymbol{\omega}\, d\mathbf{x}.$$

For thin vortex tubes, it is a measure of linking, twisting, and writhing of vortex structures.

8.8.5 Conservation of Helicity

For ideal incompressible flow under suitable boundary conditions, helicity is conserved:

$$\boxed{\frac{d}{dt}\mathcal{H} = 0.} \tag{8.23}$$

This conservation reflects the fact that vortex tubes are transported by the flow and cannot reconnect in smooth ideal motion. The linking and knotting of vortex tubes are therefore preserved as long as the ideal flow remains smooth.

A direct PDE proof of Conservation of Helicity We now give a direct proof of helicity conservation for ideal barotropic flow. Let

$$\mathcal{H}(t) = \int_M \mathbf{v} \cdot \boldsymbol{\omega}\, d\mathbf{x}, \qquad \boldsymbol{\omega} = \operatorname{curl} \mathbf{v}.$$

Assume that the flow is inviscid and barotropic, and that the body force is conservative. Then the Euler equation can be written in Lamb form:

$$\partial_t \mathbf{v} - \mathbf{v} \times \boldsymbol{\omega} = -\operatorname{grad} B,$$

where

$$B = \frac{1}{2}|\mathbf{v}|^2 + h + \Phi.$$

Here h is the specific enthalpy and Φ is the potential of the body force.

Taking the curl gives the vorticity equation

$$\partial_t \boldsymbol{\omega} = \operatorname{curl}(\mathbf{v} \times \boldsymbol{\omega}).$$

Differentiate helicity:

$$\frac{d}{dt}\mathcal{H} = \int_M \partial_t \mathbf{v} \cdot \boldsymbol{\omega}\, d\mathbf{x} + \int_M \mathbf{v} \cdot \partial_t \boldsymbol{\omega}\, d\mathbf{x}.$$

Using the Lamb form of the momentum equation,

$$\partial_t \mathbf{v} = \mathbf{v} \times \boldsymbol{\omega} - \operatorname{grad} B,$$

we obtain

$$\int_M \partial_t \mathbf{v} \cdot \boldsymbol{\omega}\, d\mathbf{x} = \int_M (\mathbf{v} \times \boldsymbol{\omega}) \cdot \boldsymbol{\omega}\, d\mathbf{x} - \int_M \operatorname{grad} B \cdot \boldsymbol{\omega}\, d\mathbf{x}.$$

The first term vanishes because

$$(\mathbf{v} \times \boldsymbol{\omega}) \cdot \boldsymbol{\omega} = 0.$$

For the second term,

$$\operatorname{div} \boldsymbol{\omega} = 0,$$

so

$$\int_M \operatorname{grad} B \cdot \boldsymbol{\omega}\, d\mathbf{x} = \int_{\partial M} B\, \boldsymbol{\omega} \cdot \boldsymbol{\nu}\, dS.$$

Thus this term vanishes if the boundary contribution is zero, for example in the periodic case, in the whole space with sufficient decay, or when

$$\boldsymbol{\omega} \cdot \boldsymbol{\nu} = 0 \quad \text{on } \partial M.$$

Next, using the vorticity equation,

$$\partial_t \boldsymbol{\omega} = \operatorname{curl}(\mathbf{v} \times \boldsymbol{\omega}),$$

we have

$$\int_M \mathbf{v} \cdot \partial_t \boldsymbol{\omega}\, d\mathbf{x} = \int_M \mathbf{v} \cdot \operatorname{curl}(\mathbf{v} \times \boldsymbol{\omega})\, d\mathbf{x}.$$

By integration by parts for curl,

$$\int_M \mathbf{v} \cdot \operatorname{curl}(\mathbf{v} \times \boldsymbol{\omega})\, d\mathbf{x} = \int_M (\mathbf{v} \times \boldsymbol{\omega}) \cdot \operatorname{curl} \mathbf{v}\, d\mathbf{x} + \text{boundary term}.$$

Since

$$\operatorname{curl} \mathbf{v} = \boldsymbol{\omega},$$

the volume term becomes

$$\int_M (\mathbf{v} \times \boldsymbol{\omega}) \cdot \boldsymbol{\omega}\, d\mathbf{x} = 0.$$

Thus, under boundary conditions for which the curl integration-by-parts boundary term vanishes,

$$\int_M \mathbf{v} \cdot \partial_t \boldsymbol{\omega}\, d\mathbf{x} = 0.$$

Combining the two parts, we obtain

$$\boxed{\frac{d}{dt}\mathcal{H}(t) = 0.}$$

Therefore helicity is conserved for inviscid barotropic flow under suitable boundary conditions.

This proof shows directly why helicity is conserved. The nonlinear term $\mathbf{v} \times \boldsymbol{\omega}$ is perpendicular to $\boldsymbol{\omega}$, and the remaining gradient term contributes only a boundary flux. Thus helicity can change only through boundary effects or through mechanisms that destroy the ideal barotropic structure, such as viscosity or baroclinicity.

Helicity is a Casmir invariant. Helicity also has a Hamiltonian meaning. In the noncanonical Hamiltonian formulation of ideal incompressible fluids, helicity is a Casimir invariant. It is preserved by the Poisson structure itself. Thus helicity is both a topological invariant of vortex geometry and a structural invariant of the Hamiltonian formulation.

Remark 8.1 (Vortex reconnection in viscous flow). In viscous flows, vortex reconnection may occur. Two vortex tubes can approach, reconnect, and change their topology. During reconnection, linking may be converted into twist, writhe, small-scale vorticity, or dissipation. Thus helicity may be redistributed among different geometric forms.

For Navier–Stokes flow, helicity is no longer exactly conserved in general. Viscosity allows vortex lines to diffuse and reconnect. Hence helicity is a useful diagnostic for how viscous effects change vortex topology.

In short, ideal flow preserves vortex topology, while viscous flow can change it through reconnection.

8.9 Impulse, Momentum, and Forces

8.9.1 Classical Impulse and Hydrodynamic Impulse

Classical impulse. In classical mechanics, force is the rate of change of momentum:

$$\mathbf{F} = \frac{d\mathbf{P}}{dt}.$$

Integrating from t_1 to t_2 gives

$$\int_{t_1}^{t_2} \mathbf{F}(t)\, dt = \mathbf{P}(t_2) - \mathbf{P}(t_1).$$

The quantity

$$\mathbf{J} = \int_{t_1}^{t_2} \mathbf{F}(t)\, dt$$

is called the impulse. Thus

$$\boxed{\mathbf{J} = \Delta\mathbf{P}.} \tag{8.24}$$

Impulse is the change of momentum over a time interval.

The dimensions are

$$[\mathbf{F}] = MLT^{-2}, \qquad [\mathbf{J}] = [\mathbf{F}]T = MLT^{-1},$$

and

$$[\mathbf{P}] = MLT^{-1}.$$

Therefore impulse and momentum have the same physical dimension:

$$[\mathbf{J}] = [\mathbf{P}].$$

For example, if a constant force $\mathbf{F}$ acts on a particle during a time interval of length Δt, then

$$\mathbf{J} = \mathbf{F}\Delta t.$$

If the particle has mass m, then

$$\mathbf{F}\Delta t = m\mathbf{v}(t_2) - m\mathbf{v}(t_1).$$

In a collision, the force may be large and act only for a short time, but the impulse still measures the net change in momentum.

For a rocket, if the thrust is $T(t)$, then the total thrust impulse is

$$I_{\text{rocket}} = \int_{t_1}^{t_2} T(t)\, dt.$$

If the thrust is approximately constant,

$$I_{\text{rocket}} = T\Delta t.$$

The unit is

$$\text{N s} = \text{kg m/s},$$

again the unit of momentum. Thus rocket impulse measures how much momentum the engine delivers during the burn.

Hydrodynamic impulse. In vortex dynamics, we need an analogous quantity. For a localized vortical flow in an unbounded incompressible fluid, the ordinary total momentum

$$\rho \int \mathbf{v}\, d\mathbf{x}$$

is often not the most useful quantity. The velocity field may extend far away, and the momentum integral may vanish, diverge, or fail to capture the momentum-like effect of the vortex structure. Instead, one uses the hydrodynamic impulse.

For an incompressible fluid of constant density ρ, the hydrodynamic impulse is defined by

$$\boxed{\mathbf{I} = \frac{1}{2}\rho \int \mathbf{x} \times \boldsymbol{\omega}\, d\mathbf{x}.} \tag{8.25}$$

Here

$$\boldsymbol{\omega} = \operatorname{curl} \mathbf{v}.$$

This quantity is built directly from the vorticity distribution. The factor $\mathbf{x} \times \boldsymbol{\omega}$ measures the first moment of vorticity, and the factor ρ converts it into a momentum-like quantity.

Relation with ordinary linear momentum. The definition of hydrodynamic impulse is closely related to ordinary linear momentum. Suppose ρ is constant and

$$\boldsymbol{\omega} = \operatorname{curl} \mathbf{v}.$$

Then

$$\mathbf{I} = \frac{1}{2}\rho \int_M \mathbf{x} \times (\operatorname{curl} \mathbf{v})\, d\mathbf{x}.$$

Using integration by parts, one obtains

$$\int_M \mathbf{x} \times (\operatorname{curl} \mathbf{v})\, d\mathbf{x} = 2 \int_M \mathbf{v}\, d\mathbf{x} + \text{boundary terms}.$$

If the boundary terms vanish, then

$$\boxed{\mathbf{I} = \rho \int_M \mathbf{v}\, d\mathbf{x}.}$$

The right-hand side is the ordinary linear momentum of the fluid:

$$\mathbf{P} = \int_M \rho \mathbf{v}\, d\mathbf{x}.$$

Thus, when boundary contributions are absent,

$$\mathbf{I} = \mathbf{P}.$$

This calculation explains the meaning of hydrodynamic impulse: it is a vorticity-based expression for the momentum of the fluid. In unbounded domains or in flows with slowly decaying velocity, the ordinary momentum integral may be inconvenient or divergent, while the vorticity moment

$$\frac{1}{2}\rho \int_M \mathbf{x} \times \boldsymbol{\omega}\, d\mathbf{x}$$

can still be the natural momentum-like quantity associated with a localized vortex structure.

Dimension of the impulse. The dimension of the hydrodynamic impulse is

$$[\rho] = ML^{-3}, \qquad [\mathbf{x}] = L, \qquad [\boldsymbol{\omega}] = T^{-1}, \qquad [d\mathbf{x}] = L^3.$$

Therefore

$$[\mathbf{I}] = ML^{-3} \cdot L \cdot T^{-1} \cdot L^3 = MLT^{-1}.$$

Thus hydrodynamic impulse has the same dimension as momentum and classical impulse:

$$[\mathbf{I}] = [\mathbf{P}] = [\mathbf{J}].$$

The meaning is that a localized vortex structure carries a momentum-like effect through the surrounding fluid. The hydrodynamic impulse measures this effect using only the vorticity distribution. This is especially useful because vortices are often easier to identify than the global pressure and velocity field.

The analogy with classical mechanics is

$$\begin{aligned} &\text{classical mechanics} \quad : && \mathbf{P} = \text{momentum}, && \mathbf{F} = \frac{d\mathbf{P}}{dt}, \\ &\text{vortex dynamics} \quad : && \mathbf{I} = \text{hydrodynamic impulse}, && \text{force is related to } \frac{d\mathbf{I}}{dt}. \end{aligned}$$

More precisely, the force exerted by a body on the fluid is related to the rate of change of impulse of the fluid, while the force exerted by the fluid on the body has the opposite sign. Schematically,

$$\mathbf{F}_{\text{body on fluid}} = \frac{d\mathbf{I}}{dt}, \qquad \mathbf{F}_{\text{fluid on body}} = -\frac{d\mathbf{I}}{dt},$$

with additional terms possible depending on the domain, boundaries, and external forces.

Thus hydrodynamic impulse provides the bridge

$$\text{vorticity distribution} \quad \Longrightarrow \quad \text{momentum-like quantity} \quad \Longrightarrow \quad \text{force}.$$

This is why impulse is central in the mechanics of vortex rings, starting vortices, lift, and wake dynamics.

Remark 8.2. he concept of vortex impulse, usually called hydrodynamic impulse or Kelvin impulse, is credited to William Thomson (Lord Kelvin). His foundational paper On Vortex Motion was read in 1867 and published in 1869.

For a constant-density fluid with localized vorticity in three dimensions, its modern expression is

$$\mathbf{I} = \frac{\rho}{2} \int_{\mathbb{R}^3} \mathbf{x} \times \boldsymbol{\omega} \, dV.$$

It measures the impulse needed to establish the vortex motion from rest.

Horace Lamb later developed and presented the theory systematically in Hydrodynamics, especially §161, "Impulse and Energy of a Vortex-System." Lamb explicitly credited the definition to Kelvin.

8.9.2 Impulse of pair of point vortices in 2D

Two-dimensional point vortices with opposite signs

In two dimensions, the hydrodynamic impulse of a vorticity distribution is

$$\mathbf{I} = \rho \int_{\mathbb{R}^2} \omega(\mathbf{x}) \, \mathbf{e}_z \times \mathbf{x} \, dA,$$

up to the sign convention for the perpendicular direction. For point vortices,

$$\omega(\mathbf{x}) = \sum_{j=1}^{N} \Gamma_j \delta(\mathbf{x} - \mathbf{x}_j),$$

this becomes

$$\boxed{\mathbf{I} = \rho \sum_{j=1}^{N} \Gamma_j \, \mathbf{e}_z \times \mathbf{x}_j.}$$

Consider two point vortices of opposite sign:

$$\Gamma_1 > 0, \qquad \Gamma_2 < 0.$$

Then

$$\mathbf{I} = \rho \left(\Gamma_1 \mathbf{e}_z \times \mathbf{x}_1 + \Gamma_2 \mathbf{e}_z \times \mathbf{x}_2 \right).$$

If their strengths have equal magnitude,

$$\Gamma_1 = \Gamma, \qquad \Gamma_2 = -\Gamma,$$

then

$$\mathbf{I} = \rho \Gamma \, \mathbf{e}_z \times (\mathbf{x}_1 - \mathbf{x}_2).$$

Thus the impulse depends only on the separation vector. This is the classical translating vortex dipole.

If the magnitudes are not equal,

$$|\Gamma_1| \neq |\Gamma_2|,$$

then the total circulation is nonzero:

$$\Gamma_{\text{tot}} = \Gamma_1 + \Gamma_2 \neq 0.$$

The two vortices no longer form a pure translating dipole. Instead, the motion is a rotation about the center of circulation

$$\mathbf{X}_c = \frac{\Gamma_1 \mathbf{x}_1 + \Gamma_2 \mathbf{x}_2}{\Gamma_1 + \Gamma_2}.$$

The distance between the vortices remains constant, but the pair rotates around $\mathbf{X}_c$. In the limiting case

$$\Gamma_1 + \Gamma_2 = 0,$$

the center of circulation is at infinity, and the rotation becomes pure translation. This is the equal-and-opposite dipole.

Besides linear impulse, two-dimensional point vortex dynamics also has an angular impulse, or angular moment of vorticity:

$$\boxed{J = \rho \int_{\mathbb{R}^2} |\mathbf{x}|^2 \omega(\mathbf{x})\, dA.} \tag{8.26}$$

For point vortices,

$$\boxed{J = \rho \sum_{j=1}^{N} \Gamma_j |\mathbf{x}_j|^2.}$$

This quantity is related to rotational motion of the vortex system. For a same-sign vortex pair, the linear impulse may vanish in center coordinates, but the angular impulse remains nonzero and records the rotational content of the configuration.

Thus, in two dimensions,

linear impulse	:	translation of vortex structures,
angular impulse	:	rotation and spatial spread of vorticity.

Two-Dimensional Point Vortices with Same Signs

In two dimensions, the hydrodynamic impulse of a vorticity distribution is

$$\mathbf{I} = \rho \int_{\mathbb{R}^2} \omega(\mathbf{x})\, \mathbf{e}_z \times \mathbf{x}\, dA,$$

up to the sign convention for the perpendicular direction. For point vortices,

$$\omega(\mathbf{x}) = \sum_{j=1}^{N} \Gamma_j \delta(\mathbf{x} - \mathbf{x}_j),$$

this becomes

$$\boxed{\mathbf{I} = \rho \sum_{j=1}^{N} \Gamma_j\, \mathbf{e}_z \times \mathbf{x}_j.} \tag{8.27}$$

Now consider two point vortices with the same sign:

$$\Gamma_1 > 0, \qquad \Gamma_2 > 0.$$

Their total circulation is

$$\Gamma_{\text{tot}} = \Gamma_1 + \Gamma_2.$$

The center of circulation is defined by

$$\boxed{\mathbf{X}_c = \frac{\Gamma_1 \mathbf{x}_1 + \Gamma_2 \mathbf{x}_2}{\Gamma_1 + \Gamma_2}.} \tag{8.28}$$

Then the impulse can be written as

$$\mathbf{I} = \rho \Gamma_{\text{tot}}\, \mathbf{e}_z \times \mathbf{X}_c.$$

Thus, in coordinates centered at $\mathbf{X}_c$, the linear impulse vanishes:

$$\mathbf{I} = 0.$$

This agrees with the dynamics: same-sign vortex pairs do not translate as a dipole. Instead, they rotate around their center of circulation.

Let

$$\mathbf{r} = \mathbf{x}_1 - \mathbf{x}_2, \qquad d = |\mathbf{r}|.$$

The point vortex equations give

$$\dot{\mathbf{x}}_1 = \frac{\Gamma_2}{2\pi} \frac{\mathbf{r}^\perp}{d^2}, \qquad \dot{\mathbf{x}}_2 = -\frac{\Gamma_1}{2\pi} \frac{\mathbf{r}^\perp}{d^2}.$$

Hence

$$\dot{\mathbf{r}} = \dot{\mathbf{x}}_1 - \dot{\mathbf{x}}_2 = \frac{\Gamma_1 + \Gamma_2}{2\pi d^2} \mathbf{r}^\perp.$$

Therefore the distance d is constant, and $\mathbf{r}$ rotates with angular velocity

$$\boxed{\Omega = \frac{\Gamma_1 + \Gamma_2}{2\pi d^2}.} \tag{8.29}$$

For equal strengths,

$$\Gamma_1 = \Gamma_2 = \Gamma,$$

this becomes

$$\Omega = \frac{\Gamma}{\pi d^2}.$$

The appropriate impulse-like quantity for this rotational motion is the *angular impulse*, or angular moment of vorticity:

$$\boxed{J = \rho \int_{\mathbb{R}^2} |\mathbf{x}|^2 \omega(\mathbf{x})\, dA.} \tag{8.30}$$

For point vortices,

$$\boxed{J = \rho \sum_{j=1}^{N} \Gamma_j |\mathbf{x}_j|^2.} \tag{8.31}$$

In coordinates centered at the center of circulation, one has

$$\Gamma_1 \mathbf{x}_1 + \Gamma_2 \mathbf{x}_2 = 0.$$

Using

$$\mathbf{r} = \mathbf{x}_1 - \mathbf{x}_2,$$

we obtain

$$\mathbf{x}_1 = \frac{\Gamma_2}{\Gamma_1 + \Gamma_2}\mathbf{r}, \qquad \mathbf{x}_2 = -\frac{\Gamma_1}{\Gamma_1 + \Gamma_2}\mathbf{r}.$$

Thus

$$\begin{aligned} J &= \rho \left(\Gamma_1 |\mathbf{x}_1|^2 + \Gamma_2 |\mathbf{x}_2|^2 \right) \\ &= \rho \frac{\Gamma_1 \Gamma_2}{\Gamma_1 + \Gamma_2} d^2. \end{aligned}$$

Hence

$$\boxed{J = \rho \frac{\Gamma_1 \Gamma_2}{\Gamma_1 + \Gamma_2} d^2.} \tag{8.32}$$

For equal strengths,

$$\Gamma_1 = \Gamma_2 = \Gamma,$$

this reduces to

$$J = \frac{1}{2} \rho \Gamma d^2.$$

Thus same-sign vortex pairs are naturally associated with angular impulse, not linear impulse. Their coherent motion is rotation about the center of circulation:

$$\text{same-sign pair} \quad \Longrightarrow \quad \text{rotating vortex pair.}$$

By contrast, equal and opposite vortices have zero total circulation and form a translating dipole, whose motion is naturally described by linear impulse.

8.9.3 Impulse of a Vortex Ring

We now compute the hydrodynamic impulse of a thin vortex ring. This example shows clearly why impulse is the natural momentum-like quantity for vortex dynamics.

Consider a thin vortex filament concentrated on a closed space curve

$$\boldsymbol{\gamma} = \boldsymbol{\gamma}(s),$$

where s is arclength. Let

$$\mathbf{T}(s) = \frac{d\boldsymbol{\gamma}}{ds}$$

be the unit tangent. If the filament carries circulation Γ, then the vorticity may be written formally as

$$\boldsymbol{\omega}(\mathbf{x}) = \Gamma \int_{\gamma} \mathbf{T}(s)\, \delta(\mathbf{x} - \boldsymbol{\gamma}(s))\, ds.$$

Equivalently,

$$\boldsymbol{\omega}(\mathbf{x}) = \Gamma \int_{\gamma} \delta(\mathbf{x} - \boldsymbol{\gamma})\, d\boldsymbol{\gamma}.$$

The hydrodynamic impulse is

$$\mathbf{I} = \frac{1}{2}\rho \int \mathbf{x} \times \boldsymbol{\omega}(\mathbf{x})\, d\mathbf{x}.$$

Substituting the filament expression gives

$$\begin{aligned}\mathbf{I} &= \frac{1}{2}\rho\Gamma \int_\gamma \boldsymbol{\gamma}(s) \times \mathbf{T}(s)\, ds \\ &= \frac{1}{2}\rho\Gamma \int_\gamma \boldsymbol{\gamma} \times d\boldsymbol{\gamma}.\end{aligned}$$

This motivates the definition of the vector area enclosed by the closed curve $\boldsymbol{\gamma}$:

$$\boxed{\mathbf{A}_\gamma = \frac{1}{2}\int_\gamma \boldsymbol{\gamma} \times d\boldsymbol{\gamma}.}$$

Hence

$$\boxed{\mathbf{I} = \rho\Gamma\mathbf{A}_\gamma.} \tag{8.33}$$

Thus the impulse of a thin closed vortex filament is density times circulation times the vector area enclosed by the filament. This is the vortex analogue of the statement that impulse is momentum-like. The vorticity distribution carries an effective momentum determined by its circulation and geometry.

For a circular vortex ring of radius R, the curve lies in a plane and has unit normal $\mathbf{B}$. Its vector area is

$$\mathbf{A}_\gamma = \pi R^2 \mathbf{B}.$$

Therefore

$$\boxed{\mathbf{I} = \rho\Gamma\pi R^2 \mathbf{B}.} \tag{8.34}$$

The direction of $\mathbf{I}$ is the direction of propagation of the ring, determined by the right-hand rule from the orientation of the circulation.

This formula also explains why a vortex ring behaves like a coherent momentum-carrying structure. Increasing the circulation Γ increases the impulse. Increasing the ring radius R increases the vector area and therefore increases the impulse. In this sense, a vortex ring transports a momentum-like quantity through the fluid.

One may also formally consider a curve-supported vorticity with variable strength:

$$\boldsymbol{\omega}(\mathbf{x}) = \int_\gamma \Gamma(s)\mathbf{T}(s)\, \delta(\mathbf{x} - \boldsymbol{\gamma}(s))\, ds.$$

Then the same calculation gives

$$\boxed{\mathbf{I} = \frac{1}{2}\rho \int_\gamma \Gamma(s)\, \boldsymbol{\gamma}(s) \times d\boldsymbol{\gamma}(s).}$$

This is a circulation-weighted vector area. However, for an isolated closed vortex filament in incompressible flow, the circulation must be constant along the filament. Indeed,

$$\operatorname{div} \boldsymbol{\omega} = 0$$

requires that no vorticity source or sink occur along the curve. A varying $\Gamma(s)$ would create a distributional divergence unless additional singular structures, endpoints, or sources are present. Therefore, for a closed isolated vortex ring, the physically admissible case is

$$\Gamma(s) = \Gamma = \text{constant}.$$

Two Vortex Rings and Leapfrogging

A circular vortex ring has impulse

$$\mathbf{I} = \rho\Gamma\pi R^2\mathbf{B},$$

where R is the ring radius, Γ is its circulation, and $\mathbf{B}$ is the axis direction. Thus the impulse is proportional to the vector area of the ring.

Now consider two coaxial vortex rings with the same orientation. Suppose both rings have circulation Γ and share the same symmetry axis, which we take to be the z-axis. Let their radii be

$$R_1(t), \qquad R_2(t),$$

and let their axial positions be

$$z_1(t), \qquad z_2(t).$$

Each ring moves for two reasons. First, each ring has a self-induced velocity caused by its own curved vorticity. Second, each ring is advected by the velocity field induced by the other ring.

For a single thin vortex ring of radius R and core radius a, with $a \ll R$, the self-induced speed along the symmetry axis is approximately

$$U_{\text{self}}(R) \approx \frac{\Gamma}{4\pi R}\left[\log\left(\frac{8R}{a}\right) - C\right],$$

where the constant C depends on the vorticity distribution inside the core. The important dependence is

$$U_{\text{self}}(R) \sim \frac{\Gamma}{4\pi R}\log\left(\frac{R}{a}\right).$$

Thus, to leading order, a smaller ring moves faster than a larger ring.

Now suppose the rear ring is behind the front ring. The velocity induced by the front ring is not uniform near the rear ring. It has both an axial component and a radial component. The axial component advects the rear ring forward. The radial component can shrink or expand the ring, depending on the relative position of the two rings.

During leapfrogging, the rear ring is pulled inward radially and therefore its radius decreases:

$$R_{\text{rear}}(t) \downarrow .$$

Since the self-induced speed increases when the radius decreases, the rear ring accelerates:

$$U_{\text{self}}(R_{\text{rear}}) \uparrow .$$

It then catches up to the front ring and passes through it.

At the same time, the front ring is pushed outward radially. Its radius increases:

$$R_{\text{front}}(t) \uparrow,$$

so its self-induced speed decreases:

$$U_{\text{self}}(R_{\text{front}}) \downarrow .$$

After the rear ring passes through the front ring, the roles are exchanged: the previously rear ring becomes the front ring, expands, and slows down; the other ring contracts and speeds up. This exchange can repeat, producing the leapfrogging motion.

Thus the qualitative mechanism is

$$\begin{aligned} \text{rear ring contracts} &\implies \text{self-induced speed increases,} \\ \text{front ring expands} &\implies \text{self-induced speed decreases,} \\ \text{rear catches front} &\implies \text{rings pass through each other.} \end{aligned}$$

The motion is not a collision. The vortex rings are material vortex tubes in an inviscid idealization, and each ring is transported by the velocity field induced by the whole vorticity distribution. When one ring passes through the other, the two vortex tubes deform smoothly.

The impulse viewpoint also helps. A thin circular ring carries impulse

$$\mathbf{I} = \rho\Gamma\pi R^2\mathbf{B}.$$

Thus changing the radius changes the impulse carried by each ring. During leapfrogging, impulse is exchanged between the two rings and the surrounding fluid, while the total impulse of the two-ring system is conserved in the absence of external forces. The process is therefore a coherent exchange of radius, velocity, and impulse.

In short,

$$\text{leapfrogging} = \text{mutual induction} + \text{radius change} + \text{self-induced speed change.}$$

This is one of the most striking examples of nonlinear interaction between three-dimensional vortex structures.

Trailing Vortices, Wake Impulse, and Lift

The same idea appears in the wake of a lifting wing. A finite wing generates bound circulation. Behind the wing, trailing vorticity is shed into the wake. Far downstream, the wake is often dominated by two counter-rotating vortex tubes. In a cross-section, these look like a two-dimensional vortex dipole.

Let the two trailing vortices have circulations

$$\Gamma \quad \text{and} \quad -\Gamma,$$

separated by a distance d. The cross-sectional impulse per unit length is analogous to the two-dimensional dipole impulse:

$$\mathbf{I}' = \rho\Gamma\,\mathbf{e}_x \times \mathbf{d},$$

where $\mathbf{e}_x$ is the downstream direction and $\mathbf{d}$ is the separation vector between the two vortices in the cross-section. This impulse points mainly downward or upward depending on the orientation convention. It represents the momentum carried by the wake.

For a lifting wing, the wake carries downward momentum. By Newton's third law, the wing experiences upward lift. Thus lift is connected to the rate at which impulse is deposited into the wake:

$$\boxed{\text{lift} \quad \Longleftrightarrow \quad \text{rate of change of wake impulse.}} \tag{8.35}$$

This gives a vortex interpretation of the Kutta–Joukowski lift formula. In two-dimensional potential flow with circulation, the lift per unit span is

$$L' = \rho U |\Gamma|.$$

In the vortex-dynamics picture, the same circulation is tied to the generation of trailing or starting vortices. The fluid receives impulse through the shed vortices, and the body experiences the opposite force.

Thus the connection is

$$\text{bound circulation} \quad \Longrightarrow \quad \text{shed vorticity} \quad \Longrightarrow \quad \text{wake impulse} \quad \Longrightarrow \quad \text{lift.}$$

This viewpoint complements the pressure-based derivation of lift in potential flow. Potential flow explains the pressure distribution once the circulation is known. Vortex impulse explains how the circulation and wake vorticity carry momentum and produce force.

Remark 8.3 (Lift, thrust, and staying in the air). An aircraft stays in the air because the total aerodynamic and propulsive forces balance its weight. In ordinary level flight, the main balance is

$$L \approx mg,$$

where L is lift and mg is weight. The wings produce lift by deflecting air downward. Equivalently, the wing creates circulation and a pressure difference: lower pressure above the wing and higher pressure below. The air gains downward momentum, and the aircraft gains upward force.

The engine is also necessary, but in steady level flight its main role is to overcome drag:

$$T \approx D,$$

where T is thrust and D is drag.

For a fighter aircraft, the force balance depends on the maneuver:

level flight	:	the wings provide most of the upward force,
steep climb	:	thrust contributes strongly against weight,
vertical climb	:	thrust may support almost all the weight,
inverted level flight	:	the wings still produce upward aerodynamic force, but with the opposite angle of attack relative to normal flight.

Thus lift should not be identified simply with "upward force." Lift is usually defined as the aerodynamic force perpendicular to the incoming relative wind. In ordinary horizontal flight this force is nearly vertical. In vertical flight, however, the lift direction may be nearly horizontal, and the force supporting the aircraft against gravity is mainly thrust.

In all cases, the basic momentum principle is the same:

$$\text{aircraft gives air downward momentum} \quad \Longrightarrow \quad \text{air gives aircraft upward force.}$$

For a wing this momentum transfer is organized by bound circulation and trailing vortices. For a rotor or jet, it is organized by thrust and a vortical wake.

Drone Rotors, Vortices, and Lift

A drone produces lift by rotating propellers. Each propeller accelerates air downward. By Newton's third law, the air exerts an upward force on the drone. Thus the basic momentum balance is

$$\text{downward momentum given to air} \quad \Longleftrightarrow \quad \text{upward lift on the drone.}$$

The flow generated by a rotor is strongly vortical. The blade tips shed trailing vortices, and these vortices form a helical wake behind the rotor. For a hovering drone, the wake is approximately a downward column of swirling air. The rotor therefore generates both

$$\text{downwash} \qquad \text{and} \qquad \text{helical tip vortices.}$$

A simple actuator-disk model captures the lift mechanism. Suppose a rotor of disk area A drives air downward with induced velocity w. The mass flux through the disk is approximately

$$\dot{m} = \rho A w.$$

The change of vertical momentum per unit time is then of order

$$\dot{m}\, w = \rho A w^2.$$

Therefore the thrust, or lift in hover, scales like

$$\boxed{T \sim \rho A w^2.}$$

More refined actuator-disk theory gives

$$T = 2\rho A w^2,$$

depending on the convention for the induced velocity at the disk and in the far wake.

From the vortex viewpoint, this downward momentum flux is organized by the vorticity shed from the rotating blades. The blade tips generate strong vortices, and the rotating wake carries circulation and impulse downward. The drone experiences the opposite force:

$$\mathbf{F}_{\text{drone}} = -\frac{d\mathbf{I}_{\text{wake}}}{dt},$$

schematically, where $\mathbf{I}_{\text{wake}}$ is the hydrodynamic impulse carried by the vortical wake.

Thus a drone rotor is not merely pushing air like a fan in a purely potential flow. It creates a vortical wake. The helical vortex system behind the propeller records the momentum and impulse transferred to the air, and this transfer is what supports the drone.

This example is parallel to the lifting wing:

$$\begin{aligned} \text{airplane wing} &: \text{bound circulation and trailing vortices,} \\ \text{drone rotor} &: \text{rotating blades and helical tip vortices.} \end{aligned}$$

In both cases, lift is connected to the generation and transport of vortex impulse in the wake.

8.9.4 Lift, Bound Circulation, and Starting Vortices

In the preceding chapter, lift in potential flow was computed from pressure using the Kutta–Joukowski formula:

$$\mathbf{L}' = \rho\, \mathbf{U}_\infty \times \boldsymbol{\Gamma}.$$

From the vortex viewpoint, the same lift is connected to circulation and vorticity. The bound circulation around an airfoil behaves like vorticity enclosed by the body. When an airfoil starts from rest, a starting vortex is shed into the wake. Kelvin's theorem then implies that an opposite circulation remains around the airfoil:

$$\Gamma_{\text{bound}} + \Gamma_{\text{starting}} = 0.$$

Thus lift is not merely a pressure phenomenon. It is also a vortex phenomenon:

$$\text{starting vortex} + \text{bound circulation} \quad \Longrightarrow \quad \text{lift}.$$

Potential flow describes the exterior irrotational motion once the circulation is known. Vortex dynamics explains how that circulation is generated and carried away.

8.9.5 Wake Momentum and Drag

Drag is also connected to vortex dynamics. A body moving through a viscous fluid generates boundary-layer vorticity. When the boundary layer separates, vorticity is shed into the wake. The wake carries momentum deficit and vortex impulse. The drag on the body is related to the rate at which momentum and impulse are transported into the wake.

This explains why inviscid steady potential flow gives d'Alembert's paradox: without a wake, there is no mechanism for sustained drag. Real drag is connected to vorticity generation, separation, and wake dynamics.

8.10 Summary and Further Reading

This chapter used the vorticity equation and circulation laws from Chapter **??** without rederiving them. The emphasis was on the geometry and mechanics of vortices: point vortices, vortex patches, vortex sheets, filaments, rings, classical vortex models, wake patterns, impulse, and velocity reconstruction.

Vortex dynamics is where the abstract structures of the previous chapters become visible. Hodge decomposition explains why vorticity alone does not always determine velocity. Hamiltonian structure appears in point vortex dynamics, helicity, and coadjoint-orbit viewpoints. Mechanics appears through impulse, lift, wakes, and vortex rings.

For classical vortex dynamics, see **?**, Lamb (1932a), and Batchelor (1967). For vorticity methods and vortex patches, see Majda and Bertozzi (2002). For vortex methods, see Chorin (1973) and Leonard (1980). For helicity and vortex topology, see Moffatt (1969) and Arnold and Khesin (1998). For cohomology-fluid and covector-fluid viewpoints, see Yin et al. (2023) and Nabizadeh et al. (2024).

Bibliography

Ralph Abraham and Jerrold E. Marsden. *Foundations of Mechanics*. Benjamin/Cummings, Reading, MA, 2 edition, 1978.

D. J. Acheson. *Elementary Fluid Dynamics*. Oxford University Press, Oxford, 1990.

John D. Anderson. *Modern Compressible Flow*. McGraw-Hill, New York, 3 edition, 2002.

Rutherford Aris. *Vectors, Tensors and the Basic Equations of Fluid Mechanics*. Dover Publications, New York, 1989.

Vladimir I. Arnold. Sur la géométrie différentielle des groupes de lie de dimension infinie et ses applications à l'hydrodynamique des fluides parfaits. *Annales de l'Institut Fourier*, 16:319–361, 1966.

Vladimir I. Arnold and Boris A. Khesin. *Topological Methods in Hydrodynamics*. Springer, New York, 1998.

G. K. Batchelor. *An Introduction to Fluid Dynamics*. Cambridge University Press, Cambridge, 1967.

Herbert B. Callen. *Thermodynamics and an Introduction to Thermostatistics*. Wiley, New York, 2 edition, 1985.

Constantin Carathéodory. Untersuchungen über die grundlagen der thermodynamik. *Mathematische Annalen*, 67(3):355–386, 1909.

Augustin-Louis Cauchy. Mémoire sur la dynamique des fluides. *Mémoires présentés à l'Académie des Sciences de l'Institut de France*, 1815.

Alexandre J. Chorin. Numerical study of slightly viscous flow. *Journal of Fluid Mechanics*, 57(4): 785–796, 1973.

Alexandre J. Chorin and Jerrold E. Marsden. *A Mathematical Introduction to Fluid Mechanics*. Springer, New York, 4 edition, 2000.

Alfred Clebsch. Über eine allgemeine transformation der hydrodynamischen gleichungen. *Journal für die reine und angewandte Mathematik*, 56:1–10, 1859.

Richard Courant and K. O. Friedrichs. *Supersonic Flow and Shock Waves*. Springer, New York, 1948.

Keenan Crane. Discrete differential geometry: An applied introduction. Course notes, 2023. Available online.

Mathieu Desbrun, Anil N. Hirani, Melvin Leok, and Jerrold E. Marsden. Discrete exterior calculus. Technical report, California Institute of Technology, 2005. Preprint.

Hans Ertel. Ein neuer hydrodynamischer wirbelsatz. *Meteorologische Zeitschrift*, 1942.

Leonhard Euler. Principes généraux du mouvement des fluides. *Mémoires de l'Académie des Sciences de Berlin*, 1755.

Enrico Fermi. *Thermodynamics*. Dover Publications, New York, 1956.

Kurt O. Friedrichs. Differential forms on riemannian manifolds. *Communications on Pure and Applied Mathematics*, 8:551–590, 1955.

J. Willard Gibbs. *The Collected Works of J. Willard Gibbs, Vol. I: Thermodynamics*. Longmans, Green and Co., New York, 1928.

Walter Greiner, Ludwig Neise, and Horst Stöcker. *Thermodynamics and Statistical Mechanics*. Springer, New York, 1995.

Hermann von Helmholtz. On integrals of the hydrodynamical equations, which express vortex-motion. *Philosophical Magazine*, 1858.

John W. Herivel. The derivation of the equations of motion of an ideal fluid by hamilton's principle. *Proceedings of the Cambridge Philosophical Society*, 51(1):344–349, 1955.

W. V. D. Hodge. *The Theory and Applications of Harmonic Integrals*. Cambridge University Press, Cambridge, 1941.

Darryl D. Holm, Jerrold E. Marsden, and Tudor S. Ratiu. The Euler–Poincaré equations and semidirect products with applications to continuum theories. *Advances in Mathematics*, 137(1): 1–81, 1998.

James R. Holton and Gregory J. Hakim. *An Introduction to Dynamic Meteorology*. Academic Press, Amsterdam, 5 edition, 2012.

Charles Kittel and Herbert Kroemer. *Thermal Physics*. W. H. Freeman, New York, 2 edition, 1980.

Nikolai E. Kochin, Ilia A. Kibel, and Nikolai V. Roze. *Theoretical Hydrodynamics*. Interscience, New York, 1964.

Joseph-Louis Lagrange. *Mécanique Analytique*. Chez la Veuve Desaint, Paris, 1788.

Horace Lamb. *Hydrodynamics*. Cambridge University Press, Cambridge, 6 edition, 1932a.

Horace Lamb. *Hydrodynamics*. Cambridge University Press, Cambridge, 6 edition, 1932b.

L. D. Landau and E. M. Lifshitz. *Statistical Physics, Part 1*, volume 5 of *Course of Theoretical Physics*. Butterworth-Heinemann, Oxford, 3 edition, 1980.

L. D. Landau and E. M. Lifshitz. *Fluid Mechanics*. Pergamon Press, Oxford, 2 edition, 1987.

Pierre-Simon Laplace. Sur la vitesse du son dans l'air. *Annales de Chimie et de Physique*, 1816.

Anthony Leonard. Vortex methods for flow simulation. *Journal of Computational Physics*, 37(3): 289–335, 1980.

Elliott H. Lieb and Jakob Yngvason. The physics and mathematics of the second law of thermodynamics. *Physics Reports*, 310(1):1–96, 1999.

H. W. Liepmann and A. Roshko. *Elements of Gasdynamics*. John Wiley & Sons, New York, 1957.

C. C. Lin. Hydrodynamics of helium II. In *Proceedings of the International School of Physics "Enrico Fermi", Course XXI*, pages 93–146. Academic Press, New York, 1963.

Andrew J. Majda and Andrea L. Bertozzi. *Vorticity and Incompressible Flow*. Cambridge University Press, Cambridge, 2002.

Jerrold E. Marsden and Thomas J. R. Hughes. *Mathematical Foundations of Elasticity*. Dover Publications, New York, 1994.

Jerrold E. Marsden and Tudor S. Ratiu. *Introduction to Mechanics and Symmetry*. Springer, New York, 1994.

L. M. Milne-Thomson. *Theoretical Hydrodynamics*. Macmillan, London, 5 edition, 1968.

H. K. Moffatt. The degree of knottedness of tangled vortex lines. *Journal of Fluid Mechanics*, 35 (1):117–129, 1969.

Charles B. Morrey. A variational method in the theory of harmonic integrals, ii. *American Journal of Mathematics*, 78(1):137–170, 1956.

Philip J. Morrison. Poisson brackets for fluids and plasmas. In *AIP Conference Proceedings*, volume 88, pages 13–46, 1982.

Philip J. Morrison. Hamiltonian description of the ideal fluid. *Reviews of Modern Physics*, 70(2): 467–521, 1998.

Philip J. Morrison. Hamiltonian fluid mechanics. In *Encyclopedia of Mathematical Physics*, volume 2. Elsevier, Amsterdam, 2006.

Mohammad Sina Nabizadeh, Ritoban Roy-Chowdhury, Hang Yin, Ravi Ramamoorthi, and Albert Chern. Fluid implicit particles on coadjoint orbits. *ACM Transactions on Graphics*, 43(6): 270:1–270:38, 2024.

Claude-Louis Navier. Mémoire sur les lois du mouvement des fluides. *Mémoires de l'Académie Royale des Sciences de l'Institut de France*, 1822.

Lionello Pogliani and Mario N. Berberan-Santos. Constantin carathéodory and the axiomatic thermodynamics. *Journal of Mathematical Chemistry*, 28:313–324, 2000.

Linda E. Reichl. *A Modern Course in Statistical Physics*. Wiley-VCH, Weinheim, 4 edition, 2016.

Frederick Reif. *Fundamentals of Statistical and Thermal Physics*. McGraw-Hill, New York, 1965.

Carl-Gustaf Rossby. Relation between variations in the intensity of the zonal circulation of the atmosphere and the displacements of the semi-permanent centers of action. *Journal of Marine Research*, 1939.

Philip G. Saffman. *Vortex Dynamics*. Cambridge University Press, Cambridge, 1992.

Rick Salmon. Hamiltonian fluid mechanics. *Annual Review of Fluid Mechanics*, 20:225–256, 1988.

Rick Salmon. *Lectures on Geophysical Fluid Dynamics*. Oxford University Press, Oxford, 1998.

Günter Schwarz. *Hodge Decomposition: A Method for Solving Boundary Value Problems*, volume 1607 of *Lecture Notes in Mathematics*. Springer, Berlin, 1995.

R. L. Seliger and G. B. Whitham. Variational principles in continuum mechanics. *Proceedings of the Royal Society of London. Series A. Mathematical and Physical Sciences*, 305(1480):1–25, 1968.

George Gabriel Stokes. On the theories of the internal friction of fluids. *Transactions of the Cambridge Philosophical Society*, 1850.

William Thomson. On vortex motion. *Transactions of the Royal Society of Edinburgh*, 1869.

Clifford Truesdell and Walter Noll. *The Non-Linear Field Theories of Mechanics*. Springer, Berlin, 2004.

Geoffrey K. Vallis. *Atmospheric and Oceanic Fluid Dynamics: Fundamentals and Large-Scale Circulation*. Cambridge University Press, Cambridge, 2 edition, 2017.

A. I. Vol'pert and S. I. Hudjaev. *Analysis in Classes of Discontinuous Functions and Equations of Mathematical Physics*. Springer, Dordrecht, 1985.

Stephanie Wang, Mohammad Sina Nabizadeh, and Albert Chern. Exterior calculus in graphics. In *ACM SIGGRAPH 2023 Courses*, SIGGRAPH '23, New York, NY, 2023. Association for Computing Machinery.

Frank M. White. *Viscous Fluid Flow*. McGraw-Hill, New York, 3 edition, 2006.

Hang Yin, Mohammad Sina Nabizadeh, Baichuan Wu, Stephanie Wang, and Albert Chern. Fluid cohomology. *ACM Transactions on Graphics*, 42(4):1–25, 2023. doi: 10.1145/3592402.